

THESIS

3

2001

LIBRARY
Michigan State
University

This is to certify that the

dissertation entitled

Spatial Organization in Soil Bacterial Communities

presented by

Christopher B. Blackwood

has been accepted towards fulfillment

of the requirements for

Ph. D. degree in Crop and Soil Sciences
Ecology, Evolutionary
Biology, and Behavior



Major professor

Date August 1, 2001

PLACE IN RETURN BOX to remove this checkout from your record.
TO AVOID FINES return on or before date due.
MAY BE RECALLED with earlier due date if requested.

DATE DUE	DATE DUE	DATE DUE
SEP 22 2007		

SPATIAL ORGANIZATION IN SOIL BACTERIAL COMMUNITIES

By

Christopher B. Blackwood

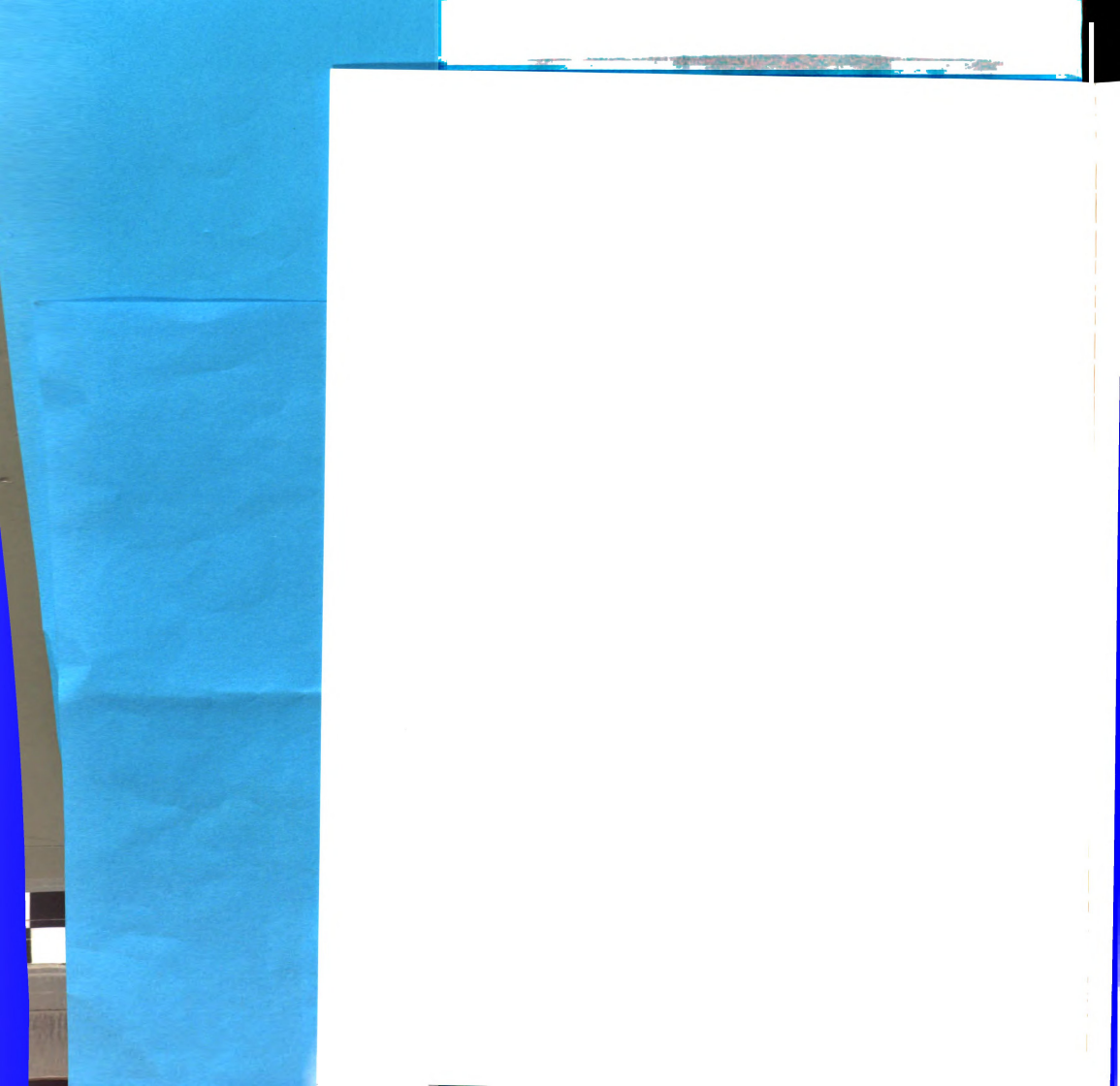
A DISSERTATION

Submitted to
Michigan State University
in partial fulfillment of the requirements
for the degree of

DOCTOR OF PHILOSOPHY

Department of Crop and Soil Sciences
Ecology, Evolutionary Biology, and Behavior Program

2001



SPATIAL ORGANIZATION IN SOIL BACTERIAL COMMUNITIES

By

Christopher B. Blackwood

AN ABSTRACT OF A DISSERTATION

Submitted to
Michigan State University
in partial fulfillment of the requirements
for the degree of

DOCTOR OF PHILOSOPHY

Department of Crop and Soil Sciences
Ecology, Evolutionary Biology, and Behavior Program

2001

Professor Eldor A. Paul

THE JOURNAL OF THE AMERICAN MEDICAL ASSOCIATION

PUBLISHED WEEKLY

CONTENTS

Original Articles
The Role of the Physician in the Community
The Role of the Physician in the Community
The Role of the Physician in the Community

Editorial

The Role of the Physician in the Community
The Role of the Physician in the Community
The Role of the Physician in the Community

Index

Published by the American Medical Association, 535 North Dearborn Street, Chicago, Ill. 60610

ABSTRACT

SPATIAL ORGANIZATION IN SOIL BACTERIAL COMMUNITIES

By

Christopher B. Blackwood

Spatial variability of soil resources is high due to the heterogeneous arrangement of pores and mineral and organic matter particles in soil, and due to the activity of plants and soil fauna. The spatial organization of soil microbial communities was investigated using terminal restriction fragment length polymorphism (T-RFLP) of eubacterial ribosomal 16S genes, a molecular genetic technique independent of the cultivation of microbes outside their natural environment. Methods for optimal data processing and multivariate statistical analysis of complex community T-RFLP profiles were investigated using analytically-replicated datasets. Spatially-defined microbial habitats were detected by testing the significance of the differences between eubacterial community T-RFLP profiles. Light fraction and shoot residue (partially-decomposed organic matter particles) were found to contain communities different from both the rhizosphere and the soil heavy fraction (soil minerals with associated humified organic matter). Communities in the external and internal portions of soil aggregates were found to be slightly different, while those of different aggregate sizes were not different. The establishment of soil fractions as distinct microbial habitats seemed to be dependent on the differences in the organic matter contents of different fractions. However, different cropping systems also caused divergence in communities which could not be explained on the basis of organic matter contents of samples. Microscopic cell counts were shown to be primarily sensitive to organic matter contents of samples, and not to qualitative

differences between cropping systems, in contrast to community composition. Number of large cells ($>0.18 \mu\text{m}^3$) was significantly affected by both soil fraction and cropping system. In another approach to understanding spatial organization of soil eubacterial communities, communities within soil samples of varying sizes and from differing locations within replicated 1.5x2 m plots were assayed by T-RFLP. The spatial structure of the communities was investigated using a generalized multivariate extension of blocked-quadrat analysis and semivariance analyses, integrating analyses based on varying sampling grain and extent. Significant hierarchical spatial structure was detected within the eubacterial communities, manifest by phase shifts in the relationship between community variability and spatial scale. These studies indicate that significant spatial organization exists in eubacterial communities in soil, which implies that soil communities are not randomly assembled and may be regulated by mechanisms analogous to those for plant and animal communities.



ACKNOWLEDGEMENTS

I am extremely grateful to Dr. Eldor Paul, my graduate advisor, for the inspiration and advice he has given me through my years at MSU. He gave me the freedom to pursue my interests while ensuring that the goals were realistic and the science was rigorous and exciting. I would also like to thank my committee members, Dr. Richard Harwood, Dr. Kay Gross, and Dr. James Tiedje for their advice and support.

Dr. Terry Marsh graciously allowed me to perform much of the molecular genetic work in this thesis in the Research On Microbial Evolution (R.O.M.E.) lab. The advice I received from Dr. Marsh and other members of the R.O.M.E. lab, and from Dr. David Treves, Hector Ayala del Rio, and Jim Stoddard was invaluable in my learning molecular techniques. Dr. Al Smucker, Dr. Curtis Dell, and Dr. Shawel Haile-Mariam shared their expertise of soil structure and helped perform some of the soil aggregate fractionation work. Discussions with Dr. Sven Bohm, Dr. Sherri Morris, Dr. Ann Marie Fortuna, and Helmut Stoyan also assisted in the formulation and accomplishment of this research. My work was shaped by discussions with many individuals from the Center for Microbial Ecology, the KBS Long Term Ecological Research site, the Living Field Lab, the Ecology, Evolutionary Biology, and Behavior Program, and the Michigan State Sustainable Agriculture Network. Financial support for my studies was provided by Dr. Tiedje through the Center for Microbial Ecology, Dr. G. Philip Robertson through the KBS LTER, and Dr. Smucker through USDA/NRI grant 97-35107-4322.

Finally, I thank my wife Andria and sons Stewart and Eli for their continued understanding and support, and my parents for providing me with the tools and confidence needed to accomplish my goals.

TABLE OF CONTENTS

List of Tables	vi
List of Figures	vii
Chapter 1: Introduction	1
Chapter 2: Methods of T-RFLP Data Analysis for Quantitative Comparison of Microbial Communities	8
Abstract	9
Introduction	10
Methods	16
Results	22
Discussion	28
Conclusions	31
Chapter 3: Eubacterial Community Structure and Population Size within the Soil Light Fraction, Rhizosphere, and Heavy Fraction of Several Agricultural Cropping Systems	47
Abstract	48
Introduction	49
Methods	52
Results	60
Discussion	67
Chapter 4: Eubacterial Community Response to Position within Soil Macroaggregates and Soil Management	89
Abstract	90
Introduction	90
Methods	94
Results	102
Discussion	108
Conclusions	110
Chapter 5: Use of Multivariate Statistics to Test Hierarchical Structure within a Soil Eubacterial community Analyzed By T-RFLP	126
Abstract	127
Introduction	128
Detection of Levels of Ecological Organization: Statistical Approaches	132
Materials and Methods	143
Data Analysis Methods	148
Results	156
Discussion	161
Conclusions	168

LIST OF TABLES

Chapter 2

Table 1: Dendrogram characteristics for cluster analysis of manually-aligned T-RFLP profiles of KBS soil fraction using a variety of data processing methods and clustering algorithms. All profiles included in the analysis.	37
Table 2: Dendrogram characteristics for cluster analyses of computer-aligned T-RFLP profiles of KBS soil fractions using a variety of data processing methods.	38
Table 3: Dendrogram characteristics for cluster analysis of manually-aligned T-RFLP profiles of KBS soil fractions using a variety of data processing methods and clustering algorithms. Only profiles with a cumulative peak height of >10,000 included in analysis.	39
Table 3: Dendrogram characteristics for cluster analyses T-RFLP profiles of bioreactor samples using a variety of data processing methods and clustering algorithms.	40
Table 5: Redundancy analysis results testing the null hypothesis that there is no difference between bioreactor sample T-RFLP profiles.	41
Table 6: Dendrogram characteristics and redundancy analysis results for the set of alfalfa soil samples.	41

Chapter 3

Table 1: Biogeochemical characteristics of soil fractions.	78
Table 2: Numbers of bacterial cells and percent of cells in different cell size classes.	79
Table 3: Redundancy analysis testing treatment effects on T-RFLP profiles derived from different soil fractions and cropping systems.	80
Table 4: Terminal restriction fragments (T-RFs) associated with the same treatment in 1998 and 1999.	81

Chapter 4

Table 1: Redundancy analysis of HF-1 and LF-1 isolated from different aggregate size classes at KBS.	117
Table 2: Redundancy analysis of pooled aggregate layer samples from KBS.	118
Table 3: Redundancy analysis of pooled aggregate layer samples from Wooster.	119

Chapter 5

Table 1: Grain-based regression analysis of T-RFLP profile variability on mean log soil weight.	178
Table 2: Distance function parameters fit with nonlinear least-squares to HV of 10 g sample T-RFLP profiles.	178
Table 3: Redundancy analysis and global Mantel tests of all fifty 10 g sample T-RFLP profiles per grid.	179

LIST OF FIGURES

Chapter 2

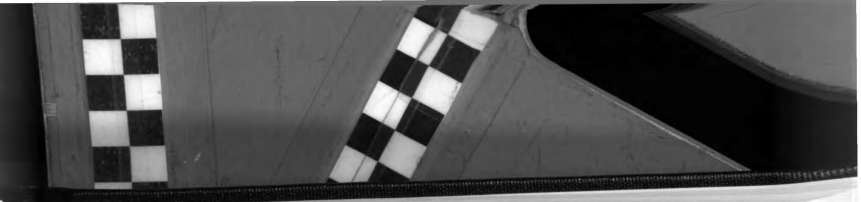
Figure 1: Example of replicated T-RFLP electropherograms	42
Figure 2: Dendrogram of manually-aligned T-RFLP profiles of KBS soil fractions constructed by Ward's cluster analysis of raw T-RF peak heights.	43
Figure 3: Dendrogram of manually-aligned T-RFLP profiles of KBS soil fractions constructed by Ward's cluster analysis of relative T-RF peak heights.	44
Figure 4: Dendrogram of manually-aligned T-RFLP profiles of KBS soil fractions constructed by UPGMA cluster analysis of relative T-RF peak heights.	45
Figure 5: Canonical principal components plots derived from redundancy analysis of bioreactor sample T-RFLP profiles (RsaI, MspI, and HhaI profiles pooled).	46

Chapter 3

Figure 1: Number of DTAF-stained cells counted per g of soil fractions.	82
Figure 2: Regression of bacterial cells per g of soil fraction against percent C of soil fraction.	83
Figure 3: Regression of percent of cells in the largest cell size class ($>0.18 \mu\text{m}^3$) against percent C of the sample.	84
Figure 4: Partial canonical principal components plots derived from redundancy analysis of 1998 RsaI T-RFLP profiles.	85
Figure 5: Dendrogram generated by Ward's method of hierarchical cluster analysis on 1999 RsaI T-RFLP profiles using Hellinger distance between profiles.	87
Figure 6: Dendrogram generated by Ward's method of hierarchical cluster analysis on 1998 RsaI T-RFLP profiles using Hellinger distance between profiles.	88

Chapter 4

Figure 1: Dendrogram of cluster analysis by Ward's method of RsaI T-RFLP profiles from aggregate layers of individual 4-6.3 mm KBS aggregates.	120
Figure 2: Plots of principal coordinates of Jaccard distance between T-RFLP profiles of layers of individual 4-6.3 mm KBS aggregates.	121
Figure 3: Dendrogram of cluster analysis by Ward's method of RsaI T-RFLP profiles from pooled KBS aggregate layers using Hellinger distance.	122
Figure 4: Biplots of sample and T-RF scores for the three canonical principal components (PCs) derived from redundancy analysis of Hellinger distance between pooled aggregate layers from KBS.	123



LIST OF FIGURES, continued

Figure 5: Aggregate layer and treatment interaction axes of canonical principal components derived from distance-based redundancy analysis of Jaccard distance between Wooster aggregate layer RsaI T-RFLP profiles.	124
Figure 6: Principal coordinates derived from Jaccard distance between Wooster aggregate layer RsaI T-RFLP profiles.	124
Figure 7: Dendrogram of cluster analysis by Ward's method of RsaI T-RFLP profiles from Wooster aggregate layers using Jaccard distance.	125
Chapter 5	
Figure 1: Sampling map for grid 1.	180
Figure 2: MAD-t scores derived from DNA extraction experiment.	181
Figure 3: Grain-based analysis using three variability statistics.	182
Figure 4: Hellinger variance as a function of separation distance.	183
Figure 5: Integration of extent-based and grain-based analyses of Hellinger variance.	185
Figure 6: Principal coordinates analysis of correlation super-matrix of covariance matrices constructed from different distance classes in grid 2, RsaI digest.	186
Figure 7: Cluster analysis correlation super-matrix describing covariance matrices constructed from different distance classes in grid 2, RsaI digest.	187
Figure 8: Normalized Mantel correlogram of Hellinger and Jaccard distances for all 10 g samples.	188
Appendix A: Total number of T-RFs detected in sets of samples at multiple-grain sampling locations.	189

Chapter 1

Introduction



The spatial structure of soil is a complex interconnected framework characterized by pores of various sizes and tortuosity, and zones of varying bulk density and stability, (Christensen 1996, Young and Ritz 2000). Among the mineral particles are heterogeneously distributed particles of decomposing plant residue (Parkin 1993, Staricka et al. 1991). Plant roots, fungal hyphae, and soil fauna grow through this matrix and modify its spatial structure by forcing through narrow pores and entangling particles (Oades 1993, Tisdall 1996). These organisms also process resources and energy, creating gradients of organic matter, water, redox potential, and inorganic nutrients (Juma 1994, Smucker 1993). Soil resources are heterogeneously distributed at larger scales as well, from one to hundreds of meters (Boerner et al. 1998, Dobermann et al. 1995, Robertson et al. 1997, Stoyan et al. 2000).

The major goal in this thesis is to investigate how soil bacterial communities respond to spatial structure in their environment. The approach taken tests for patterns in the distributions over all species in an environment. The patterns detected are thus community-wide, and reflect the strength of interactions and similarities between different species as well as their individual responses to the environment. This approach required the use of multivariate statistical techniques. Multivariate hypothesis-testing methods based on permutation tests were used where possible so that the interpretation of results is not a subjective matter.

Microbial community composition was assayed using terminal restriction fragment length polymorphism (T-RFLP) of eubacterial 16S ribosomal sequences amplified by PCR from environmental genomic DNA extracts. This method is not dependent on the growth of the bacteria in the laboratory, which is known to result in

severe biases in the species detected (Felske et al. 1999, Madsen 1996). There are commonly occurring species in soil that have never been successfully isolated in the laboratory, but can be detected via molecular methods (Head et al. 1998, Hugenholtz et al. 1998).

In Chapter 2 of this thesis, several methods of processing T-RFLP data and examining relationships between profiles using multivariate statistical methods are tested. Four sets of T-RFLP profiles are used, representing a wide range in degree of divergence between samples, from a set of soil samples taken in different regions of the United States to a set of samples taken from within one meter of each other in an alfalfa field. Each set contained analytical replicates of the sample profiles. The data processing and statistical methods were tested for their sensitivity to analytical variability present in T-RFLP profiles. The methods found to be most robust are used in the remainder of the chapters, including analysis of Hellinger distance and Jaccard distance between T-RFLP profiles with the multivariate hypothesis-testing method redundancy analysis.

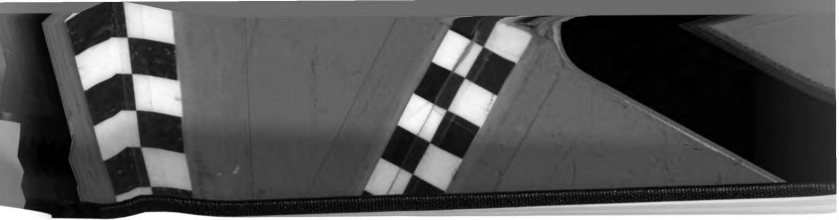
Chapter 3 is an investigation into the possibility that different microbial communities are associated with different soil fractions, which could then be classified as distinct soil habitats. The fractions investigated were hypothesized to contain different communities due to differences in the age and types of organic matter found within them. The fractions included the light and heavy fractions, shoot residue > 2 mm, and the rhizosphere. Communities in all fractions were shown to be different from each other, except for light fraction and shoot residue, which were essentially the same. The rhizosphere is well-accepted as a habitat that has a community distinct from the bulk soil. Detection of the light fraction/shoot residue habitat shows that organization of soil

microbial communities around organic matter is more general than the rhizosphere – bulk soil dichotomy. Differentiation of communities due to cropping system shows that other aspects of the environment critically affect the community present, in addition to the total amount of organic matter present. This is also shown for the relationship between organic matter and total number of bacterial cells.

Hierarchical aggregate structure is currently the dominant model of soil structure and has been shown to be useful in the study of organic matter turnover in soils. In Chapter 4 the hypotheses that aggregates of different sizes and that layers within aggregates contain different communities was tested. A new method of isolating the outer portion of aggregates and its bacterial community was used, resulting in knowledge of the precise location of the sample within the aggregate. Analysis of individual aggregates using a split-plot design was found to be the most satisfactory approach for investigating whether the communities in different aggregate layers were different. Aggregate layers had communities which were only slightly different. Aggregate-to-aggregate variability was large. The effect of aggregate size on eubacterial communities was quite weak. Organization of eubacterial communities due to position within and size of soil aggregates was not as pronounced as organization by organic matter found in Chapter 3. Organization by the particular tertiary structure of the soil (arrangement of aggregates in relation to shoot residue, roots, macropores, etc.) is hypothesized to be more important in the determination of the types of microbial communities present in aggregates.

Spatial organization is a scale-dependent phenomenon. Hierarchical spatial organization is one hypothetical way in which organization can change with scale,

incorporating the concept of levels of organization that operate over different scale domains. Chapter 5 is a test of the hierarchical spatial organization of soil eubacterial communities. Size and location of soil samples are varied, resulting in two datasets measuring different aspects of how spatial structure of the communities changes with scale. These are analyzed and integrated using a generalized multivariate extension of paired-quadrat analysis and semivariance analysis that is called variability-scale analysis. The variability-scale analysis is compared to Mantel methods and spatially-constrained ordination. An approach called the correlation super-matrix is also proposed for examining how species or T-RF covariance structure changes with scale. Soil eubacterial communities within 1.5x2 m plots were found to be organized by three hierarchical levels which are described.



References

- Boerner, R.E.J., A.J. Scherzer, J.A. Brinkman. 1998. Spatial patterns of inorganic N, P availability, and organic C in relation to soil disturbance: a chronosequence analysis. *Applied Soil Ecology* 7:159-177.
- Christensen, B.T. 1996. Carbon in primary and secondary organomineral complexes. In *Structure and Organic Matter Storage in Agricultural Soils*, edited by M. R. Carter and B. A. Stewart. Boca Raton: CRC Press.
- Dobermann, A., P. Goovaerts, T. George. 1995. Sources of soil variation in an acid Ultisol of the Philippines. *Geoderma* 68:173-191.
- Felske, A., A. Wolterink, R.v. Lis, W.M.d. Vos, A.D.L. Akkermans. 1999. Searching for predominant soil bacteria: 16S rDNA cloning versus strain cultivation. *FEMS Microbial Ecology* 30:137-145.
- Head, I.M., J.R. Saunders, R.W. Pickup. 1998. Microbial evolution, diversity, and ecology: a decade of ribosomal RNA analysis of uncultivated microorganisms. *Microbial Ecology* 35:1-21.
- Hugenholtz, P., B.M. Goebel, N.R. Pace. 1998. Impact of culture-independent studies on the emerging phylogenetic view of bacterial diversity. *Journal of Bacteriology* 180:4765-4774.
- Juma, N.G. 1994. A conceptual framework to link carbon and nitrogen cycling to soil structure formation. *Agriculture, Ecosystems and Environment* 51:257-267.
- Madsen, E.L. 1996. A critical analysis of methods for determining the composition and biogeochemical activities of soil microbial communities in situ. In *Soil Biochemistry*, edited by G. Stotzky and J. Bollag. New York: Marcel Dekker.
- Oades, J.M. 1993. The role of biology in the formation, stabilization, and degradation of soil structure. *Geoderma* 56:377-400.
- Parkin, T.B. 1993. Spatial variability of microbial processes in soil - a review. *Journal of Environmental Quality* 22:409-417.
- Robertson, G.P., K.M. Klingensmith, M.J. Klug, E.A. Paul, J.R. Crum, B.G. Ellis. 1997. Soil resources, microbial activity, and primary production across an agricultural ecosystem. *Ecological Applications* 7:158-170.
- Smucker, A.J.M. 1993. Soil environmental modifications of root dynamics and measurement. *Annual Review of Phytopathology* 31:191-216.



Staricka, J.A., R.R. Allmaras, W.W. Nelson. 1991. Spatial variation of crop residue incorporated by tillage. *Soil Science Society of America Journal* 55:1668-1674.

Stoyan, H., H. De-Polli, S. Böhm, G.P. Robertson, E.A. Paul. 2000. Spatial heterogeneity of soil respiration and related properties at the plant scale. *Plant and soil* 222:203-214.

Tisdall, J.M. 1996. Formation of soil aggregates and accumulation of soil organic matter. In *Structure and Organic Matter Storage in Agricultural Soils*, edited by M. R. Carter and B. A. Stewart. Boca Raton: CRC Press.

Young, I.M., K. Ritz. 2000. Tillage, habitat space and function of soil microbes. *Soil & Tillage Research* 53:201-213.

Chapter 2

Methods of T-RFLP Data Analysis for Quantitative Comparison of Microbial Communities

Abstract

Terminal restriction fragment length polymorphism (T-RFLP) is a culture-independent method of obtaining a fingerprint of the composition of a microbial community. T-RFLP profiles of complex eubacterial communities were generated following PCR amplification of the 16S ribosomal gene. Profiles of each sample were replicated so that the relative utility of different methods of statistical analysis, T-RF alignment, and computing the difference (or distance) between profiles could be compared. Four sets of samples were used, representing a wide range in degree of divergence between environmental conditions. These sets of samples included: soil samples collected from three regions of the United States, different soil fractions derived from three agronomic fields at one site, soil samples taken from within one meter of each other within an alfalfa field, and replicate laboratory bioreactors. All methods of analysis could be used to differentiate between samples in the most divergent set, but only a subset were successful on the more similar sets. Ward's method of cluster analysis was more effective at finding major groups within sets of profiles, while the average or UPGMA method of cluster analysis had a slightly reduced error rate in clustering of replicate profiles and was more sensitive to outliers. Analyses based on Euclidean distance between profiles of raw T-RF peak heights did not result in clustering of replicate profiles, while most replicate profiles were grouped together using Euclidean distance between relative peak height profiles or Hellinger distance between profiles. It was found that the multivariate hypothesis-testing technique redundancy analysis was more effective at detecting differences between very similar samples than was cluster analysis. Redundancy analysis using Hellinger distance was more sensitive than using



Euclidean distance between relative peak height profiles (i.e. a lower p-value was obtained in testing the null hypothesis that the profiles of different samples were the same). Analysis of Jaccard distance between profiles, which only takes into account presence/absence of a T-RF, was the most sensitive in redundancy analysis, and equally sensitive in cluster analysis, compared to the other distance metrics, but only if all profiles had cumulative peak heights greater than 10,000 fluorescence units. It was concluded T-RFLP was a very sensitive method of differentiating between microbial communities when the appropriate statistical methods were used.

Introduction

Culture-independent methods of microbial community analysis involve the analysis of signature biochemicals extracted directly from environmental samples. Molecular genetic techniques, utilizing extracted genomic or ribosomal nucleic acids, allow microbial community analysis to be coupled with a comprehensive phylogenetic framework (Amann et al. 1995, Woese 1987). The use of such techniques has shown that methods relying on growth of the organisms *ex situ* reveal a small fraction of the diversity present in soil microbial communities (e.g. Torsvik et al. 1990, Ward et al. 1992). This uncultured diversity includes both species that are closely related to cultured organisms and species that represent virtually uncultured phylogenetic lineages (Head et al. 1998, Hugenholtz et al. 1998, Kuske et al. 1997).

A variety of molecular techniques have been developed for rapidly assaying community structure. Most methods involve the separation of PCR amplicons based on differences in DNA sequence of genes of functional or phylogenetic interest, often the



16S ribosomal RNA gene. These include denaturing gradient gel electrophoresis (DGGE, Muyzer et al. 1993), ribosomal intergenic spacer analysis (RISA, Borneman and Triplett 1997), single strand conformation polymorphism (SSCP, Simon et al. 1993), amplified ribosomal DNA restriction analysis (ARDRA, Massol-Deya et al. 1995), and terminal restriction fragment length polymorphism (T-RFLP, Bruce 1997, Liu et al. 1997). These methods do not reveal diversity per se unless the community is very simple, since a fraction of the species revealed by DNA rehybridization rates or sequence analysis of a clone library can be visualized on a gel (Dunbar et al. 2000, Nakatsu et al. 2000). However, these methods do provide a way to determine the relative abundance of common species present in a sample, free of the constraint that the organisms must be amenable to growth in the laboratory. They are valuable as rapid methods of finding major differences between communities, and testing hypotheses based on a comparison of samples.

T-RFLP has been shown to be effective at discriminating between microbial communities in a wide range of environments and has several advantages over other techniques (Tiedje et al. 1999). T-RFLP involves tagging one end of PCR amplicons through the use of a fluorescent molecule attached to a primer. The amplified product is then cut with a restriction enzyme. Terminal restriction fragments (T-RFs) are separated by electrophoresis and visualized by excitation of the fluor. T-RFLP analysis provides quantitative data about each T-RF detected, including size in base pairs (bp) and intensity of fluorescence (peak height). T-RF sizes can be directly compared to a database of theoretical T-RFs derived from sequence information (e.g. Dunbar et al. 2001, Marsh et

al. 2000). In addition, T-RFLP has been found to detect a greater number of operational taxonomic units compared to DGGE (Marsh et al. 1998, Moeseneder et al. 1999).

T-RFLP profiles have been shown to be relatively stable to variability in PCR conditions (Osborn et al. 2000, Ramakrishnan et al. 2000). Currently the least well-defined technical aspect of T-RFLP, as well as many other methods of microbial community analysis, is the data processing and analysis of profiles. A wide range of methods have been used in the literature. The goal of this study was to find the optimal procedure for use in comparing complex environmental T-RFLP profiles, resulting in the lowest probability of type II errors (not finding differences between profiles when they are actually different). The possibility of alignment of T-RFLP peaks using non-hierarchical K-means cluster analysis was also examined.

The sensitivity of statistical methods to pre-analysis data processing or changes in the statistical procedures is dependent not only on the analytical consistency of replicate profiles, but also on the degree of divergence between profiles in the dataset. Therefore four sets of samples were used, representing a wide range in biological complexity and environmental differentiation. The most divergent set of samples were soil samples collected from three regions of the United States, with differing levels of environmental contamination and disturbance. Representing an intermediate level of divergence, soil samples from one site were divided into chemically and physically distinct fractions. Two sets of samples were characterized by quite low divergence in environmental characteristics: a set of replicate laboratory bioreactors, and a set of soil samples taken from within a 1.5x2 meter area of alfalfa. It is expected that microbial communities will diverge in species composition and relative abundance in accordance with the divergence

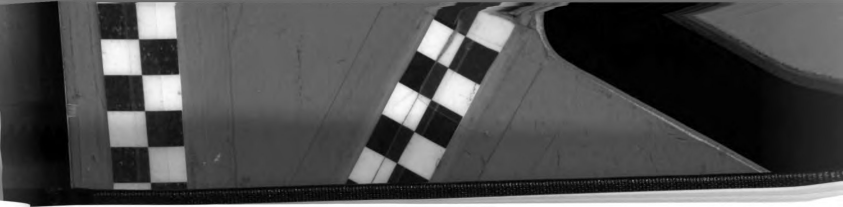


of their habitats. While this is supported by the analyses presented in this paper, the hypothesis and the nature of the differences, with respect to spatial structure in soil, is more fully explored in subsequent chapters.

The threshold for including an electropherogram peak as a valid T-RF is often left unspecified, but has been set to 100 fluorescence units (Franklin et al. 2001, Osborn et al. 2000), 50 units (Kerkhof et al. 2000), and 25 units (Dunbar et al. 2000, Dunbar et al. 2001). Other researchers have limited the number of peaks analyzed by rarefaction (Hedrick et al. 2000) or by including only those comprising greater than one percent of relative abundance in a sample (Derakshani et al. 2001, Lukow et al. 2000), or present in all analytical replicates (Dunbar et al. 2000).

To compare T-RFLP profiles in cases where the community is very simple or the primers targeted a small group of organisms, a simple inspection of electropherograms, tables, or barcharts is normally used (e.g. Bernhard and Field 2000, Bruce 1997, Chin et al. 1999, Flynn et al. 2000, Ramakrishnan et al. 2000). While raw data is sometimes relied upon to compare complex profiles (e.g. Derakshani et al. 2001, Gonzalez et al. 2000, Kerkhof et al. 2000, Leser et al. 2000, Lüdemann et al. 2000), quantitative statistical approaches can also be employed. These have included cluster analysis (Dunbar et al. 2000, Liu et al. 1997, Moeseneder et al. 1999, Scala and Kerkhof 2000), MANOVA (Lukow et al. 2000), and principal components analysis (Clement et al. 1998, Franklin et al. 2001).

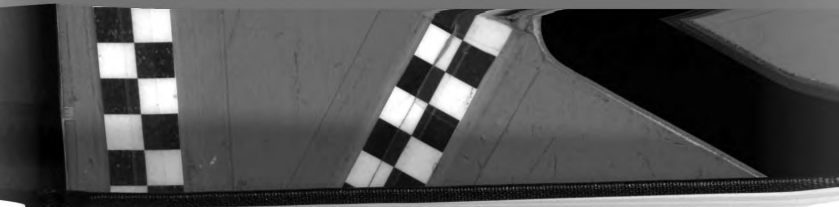
Statistical methods for assessing differences between T-RFLP profiles that were tested in this study include redundancy analysis and the unweighted-pair group method using arithmetic averages (UPGMA) and Ward's method of hierarchical cluster analysis.



Redundancy analysis is equivalent to a principal components analysis of fitted values derived from a multiple linear regression of each variable (or T-RF). To test for differences between experimental groups, the linear regression is performed with a set of dummy variables indicating group identity for each sample (Legendre and Legendre 1998). The proportion of total variance in the original nonfitted dataset that the canonical principal components can account for is then calculated, with an associated pseudo-F statistic. The F statistic is then compared to a distribution generated by random permutation of the data with respect to the dummy variables to obtain a p-value. Calculation of a p-value by random permutation avoids the assumptions of multinormality and restrictions on the number of variables that can be analyzed (Legendre and Anderson 1999).

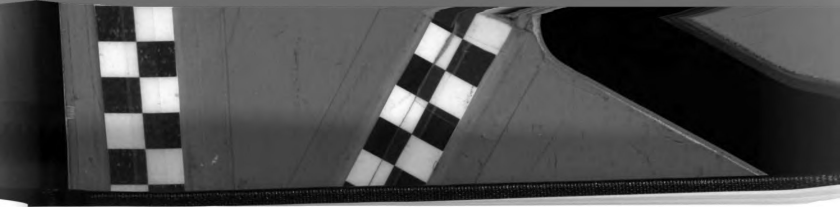
Cluster analysis is essentially a tool for exploratory data analysis, and should not be used as final proof in testing of hypotheses (Krzanowski and Marriott 1994). Cluster analysis summarizes all the variability, and therefore all phenomena affecting the data, within a dendrogram. The difference between the UPGMA and Ward's methods of cluster analysis is in how they calculate the distances between groups of samples (Jobson 1992). The UPGMA method uses the average distance between samples calculated from all possible pairs of samples from the two groups. Ward's method uses the distance between the group centroids, weighted by the total number of samples in both groups. The distance between group centroids is equivalent to the semi-partial r-squared, or the proportion of total variance that would be accounted for by joining the two groups.

The statistical methods discussed above must be based on some measurement of the distance (or difference) between profiles. Cluster analysis or redundancy analysis



using raw peak heights results is based on Euclidean distance. Several kinds of transformations can be made to peak height before statistical analysis, resulting in analyses based on other distance metrics. Use of relative peak height (or height divided by the cumulative peak height of the profile), is a common method (Bruce 1997, Chin et al. 1999, Derakshani et al. 2001, Gonzalez et al. 2000, Lüdemann et al. 2000, Ramakrishnan et al. 2000). Legendre and Gallagher (in press) examined several data transformations that could be performed prior to statistical analysis that result in analyses based on ecologically appropriate distance metrics instead of Euclidean distance. They found that use of relative abundance was an improvement but still unsatisfactory for simulated community composition data. Analyses based on the Hellinger distance can be performed by finding the Euclidean distance between profiles after the Hellinger transformation, which is simply a square root transformation of relative abundance (Legendre and Gallagher in press). Lukow et al. (2000) used this transformation in an attempt to normalize peak height distribution.

Other studies have based comparison of T-RFLP profiles on binary indicators of peak presence (Bernhard and Field 2000, Clement et al. 1998, Flynn et al. 2000, Franklin et al. 2001, Kerkhof et al. 2000, Leser et al. 2000, Liu et al. 1997, Moeseneder et al. 1999, Scala and Kerkhof 2000) or binary indicators after deletion of peaks falling below a height threshold due to standardization (Dunbar et al. 2000, Dunbar et al. 2001). Several similarity coefficients can be used to quantitatively compare profiles using binary indicators; in this study we subtract Jaccard's coefficient from one to transform it into a distance metric, and refer to this as Jaccard's distance. Redundancy analysis using Jaccard distance requires the alternate procedure, distance-based redundancy analysis, to



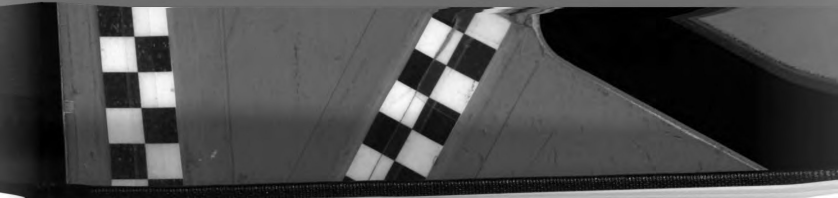
be employed. Any distance metric can be employed in distance-based redundancy analysis because, prior to the redundancy analysis, principal coordinates analysis is used to project the distances between profiles into a Euclidean space (Legendre and Anderson 1999). Distance-based redundancy analysis has the disadvantages of being somewhat more complex and, unlike standard redundancy analysis, the impact of individual variables (or T-RFs) on the results cannot be determined directly.

Methods

Sample collection

Four sets of samples were used in this study:

1. *KBS Soil Fractions.* Soil samples were collected from the agricultural field plots of the Long Term Ecological Research (LTER) site and the Living Field Lab (LFL) at the W.K. Kellogg Biological Station in southwestern Michigan, USA. Three blocks of soil weighing approximately 350 g were excavated and pooled from each plot. Sampling depth was 10 cm. Field treatments included continuous alfalfa, conventionally managed continuous corn, and organically managed first year corn in a corn-corn-soybean-wheat rotation with cover crops. Details of the field treatments are described elsewhere (Jones et al. 1998, <http://lter.kbs.msu.edu/Agronomics>). The soil was fractionated into rhizosphere, shoot residue, and light and heavy fractions from various sizes of soil macroaggregates. Details of the soil fractionation and results from comparison of field treatments and soil fractions are described in chapters 3 and 4.
2. *Bioreactor Samples.* Bioreactor samples were taken from a fluidized-bed reactor with activated carbon as the particulate carrier. The reactor was inoculated with an anaerobic



enrichment culture and fed continuously with ethanol and essential nutrients. Samples were removed, pelleted, and stored at -20°C until needed. Sample collection and T-RFLP analysis as described below was performed by Dr. Terry Marsh, who kindly provided the T-RFLP profiles for statistical analysis.

3. KBS Alfalfa Soil Samples. A ten g soil sample was collected from each of five locations within a 1.5 x 2 m plot within an alfalfa field at the KBS LTER site. Samples were collected from the layer of soil 2 to 4 cm deep. These samples were part of a larger study of the spatial structure of soil microbial communities described in chapter 5.

4. Multi-Region Soil Samples. Soils were collected from Sault Saint Marie, MI, Milan, TN, and Hawthorne NV. Approximately 500 grams of soil were removed from the top 5 centimeters of soil, homogenized, and aliquoted to 100 ml specimen containers. Samples were stored at -20°C until needed. Sample collection and T-RFLP analysis as described below was performed by Dr. Terry Marsh, who kindly provided the T-RFLP profiles for statistical analysis.

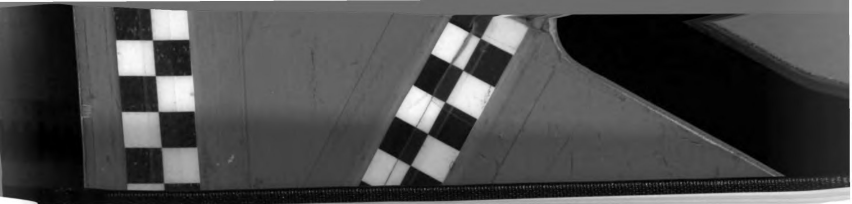
T-RFLP

Mixed community DNA was extracted from the KBS LFL and LTER soil fractions (0.3 g) and alfalfa soil samples (10 g) using the standard or Large-Scale Ultraclean Soil DNA extraction kit, respectively, following the manufacturers instructions (Mo Bio Laboratories, Solana Beach, CA). Genomic DNA was found to be of sufficient purity to be used directly in PCR reactions. PCR was performed using a standard reaction mixture of 160 μ M of each deoxynucleoside triphosphate, 3 mM $MgCl_2$, 0.05 U/ μ L Taq DNA polymerase and the appropriate volume of accompanying 10X PCR buffer (Gibco BRL, Gaithersburg, MD), and 0.2 μ g/mL bovine serum albumin



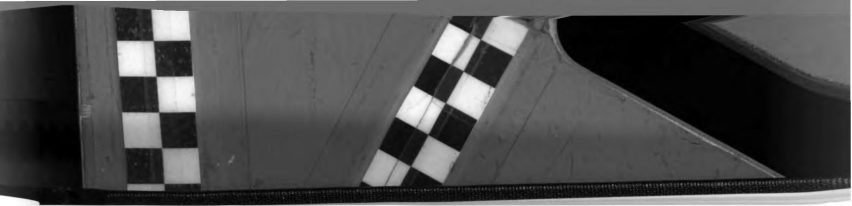
(Boehringer Mannheim Biochemicals, Indianapolis, IN). Primers used were the general eubacterial primer 8-27F (AGAGTTTGATCCTGGCTCAG, *E. coli* numbering, Amann et al. 1995, Integrated DNA Technologies, Coralville, IA) and the universal primer 1392-1406R (ACGGGCGGTGTGTACA) amplifying the 16S ribosomal gene. PCR reactions were optimized for each sample of genomic DNA using a master mix with primer concentrations of 0.4 μ M. PCR was performed in a Perkin-Elmer 9600 thermocycler using an initial denaturation step of 95°C followed by 22 cycles of the following program: denaturation at 94°C for 30 sec., primer annealing at 55°C for 30 sec., and extension at 72°C for 30 sec. A modified hot start procedure was used where PCR tubes were not placed in the thermocycler until the block temperature had reached 80°C. A final extension at 72°C for 7 min. was performed after the programmed number of cycles was complete. PCR product concentration and specificity was checked by electrophoresis on a 1% agarose gel, followed by staining with ethidium bromide. Optimizations were performed by adjusting the amount of genomic DNA extract used (0.4 to 2 μ L) in order to obtain a strong band without visible non-specific product.

PCR reactions (50-75 μ L) were performed in triplicate for each sample using the optimal conditions found previously. These reactions were performed using the same PCR master mix and program described above except that the forward primer was 0.6 μ M hexachlorofluorescein (hex)-labeled 8-27F (Integrated DNA Technologies). PCR replicates were then pooled and purified using the Promega PCR Preps Wizard Kit as directed by the supplier, except that elution was performed with 19 μ L of sterile water heated to 55-65°C. Five μ L of purified PCR product was mixed with 5 μ L of restriction enzyme master mix containing 1.5 U/ μ L of restriction enzyme and one μ L of the



accompanying reaction buffer (Gibco). Restriction reactions were incubated for three hours at 37°C, followed by 16 min. at 65°C to denature the restriction enzyme. Three μL of the restricted PCR product was mixed with one μL of 2500 TAMRA size standard (Applied Biosystems Instruments, Foster City, CA). DNA fragments were separated by size by electrophoresis at 1800 V for 14 hours on an ABI 373 automated DNA sequencer at Michigan State University's DNA Sequencing Facility. The 5' terminal fragments were visualized by excitation of the hex molecule attached to the forward primer. The gel image was captured and analyzed using Genescan Analysis Software 3.1. A peak height threshold of 50 fluorescence units was used in the initial analysis of the electropherogram. Negative controls (no genomic DNA) were conducted with every PCR and run on several Genescan gels. Contamination in PCR reactions was not detected. Small peaks occasionally appeared in negative control lanes on Genescan gels, but the cumulative peak height was always below 1000 units.

Amplification of bioreactor and multi-region soil samples were performed as described above with the following modifications. 16S rRNA genes were amplified from community DNAs using primers 8-27F and 1492R (5'-GGTTACCTTGTTACGACTT-3'). The PCR reaction mixture (100 μL) contained 1X PCR buffer, 0.2 mM dNTPs, 1.5 mM MgCl_2 , 0.4 μM of 8-27F primer, 0.2 μM of 1492R primer, 0.1 μg BSA/ μL , 0.2 ng template DNA/ μL , 0.05 U Taq polymerase/ μL (PE Amplitaq). Thermocycling was performed in a GeneAmp 2400 PCR System thermal cycler (Perkin Elmer, Norwalk, CT) at 94°C for 5 min followed by 30 cycles of 94°C for 50 sec, 55°C for 50 sec, 72°C for 1 min 30 sec, and a final extension step at 72°C for 7 min. Amplifications that checked positively on a 1.2% agarose gel were cleaned and concentrated using a Microcon YM-




100 (Millipore Corp. Bedford, MA). DNA concentrations were determined spectrophotometrically. Purified PCR products (600 ng/reaction) were digested with HhaI, MspI, or RsaI restriction endonuclease at 37°C for 3-4 hrs.

Replication experiments

For the set of KBS soil fraction samples, 32 samples were run on two Genescan gels. Several other samples were also run once. For the remaining sets of samples, two sets of PCR reactions were performed and pooled separately for each sample. Each of these were then restricted and run twice on the same Genescan gel, for a total of four replicate runs per sample.

Profile alignment and statistical analyses

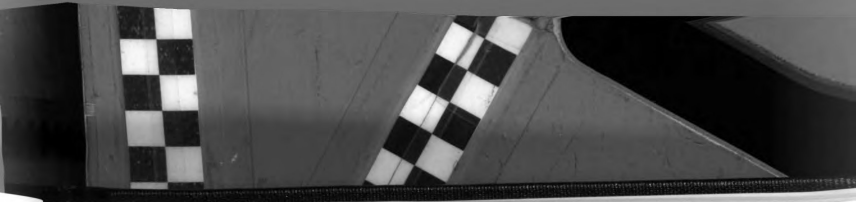
Peak (or T-RF) heights in fluorescence units and sizes in base pairs (bp) were transferred to an Excel file. T-RFs were aligned between samples either by inspection of the electropherogram and manual grouping of peaks into categories, or by use of a custom algorithm written in SAS (Version 8 IML and Stat components) based on K-means cluster analysis of the T-RF sizes. The algorithm also separated T-RFs when multiple T-RFs from the same sample were clustered together. In this event, a new cluster was generated and any T-RFs from samples with two or more T-RFs present in the original cluster were placed into the new cluster. The process was then repeated for the new cluster. The algorithm also allowed a maximum range in bp to be set for all clusters. Alignments were generated using this algorithm with maximum ranges of from 1 to 10 bp. Computer alignment was only tested on the set of KBS soil fraction samples. Alignment of peaks by manual inspection was done in Excel and was based primarily on the size of peaks in bp. The pattern of peaks was also used to determine their alignment



when groups of overlapping peaks were found between samples. The identities of samples were concealed during manual alignment.

Hierarchical cluster analysis was performed on aligned T-RFLP profiles using SAS Version 8. Clustering was performed using the unweighted-pair group method using arithmetic averages (UPGMA) and Ward's method (SAS Institute Inc., Jobson 1992). Several methods of data processing were compared. The baseline for including a peak was set to 50, 100, or 200 fluorescence units. Rarefaction was also used as a method of determining which small peaks should be included in the analysis, following the procedure of Hedrick et al. (2000). Clustering was then based on Euclidean distance between raw or relative peak height, Hellinger distance, or one minus Jaccard's coefficient (referred to as Jaccard distance). Hellinger distance is equivalent to the Euclidean distance between profiles after square-root transformation of relative peak heights (Legendre and Gallagher in press). Jaccard's coefficient is based on binary variables of peak presence and is equal to the ratio of the number of T-RFs present in both profiles being compared to the total number of T-RFs present in either profile. Clustering was performed both with and without samples whose peak heights summed to greater than 10,000 fluorescence units. The cophenetic correlation was calculated for dendrograms using an algorithm written in SAS IML.

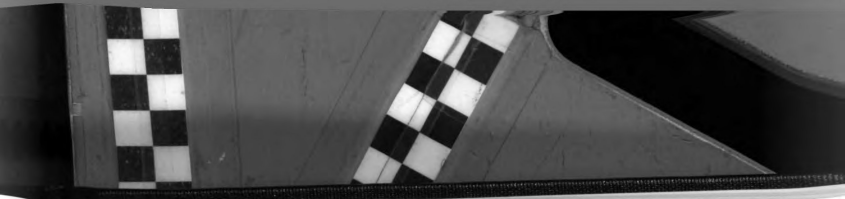
Statistical significance of the difference between samples, and as a corollary the similarity of replicate profiles, was tested using redundancy analysis with the computer software Canoco (Microcomputer Power, Ithaca, NY). This analysis compares a pseudo-F statistic, calculated from the proportion of the total variance explained by sample identity, to the values of F of 9999 random permutations of the sample identities of the



profiles (Legendre and Legendre 1998). Distance-based redundancy analysis was used to determine significance using Jaccard distance (Legendre and Anderson 1999). The Jaccard distance matrix and its principal coordinates were calculated using an algorithm written in SAS IML, adapted from original code provided by Dr. Carl Ramm at Michigan State University.

Results

An example of several T-RFLP electropherograms is shown in Figure 1. Occasionally the baseline fluorescence of the T-RFLP electropherograms was elevated (i.e. fluorescence did not reach zero between widely-spaced peaks). If the value of the baseline could be ascertained, the baseline was subtracted from peak height in that region. If the baseline varied inconsistently the sample was re-run. Evaluation of clustering errors was performed using dendrograms showing the hierarchical relationships between T-RFLP profiles as found by the clustering procedure (see Figures 2-4 for examples). The number of clusters chosen to be examined was equal to the number required to explain 50 percent of the variance in the entire dataset. An error was counted when two replicate T-RFLP profiles (i.e. profiles derived from the same DNA extract) were clustered into different groups. Errors in the dendrograms in Figures 2-4 occur where lines joining analytical replicates cross group divisions. Group colors were exchanged for the profiles where errors occur in an attempt to allow the degree of error in the dendrogram to be assessed intuitively.



1. KBS LTER soil fraction samples

In the first set of samples there were 32 replicated profiles (see Table 1 and Figures 2-4). Clustering using raw, unstandardized peak height consistently resulted in the greatest number of errors. Use of relative peak height (peak height divided by the cumulative peak height of the given sample) resulted in the fewest number of errors. Clustering using binary variables (Jaccard distance) had an error rate higher than for relative peak height, but still much lower than for raw peak heights (see Table 1). Deleting peaks with heights less than 100 fluorescence units, less than one percent of the cumulative peak height for a given sample, or by rarefaction did not result in improvement of clustering on any variable, compared to use of all peaks with heights greater than 50. Deleting all peaks with heights less than 200 increased the number of errors (see Table 1). Use of the Hellinger transformation resulted in an increase of between zero and two errors over the analogous dendrogram based on relative peak height. UPGMA clustering normally contained one to two fewer errors than clustering by Ward's method, and also resulted in a higher cophenetic correlation (or correlation between elements of the original distance matrix and a distance matrix constructed from the results of the cluster analysis). However, clustering by Ward's method required fewer groups to explain 50 percent of the variance in the dataset.

After alignment of T-RFLP profiles by the computer algorithm described in the Methods, the minimum number of errors present in a dendrogram equaled four (using Ward's method; see Table 2). The computer alignment resulting in this dendrogram had a maximum range of 4 bp and a mean range of 1.3 bp for groups of peaks (i.e. peaks in different samples considered to represent the same T-RF). The manual alignment had a

maximum range of 4.4 bp and a mean range of 1.4 bp for groups of peaks. Deletion of samples with cumulative peak height less than 10,000 fluorescence units resulted in 22 replicated profiles (see Table 3; the minimum of the full dataset was 4650). Using the manual alignment of profiles, the number of errors was zero or one for all combinations of clustering methods and distance metrics (raw peak height was not analyzed). The number of errors resulting from Ward's cluster analysis of the computer-aligned profiles was found to be fewest using a maximum range of 2 bp for groups of peaks (mean = 0.9 bp). However, the number of errors was still higher than that for manually-aligned profiles.

2. Bioreactor samples

The various methods of data processing and analysis did not greatly affect the error rate of clustering of bioreactor replicates, and no method appeared to perform the best (see Table 4). This was consistent for *Rsa*I, *Msp*I, and *Hha*I digests analyzed separately, as well as for analysis of all three digests simultaneously. Since there were four replicate profiles per sample, the error rate of nine out of 18 potential errors, which is typical for this set of samples, could be generated by a variety of dendrograms. These could include 1. the clustering of three replicates of each sample into distinct groups, with the fourth of each sample an outlier, or 2. the perfect clustering of replicates of one sample, a second sample being split evenly between two groups, and a third with no replicates in the same group.

The significance of the differences between sample profiles was tested using redundancy analysis of standardized peak heights, Hellinger-transformed peak heights, and principal coordinates of Jaccard distance. The sample identities were found to



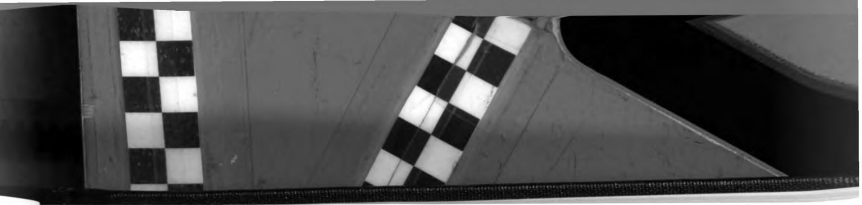
explain a significant amount of variance in the dataset for the RsaI and HhaI profiles analyzed separately and for the RsaI, MspI, and HhaI profiles analyzed together (see Table 5). Sample identities were significant for the MspI profiles only for Jaccard distance. P-values for all digests were lowest for analysis of Jaccard distance, and highest for standardized peak heights, except for the RsaI profile where analysis of Jaccard distance had the highest p-value. The RsaI dataset included several profiles where the cumulative peak height was less than 10,000 fluorescence units. Plots of the first two canonical principal components generated by the redundancy analyses are shown in Figure 5.

3. Alfalfa soil samples

While clustering Jaccard distance resulted in the lowest number of errors for the alfalfa soil samples, all dendrograms had error rates that were quite high (see Table 6). The errors could again be generated by a variety of dendrogram topologies since there were four replicates per sample. Redundancy analysis detected significant differences between community profiles when analyzing Hellinger-transformed variables and principal coordinates of Jaccard distance, but not relative peak height variables.

4. Multi-Regional Soil Samples

No errors were observed in cluster analysis of replicate profiles from the multi-regional set of soil samples using any method of processing and analysis (data not shown). This result was consistent for RsaI, MspI, and HhaI digests. In general, two groups were required to explain 50 percent of the variance in the dataset. This grouping divided all replicate profiles of one sample from the eight replicate profiles of the



remaining two samples. Three groups explained 75 to 85 percent of the total variance in the dataset, with each group being made up by all of one sample's replicate profiles.

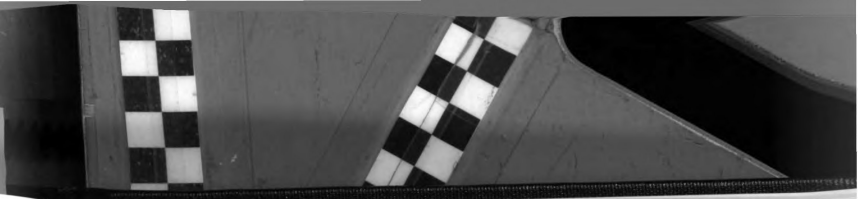
Comparison of Statistical Methods

The number of errors found in cluster dendrograms was dependent on the set of samples being analyzed. The error rate was lower using UPGMA compared to Ward's method if some profiles had cumulative peak height less than 10,000 fluorescence units (see Table 1). However, the two methods had essentially equivalent error rates if all samples had cumulative peak heights greater than 10,000 (see Table 3). UPGMA clustering was more true to the original distances between samples, as indicated by higher cophenetic correlation (Jobson 1992). This also leads, however, to an increase in the number of groups required to explain 50 percent of the total variance in the datasets, and a greater influence of outliers on dendrogram topology (see Figures 3 and 4).

Redundancy analysis was able to detect significant differences between samples, and as a corollary significant similarities between analytical replicates, for all datasets tested. The cause of significant differences can be assessed using plots of canonical principal components (see Figure 5), although it should be noted that these plots are biased to show group differences, compared to standard principal components analysis, due to the nature of redundancy analysis.

Profile Alignment and Peak Height Baseline

Alignment of profiles was shown to be best performed manually, aided by patterns within the peak positions as well as the putative fragment sizes calculated using the internal lane standard. Deletion of the smallest peaks using any of a variety of algorithms was shown to have relatively little effect on the error rate of analyses, except

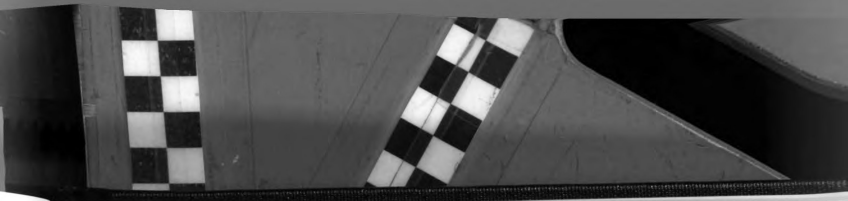


that an increase in the number of errors was observed where larger peaks started to be deleted as well (i.e. peaks with heights between 100 and 200 fluorescence units).

Comparison of Community Distance Metrics

Cluster analyses based on Euclidean distance calculated from raw peak heights resulted in an unacceptable number of errors for all sets of samples except the most divergent (for example, compare figures 2 and 3). The Hellinger transformation had inconsistent results on the number of clustering errors compared to clustering based on relative peak height, sometimes decreasing and sometimes increasing the error rate. The Hellinger transformation did consistently result in a greater number of groups being required to account for 50 percent of the variance in the dataset, although other changes in the topologies of the dendrograms were minor. However, the Hellinger transformation also consistently resulted in a lower p-value when redundancy analysis was performed to test the significance of the differences between samples. This reduction in p-value was dramatic for the set of closely-spaced alfalfa soil samples. Other data transformations examined by Legendre and Gallagher (in press) were either discarded in preliminary analyses (i.e. the chord distance) or because of the heavy weighting of rare T-RFs (e.g. the chi-square distance). The latter property makes a distance metric inappropriate for T-RFLP data since rarity of a T-RF might not reflect rarity of the associated genotype, but simply sampling variability in detection of less-abundant (i.e. low population size or mean peak heights), but still common, species (see Legendre and Gallagher in press, and Legendre and Legendre 1998 for discussions on weighting of rare species).

Use of Jaccard distance when some profiles had low cumulative peak height (<10,000 fluorescence units) resulted in a large number of errors in cluster analysis and a

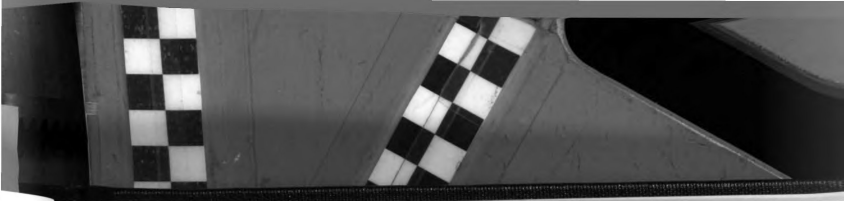


higher p-value in redundancy analysis. When all profiles analyzed had cumulative peak height >10,000, clustering using Jaccard distance was as good as relative or Hellinger-transformed peak height, and redundancy analysis was more sensitive (with a lower p-value).

Discussion

A primary weakness in many microbial community analysis studies is the lack of quantitative statistical comparison of community profiles. This may be appropriate if the methodology used only allows for qualitative comparisons, but in such cases conclusions may be affected by subjective interpretation. This study is designed to aid in the choice of methods to process and analyze quantitative T-RFLP data. The results may also be useful for other methods of community analysis such as DGGE or RISA. The results are based on analytical replicates with the goal of finding a method of data analysis such that further analyses will not need to be replicated at the analytical level. Analytical replication may be prohibitive in molecular work if there are a large number of samples due to the relatively high cost and time involved. Analysis of treatment or field replicates is always a necessity.

The results of the analyses are different, in absolute terms, for each of the sets of samples examined because the sets represent a wide range in degree of sample divergence. The trends in sensitivity of data analysis methods are consistent across this gradient and resulted in some methods being clearly preferable. As expected, the multi-regional set of soil samples resulted in the most divergent set of T-RFLP profiles, and the bioreactor and alfalfa soil samples resulted in the least divergent T-RFLP profiles. This

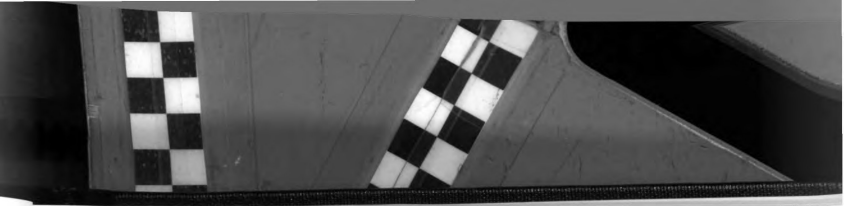


gradient was useful in showing the relative sensitivities of the various methods to the analytical variability present in T-RFLP profiles.

Ward's method of hierarchical cluster analysis seems to sacrifice some precision in clustering for the ability to more efficiently identify major groups within T-RFLP datasets. This efficiency results in Ward's analyses accounting for a larger proportion of the total variance with fewer groups compared to UPGMA. Also the scale of the dendrogram plot is more heterogeneous across different levels in the hierarchy (see Figures 3 and 4), resulting in the ability to more easily choose the number of major groups in the dendrogram. Dendrograms constructed from UPGMA analyses could be plotted using the semi-partial r -squared scale (and perhaps they should be when looking for natural groups), but inversions will be present. The UPGMA method may be considered a more conservative method of finding natural groups and outliers within sets of T-RFLP profiles, which is in agreement with comments by Jobson (1992).

The problems associated with choosing the number of important groups that are present when comparing dendrograms with differing scales were avoided in the current study by examining whatever number of groups was required to account for 50 percent of the total variance. This was done in order to compare error rates of dendrograms on an equal basis, but is not recommended for applications of cluster analysis other than assessing error rates since the 50 percent level may not correspond to a biologically meaningful number of groups.

Redundancy analysis and cluster analysis are fundamentally different types of methods, and are hence not directly comparable. The goal of redundancy analysis is not to summarize all variability within the dataset, but to explicitly test whether that

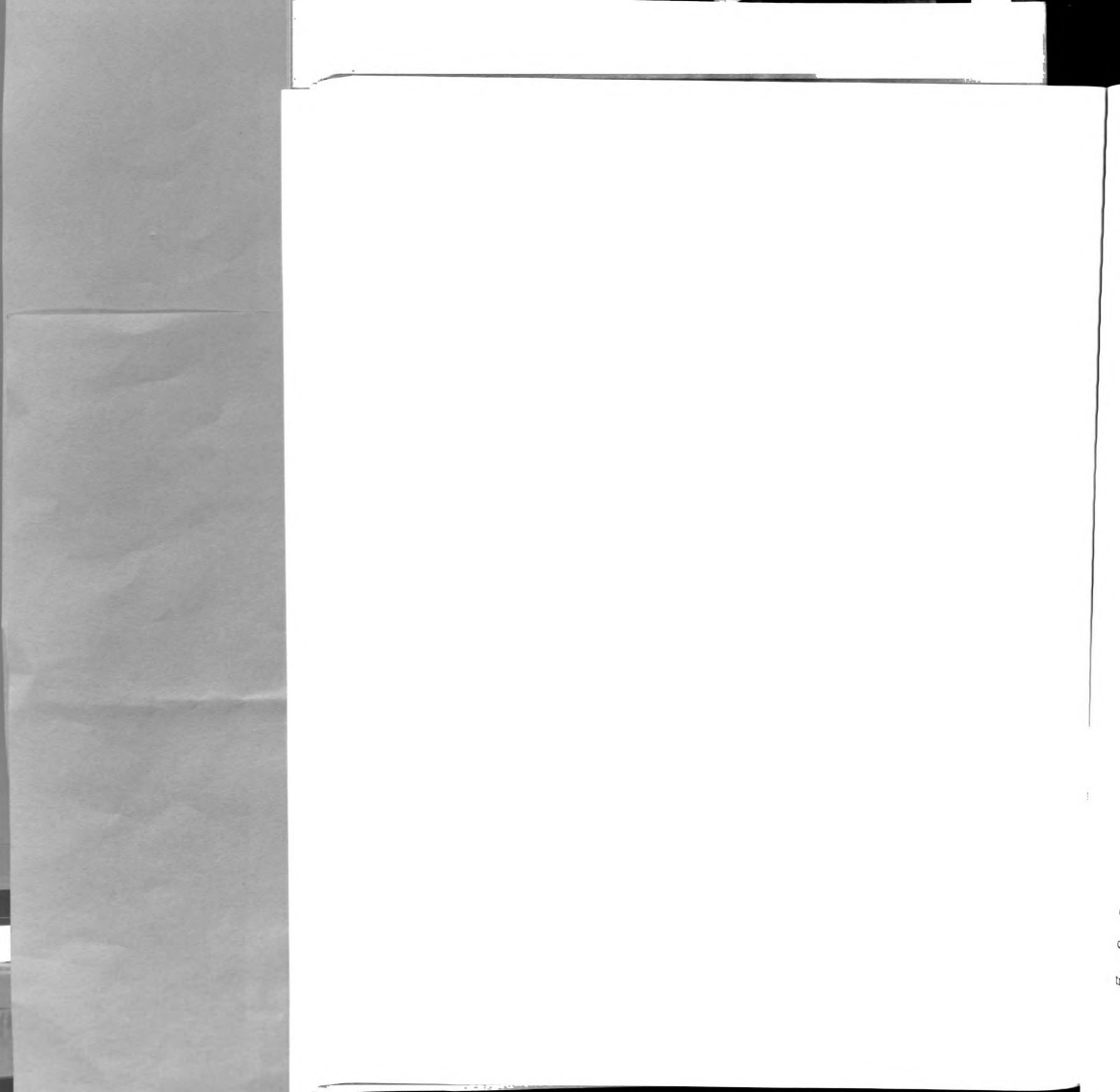


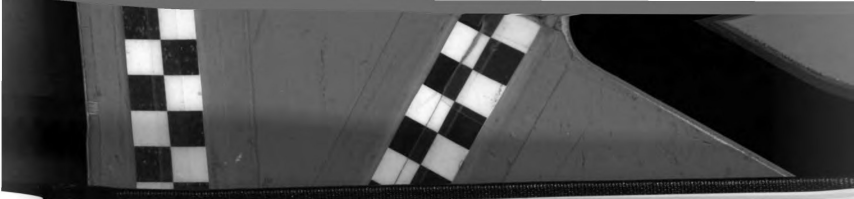
variability that can be attributed to the differences between experimental groups is significant. In that case, it would be expected that redundancy analysis detected significant differences between samples in the less divergent sample sets, while cluster analysis often failed to show them, because these differences accounted for only 25-40% of the variance in the datasets.

The failure of our T-RFLP profile alignment algorithm compared to alignment by hand was a disappointment. Future work should focus on development of computer algorithms which can take these patterns into account, since at this point manual alignment of profiles represents the least standardized or objective step of quantitative T-RFLP analysis.

The fact that deletion of the smallest peaks had relatively little effect on dendrogram error rate is somewhat surprising because small peaks tend to be the "noisiest", with inconsistent presence in replicates of a single sample. An effect of deletion of small peaks was particularly expected to occur for the analysis of Jaccard distance since, in that case, small peaks are given equal weight to large peaks. However, Jaccard distance does weight "common" (or frequently-present) T-RFs more than "rare" (infrequently-present) T-RFs, and noisy peaks are by definition rare. These results imply there were a number of T-RFs with generally low peak heights that were important for distinguishing between samples.

Problems associated with Euclidean distance between profiles (raw peak height) are likely associated with variability in the amount of DNA loaded into each gel lane. This can result in variability in absolute peak height and presence of some of the smaller peaks. Analysis of relative peak height led, in general, to optimal performance in cluster





analysis (equal to Hellinger distance), but not redundancy analysis. Use of the Hellinger distance for T-RFLP data is superior based both on the present empirical results and the theoretical considerations previously discussed (Legendre and Galagher in press). Jaccard distance performed well in cluster analysis and superior to other distance metrics in redundancy analysis only when DNA load was uniformly high. The difference in performance with changes in cumulative peak height may be due to increased stability of small peaks when DNA load is high.

Conclusions

T-RFLP has been shown to be a valuable method of assaying microbial community structure. Given statistical analyses that were sensitive enough (low probabilities of type II error), it was possible to use T-RFLP to reject the null hypotheses that communities were identical in replicate bioreactors, or in soil samples collected within two meters of each other. With this level of sensitivity, the utility of T-RFLP in quantitative comparison of microbial communities is obvious. If the experimental design is such that appropriate hypotheses can be formulated, redundancy analysis of Hellinger-transformed peak height and/or distance-based redundancy analysis of Jaccard distance (if all profiles have a cumulative peak height greater than 10,000) are recommended as the most sensitive methods to distinguish between groups of profiles. If the goal of analysis is exploratory data analysis, clustering using both Ward's method, to find natural groups, and UPGMA, to identify potential outliers, is recommended. The validity of clustering results are basically equivalent using relative peak height, Hellinger-transformed peak height, or Jaccard distance (if all samples have cumulative peak height

greater than 10,000). This study was not an exhaustive examination of all multivariate statistical methods that could be used for T-RFLP data. Future work could examine the potential of other distance metrics and other methods of data analysis, such as correspondence analysis, principal coordinates plots, and use of artificial neural networks. The use of quantitative statistical analysis coupled with molecular methods creates new opportunities for addressing applied and ecological problems in microbial community analysis.

greater than 10,000
statistical methods
potential of this
correspondence
networks. This
creates new
community an

References

- Amann, R.I., W. Ludwig, K. Schleifer. 1995. Phylogenetic identification and in situ detection of individual microbial cells without cultivation. *Microbiological Reviews* 59:143-169.
- Bernhard, A.E., K.G. Field. 2000. Identification of nonpoint sources of fecal pollution in coastal waters by using host-specific 16S ribosomal DNA genetic markers from fecal anaerobes. *Applied and Environmental Microbiology* 66:1587-1594.
- Borneman, J., E.W. Triplett. 1997. Molecular microbial diversity in soils from Eastern Amazonia: evidence for unusual microorganisms and microbial population shifts associated with deforestation. *Applied and Environmental Microbiology* 63:2647-2653.
- Bruce, K.D. 1997. Analysis of *mer* gene subclasses within bacterial communities in soils and sediments resolved by fluorescent-PCR-restriction fragment length polymorphism profiling. *Applied and Environmental Microbiology* 63:4914-4919.
- Chin, K., T. Lukow, R. Conrad. 1999. Effect of temperature on structure and function of the methanogenic archaeal community in an anoxic rice field soil. *Applied and Environmental Microbiology* 65:2341-2349.
- Clement, B.G., L.E. Kehl, K.L. DeBord, C.L. Kitts. 1998. Terminal restriction fragment patterns (TRFPs), a rapid, PCR-based method for the comparison of complex bacterial communities. *Journal of Microbiological Methods* 31:135-142.
- Derakshani, M., T. Lukow, W. Liesack. 2001. Novel bacterial lineages at the (sub)division level as detected by signature nucleotide-targeted recovery of 16S rRNA genes from bulk soil and rice roots of flooded rice microcosms. *Applied and Environmental Microbiology* 67:623-631.
- Dunbar, J., L.O. Ticknor, C.R. Kuske. 2000. Assessment of microbial diversity in four southwestern United States soils by 16S rRNA gene terminal restriction fragment analysis. *Applied and Environmental Microbiology* 66:2943-2950.
- Dunbar, J., L.O. Ticknor, C.R. Kuske. 2001. Phylogenetic specificity and reproducibility and new method for analysis of terminal restriction fragment profiles of 16S rRNA genes from bacterial communities. *Applied and Environmental Microbiology* 67:190-197.
- Flynn, S.J., F.E. Löffler, J.M. Tiedje. 2000. Microbial community changes associated with a shift from reductive dechlorination of PCE to reductive dechlorination of *cis*-DCE and VC. *Environmental Science and Technology* 34:1056-1061.
- Franklin, F.B., J.L. Garland, C.H. Bolster, A.L. Mills. 2001. Impact of dilution of microbial community structure and functional potential: comparison of numerical

simulations and batch culture experiments. *Applied and Environmental Microbiology* 67:702-712.

Gonzalez, J.M., R. Simo, R. Massana, J.S. Covert, E.O. Casamayor, C. Pedros-Alio, M.A. Moran. 2000. Bacterial community structure associated with a dimethylsulfoniopropionate-producing North Atlantic algal bloom. *Applied and Environmental Microbiology* 66:4237-4246.

Head, I.M., J.R. Saunders, R.W. Pickup. 1998. Microbial evolution, diversity, and ecology: a decade of ribosomal RNA analysis of uncultivated microorganisms. *Microbial Ecology* 35:1-21.

Hedrick, D.B., A. Peacock, J.R. Stephen, S.J. Macnaughton, J. Brüggman, D.C. White. 2000. Measuring soil microbial community diversity using polar lipid fatty acid and denaturing gradient gel electrophoresis data. *Journal of Microbiological Methods* 41:235-248.

Hugenholtz, P., B.M. Goebel, N.R. Pace. 1998. Impact of culture-independent studies on the emerging phylogenetic view of bacterial diversity. *Journal of Bacteriology* 180:4765-4774.

Jobson, J.D. 1992. *Applied Multivariate Data Analysis Volume II: Categorical and Multivariate Methods*. New York: Springer-Verlag.

Jones, M.E., R.R. Harwood, N.C. Dehne, J. Smeenk, E. Parker. 1998. Enhancing soil nitrogen mineralization and corn yield with overseeded cover crops. *Soil and Water Conservation* 53:245-249.

Kerkhof, L., M. Santoro, J. Garland. 2000. Response of soybean rhizosphere communities to human hygiene water addition as determined by community level physiological profiling (CLPP) and terminal restriction fragment length polymorphism (T-RFLP) analysis. *FEMS Microbiology Letters* 184:95-101.

Krzanowski, W.J., F.H.C. Marriott. 1994. *Multivariate Analysis Part 2: Classification, Covariance Structures and Repeated Measurements*. London: Arnold.

Kuske, C.R., S.M. Barns, J.D. Busch. 1997. Diverse uncultivated bacterial groups from soils of the arid southwestern United States that are present in many geographic regions. *Applied and Environmental Microbiology* 63:3614-3621.

Legendre, P., M.J. Anderson. 1999. Distance-based redundancy analysis: testing multispecies responses in multifactorial ecological experiments. *Ecological Monographs* 69:1-24.

Legendre, P., E.D. Gallagher. in press. Ecologically meaningful transformations for ordination of species data. *Oecologia*.

1987

1987

1987

1987

1987

1987

1987

1987

1987

1987

1987

1987

Legendre, P., L. Legendre. 1998. *Numerical Ecology*. 2 ed. Amsterdam: Elsevier.

Leser, T.D., R.H. Lindecrona, T.K. Jensen, B.B. Jensen, K. Moller. 2000. Changes in bacterial community structure in the colon of pigs fed different experimental diets and after infection with *Brachyspira hyodysenteriae*. *Applied and Environmental Microbiology* 66:3290-3296.

Liu, W.-T., T.L. Marsh, H. Cheng, L.J. Forney. 1997. Characterization of microbial diversity by determining terminal restriction fragment length polymorphisms of genes encoding 1S rRNA. *Applied and Environmental Microbiology* 63:4516-4522.

Lüdemann, H., I. Arth, W. Liesack. 2000. Spatial changes in the bacterial community structure along a vertical oxygen gradient in flooded paddy soil cores. *Applied and Environmental Microbiology* 66:754-762.

Lukow, T., P.F. Dunfield, W. Liesack. 2000. Use of the T-RFLP technique to assess spatial and temporal changes in the bacterial community structure within an agricultural soil planted with transgenic and non-transgenic potato plants. *FEMS Microbiology Ecology* 32:241-247.

Marsh, T.L., W. Liu, L.J. Forney, H. Cheng. 1998. Beginning a molecular analysis of eukaryal community in activated sludge. *Water Science and Technology* 37:455-460.

Marsh, T.L., P. Saxman, J. Cole, J. Tiedje. 2000. Terminal restriction fragment length polymorphism analysis program, a web-based research tool for microbial community analysis. *Applied and Environmental Microbiology* 66:3616-3620.

Massol-Deya, A.A., D.A. Odelson, R.F. Hickey, J.M. Tiedje. 1995. Bacterial community fingerprinting of amplified 16S and 16-23S ribosomal DNA gene sequences and restriction endonuclease analysis (ARDRA). In *Molecular Microbial Ecology Manual*, edited by A. D. L. Akkermans, J. D. V. Elsas and F. J. D. Bruin. Dordrecht: Kluwer Academic Publishers.

Moeseneder, M.M., J.M. Arrieta, G. Muyzer, C. Winter, G.J. Herndl. 1999. Optimization of terminal-restriction fragment length polymorphism analysis for complex marine bacterioplankton communities and comparison with denaturing gradient gel electrophoresis. *Applied and Environmental Microbiology* 65:3518-3525.

Muyzer, G.A., E.C.d. Waal, A.G. Uitterlinden. 1993. Profiling of complex microbial populations by denaturing gradient gel electrophoresis analysis of polymerase chain reaction-amplified genes coding for 16S rRNA. *Applied and Environmental Microbiology* 59:695-700.

- Nakatsu, C.H., V. Torsvik, L. Øvreås. 2000. Soil community analysis using DGGE of 16S rDNA polymerase chain reaction products. *Soil Science Society of America Journal* 64:1382-1388.
- Osborn, A.M., E.R.B. Moore, K.N. Timmis. 2000. An evaluation of terminal-restriction fragment length polymorphism (T-RFLP) analysis for the study of microbial structure and dynamics. *Environmental Microbiology* 2:39-50.
- Ramakrishnan, B., T. Lueders, R. Conrad, M. Friedrich. 2000. Effect of soil aggregate size on methanogenesis and archaeal community structure in anoxic rice field soil. *FEMS Microbiology Ecology* 32:261-270.
- Scala, D.J., L.J. Kerkhof. 2000. Horizontal heterogeneity of denitrifying bacterial communities in marine sediments by terminal restriction fragment length polymorphism analysis. *Applied and Environmental Microbiology* 66:1980-1986.
- Simon, L., R.C. Lévesque, M. Lalonde. 1993. Identification of endomycorrhizal fungi colonizing roots by fluorescent single-strand conformation polymorphism-polymerase chain reaction. *Applied and Environmental Microbiology* 59:4211-4215.
- Tiedje, J.M., S. Asuming-Brempong, K. Nüsslein, T.L. Marsh, S.J. Flynn. 1999. Opening the black box of soil microbial diversity. *Applied Soil Ecology* 13:109-122.
- Torsvik, V., J. Goksoyr, F.L. Daae. 1990. High diversity of DNA of soil bacteria. *Applied and Environmental Microbiology* 56:782-787.
- Ward, D.M., M.M. Bateson, R. Weller, A.L. Ruff-Roberts. 1992. Ribosomal RNA analysis of microorganisms as they occur in nature. In *Advances in Microbial Ecology*, edited by K. C. Marshall. New York: Plenum Press.
- Woese, C.R. 1987. Bacterial evolution. *Microbiological Reviews* 51:221-271.

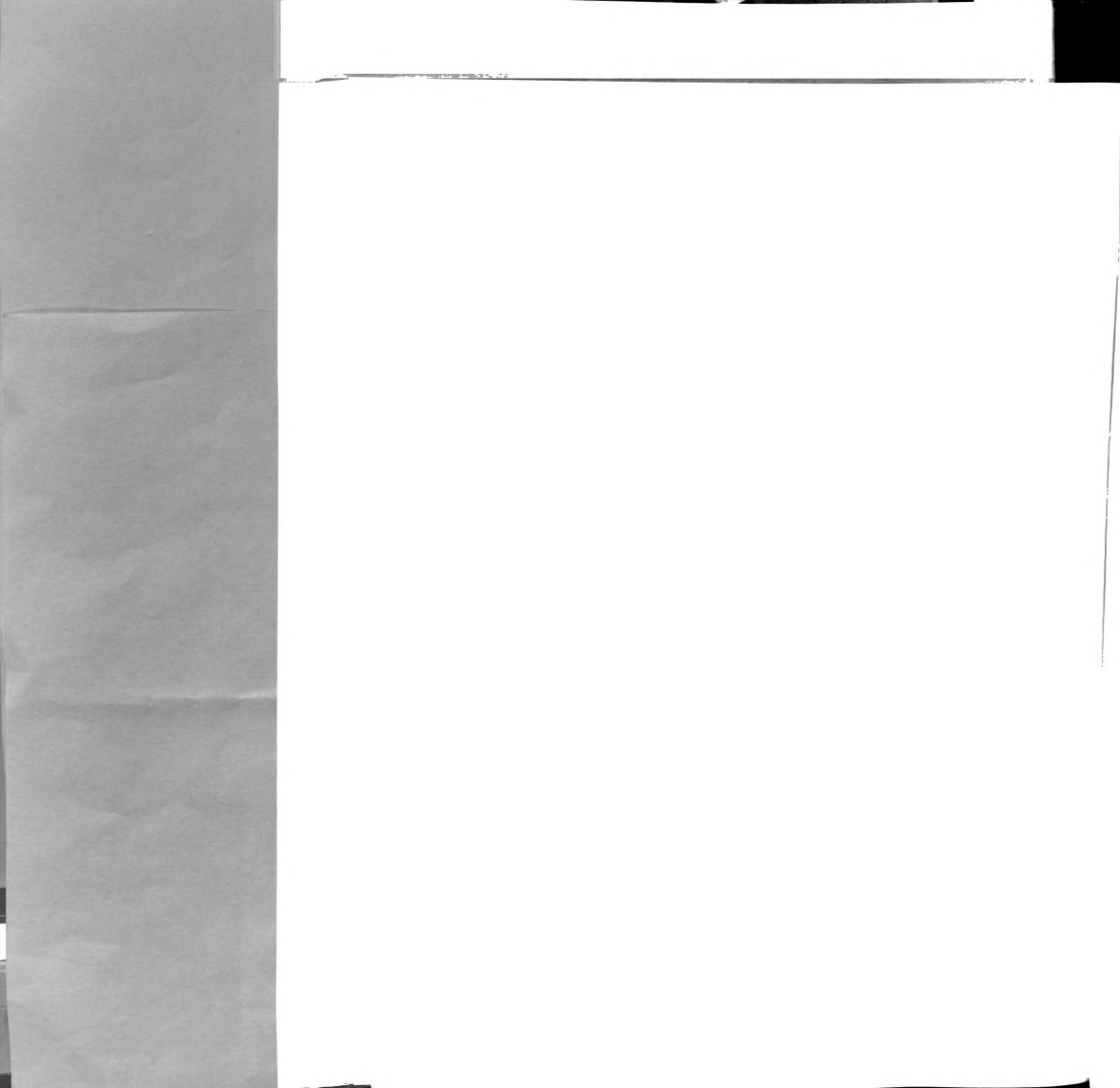


Table 1: Dendrogram characteristics for cluster analyses of manually-aligned T-RFLP profiles of KBS soil fractions using a variety of data processing methods and clustering algorithms. All profiles included in analysis.

Variable	Baseline	Ward's		UPGMA	
		Errors out of 32	# Groups	Errors out of 32	# Groups
Height	50	14	6	12	9
	100	14	6	12	9
	200	18	6	12	9
Relative Height	50	2	6	1	10
	100	2	6	1	8
	200	3	6	5	7
	Rarefraction	2	6	1	9
	1%	2	6	1	10
Hellinger-Transformed	50	2	11	1	13
	100	2	11	1	13
	200	7	11	5	12
	Rarefraction	4	11	2	12
	1%	3	11	2	12
Jaccard distance	50	6	6	5	8
	100	11	5	5	7
	200	8	4	9	4
	Rarefraction	7	7	3	9
	1%	5	7	4	7

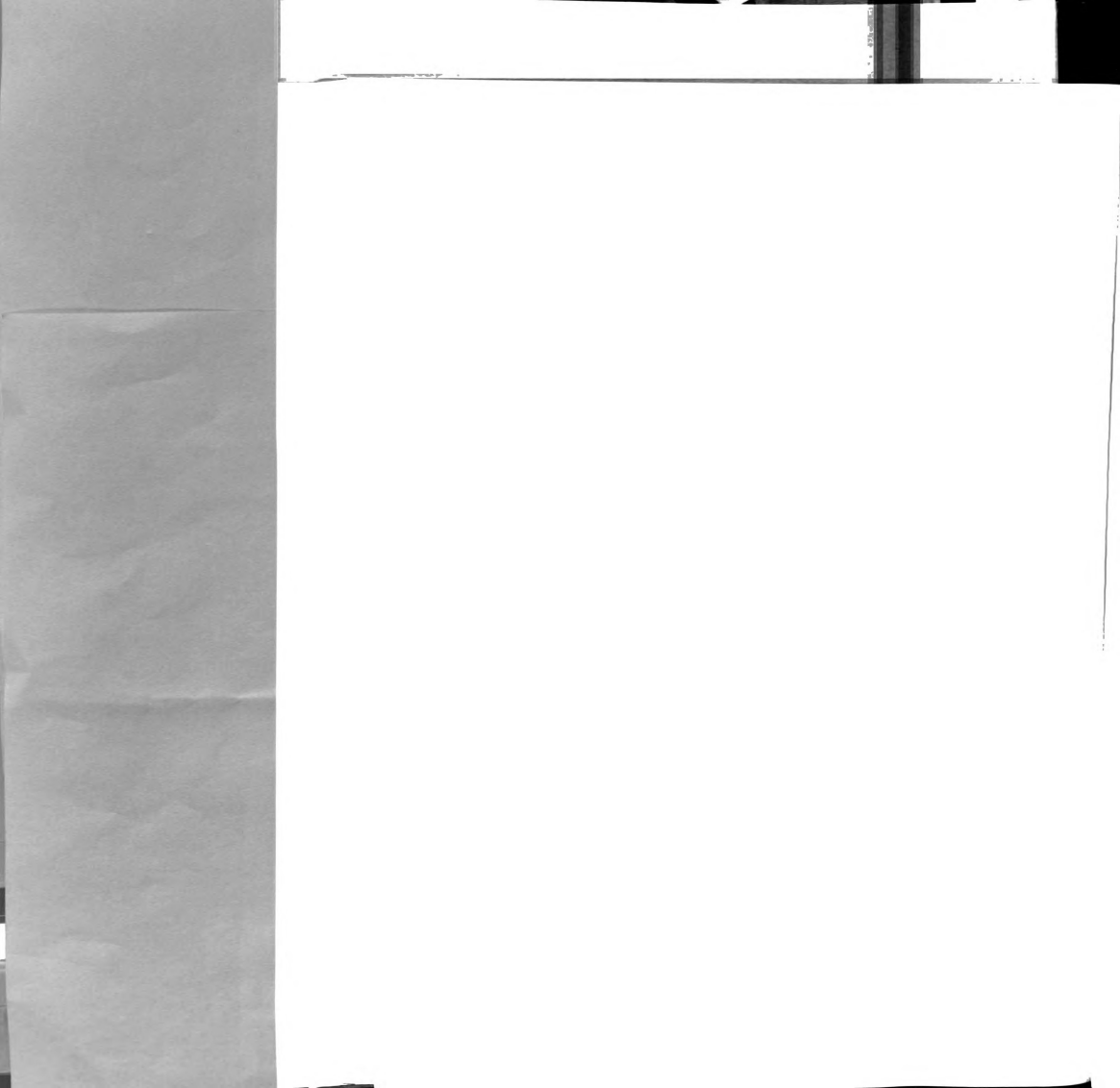


Table 2: Dendrogram characteristics for cluster analyses of computer-aligned T-RFLP profiles of KBS soil fractions using a variety of data processing methods.

Variable	Baseline	Maximum Range	Mean Range	Errors out of 32
All Samples				
Height	50	2	1.1	15
	50	2	1.1	5
Relative Height	1%	2	1.1	5
	1%	3	1.5	11
	1%	4	2.1	4
	1%	7	4	10
	1%	10	5.8	12
	50	2	1.1	7
Jaccard distance	1%	1	0.5	11
	1%	2	1.1	6
	1%	3	1.5	10
	1%	4	2.1	8
	1%	7	4	14
	1%	10	5.8	14
Samples with cumulative peak height > 10,000				
Relative Height	1%	2	1.1	2
	1%	3	1.5	6
	1%	4	2	7

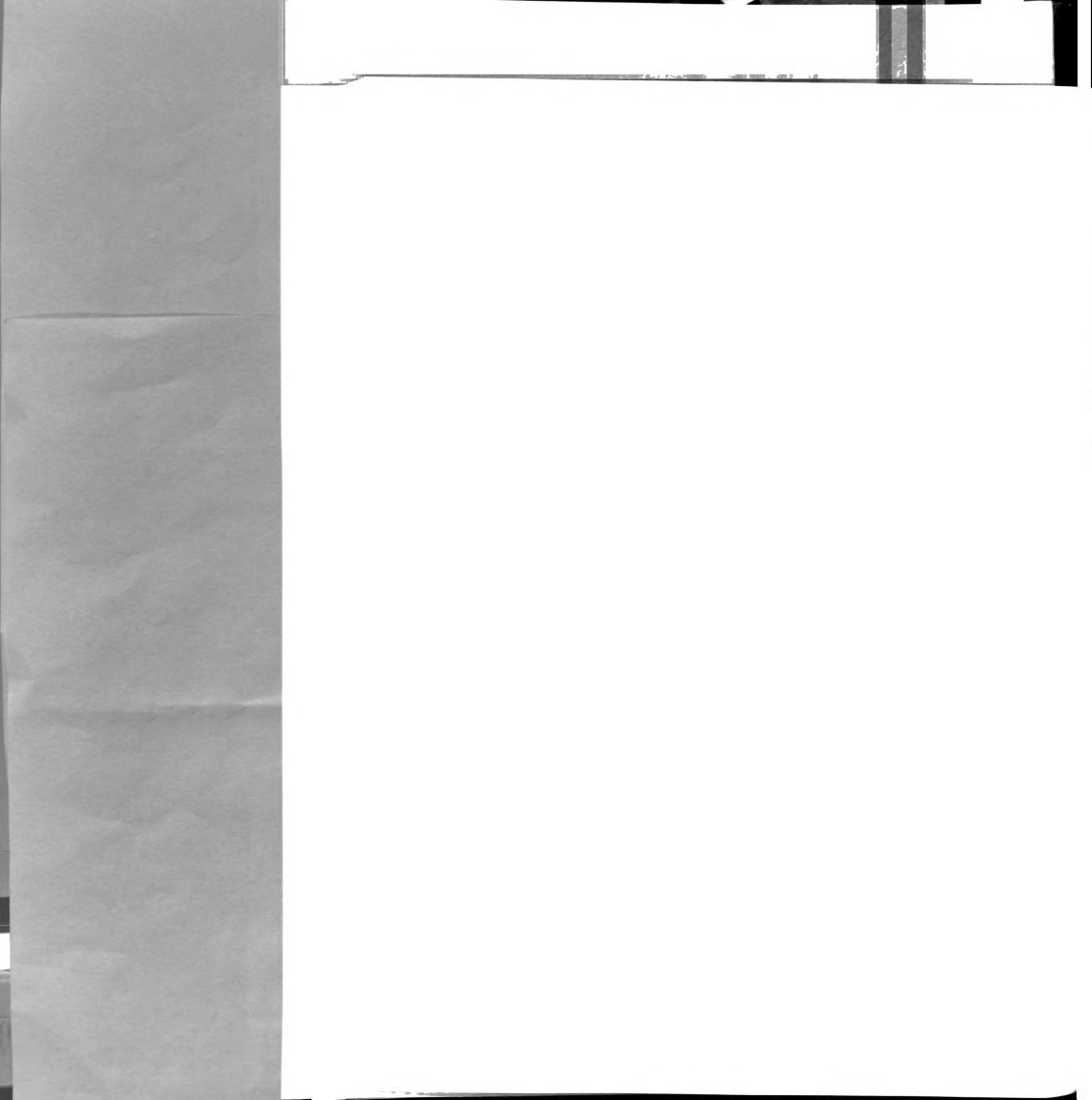


Table 3: Dendrogram characteristics for cluster analyses of manually-aligned T-RFLP profiles of KBS soil fractions using a variety of data processing methods and clustering algorithms. Only profiles with a cumulative peak height of > 10,000 included in analysis.

Variable	Baseline	Ward's			UPGMA		
		Errors out of 22	# Groups	Cophenetic correlation	Errors out of 22	# Groups	Cophenetic correlation
Relative Height	50	1	7	0.61	0	8	0.77
Relative Height	0.5%	1	7	0.61	0	8	0.77
Hellinger-transformed	50	0	10	0.59	1	12	0.88
Hellinger-transformed	0.5%	0	10	0.58	1	12	0.88
Jaccard distance	50	0	6	0.54	0	7	0.84
Jaccard distance	0.5%	1	8	0.52	1	9	0.81

Table 4: Dendrogram characteristics for cluster analyses of T-RFLP profiles of bioreactor samples using a variety of data processing methods and clustering algorithms.

		Ward's			UPGMA		
Variable	Baseline	Errors out of 18	# Groups	Cophenetic correlation	Errors out of 18	# Groups	Cophenetic correlation
Average statistics for Mspl, RsaI, and HhaI profiles analyzed separately							
Height	100	9.7	3.3	0.81	10.3	3.3	0.92
Relative Height	100	8.3	3.7	0.80	9.7	3.7	0.94
Relative Height	Rarefraction	8.3	3.7	0.79	9.7	3.7	0.94
Hellinger-transformed	100	9	4	0.82	9	4.3	0.96
Hellinger-transformed	Rarefraction	8.7	3.7	0.82	9	4	0.96
Jaccard distance	100	9.7	3.4	0.74	6.3	3.7	0.94
Jaccard distance	Rarefraction	7.3	3.3	0.75	7.7	3.3	0.94
Statistics for Mspl, RsaI, and HhaI profiles analyzed together							
Height	100	13	4	0.79	12	4	0.94
Relative Height	100	13	5	0.77	14	5	0.95
Relative Height	Rarefraction	11	4	0.78	14	5	0.94
Hellinger-transformed	100	13	5	0.80	8	5	0.97
Hellinger-transformed	Rarefraction	13	5	0.81	8	5	0.97
Jaccard distance	100	7	4	0.74	8	4	0.97
Jaccard distance	Rarefraction	5	4	0.78	6	4	0.97

Table 5: Redundancy analysis results testing the null hypothesis that there is no difference between bioreactor sample T-RFLP profiles.

Profile	Variable	Proportion Explained	F	p-value
RsaI	Relative Height	46%	3.8	0.0017
	Hellinger-transformed	35%	2.4	0.0003
	Jaccard distance	35%	2.4	0.0119
MspI	Relative Height	23%	1.3	0.1925
	Hellinger-transformed	22%	1.3	0.1489
	Jaccard distance	24%	1.5	0.0054
HhaI	Relative Height	33%	2.2	0.0235
	Hellinger-transformed	33%	2.2	0.0061
	Jaccard distance	29%	1.8	0.0005
MspI, RsaI, HhaI	Relative Height	30%	2.0	0.0071
	Hellinger-transformed	28%	1.8	0.0032
	Jaccard distance	26%	1.6	0.0003

Table 6: Dendrogram characteristics and redundancy analysis results for the set of alfalfa soil samples.

Variable	Ward's			UPGMA			Redundancy Analysis		
	Errors out of 30	# Groups	Cophenetic correlation	Errors out of 30	# Groups	Cophenetic correlation	Proportion Explained	F	p-value
Relative Height	15	3	0.83	16	4	0.90	30%	1.6	0.1194
Hellinger-transformed	21	5	0.76	14	5	0.95	31%	1.7	0.0093
Jaccard distance	13	4	0.68	9	5	0.92	32%	1.8	0.0001

Figure 1: Example of replicated T-RFLP electropherograms. Horizontal axis is size of fragments in base pairs, vertical axes are fluorescence intensity. Each profile was assigned a number; analytical replicates differ by the last digit.

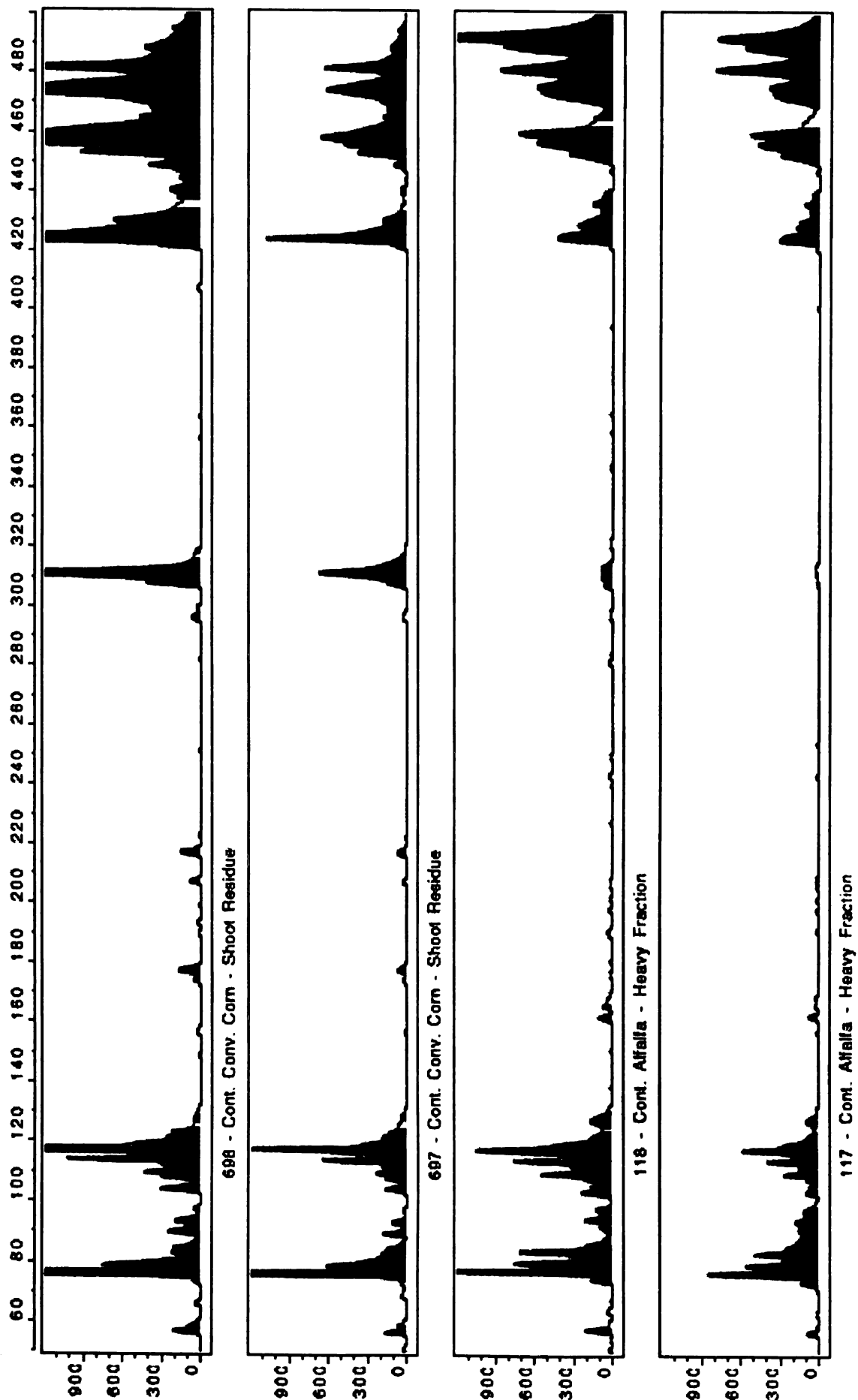
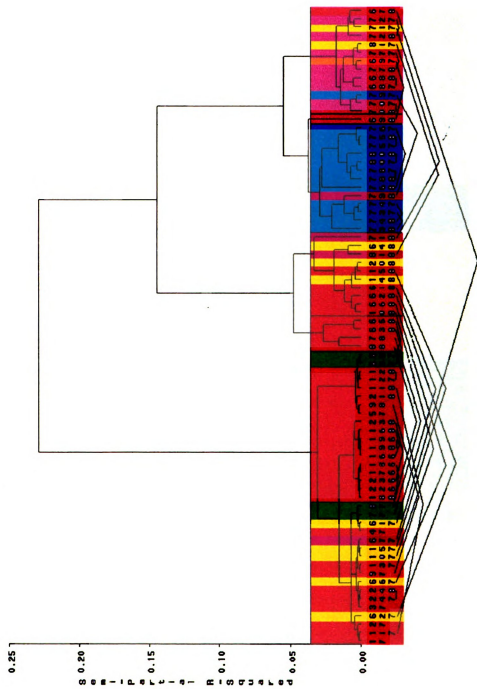




Figure 2: Dendrogram of manually-aligned T-RFLP profiles of KBS soil fractions constructed by Ward's cluster analysis of raw T-RF peak heights. Replicate profiles differ by the last digit of the profile name and are connected by a line. Each group required to explain 50% of the total variance was assigned a color. When replicates were clustered into different groups the colors of the groups at these positions were exchanged. *This figure is in color.*



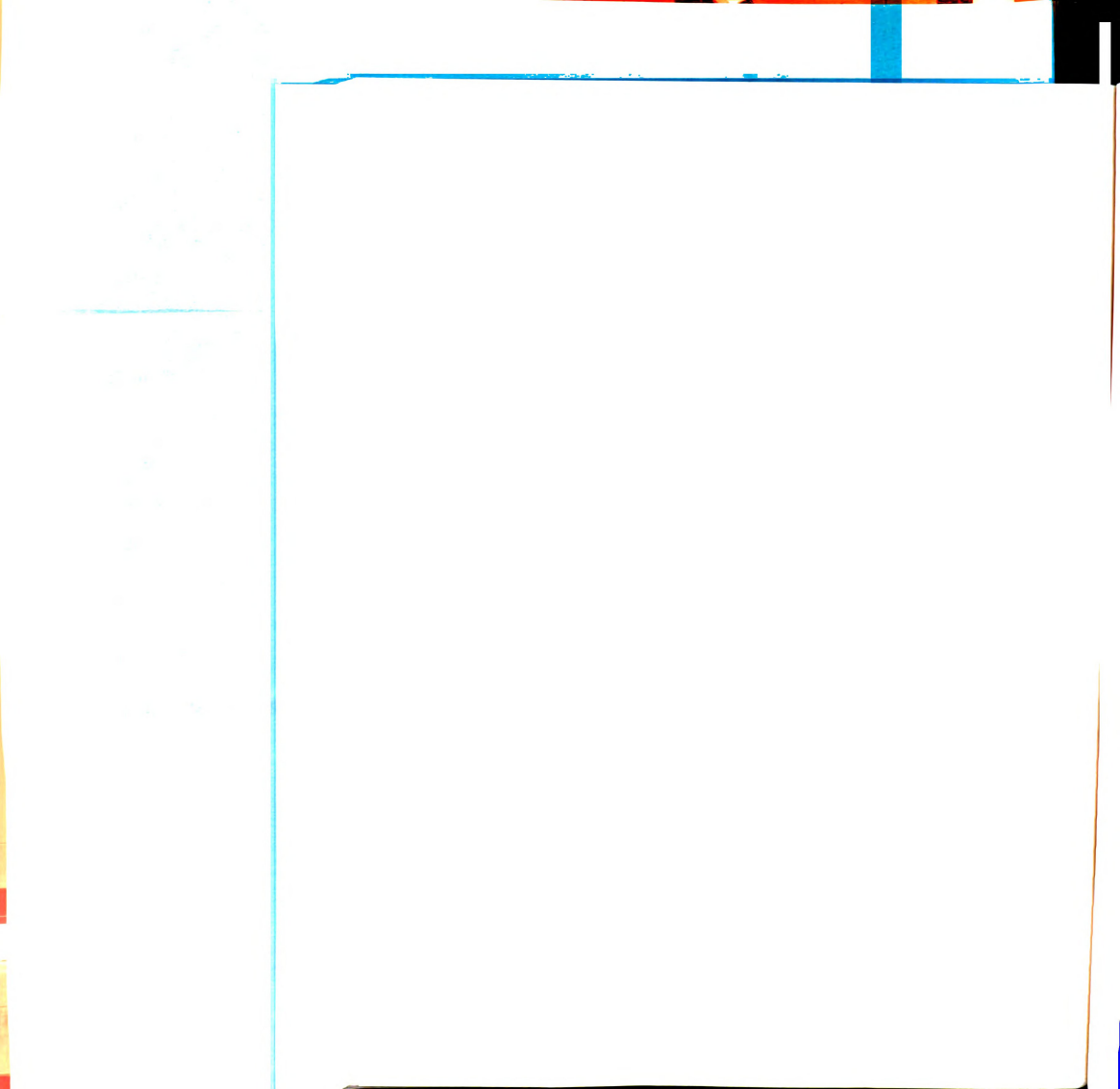
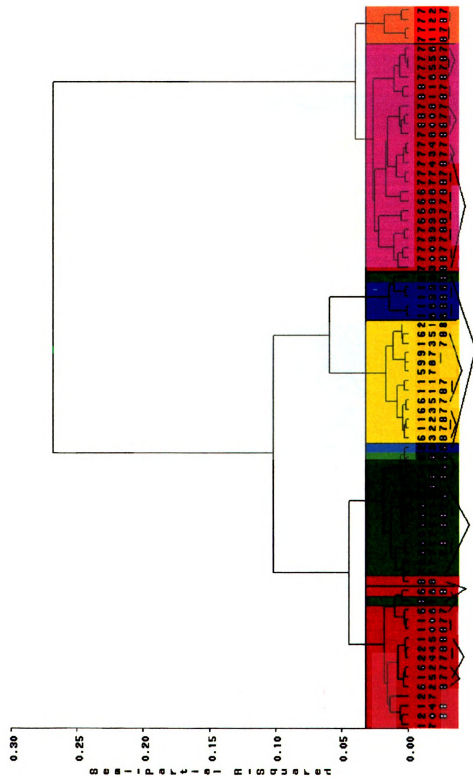


Figure 3: Dendrogram of manually-aligned T-RFLP profiles of KBS soil fractions constructed by Ward's cluster analysis of relative T-RF peak heights. Replicate profiles differ by the last digit of the profile name and are connected by a line. Each group required to explain 50% of the total variance was assigned a color. When replicates were clustered into different groups the colors at these positions were exchanged. *This figure is in color.*



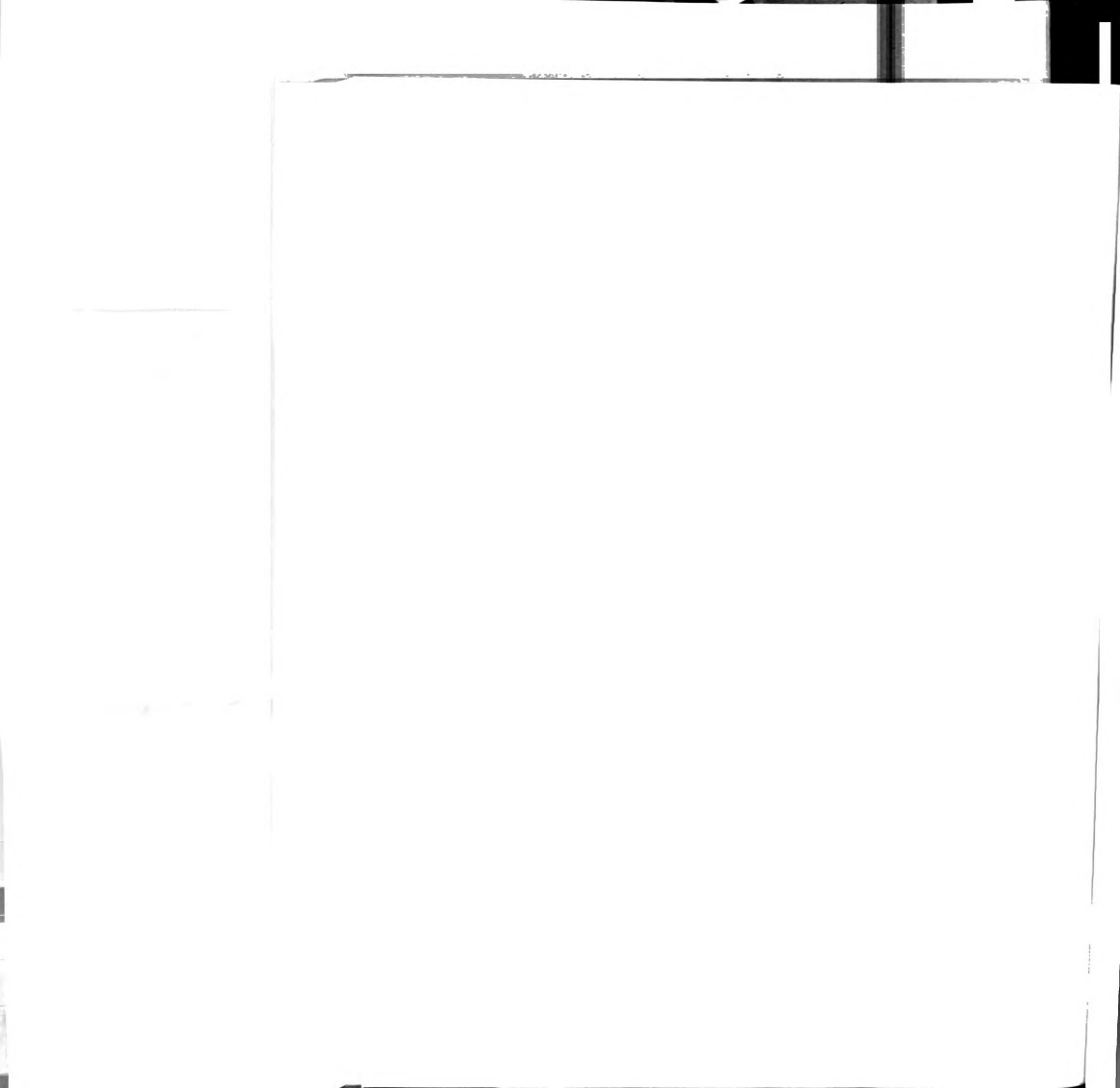
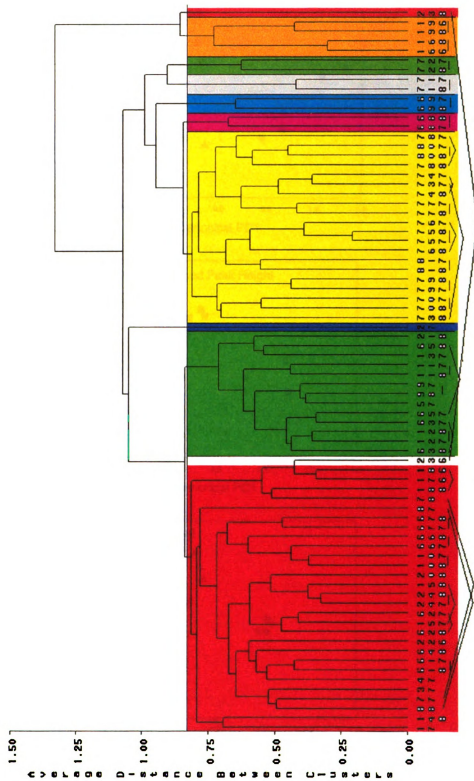


Figure 4: Dendrogram of manually-aligned T-RFLP profiles of KBS soil fractions constructed by UPGMA cluster analysis of relative T-RF peak heights. Replicate profiles differ by the last digit of the profile name and are connected by a line. Each group required to explain 50% of the total variance was assigned a color. When replicates were clustered into different groups the colors at these positions were exchanged. *This figure is in color.*



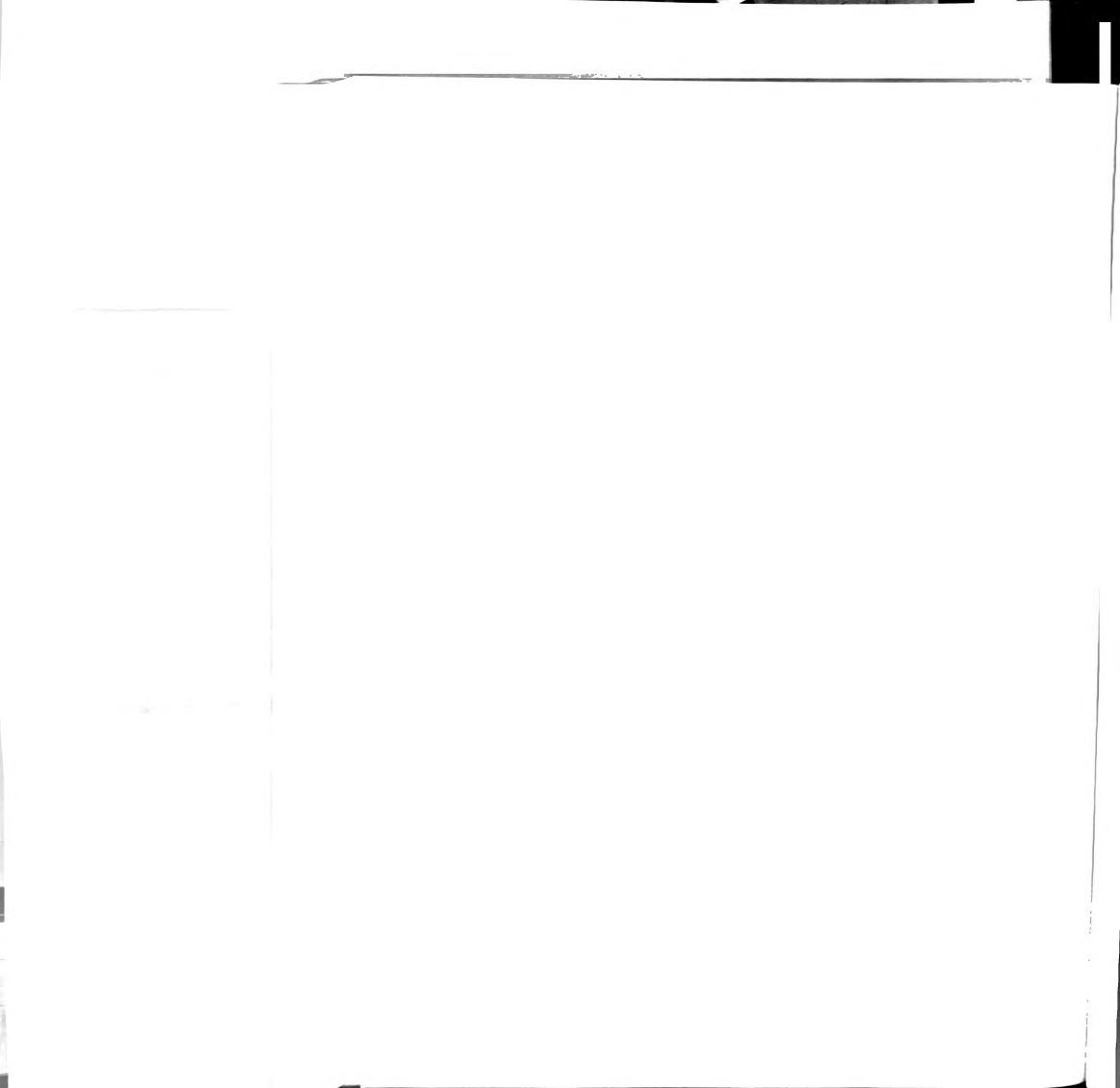


Figure 5: Canonical principal components plots derived from redundancy analysis of bioreactor sample T-RFLP profiles (RsaI, MspI, and HhaI profiles pooled).

▲ = bioreactor sample 27; ● = bioreactor sample 12; ■ = bioreactor sample 19

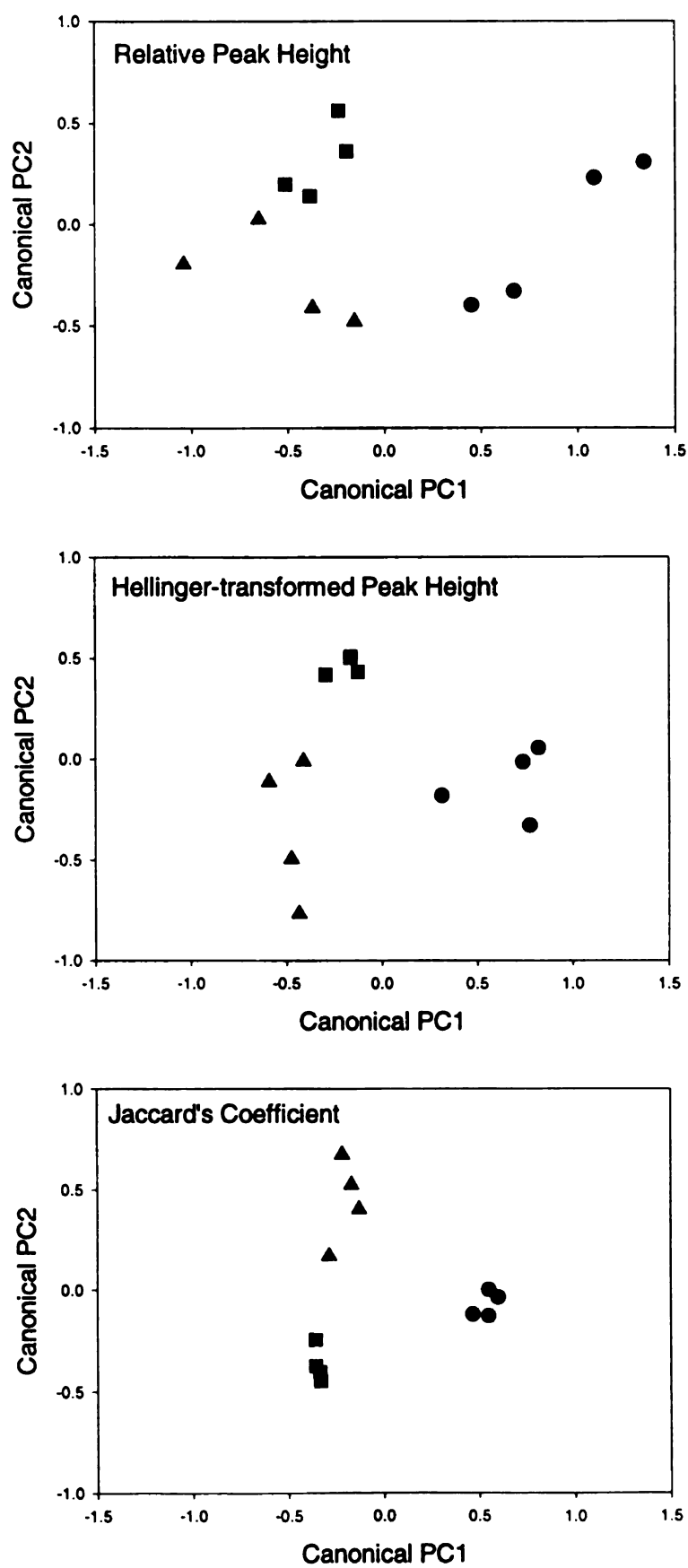
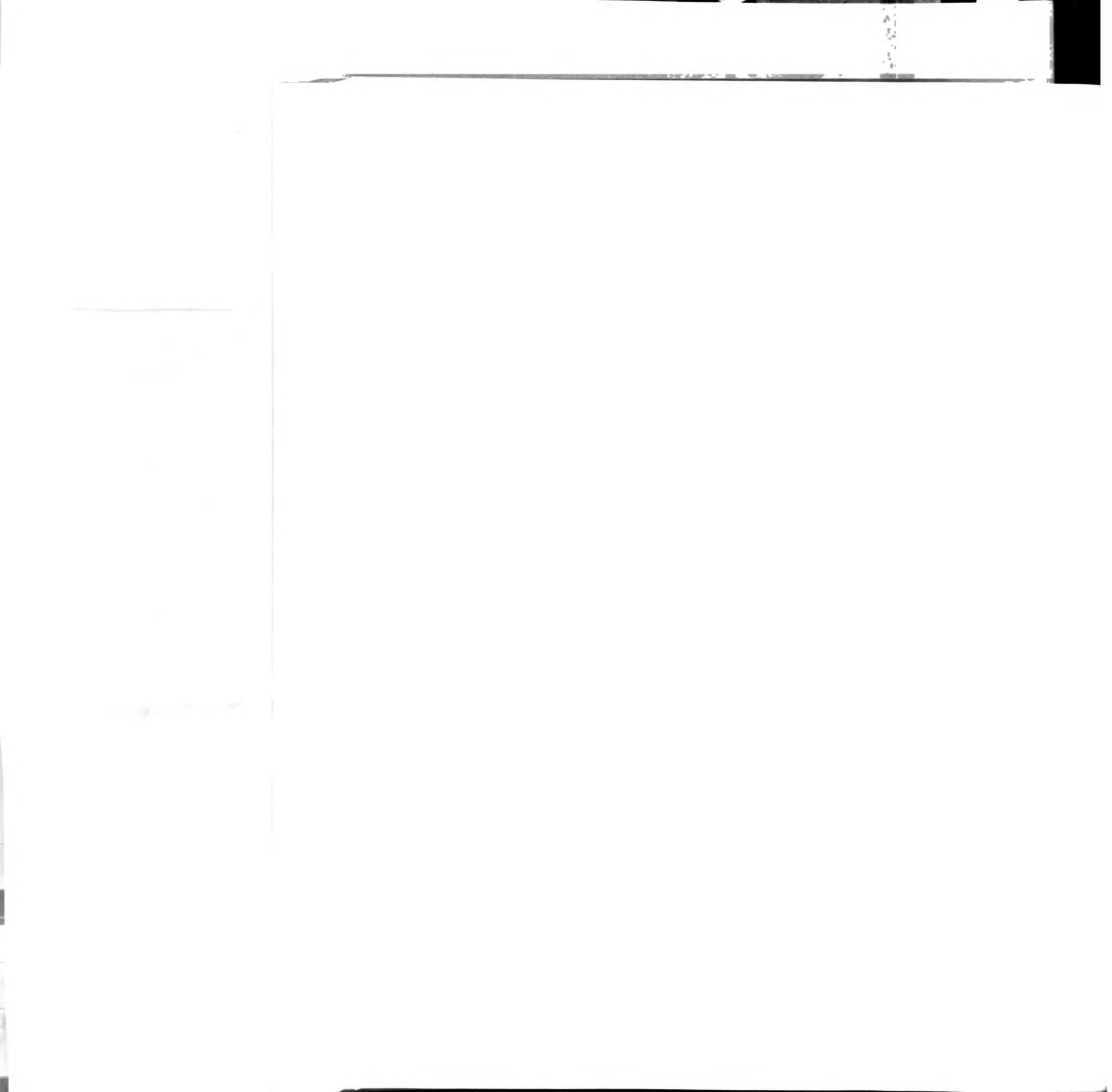


Figure 3: Canonical plot
bioreactor sample 1 (left)
vs bioreactor sample 2 (right)



Chapter 3

Eubacterial Community Structure and Population Size within the Soil Light Fraction, Rhizosphere, and Heavy Fraction of Several Agricultural Cropping Systems



Abstract

Soil fractions were hypothesized to be distinct microbial habitats on the basis of differences in the age and types of organic matter they contain. This was tested in several agronomic cropping systems by comparison of the eubacterial community composition and numbers of bacterial cells present. Terminal restriction fragment length polymorphism (T-RFLP) profiles were significantly affected by both soil fraction and cropping system, accounting for 35-50% of the variability in the profiles. There was a major difference between heavy fraction of soil, which includes the mineral particles and associated humified organic matter, and the rhizosphere and light fraction/shoot residue in soil, which includes soil organic matter particles. Differences were not based on organic carbon content of fractions alone, however, since T-RFLP profiles were also significantly differentiated by cropping system and by rhizosphere versus light fraction/shoot residue. Heavy fraction communities were found have the least amount of random variability in T-RFLP profiles, resulting in the clearest cropping system effects, while rhizosphere communities were the most variable. Profiles from organically-managed corn soil were more variable than for either conventionally-managed corn or alfalfa. The percentage of cells $>0.18 \mu\text{m}^3$ was also better explained by treatment effects than by organic carbon content of samples. In contrast, total number of bacterial cells/g fraction was not explained better by treatment differences than by carbon content of samples. The results show that habitat diversity in soil, related both to the amounts and types of organic matter, as well as other potential factors, may be important in maintaining the high soil bacterial species diversity and evenness that is found in soil.

Introduction

Particles of organic matter isolated by flotation in liquids of varying density are known as light fraction (LF) and have been shown to be useful predictors of soil respiration and nitrogen mineralization (Biederbeck et al. 1994, Hassink 1995, Janzen et al. 1992). Light fraction is sensitive to soil management regimes (Bremer et al. 1994, Cambardella and Elliott 1993) and has been proposed as an important component of soil quality (Gregorich et al. 1994, Yakovchenko et al. 1998). It has also been shown to be critical in the formation and stabilization of soil aggregates (Golchin et al. 1994a). The LF is composed of recently deposited organic matter particles (primarily plant residues), with greater rates of turnover than other soil organic matter fractions (Buyanovsky et al. 1994, Gregorich et al. 1995), higher carbohydrate contents, and higher C:N ratios (Christensen 1996). This is particularly true for the “free” LF isolated from outside of soil aggregates (Golchin et al. 1994b, 1995).

The presence of a spatially-distinct component of soil with easily-utilizable substrates raises the question of whether this fraction is colonized and inhabited by a community of microorganisms different from other soil fractions. Such habitat diversity in soil could explain the high microbial species richness and evenness (or non-dominance by any species) detected by ribosomal sequencing (Borneman and Triplett 1997, Nakatsu et al. 2000, Nüsslein and Tiedje 1998) and DNA rehybridization rate studies (Sandaa et al. 1999, Torsvik et al. 1990). Competitive exclusion will not occur if species remain in different habitat types and do not interact (Huston 1999). When competing species do colonize the same habitats, patchiness of the habitat can allow for the coexistence of the

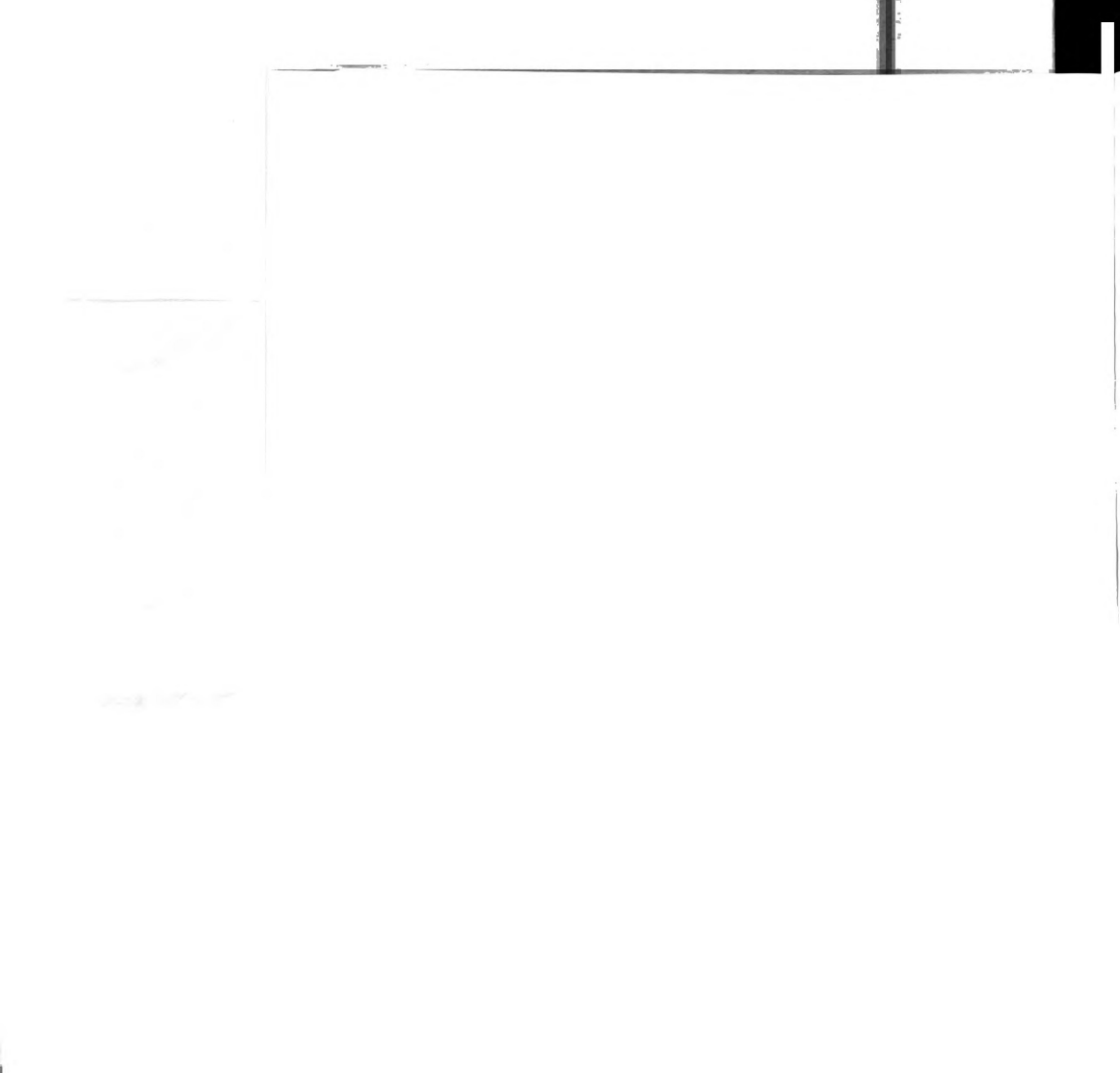
species through differential dispersal ability (fugitive species), or independently spatially-aggregated distributions coupled with limited dispersal (Hanski 1995, Pacala and Levin 1997). Plant residues are known to be patchily distributed in soil (Staricka et al. 1991). Differing limiting resources in patches can lead to differences in local competitive equilibria, resulting in coexistence of competing species by spatial resource partitioning (Tilman 1982). Nitrogen limits microbial growth in LF, resulting in N immobilization during LF decomposition (Janzen et al. 1992, Yakovchenko et al. 1998), whereas available C generally limits microbial growth in bulk soil (Smith and Paul 1990). These mechanisms of enhancing species coexistence are not mutually-exclusive. All of them, except for the spatial-aggregation hypothesis, require some difference in the ability of species to proliferate in the LF patches compared to other soil fractions. Therefore they are not supported if the community in LF are not significantly different from those in other soil fractions. If the LF microbial community is different from that in other soil fractions, the LF represents a distinct soil habitat that should be considered to contain potentially unique ecological dynamics.

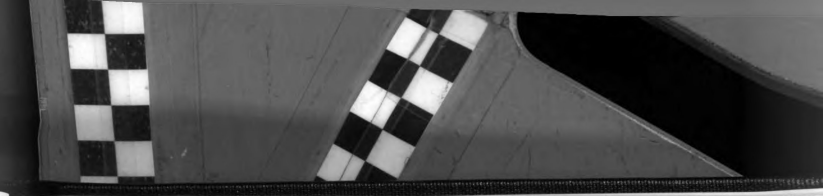
The rhizosphere, or the region of soil adjacent to and under direct influence of plant roots, is a well-recognized soil habitat (Bolton et al. 1993). Enhanced microbial growth is supported by root exudates and sloughed cells (Breland and Bakken 1991, Rouatt et al. 1960, Söderberg and Bååth 1998). The rhizosphere is colonized by and supports a community different from that in the “bulk soil” (Maloney et al. 1997, Marilley and Aragno 1999, Ringelberg et al. 1997). Other ecological dynamics distinctive of the rhizosphere (compared to the bulk soil) include interactions with other plant symbionts (Budi et al. 1999, Christensen and Jakobsen 1993, Denton et al. 1999),

reduced allocation of C to storage molecules (Tunlid et al. 1985), enhanced predation (Badalucco et al. 1996), increased proportion of species with copiotrophic growth strategies (Mahaffee and Kloepper 1997), and unique spatial structure (Bowen and Rovira 1991).

Some microbiological studies have supported the hypothesis that LF or particulate plant residues are habitats with unique effects on the microbial community. The large increases in the number and activity of bacterial cells in soil microsites containing decomposing plant residues has been recognized for a long time (e.g. Thom 1935). Kanazawa and Filip (1986) found that the LF contained 27-42% of the total numbers of culturable microorganisms, depending on growth strategy, and 67% of the total soil ATP. This was similar to the proportion of the total organic C stored in the LF, 42%. Ahmed and Oades (1984) reported only 0.2-0.4% of the total soil ATP was contained in the LF, whereas it contained 11-12% of the total soil organic C. This conflict between reports remains unresolved (Gregorich and Janzen 1996). Experimental additions of plant residue to soil microcosms has induced localized increases in dehydrogenase activity (Gaillard et al. 1999, Rønn et al. 1996), microbial biomass (Chotte et al. 1998), soil microfauna (Gaillard et al. 1999), and bacterial conjugation (Sengeløv et al. 2000).

We tested the hypothesis that the LF, HF, and rhizosphere are distinct soil microbial habitats containing differing eubacterial communities. We also examined the macroscopic shoot residue that is present in soil and is normally excluded from analysis because it is larger than 2 mm in diameter. Microbial community analysis was conducted using terminal restriction fragment length polymorphism (T-RFLP) of the 16S ribosomal gene which was PCR-amplified from eubacteria. Bacterial number within soil fractions





was assessed to contribute to the issue outlined above. The responses of the communities within fractions to differing cropping systems was examined to determine whether communities in different micro-habitats respond differently to environmental conditions varying at a larger scale.

Methods

Field Sites and Sample Collection

Samples were collected from two field experiments at the W.K. Kellogg Biological Station in Southwestern Michigan. Soils at the site are Typic Hapludalfs and approximately 43% sand and 40% silt (Robertson et al. 1997). Two field treatments of the Living Field Laboratory site were sampled: conventionally-managed continuous corn and organically-managed first-year corn. The conventionally-managed continuous corn receives synthetic fertilizer and pesticides on a regular basis. The organically-managed first-year corn is in a corn-corn-soybean-wheat rotation, with cover crops planted after corn and wheat. Organically-managed corn receives compost (dairy manure and deciduous tree leaves) at the beginning of each growing season. The experiment includes rotation entry point plots in a randomized block design (with four replicate blocks), so first-year corn can be sampled every year. Treatments were begun in 1993. Secondary tillage is used to control weeds in organically-managed corn. Details of the management of this site can be found in Jones et al. (1998). Samples were collected from within rows, between corn plants in each of the four replicate fields per treatment.

Samples were also collected from the perennial alfalfa treatment of an adjacent experiment, the Kellogg Biological Station Long Term Ecological Research site. Alfalfa

fields were established in 1989, and plants were killed every five years with herbicide and replanted to maintain stand vigor. This occurred in the spring of 1999, between dates sampled in this study. Alfalfa plants receive occasional lime amendments and pesticide application (<http://lter.kbs.msu.edu/Agronomics>). Samples were collected in September of 1998 and August of 1999 nearby permanent sampling locations in four of the replicate fields. Samples were 10 cm deep. In 1998, nine replicate soil cores were collected with a 1.9 cm diameter soil probe from each field. These were pooled in the field and stored in Whirlpak bags for transportation to the lab. In 1999, three 350 g soil blocks were excavated per field, and were transferred intact to glass jars for transportation. Samples were stored at 4°C until fractionation was complete, which was within 3 weeks in 1998 and 8 weeks in 1999.

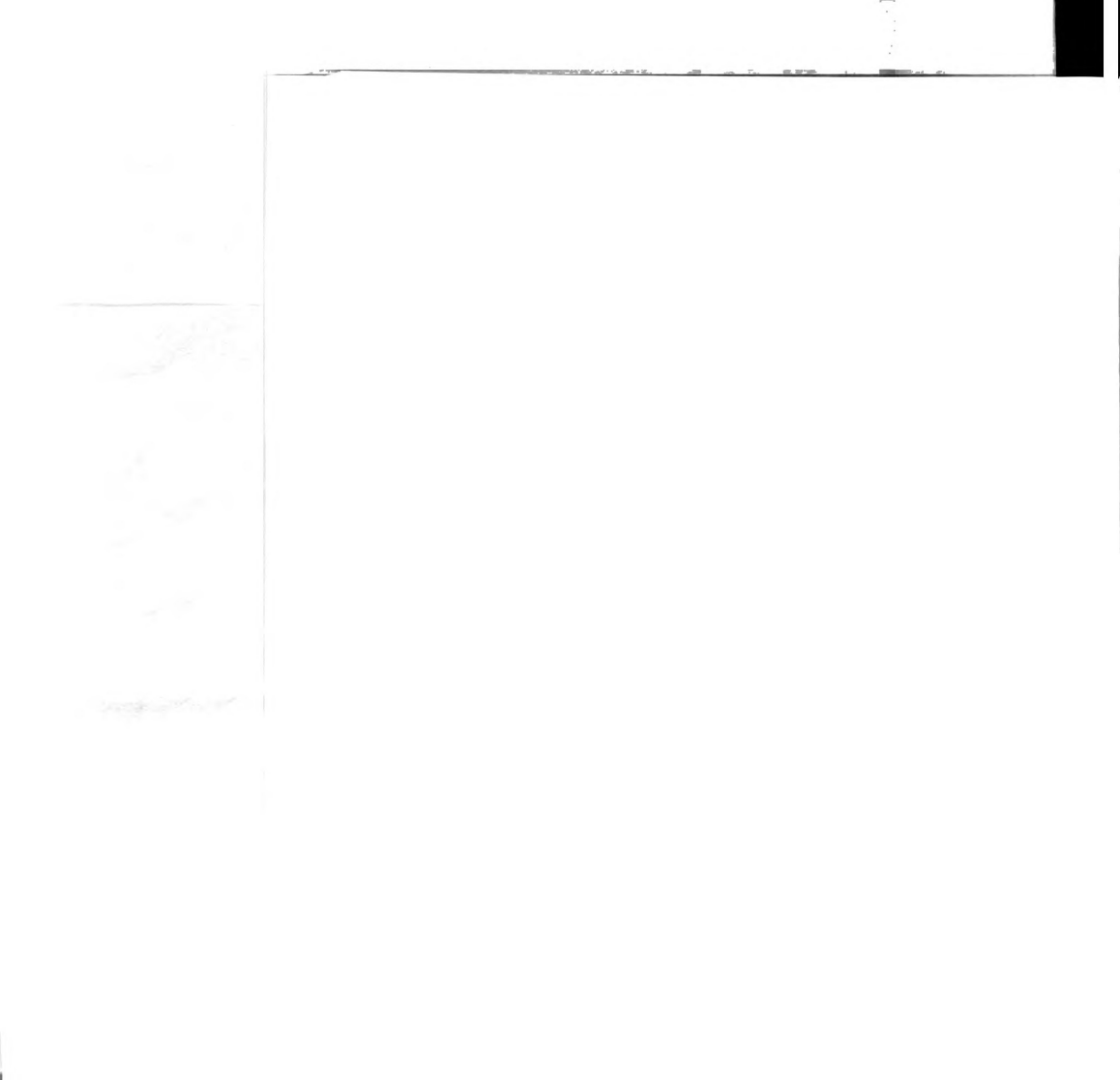
Soil Fractionation

Density separations are performed in liquids of two different densities in this study, 1 and 1.7 g/cc. To distinguish between the fractions, the density at which the fraction was isolated will follow its abbreviation; hence LF isolated using water will be designated LF-1.

Soil cores from 1998 were mixed by hand and a whole-soil subsample was removed for weighing and drying at 65°C. Samples were forced through a 2 mm sieve by gently breaking aggregates along planes of weakness. Roots and shoot residue > 2 mm were removed with forceps. Layers of soil < 1 mm thickness clinging to the roots and shoot residue were included with those fractions. Density separation was performed using a procedure modified from Golchin et al. (1994b) to isolate free or inter-aggregate LF. Bulk soil samples (with roots and shoot residue removed) weighing 50 to 75 g were

placed in sterile centrifuge bottles. Sterile water was added to a total volume of < 200 mL. Tubes were then inverted by hand 10 times and material clinging to sides of tubes and caps was washed into the suspension with sterile water. The total volume within the bottle was brought to 200 mL, and particles were allowed to settle 30 minutes. Bottles were then centrifuged in a swinging-bucket centrifuge at 3000 rpm for 30 minutes. The water and floating particles were isolated by aspiration into a filtration flask. This suspension was rinsed on a 20 μ m sieve, and then LF-1 particles were transferred to filter paper and collected with forceps. All fractions (roots/rhizosphere, shoot residue, LF-1 and HF-1) were divided into three subsamples. These were: 1. frozen for DNA extraction 2. stored in 4.9% formaldehyde 3. weighed before and after drying at 65°C. Density separation was also performed on bulk soil samples using a solution of sodium polytungstate adjusted to a density of 1.7 g/mL.

Samples collected in 1999 were fractionated in essentially the same way except that whole soil blocks were gently separated along planes of weakness over a nest of sieves with mesh sizes of 6.3, 4, and 2 mm. Soil clods were broken down until they fit through the 6.3 mm sieve. The nest of sieves was then shaken by hand until only stable aggregates that would not fit through the mesh were left on the 4 and 2 mm sieves. This resulted in isolation of aggregates of sizes 4-6.3, 2-4, and 0-2 mm. The 4-6.3 and 2-4 mm macroaggregate fractions were subsampled for analysis of aggregate layers, described in chapter 4. Density separation was performed as described above after macroaggregates had been forced through a 2 mm sieve. This resulted in a LF-1 and HF-1 for each aggregate size class. Isolation of roots/rhizosphere and shoot residue was performed



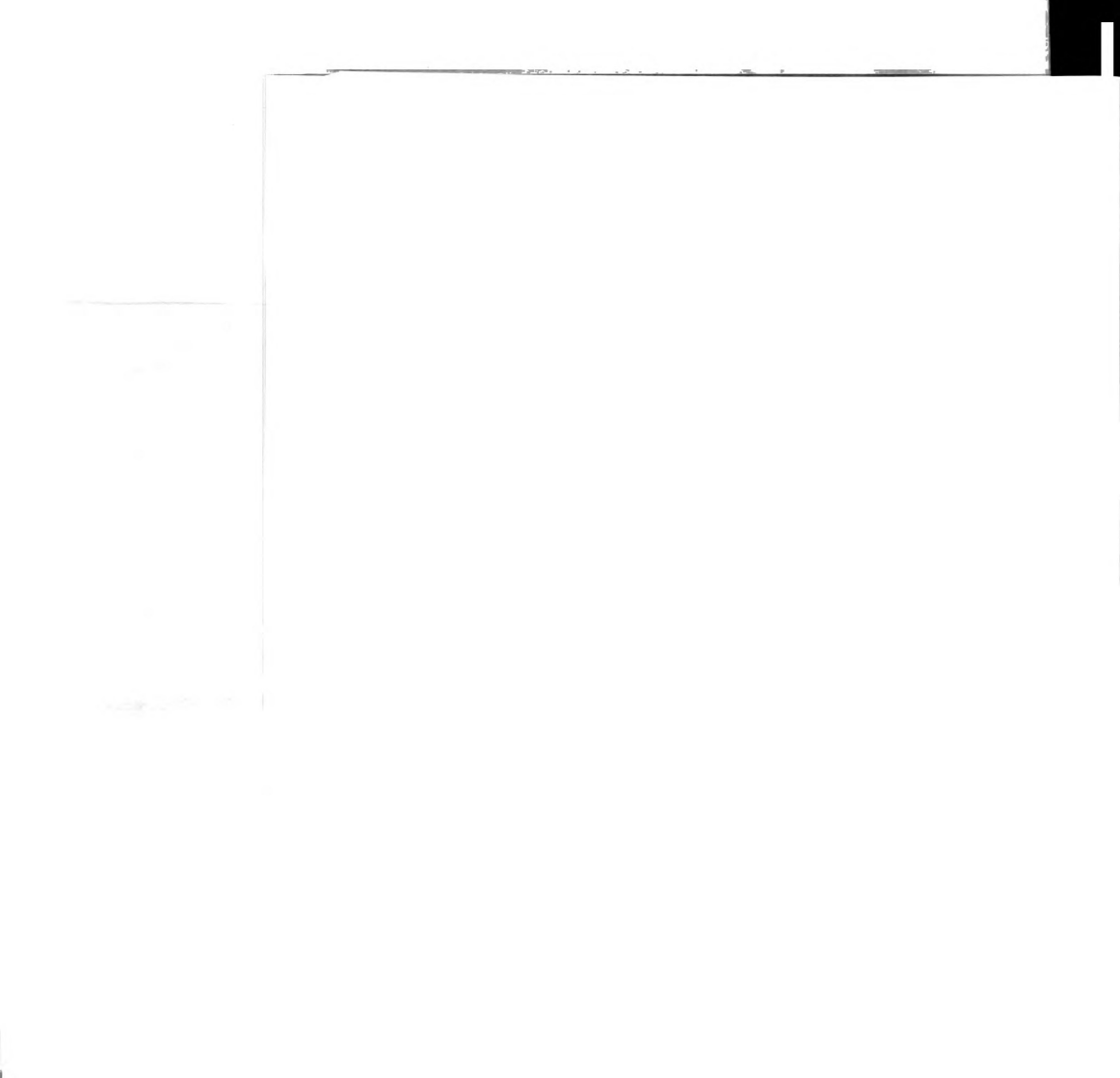
during sieving steps. Fractions and whole-soil were subsampled and stored as described above.

Carbon and Nitrogen Analyses

Carbon and nitrogen contents of dried, ground 1998 samples were obtained using a Carlo-Erba NA1500 series 2 Nitrogen-Carbon-Sulfur Analyzer.

Direct Microscopy

Samples preserved with formaldehyde were dispersed by blending in a Waring blender (HF and whole soil), or by vortexing a sample diluted with 5 mL of water for 5 minutes with approximately 1 mL of 1 mm diameter glass beads (LF, rhizosphere, shoot residue). Bacterial cell numbers were determined microscopically in samples from 1998 following Paul et al. (1999). Briefly, 4 μ L of diluted fraction was placed in each of five 6 mm diameter wells of an analytical microscope slide (Cel-Line Associates, Newfield, NJ) and allowed to dry overnight. Dried sample smears were then stained with 5-(4,6-dichlorotriazin-2-yl) aminofluoroscein (DTAF) for 40 minutes, followed by rinsing in phosphate buffer (30 minutes X 3 rinses) and water (30 minutes). Wells were flooded with type FF immersion oil and then a coverslip was glued in place. Bacteria were observed with a Leitz Orthoplan 2 microscope at 1000X magnification using a 63X objective, 10X eyepiece, and 1.6X zoom. Digital images of bacteria were obtained using a Princeton Instruments CCD microscope camera. Cells were counted and measured by a script written in the image analysis program IPLab (Princeton Instruments, Trenton, NJ). Calculations of cell biovolume were based on formulas in Paul and Clark (1996).

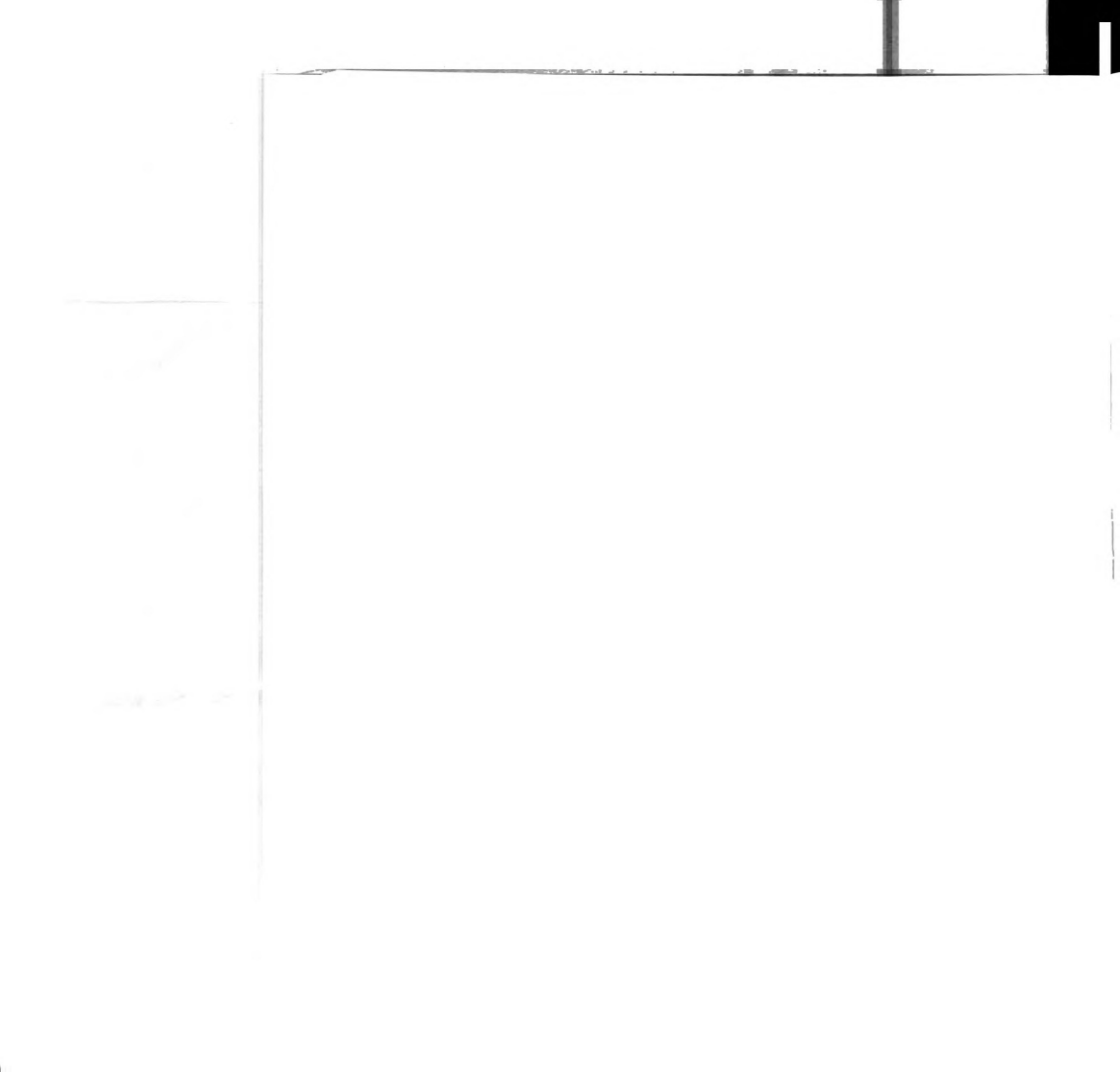


T-RFLP Analysis

T-RFLP was performed essentially as described in Liu (1997) and in Chapter 2. Community DNA was extracted from samples using the standard Ultraclean Soil DNA extraction kit (Mo Bio Laboratories, Solana Beach, CA). Genomic DNA was found to be of sufficient purity to be used directly in PCR reactions. PCR was performed using a standard reaction mixture of 160 μM of each deoxynucleoside triphosphate, 3 mM MgCl_2 , 0.05 U/ μL Taq DNA polymerase and the appropriate volume of accompanying 10X PCR buffer (Gibco BRL, Gaithersburg, MD), and 0.2 $\mu\text{g/mL}$ bovine serum albumin (Boehringer Mannheim Biochemicals, Indianapolis, IN). PCR mastermix, without primers, and PCR reaction tubes were sterilized for 14 minutes with direct ultraviolet radiation in a Cleanspot PCR/UV workstation. Primers used were the general eubacterial primer 8-27F (AGAGTTTGATCCTGGCTCAG, *E. coli* numbering, Amann et al. 1995, Integrated DNA Technologies, Coralville, IA) and the universal primer 1392-1406R (ACGGGCGGTGTGTACA). PCR reactions were optimized for each sample of genomic DNA using a master mix with primer concentrations of 0.4 μM . Optimizations were performed by adjusting the amount of genomic DNA extract used (0.4 to 7.5 $\mu\text{L}/50$ μL reaction) and the number of PCR cycles run (22 or 28) to obtain a strong band without visible non-specific product. PCR was performed in a Perkin-Elmer 9600 thermocycler using an initial denaturation step of 95°C followed by 22-28 cycles of the following program: denaturation at 94°C for 30 sec., primer annealing at 55°C for 30 sec., and extension at 72°C for 30 sec. A modified hot start procedure was used where PCR tubes were not placed in the thermocycler until the block temperature had reached 80°C. A final extension at 72°C for 7 min. was performed after the programmed number of cycles

was complete. PCR product concentration and specificity was checked by electrophoresis on a 1% agarose gel, followed by staining with ethidium bromide.

PCR reactions (50-75 μ L) were performed in triplicate for each sample using the optimal conditions found previously. These reactions were performed using the same PCR master mix and program described above except that the forward primer was 0.6 μ M hexachlorofluorescein (hex)-labeled 8-27F (Integrated DNA Technologies). PCR replicates were pooled and purified using the Promega PCR Preps Wizard Kit as directed by the supplier, except that elution was performed with 19 μ L of sterile water heated to 55-65°C. Five μ L of purified PCR product was mixed with 5 μ L of restriction enzyme master mix containing 1.5 U/ μ L of restriction enzyme and one μ L of the accompanying reaction buffer (Gibco). Restriction reactions were incubated for three hours at 37°C, followed by 16 min. at 65°C to denature the restriction enzyme. Three μ L of the restricted PCR product was mixed with one μ L of 2500 TAMRA size standard (Applied Biosystems Instruments, Foster City, CA). DNA fragments were separated by size by electrophoresis at 1800 V for 14 hours on an ABI 373 automated DNA sequencer at Michigan State University's DNA Sequencing Facility. The 5' terminal fragments (T-RFs) were visualized by excitation of the hex molecule attached to the forward primer. The gel image was captured and analyzed using Genescan Analysis Software 3.1. A peak height threshold of 50 fluorescence units was used in the initial analysis of the electropherogram. Negative controls (no genomic DNA) were conducted with every PCR and run on several Genescan gels. Contamination in PCR reactions was not detected. Small peaks occasionally appeared in negative control lanes on Genescan gels,



but the cumulative peak height was always below 1000 units. Samples were re-run if the cumulative peak height was below 9500 fluorescence units.

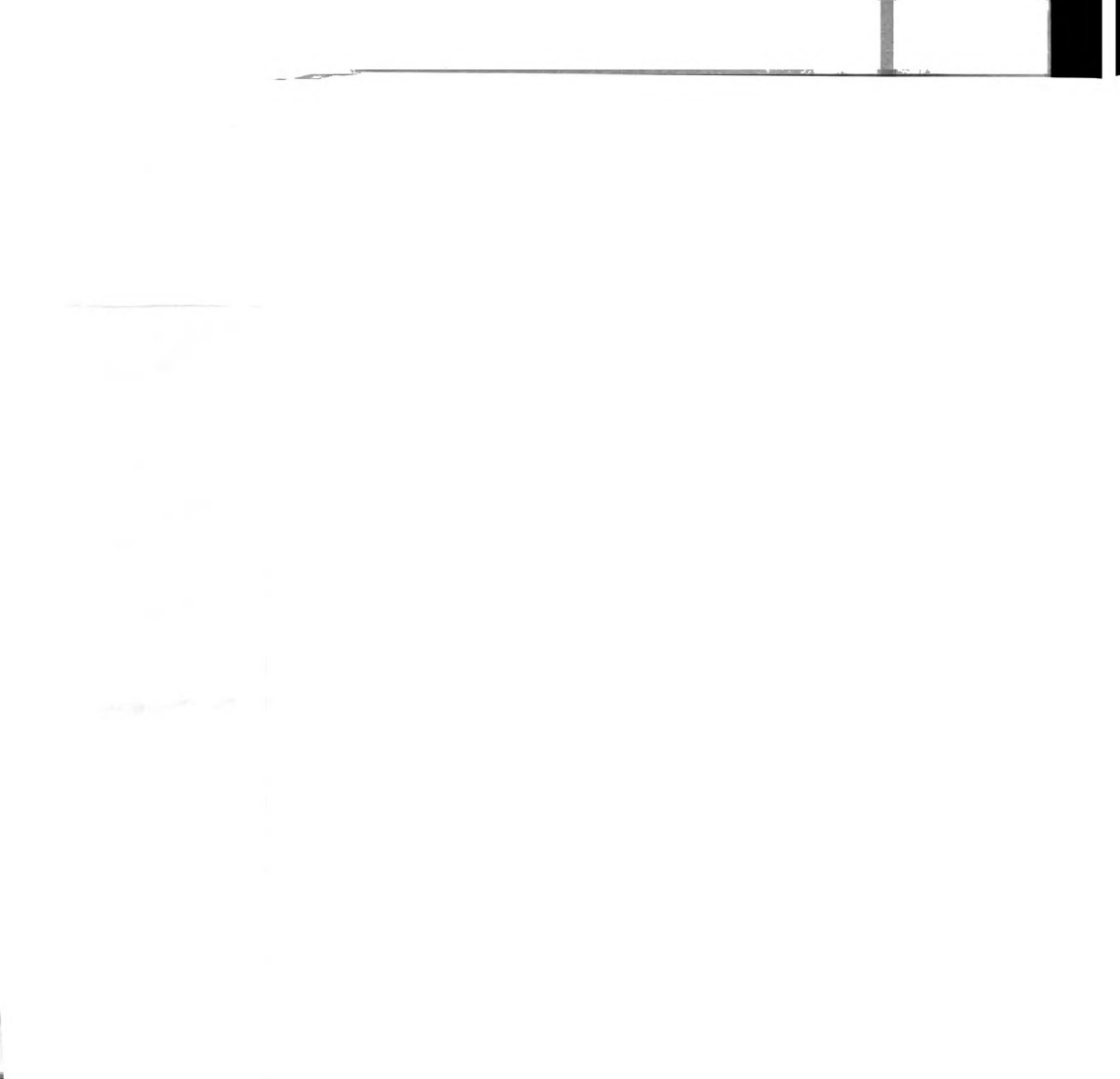
T-RFLP profiles for all samples were generated using the restriction enzyme *Rsa*I. *Msp*I was used to generate additional profiles for replicates 1,2, and 3 of 1998 rhizosphere, LF-1, and HF-1, and in 1999 for all rhizosphere replicates and replicates 3 and 4 of 0-2 mm and 4-6.3 mm aggregate LF-1 and HF-1. T-RFs of sizes between 50 and 500 bp were aligned against a previously-defined database with identities of samples concealed.

Statistical Analysis

Most statistical analyses were performed using SAS Version 8 Stat and IML components, Sigmastat, and Excel. Redundancy analysis was performed using Canoco. All analyses were performed taking into account blocking of replicates in the field and lab, which was not found to be significant.

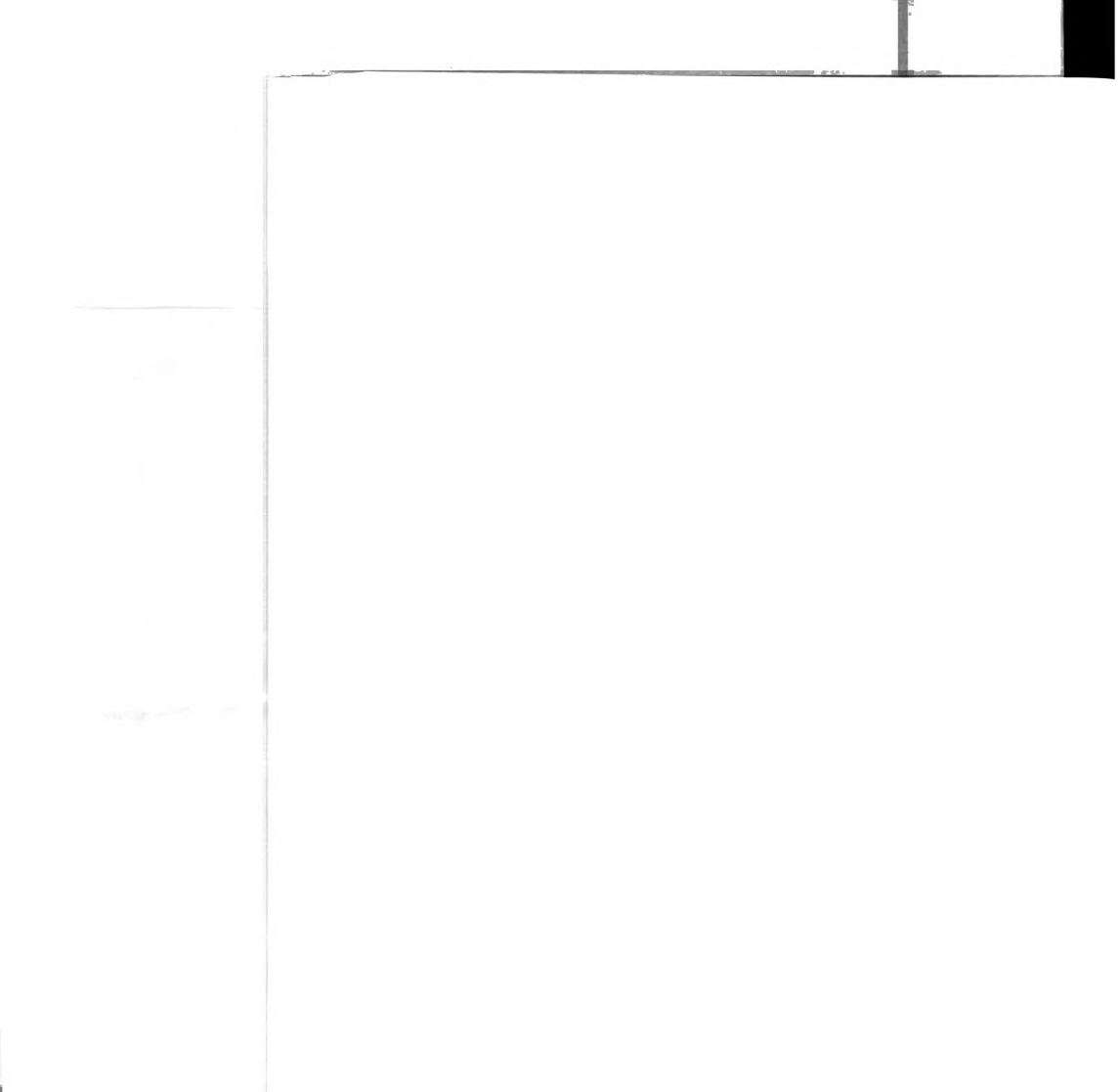
Percent C and N was analyzed using one-way analysis of variance (ANOVA) to test for a significant effect of cropping system. Total numbers of cells and percent of cells in the largest and smallest size classes were analyzed by two-way ANOVA with cropping system and soil fraction as factors, as well as by regression against C and N contents of samples. The significance of the increased fit by more complex ANOVA models compared to regression models was assessed with a partial F-test.

Relationships between T-RFLP profiles were examined using Hellinger distance and Jaccard distance (see chapter 2 for a discussion of data analysis of T-RFLP profiles). Differentiation of eubacterial T-RFLP profiles was tested using redundancy analysis (or distance-based redundancy analysis in the case of Jaccard's distance) with dummy



variables coding for cropping system, soil fraction, and interaction terms. Coding followed the method described in (Legendre and Anderson 1999). Distributions of partial pseudo-F statistics were generated with 9999 random permutations of the identities of profiles in the software Canoco. To test for fraction effects in 1999, four HF-1 and LF-1 profiles per cropping system needed to be used, instead of 12, to be balanced with the number of root/rhizosphere and shoot residue replicates. Aggregate size class was shown to not be a significant influence on HF-1 or LF-1 profiles in this dataset (see chapter 4), so 4-6.3 mm aggregates were randomly chosen to represent the different aggregate size classes in 1999. A 1999 alfalfa shoot residue RsaI profile and a 1999 conventional corn rhizosphere MspI profile were missing due to inability to obtain adequately strong T-RFLP profiles. These were replaced by the mean vector generated from the other three replicates of the respective treatment, following the method of Legendre and Anderson (1999). Relationships between profiles were also examined using Ward's method of hierarchical cluster analysis, principal components analysis, and canonical principal components plots obtained from the redundancy analysis. Percent C and N were also tested for significant effects on T-RFLP profiles using redundancy analysis.

The association of individual T-RFs with cropping systems and soil fractions was assessed using percentages of variability explained by the different factors in redundancy analysis, followed by examination of indicator values (IndVal) calculated according to Dufrêne and Legendre (1997). These were calculated for each T-RF-treatment combination, with and without interaction between treatments. IndVal is equal to the proportion of samples within the treatment where the T-RF is present times the mean



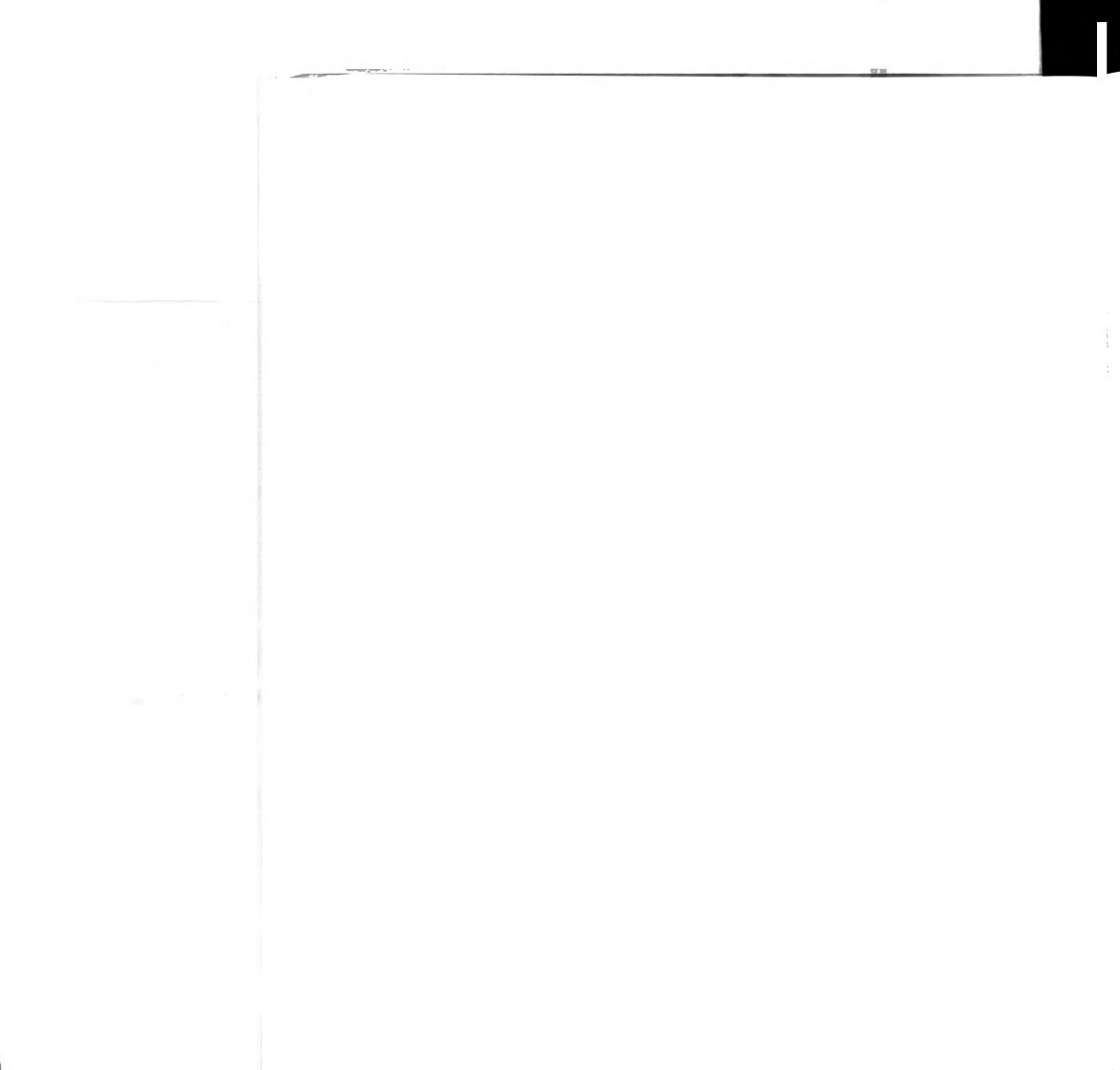
(Hellinger-transformed) T-RF abundance in that treatment divided by the sum of the mean abundances across all treatments. It is maximum when all occurrences of a T-RF are within the treatment being examined, and is sensitive to changes in both abundance and frequency between treatments.

T-RFs that were found to be consistently affected by treatment in 1998 and 1999 were compared to sequences in the Ribosomal Database Project version 8.1 (<http://rdp.cme.msu.edu>) using the online TAP-TRFLP software (Marsh et al. 2000).

Results

Fraction Mass and C and N Content

The proportion of the total C and N stored in the root/rhizosphere, shoot residue and LF-1 fractions is disproportionate (1-5% in each fraction) compared to the proportion of the total soil mass they take up (<0.5% in each fraction, see Table 1). The light fraction isolated using liquid with a specific gravity of 1.0 g/cc (LF-1) was 5 to 10 times less than that isolated using sodium polytungstate at a density of 1.7 g/cc (LF-1.7). Percent organic C in LF-1.7 was slightly less than in LF-1. Cropping system had a significant effect on the proportion of the total soil mass, percent C and N, and proportion of total C and N present in most soil fractions in 1998, tested using one-way ANOVA (see Table 1). Alfalfa soil consistently contained the lowest amounts of root/rhizosphere, shoot residue and LF-1, and conventional corn soil contained the greatest amounts. Proportion of total soil C and N stored in these fractions followed the same trends. The organic corn soil contained the greatest amount of LF-1.7, as well as C and N stored in that fraction. Percent C and N within shoot residue, LF-1, and LF-1.7 increased in the

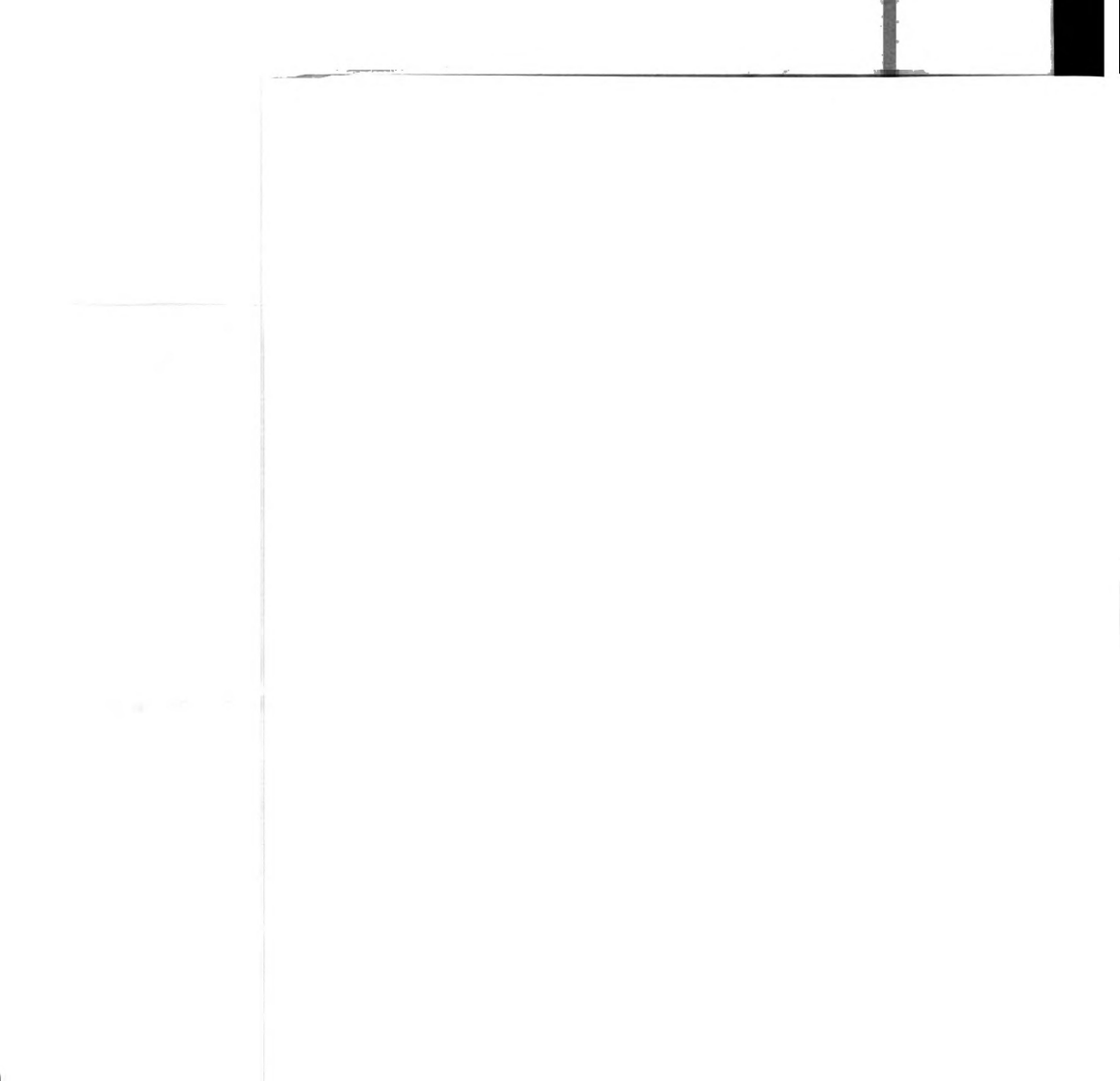


order of alfalfa, organic corn, and conventional corn (see Table 1). Percent C and N was lower in conventional corn HF-1 than in the other cropping systems. C to N ratio was approximately 18 in all fractions except HF-1, where it was 10-11. C to N ratio did not vary significantly due to cropping system. Proportion of total soil weight in the different soil fractions was similar for 1999 samples (data not shown), although more variable within cropping system treatments.

Microscopic Bacterial Cell Counts

Two-way ANOVA found that bacterial cell numbers expressed as cells/g fraction were significantly different between all fractions ($p < 0.0001$), with cells/g LF-1 being the highest and cells/g HF-1 being the lowest (see Figure 1). There were no significant effects of cropping system or interaction effects between fraction and cropping system on cell numbers. HF-1 contained 94-98% of all bacteria detected in soil, which was calculated as the weighted sum of the bacteria detected in all soil fractions (see Table 2). Number of cells detected in bulk soil was almost the same as that in HF-1, indicating that fractionation did not result in significant loss or destruction of bacteria.

Linear regression of cells/g fraction against percent C was significant at the 0.0001 significance level ($R^2 = 0.61$, see Figure 2). Variability of cells/g fraction increased with percent C, with two strong outliers present. Analysis without these outliers did not change the significance of the regression, but increased the R^2 to 0.76. Both outliers were alfalfa LF-1 samples. A partial F-test did not find that the ANOVA model with significant effects (soil fraction) fit cells/g fraction significantly better than the regression against percent C ($F = 1.5$, d.o.f.=3,58, $p = 0.20$). Nitrogen content of samples had no significant effects on any microscopic measurements.

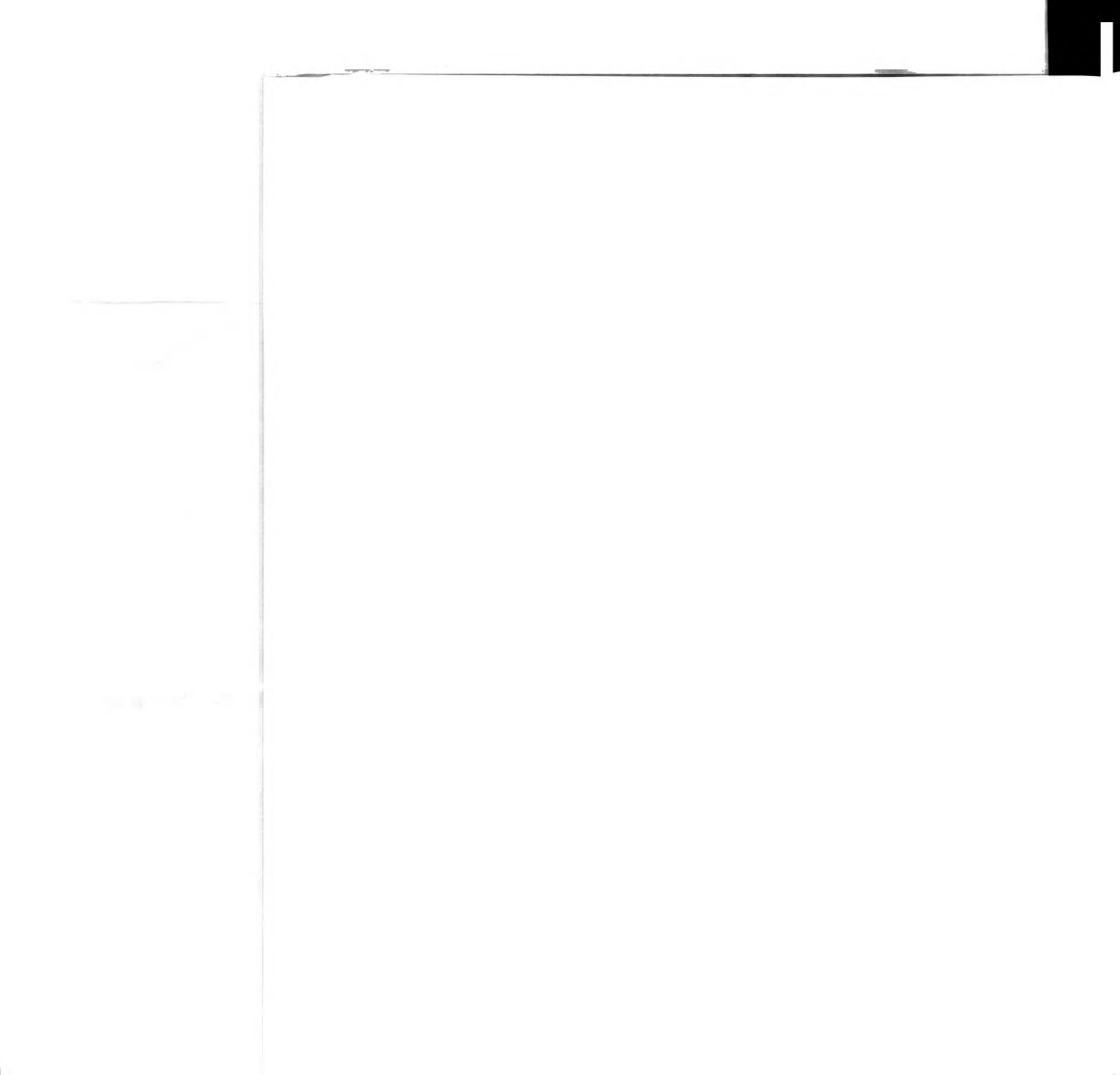


Despite the overall linear relationship between number of cells per g fraction and amount of C per g of fraction, the number of cells/ μg C was significantly affected by fraction ($p<0.0001$) and fraction-cropping system interaction ($p=0.0246$) in two-way ANOVA. The number of cells/ μg C is significantly greater in HF-1 than in other fractions, and within HF-1 the number of cells/ μg C is significantly greater in alfalfa than in either corn system (see Table 2). This can be seen in Figure 2 as a slightly increased rate of change of numbers of cells with C content in the HF-1 range of C content (0-5%) compared to the rate of change at greater C contents.

The percentage of cells in the largest size class ($>0.18 \mu\text{m}^3$) was significantly affected by both soil fraction ($p<0.0001$) and cropping system ($p<0.01$), but there was no interaction effect ($R^2=0.53$, see Table 2). Alfalfa samples contained a significantly larger proportion of large cells than either corn system (see Table 2). Percentage large cells increased with C content of fraction (see Figure 3), although the fit of the two-way ANOVA model was significantly better ($F=3.4$, d.o.f.=5,53, $p<0.01$). The percentage of cells in the smallest size class ($<0.065 \mu\text{m}^3$) followed the inverse of the trends in the largest size class, except that there was no significant cropping system effect (see Table 2). While cells in the smallest size class constituted the majority of cells in all samples (50 to 70%), they made up only 10 to 15% of the soil microbial biomass.

Eubacterial Community T-RFLP Analysis

The effects of cropping system and soil fraction were examined in four T-RFLP datasets: *RsaI* and *MspI* profiles of sets of samples collected in 1998 and 1999. There were 120 T-RFs detected in profiles generated by the restriction enzyme *RsaI* in 1998,



and 104 in 1999. There were 124 T-RFs detected in profiles generated by the restriction enzyme MspI in 1998, and 114 in 1999.

Redundancy analysis indicated that there were significant effects of cropping system and soil fraction on both RsaI and MspI T-RFLP profiles in both 1998 and 1999 (see Table 3). Interaction effects were also significant, indicating that the effects of soil fraction were not uniform for different cropping systems, and/or the effects of cropping systems were not uniform for different soil fractions. Treatment effects together accounted for 40 to 55% of the total variance in Hellinger-transformed profiles, and 35 to 38% of the total variance in Jaccard distances between profiles (see Table 3). Percent C and N, and C to N ratio of samples accounted for a significant amount of variation in the Hellinger-transformed T-RFLP profiles ($p=0.0001$, 15.5%, data not shown). Effects of nutrient concentration per se were not analyzed further because the variation between samples in C and N contents was mainly due to fraction and cropping system differences, and these treatments accounted for greater proportions of the total variability than did nutrient contents.

Figure 4 shows partial canonical principal components plots derived from the redundancy analysis of 1998 RsaI profiles, which are typical of all the datasets. These plots are efficient ways to examine why the redundancy analysis found overall significant treatment effects. In Figure 4a the effects of cropping system and the interaction between cropping system and soil fraction are partialled out, and the separation of samples due to soil fraction is maximized. A division between HF-1 and other fractions is the major cause of variability from soil fraction, and is captured in the first canonical axis. Rhizosphere samples are separated from LF-1 and shoot residue on the second axis. In

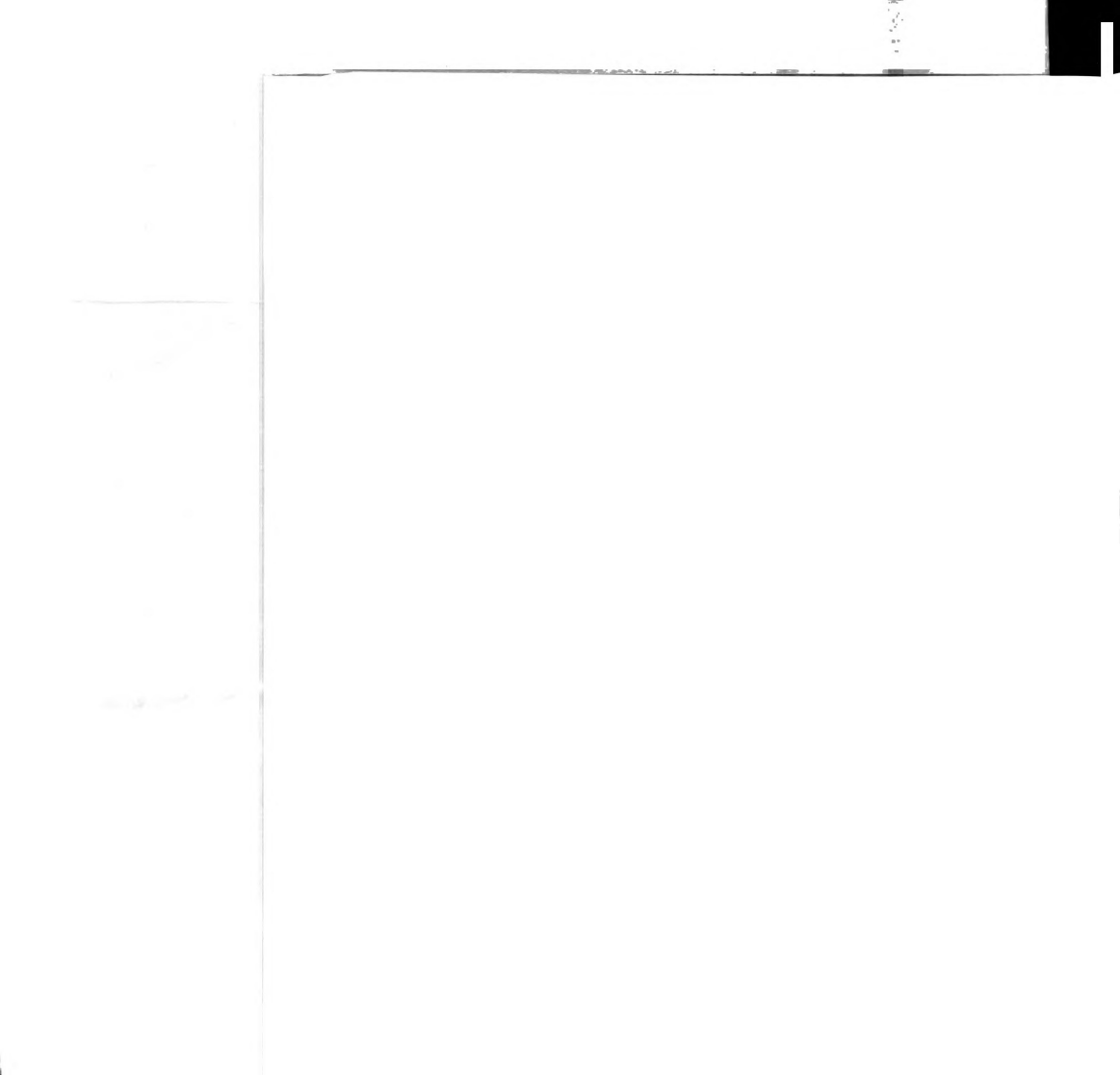
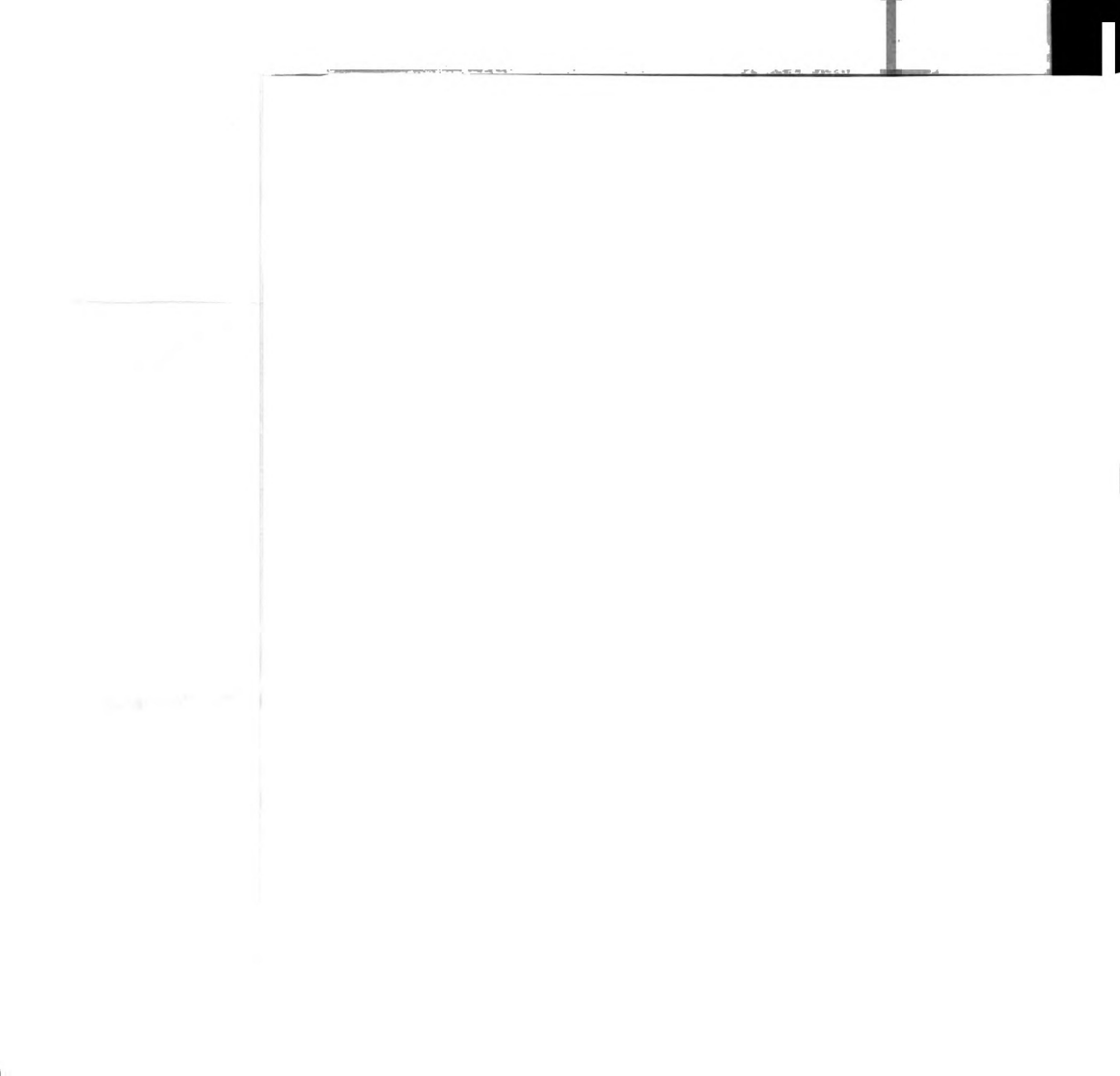


Figure 4b the interaction effects have been shown in addition to the variability due to soil fraction, with only effects of cropping system partialled out. While the same overall topology is present, interaction effects cause alfalfa samples to separate from the other cropping systems, and conventional corn rhizosphere samples become undifferentiated from other corn LF-1 and shoot residue samples.

Figure 4c shows the variability due only to cropping system, resulting in separation of alfalfa and conventional corn samples by the first canonical axis and separation of organic corn samples from other cropping systems by the second axis. Including interaction effects in the cropping systems plot had little effect on the grouping of samples and is not shown. Including all treatment effects results in Figure 4d, where a division between HF-1 of alfalfa and conventional corn from the other samples is captured on the first axis, along with separation of organic corn LF-1, HF-1, and shoot residue from other cropping system within each soil fraction. The second axis divides alfalfa from conventional corn samples in LF-1, HF-1, and shoot residue. Note that other divisions among the treatments that were evident in plots 4a,b,c are also included in the ordination including all treatment effects, but are not shown because they occur in higher-order canonical principal components. The percentage of the total variability accounted for by individual axes in Figure 4 is relatively low because of the large number of treatments involved in the dataset, requiring a large number of canonical principal components to account for all the variability due to treatment effects (see Table 3).

The 1998 MspI, 1999 RsaI, and 1999 MspI clustering dendrograms had the same general topology as the canonical ordination plots. The major division of samples evident was between an HF-1 group (including whole soil, analyzed in 1999) and another



group including LF-1, shoot residue and rhizosphere (see Figure 5). Samples from different cropping systems are separated within each of the major soil fraction groups. Alfalfa and conventional corn samples are always separated, with organic corn samples sometimes forming a third group and sometimes being split between groups characterized by the other cropping systems. Among the fractions, rhizosphere samples were most often outliers from a cropping system group.

The exception to this pattern is the 1998 *RsaI* dendrograms (see Figure 6), where alfalfa and conventional corn are divided first, with organic corn soil samples split between the groups. Limited grouping of soil fraction and cropping system samples occurs in smaller clusters.

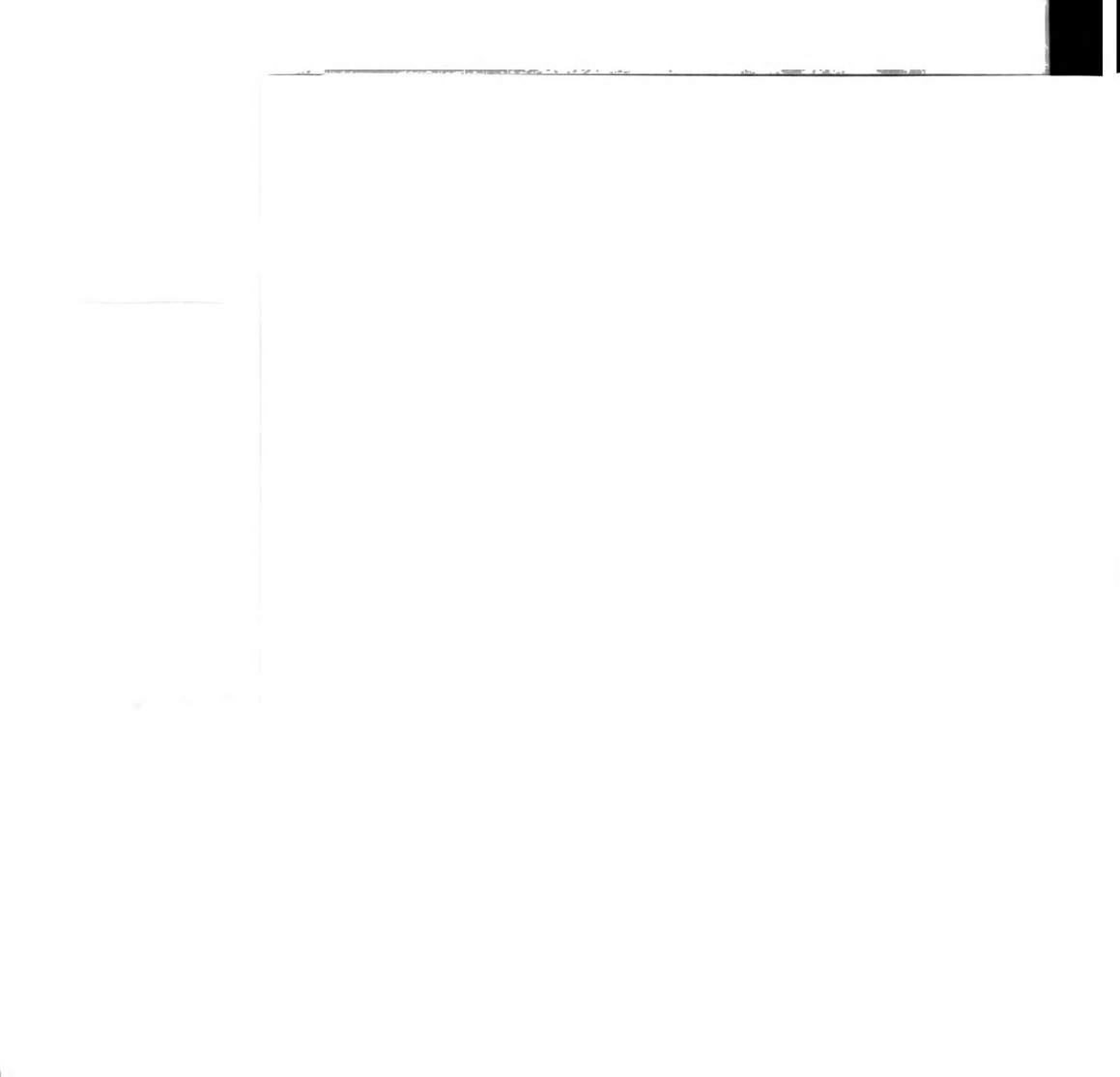
Twenty *RsaI* T-RFs in 1998, and 13 in 1999, had at least 20% of the variability in their Hellinger-transformed peak heights explained by soil fraction in the redundancy analysis, accounting for variability due to cropping system. Of these, 9 were T-RFs of the same size, potentially representing the same organisms in both years. Six of these were associated with the same fraction in each year, as indicated by *IndVal* scores (see Table 4). Out of 22 *MspI* T-RFs in 1998 and 27 T-RFs in 1999 that were associated with particular soil fractions, 3 *MspI* fragments were affected by soil fraction in both years in the same way. No sequence was found in the RDP database that would produce both an *RsaI* and an *MspI* T-RF that was found in this study to be consistently affected by soil fraction in the same way across years. One *MspI* fragment of size 405-408 bp that was found to be associated predominantly with roots/rhizosphere is close in size to the *MspI* fragment that would be generated from the garden pea chloroplast sequence in the database (404 bp). Hence the 405-408 bp *MspI* fragment detected in the rhizosphere may



be due to the presence of plant DNA in the genomic DNA extract from those samples. The overall importance of any particular T-RF to the statistical tests and community ordination described above is small, however, due to the large number of fragments that were found to be important in separating different fractions (>20 MspI fragments in each year). RsaI fragments generated from the garden pea chloroplast sequences are outside the range analyzed (i.e. >500 bp).

Sixteen RsaI T-RFs in 1998, and 18 in 1999, had at least 20% of the variability in their Hellinger-transformed peak heights explained by cropping system in the redundancy analysis, after accounting for the variability due to soil fraction. Six of these were the same size T-RFs and were associated with the same cropping systems across sampling years (see Table 4). Four MspI T-RFs were associated with cropping system in the same way both years, out of 35 in 1998 and 11 in 1999. No sequences were present in the database that would generate both an RsaI and an MspI T-RF that was found to be consistently affected by cropping system across years.

Twenty-four RsaI T-RFs in 1998, and 23 in 1999, had at least 20% of the variability in their Hellinger-transformed peak heights explained by interaction terms, or after correcting for the variability due to cropping system and soil fraction. Seven of these T-RFs were the same size. IndVal scores were low overall for these T-RFs when calculated for cropping system-soil fraction treatments, and the T-RFs were not strongly associated with the same treatments in different years. The case was quite different for MspI digests, where 28 T-RFs in 1998 and 27 in 1999 had at least 20% of the variability in their Hellinger-transformed peak heights explained by interaction terms, or by an

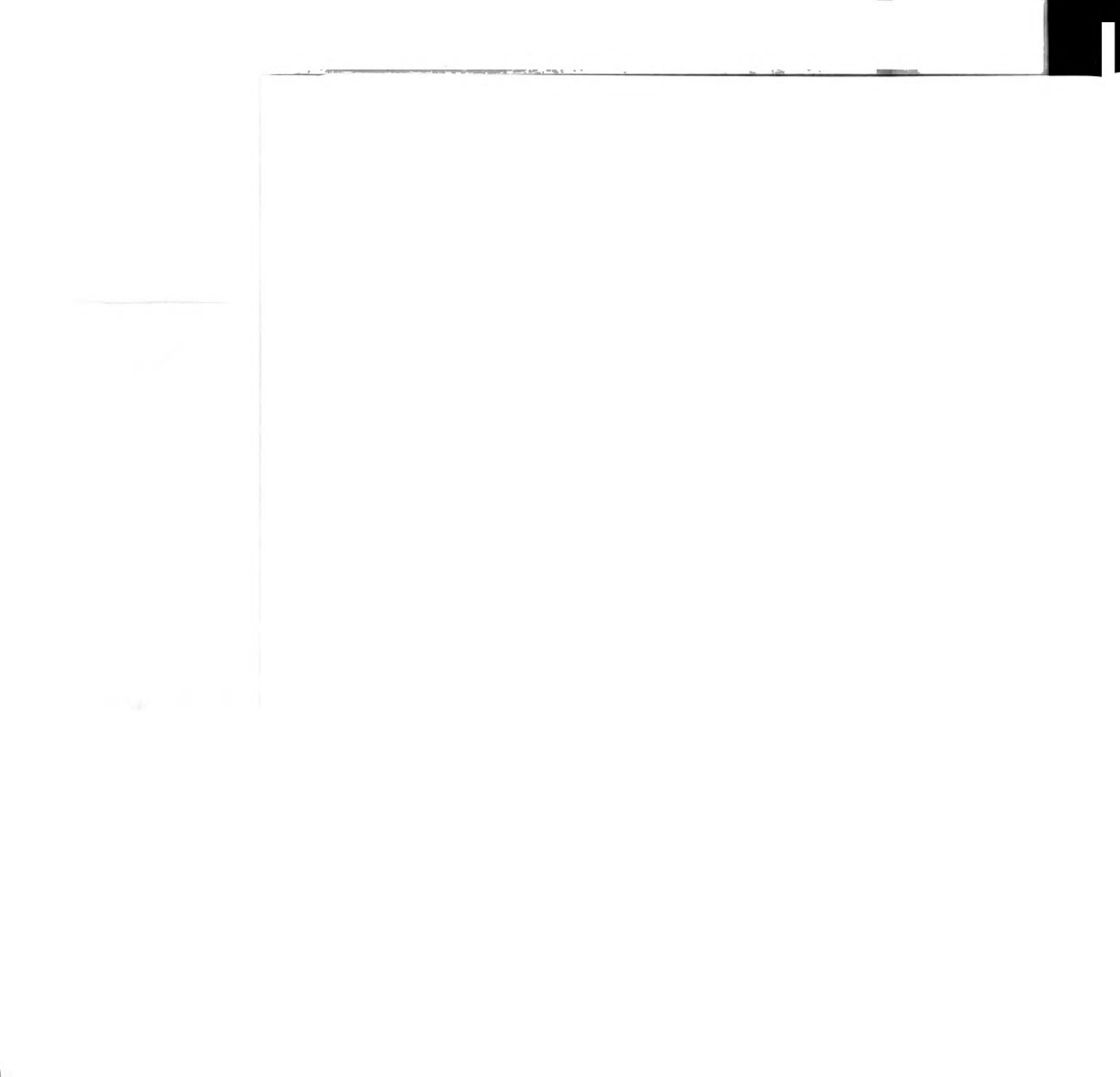


interaction term and cropping system or soil fraction. Seven of these fragments were the same size and were similarly affected in 1998 and 1999 (see Table 4).

Discussion

The light fraction has been shown to be a physically-defined soil fraction that harbors a eubacterial community that is distinct from that found in the majority of the soil, as assayed by T-RFLP. The LF-1 community is also different from the rhizosphere community, although these communities are more similar to each other than to HF-1. This is not surprising: LF-1 and the rhizosphere are both characterized by high amounts of labile C, increased bacterial growth rates and increased predator populations. They differ by the formation of mutualistic associations between roots and certain other organisms (e.g. mycorrhizal fungi, *Rhizobium*). Also the availability of complex carbohydrates and lignin contained within plant cell walls is probably much greater in LF, presenting very different catabolic enzyme requirements to the microbial community. LF-1, shoot residue, and the rhizosphere had C to N ratios of approximately 18, lower than that found in plant tissue (60-80), and higher than that in bulk soil or HF-1 (10-13). For LF-1 the intermediate C to N ratio is evidence of the microbial biomass present and the partially decomposed state of the organic particles, since all mineral soil particles are washed away. For the rhizosphere the increased C to N ratio represents the balance between the C to N ratios of the soil particles clinging to the roots and the roots themselves, which were included in rhizosphere in this study.

The shoot residue > 2 mm was the soil fraction with the eubacterial community that was most like the LF-1's. Shoot residue and LF-1 are soil fractions that are



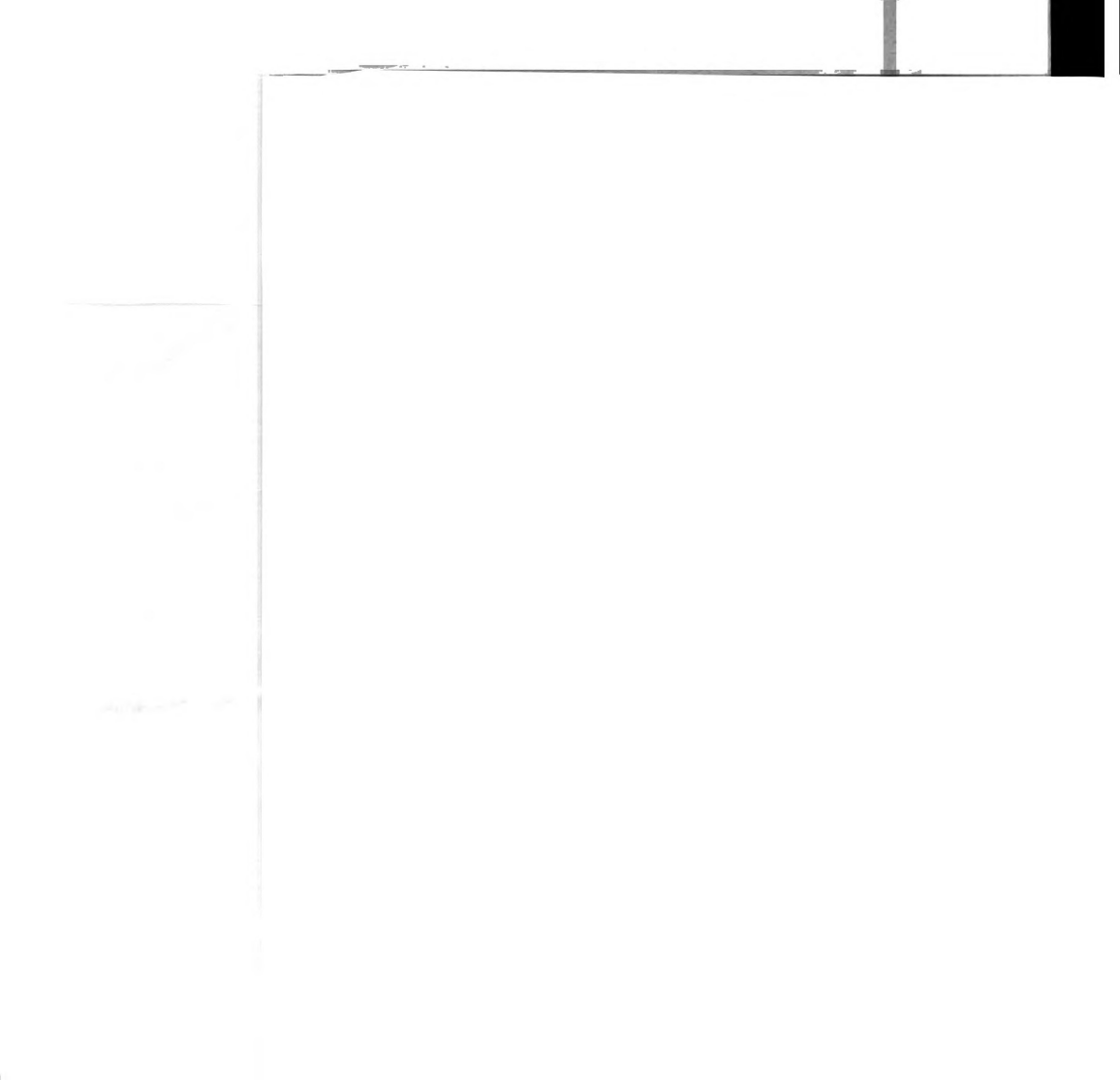
chemically and physically very similar, differing primarily by particle size and artifacts associated with their isolation. These include time and method of isolation, and the washing away of mineral soil particles clinging to the organic particles of LF-1 but not shoot residue. The LF-1/shoot residue effect cannot be attributed simply to the steps involved in fractionation because the communities of these fractions are so similar.

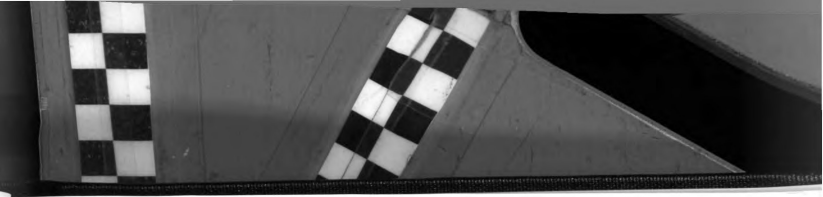
Cropping system also had a large effect on T-RFLP profiles. The increased variability of the organically-managed corn system, at the field replicate level, was expected since it involved a plant community that was temporally more diverse than either of the other two cropping systems. The organically-managed fields also received composted manure and leaves and more frequent tillage, which may affect the soil bacterial communities. Previous work at the KBS Living Field Lab has shown that addition of compost increases the content of particulate ($>53\ \mu\text{m}$) organic matter (Wilson et al. 2001). It is also probable that the addition of compost increases LF-1 in the organically-managed plots. This may be the cause for the differences in T-RFLP profiles in organic compared to conventionally-managed soils, as well as the increased variability in the organically-managed soil. These findings support previous reports of an effect of cropping system or other agricultural soil management on microbial community structure at other sites (Bossio et al. 1998, Lukow et al. 2000, Zelles et al. 1995). In contrast, Buckley (2000) used 16S ribosomal RNA oligonucleotide probing and did not find shifts in the composition of the bacterial community due to agronomic treatment at the KBS LTER site. This difference may be due to the fact that the probes used by Buckley (2000) detect shifts in relative abundance of phylogenetically very broad groups, whereas the T-RFLP procedure used in this study can potentially detect shifts in populations of



individual species. No changes in nitrifier community composition were detected due to agronomic treatments at the KBS LTER using DGGE of the nitrifier 16S ribosomal genes (Phillips et al. 2000). Increased ectomycorrhizal fungal species diversity has been observed in Poplar plots compared to annual crop plots (K. Kosola and E.A. Paul, in preparation). In a comparison of the more divergent environments at KBS, native never-tilled deciduous forest and agronomic or historically-tilled plots, changes in the relative abundance of phylogenetically broad bacterial groups and nitrifier species has been detected (Buckley 2000, Bruns 1999).

The stability of grouping soil fraction samples in dendrograms and ordinations, and of grouping cropping system within each soil fraction, decreased in the order HF-1, LF-1/shoot residue, and rhizosphere. Rhizosphere samples were never differentiated as a fraction-group in dendrograms, and were at times split between the HF-1 and LF-1 groups. Rhizosphere samples frequently caused noise in the grouping of cropping systems. This was the opposite of the expected trend, since the rhizosphere is frequently cited as exerting a selective pressure on microbial communities. The results here indicate that there is a group of organisms that are well-adapted to the HF-1 habitat, and changes in this habitat (e.g. due to cropping system) can result in quite stable shifts in community composition. The temporal scale of the cropping system treatments may be important in determining the stability of changes within fractions. In this study the treatments had been in place 6 to 10 years, whereas studies finding greater effects of plant species on the rhizosphere are often in place one year (e.g. Latour et al. 1996, Maloney et al. 1997). The rhizosphere community is consistently different from other habitats, but may be assembled more randomly, perhaps due to proliferation of randomly-encountered





dormant bacteria in HF-1 that have the life history traits enabling them to respond to high amounts of labile C. The same line of reasoning could apply to the LF-1/shoot residue habitat, except that it displayed increased stability, and may require more specialized organisms since the substrate is generally more complex.

Attempts to identify particular T-RFs that were found to be consistently important in defining differences between treatments were hindered by our use of very broad PCR primers. These primers amplify the 16S gene from most eubacterial organisms (Amman 1995), resulting in an analysis that broadly assays the community for major structural changes. The number of sequences that can produce any individual T-RF is potentially large. We attempted to work around this problem by performing digests with two restriction enzymes, but no sequences could be found in the database that would match similarly-acting T-RFs from the different digests. This could be due to the importance of organisms with no sequences currently represented in the database. It may be necessary to use more specific primers if the goal is to obtain phylogenetic information about the very complex communities, as has also been pointed out by Dunbar et al. (2001).

Expressed as a proportion of total numbers of cells in the soil, the bacterial populations present in LF and rhizosphere in this study may seem low; however they are very close to the proportion of the total amount of C found in the fractions (see Tables 1 and 2). This proportional relationship between bacterial cells and organic C is similar to what was found by Kanazawa and Filip (1986). The relationship was further generalized in this study because it was found that percent C could explain the majority of the variation in cell numbers across cropping systems and fractions. The slightly increased

100-100-100

ratio of cells to organic C present in HF-1 is probably due to the accumulation of inactive cells, as indicated by the larger percentage of small cells in this fraction.

These results contrast with those of Ahmed and Oades (1984), who found that 0.2-0.4% of the total soil ATP and 11-12% of the total C was contained in the LF. The liquid used for density separation by Ahmed and Oades (1984) was ZnBr_2 at a density of 1.6 g/cc, whereas in the present study and in Kanazawa and Filip (1986) water at a density of 1.0 g/cc was used. Osmotic pressure or other toxicity exerted by concentrated ZnBr_2 may have caused cell lysis and lead to destruction of ATP preferentially in the LF of Ahmed and Oades (1984), while a large portion of HF cells could have been protected inside microaggregates. Preliminary experiments with the fluorescent redox indicator 5-cyano-2,3-ditolyl tetrazolium chloride (CTC) indicated that sodium polytungstate solution with density of 1.7 g/cc inactivated cells; we therefore recommend the use of water for isolation of LF for microbiological work until a more complete analysis of the effects of dense liquids on microorganisms is carried out. The dispersion methods used by Ahmed and Oades (1984) prior to density separation were also more vigorous than those used in this study or by Kanazawa and Filip (1986). This could have resulted in the redistribution of bacterial cells prior to analysis. The alternative explanation is that the different dispersion technique and density used resulted in the isolation of a soil fraction with very different microbiological properties than what was isolated here.

Increased growth rate of bacteria in LF and decomposing shoot residue is supported by the finding in this study that there was an increase in the percentage of large cells in those fractions (Baath 1994), which was also explained in part by increased C concentration. While C content explained changes in cell numbers across soil fractions

ratio of cells to organic carbon was 1.0 to 1.0.

Cells as indicated by the presence of nucleic acids.

These results are consistent with the findings of

0.3-0.4% of the total organic carbon in the

liquid used for the isolation of the bacteria.

1.6 g/l. of the organic carbon in the liquid

density of 1.0 g/l. of the liquid used for

Zeller's may have been the cause of the

of Ahmed and Odeh (1968) in the isolation

inside microorganisms from the liquid

(cane-2,3-diol) from the liquid used for

solution with density of 1.0 g/l. of the

water for isolation of the bacteria from

effects of some (pH) of the liquid used

by Ahmed and Odeh (1968) in the isolation

incubated in this study and the results

reproduction of bacteria from the liquid

different species of bacteria from the

with very different results from the

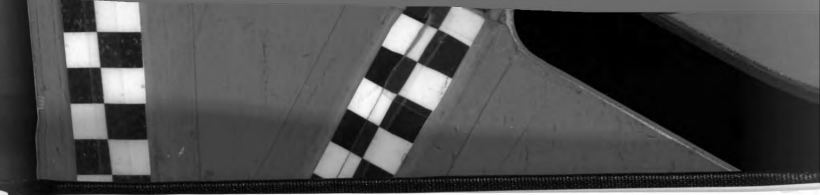
increased growth rate of the bacteria

suggested by the finding in the liquid

cells in these fractions (Table 1) and

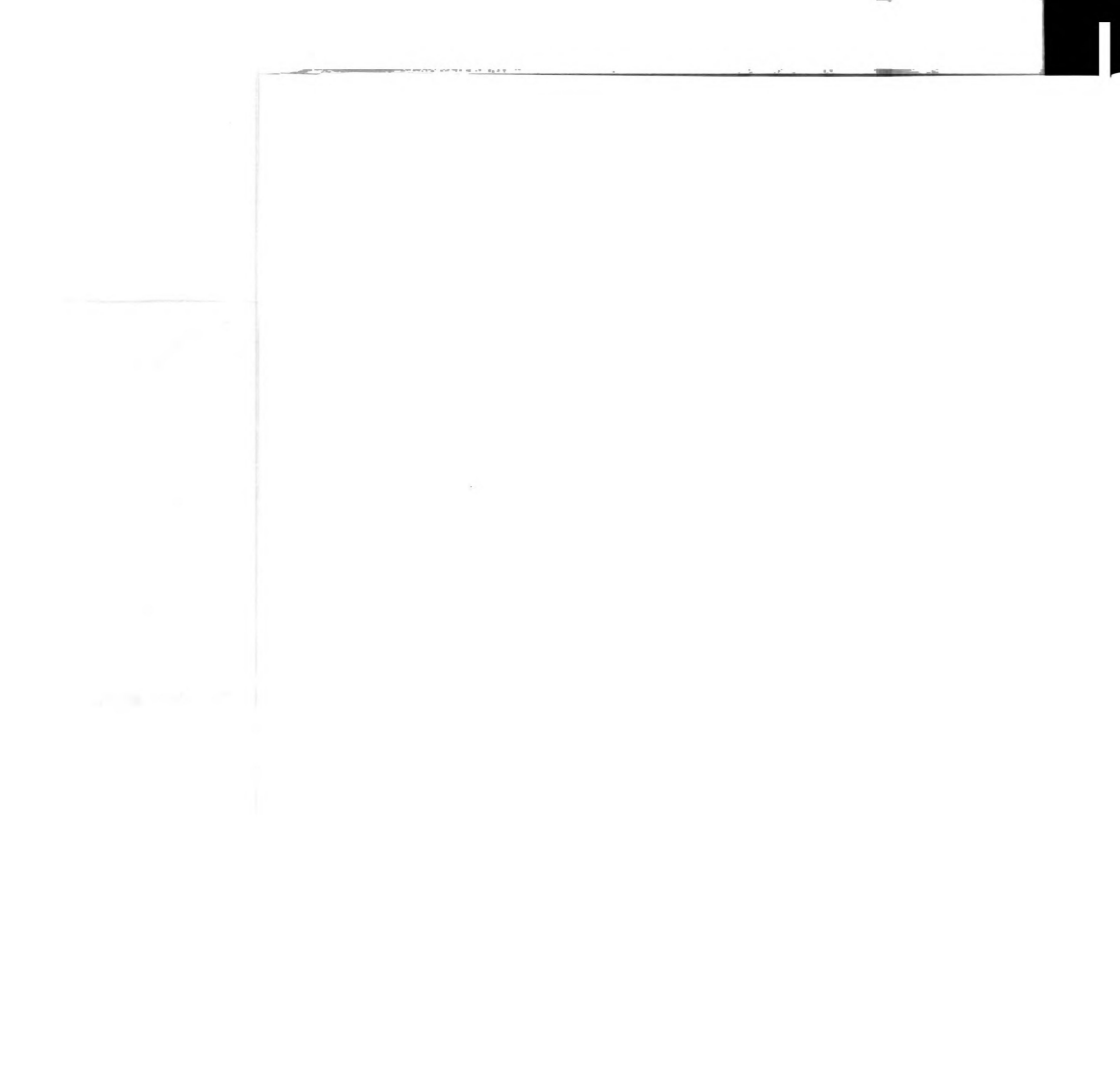
concentration. While C content was

concentration of the bacteria from the



and cropping systems, changes in eubacterial T-RFLP profiles and in the percentage of cells in the largest size class were not explained as well by C content of samples as by their treatment identities. Hence while C content is important in defining habitats in soil, other factors must also play a role. These could include the quality of the organic matter, physical disruption, or species interactions.

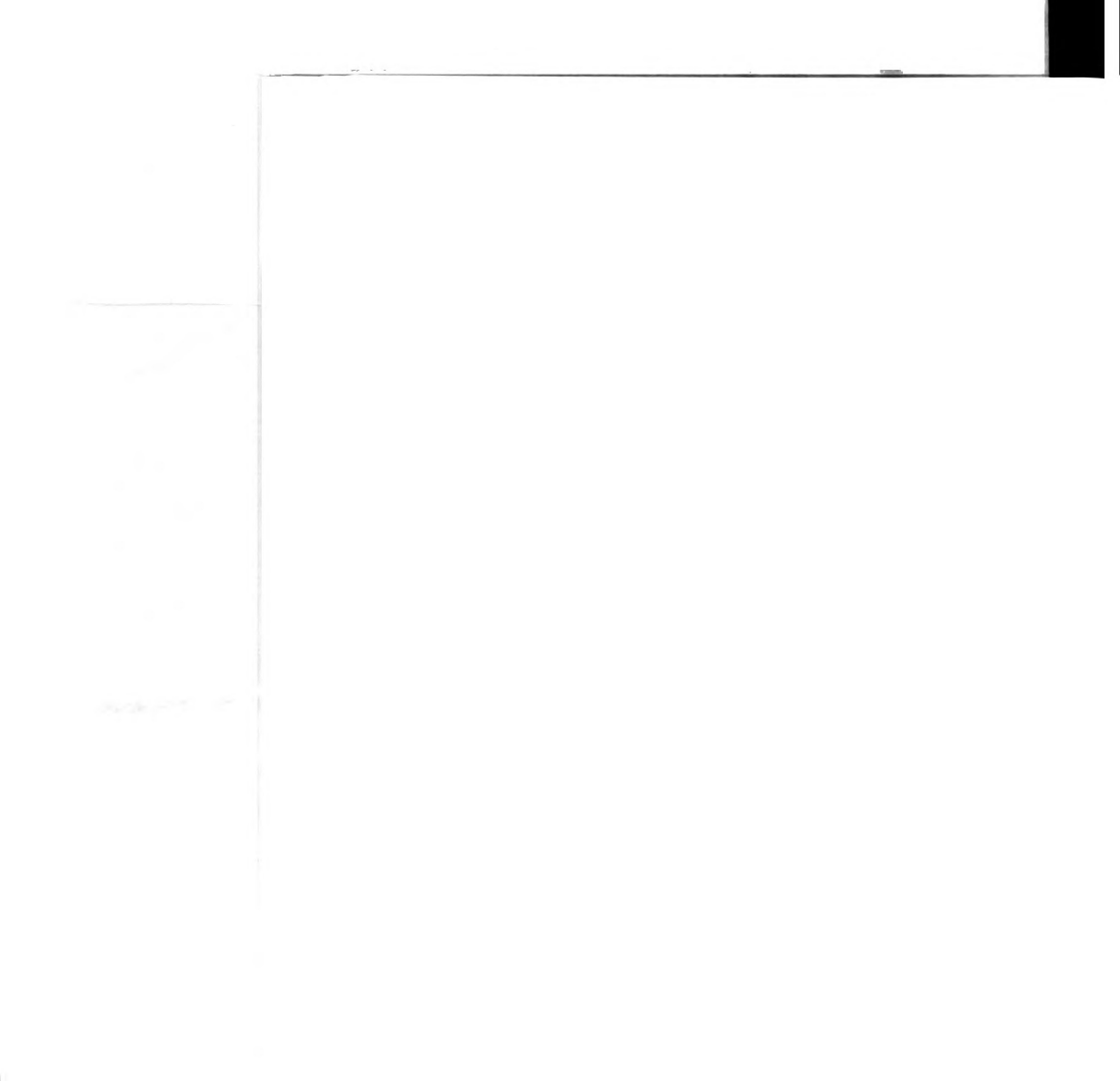
The hypothesis that habitat diversity enhances soil microbial diversity is supported by the detection of unique communities in different soil fractions. Future studies could examine the individual mechanisms of habitat diversity enhancing microbial diversity that were outlined in the Introduction. It is necessary to learn how microbial communities organize themselves to be able to manage the communities to the degree that is sometimes called for (e.g. Beare 1997, Kennedy 1999, Smith and Paul 1990). If communities are organized into separate habitats, these should be taken into consideration when looking for management effects because effects may be present in some habitats and not others. Different habitats may also represent opportunities for management, such as refuges from competition or locations of enhanced nutrient availability to be exploited by beneficial organisms.



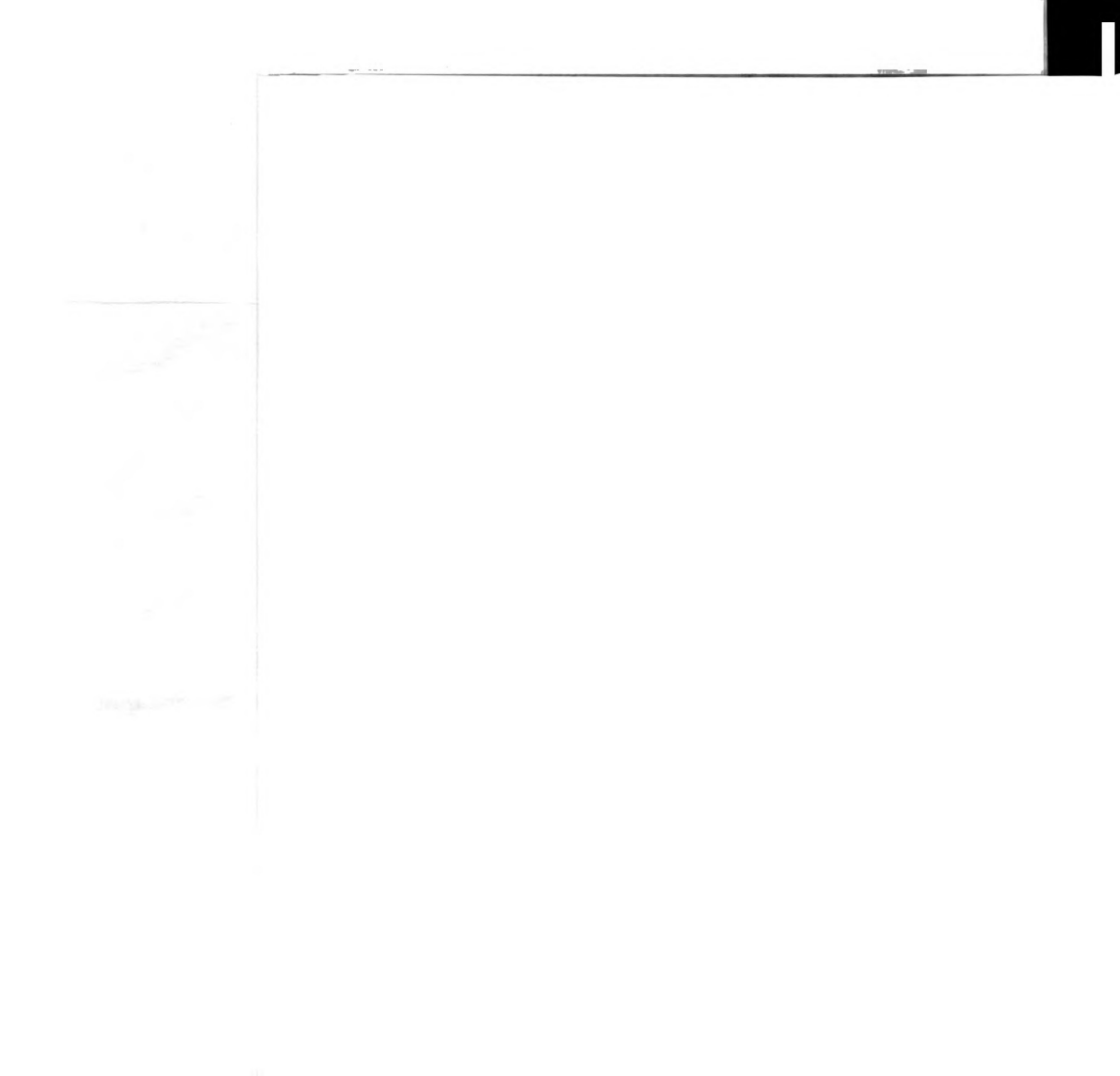
References

- Ahmed, M., J.M. Oades. 1984. Distribution of organic matter and adenosine triphosphate after fractionation of soils by physical procedures. *Soil Biology and Biochemistry* 16:465-470.
- Amann, R.L., W. Ludwig, K. Schleifer. 1995. Phylogenetic identification and in situ detection of individual microbial cells without cultivation. *Microbiological Reviews* 59:143-169.
- Baath, E. 1994. Thymidine and leucine incorporation in soil bacteria with different cell size. *Microbial Ecology* 27:267-278.
- Badalucco, L., P.J. Kuikman, P. Nannipieri. 1996. Protease and deaminase activities in wheat rhizosphere and their relation to bacterial and protozoan populations. *Biology and Fertility of Soils* 23:99-104.
- Beare, M.H. 1997. Fungal and bacterial pathways of organic matter decomposition and nitrogen mineralization in arable soils. In *Soil Ecology in Sustainable Agricultural Systems*, edited by L. Brussaard and R. Ferrara-Cerrato. Boca Raton: CRC Press.
- Biederbeck, V.O., H.H. Janzen, C.A. Campbell, R.P. Zentner. 1994. Labile soil organic matter as influenced by cropping practices in an arid environment. *Soil Biology and Biochemistry* 26:1647-1656.
- Bolton, H., Jr, J.K. Frederickson, L.F. Elliott. 1993. Microbial ecology of the rhizosphere. In *Soil Microbial Ecology: Applications in Agricultural and Environmental Management*, edited by F. B. Metting, Jr. New York: Marcel Dekker.
- Borneman, J., E.W. Triplett. 1997. Molecular microbial diversity in soils from Eastern Amazonia: evidence for unusual microorganisms and microbial population shifts associated with deforestation. *Applied and Environmental Microbiology* 63:2647-2653.
- Bossio, D.A., K.M. Scow, N. Gunapala, K.J. Graham. 1998. Determinants of soil microbial communities: effects of agricultural management, season, and soil type on phospholipid fatty acid profiles. *Microbial Ecology* 36:1-12.
- Bowen, G.D., A.D. Rovira. 1991. The rhizosphere: the hidden half of the hidden half. In *Plant Roots: The Hidden Half*, edited by Y. Waisel, A. Eshel and U. Kafafi. New York: Marcel Dekker.
- Breland, T.A., L.R. Bakken. 1991. Microbial growth and nitrogen immobilization in the root zone of barley (*Hordeum vulgare* L.), Italian ryegrass (*Lolium multiflorum* L.), and white clover (*Trifolium repens* L.). *Biology and Fertility of Soils* 12:154-160.

- Bremer, E., H.H. Janzen, A.M. Johnston. 1994. Sensitivity of total, light fraction and mineralizable organic matter to management practices in a Lethbridge soil. *Canadian Journal of Soil Science* 74:131-138.
- Bruns, M.A., J.R. Stephen, G.A. Kowalchuk, J.I. Prosser, E.A. Paul. 1999. Comparative diversity of ammonia oxidizer 16S rRNA gene sequences in native, tilled, and successional soils. *Applied and Environmental Microbiology* 65:2994-3000.
- Buckley, D. H. 2000. The Diversity and Dynamics of Microbial Groups in Soils from Agroecosystems. PhD Dissertation. Michigan State University, East Lansing.
- Budi, S.W., D.V. Tuinen, G. Martinotti, S. Gianinazzi. 1999. Isolation from the *Sorghum bicolor* mycorrhizosphere of a bacterium compatible with arbuscular mycorrhiza development and antagonistic towards soilborne fungal pathogens. *Applied and Environmental Microbiology* 65:5148-5150.
- Buyanovsky, G.A., M. Aslam, G.H. Wagner. 1994. Carbon turnover in soil physical fractions. *Soil Science Society of America Journal* 58:1167-1173.
- Cambardella, C.A., E.T. Elliott. 1993. Carbon and nitrogen in aggregates from cultivated and native grassland soils. *Soil Science Society of America Journal* 57:1071-1076.
- Chotte, J.L., J.N. Ladd, M. Amato. 1998. Sites of microbial assimilation, and turnover of soluble and particulate ¹⁴C-labelled substrates decomposing in a clay soil. *Soil Biology and Biochemistry* 30:205-218.
- Christensen, B.T. 1996. Carbon in primary and secondary organomineral complexes. In *Structure and Organic Matter Storage in Agricultural Soils*, edited by M. R. Carter and B. A. Stewart. Boca Raton: CRC Press.
- Christensen, H., I. Jakobsen. 1993. Reduction of bacterial growth by a vesicular-arbuscular mycorrhizal fungus in the rhizosphere of cucumber (*Cucumis sativus* L.). *Biology and Fertility of Soils* 15:253-258.
- Denton, C.S., R.D. Bardgett, R. Cook, P.J. Hobbs. 1999. Low amounts of root herbivory positively influence the rhizosphere microbial community in a temperate grassland soil. *Soil Biology and Biochemistry* 31:155-165.
- Dufrêne, M., P. Legendre. 1997. Species assemblages and indicator species: the need for a flexible asymmetric approach. *Ecological Monographs* 67:345-366.
- Dunbar, J., L.O. Ticknor, C.R. Kuske. 2001. Phylogenetic specificity and reproducibility and new method for analysis of terminal restriction fragment profiles of 16S rRNA genes from bacterial communities. *Applied and Environmental Microbiology* 67:190-197.



- Gaillard, V., C. Chenu, S. Recous, G. Richard. 1999. Carbon, nitrogen and microbial gradients induced by plant residues decomposing in soil. *European Journal of Soil Science* 50:567-578.
- Golchin, A., J.M. Oades, J.O. Skjemstad, P. Clarke. 1994a. Soil structure and carbon cycling. *Australian Journal of Soil Research* 32:1043-1068.
- Golchin, A., J.M. Oades, J.O. Skjemstad, P. Clarke. 1994b. Study of free and occluded particulate organic matter in soils by solid state ^{13}C CP/MAS NMR spectroscopy and scanning electron microscopy. *Australian Journal of Soil Research* 32:285-309.
- Golchin, A., J.M. Oades, J.O. Skjemstad, P. Clarke. 1995. Structural and dynamic properties of soil organic matter as reflected by ^{13}C natural abundance, pyrolysis mass spectrometry and solid-state ^{13}C NMR spectroscopy in density fractions of an Oxisol under forest and pasture. *Australian Journal of Soil Research* 33:59-76.
- Gregorich, E.G., M.R. Carter, D.A. Angers, C.M. Monreal, B.H. Ellert. 1994. Towards a minimum data set to assess soil organic matter quality in agricultural soils. *Canadian Journal of Soil Science* 74:367-385.
- Gregorich, E.G., B.H. Ellert, C.M. Monreal. 1995. Turnover of soil organic matter and storage of corn residue carbon estimated from natural ^{13}C abundance. *Canadian Journal of Soil Science* 75:161-167.
- Gregorich, E.G., H.H. Janzen. 1996. Storage of soil carbon in the light fraction and macroorganic matter. In *Structure and Organic Matter Storage in Agricultural Soils*, edited by M. R. Carter and B. A. Stewart. Boca Raton: CRC Press.
- Hanski, I. 1995. Effects of landscape pattern on competitive interactions. In *Mosaic Landscapes and Ecological Processes*, edited by L. Hansson, L. Fahrig and G. Merriam. London: Chapman & Hall.
- Hassink, J. 1995. Density fractions of soil macroorganic matter and microbial biomass as predictors of C and N mineralization. *Soil Biology and Biochemistry* 27:1099-1108.
- Huston, M.A. 1999. Local processes and regional patterns: appropriate scales for understanding variation in the diversity of plants and animals. *Oikos* 86:393-401.
- Janzen, H.H., C.A. Campbell, S.A. Brandt, G.P. Lafond, L. Townley-Smith. 1992. Light-fraction organic matter in soils from long-term crop rotations. *Soil Science Society of America Journal* 56:1799-1806.
- Jones, M.E., R.R. Harwood, N.C. Dehne, J. Smeenk, E. Parker. 1998. Enhancing soil nitrogen mineralization and corn yield with overseeded cover crops. *Soil and Water Conservation* 53:245-249.



Kanazawa, S., Z. Filip. 1986. Distribution of microorganisms, total biomass, and enzyme activities in different particles of brown soil. *Microbial Ecology* 12:205-215.

Kennedy, A.C. 1999. Microbial diversity in agroecosystem quality. In *Biodiversity in Agroecosystems*, edited by W. W. Collins and C. O. Qualset. Boca Raton: CRC Press.

Latour, X., T. Corberand, G. Laguerre, F. Allard, P. Lemanceau. 1996. The composition of fluorescent *Pseudomonad* populations associated with roots as influenced by plant and soil type. *Applied and Environmental Microbiology* 62:2449-2456.

Legendre, P., M.J. Anderson. 1999. Distance-based redundancy analysis: testing multispecies responses in multifactorial ecological experiments. *Ecological Monographs* 69:1-24.

Lukow, T., P.F. Dunfield, W. Liesack. 2000. Use of the T-RFLP technique to assess spatial and temporal changes in the bacterial community structure within an agricultural soil planted with transgenic and non-transgenic potato plants. *FEMS Microbiology Ecology* 32:241-247.

Mahaffee, W.F., J.W. Kloepper. 1997. Temporal changes in the bacterial communities of soil, rhizosphere, and endorhiza associated with field-grown cucumber (*Cucumis sativus* L.). *Microbial Ecology* 34:210-223.

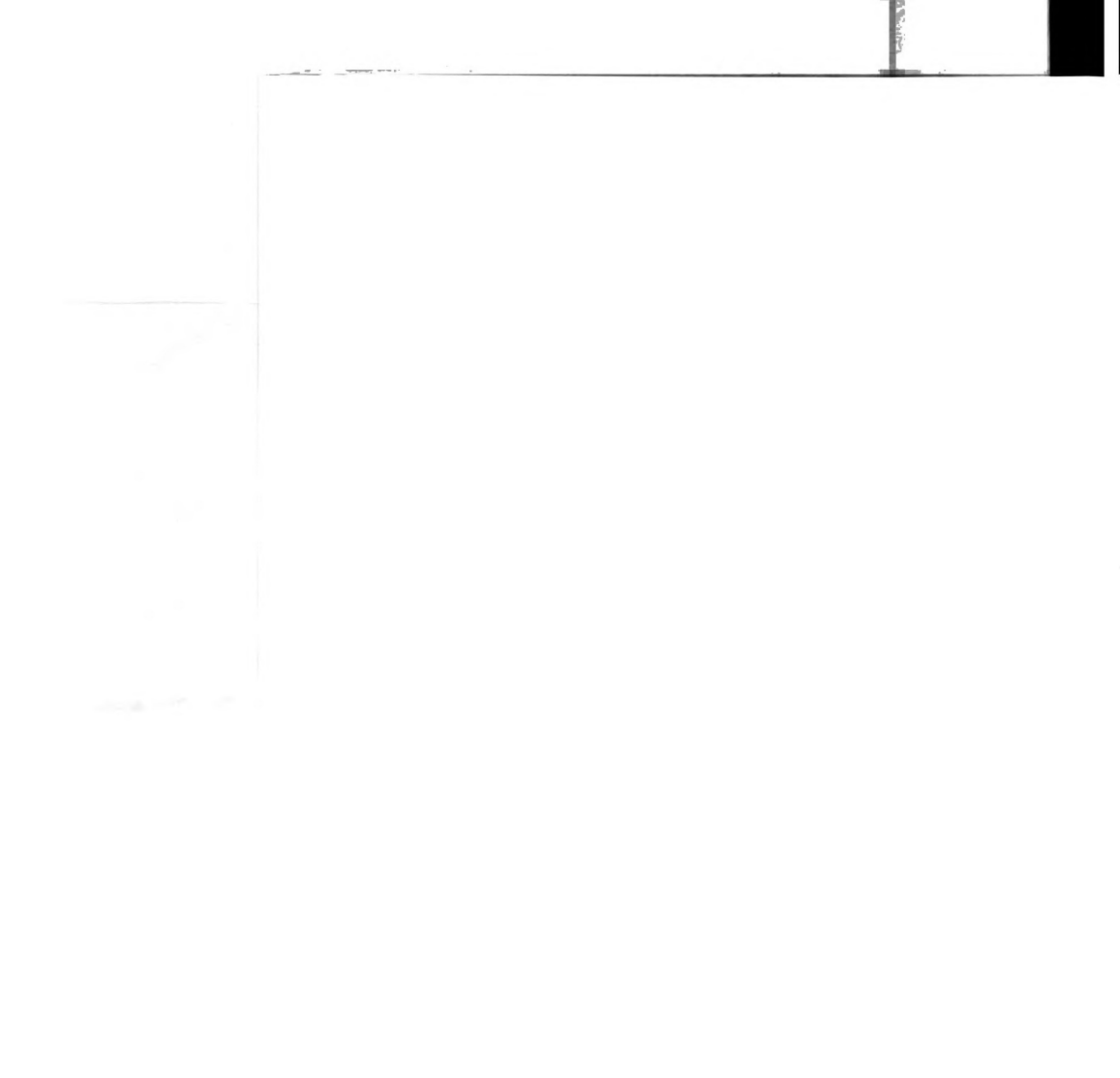
Maloney, P.E., A.H.C.v. Bruggen, S. Hu. 1997. Bacterial community structure in relation to the carbon environments in lettuce and tomato rhizospheres and in bulk soil. *Microbial Ecology* 34:109-117.

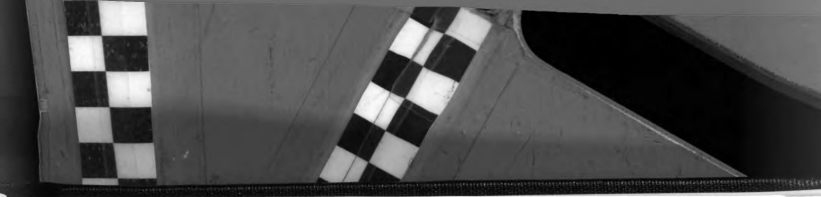
Marilley, L., M. Aragno. 1999. Phylogenetic diversity of bacterial communities differing in degree of proximity of *Lolium perenne* and *Trifolium repens* roots. *Applied Soil Ecology* 13:127-136.

Marsh, T.L., P. Saxman, J. Cole, J. Tiedje. 2000. Terminal restriction fragment length polymorphism analysis program, a web-based research tool for microbial community analysis. *Applied and Environmental Microbiology* 66:3616-3620.

Nakatsu, C.H., V. Torsvik, L. Øvreås. 2000. Soil community analysis using DGGE of 16S rDNA polymerase chain reaction products. *Soil Science Society of America Journal* 64:1382-1388.

Nüsslein, K., J.M. Tiedje. 1998. Characterization of the dominant and rare members of a young Hawaiian soil bacterial community with small-subunit ribosomal DNA amplified from DNA fractionated on the basis of its guanine and cytosine composition. *Applied and Environmental Microbiology* 64:1283-1289.





Pacala, S.W., S.A. Levin. 1997. Biologically generated spatial pattern and the coexistence of competing species. In *Spatial Ecology: The Role of Space in Population Dynamics and Interspecific Interactions*, edited by D. Tilman and P. Kareiva. Princeton: Princeton University Press.

Paul, E.A., F.E. Clark. 1996. *Soil Microbiology and Biochemistry*. 2 ed. San Diego: Academic Press.

Paul, E.A., D. Harris, M.J. Klug, R.W. Ruess. 1999. The determination of microbial biomass. In *Standard Soil Methods for Long Term Ecological Research*, edited by G. P. Robertson, D. C. Coleman, C. S. Bledsoe and P. Sollins. New York: Oxford University Press.

Phillips, C.J., D. Harris, S.L. Dollhopf, K.L. Gross, J.I. Prosser, E.A. Paul. 2000. Effects of agronomic treatment on structure and function of ammonia-oxidizing communities. *Applied and Environmental Microbiology* 66:5410-5418.

Ringelberg, D.B., J.O. Stair, J. Almeida, R.J. Norby, E.G. O'Neill, D.C. White. 1997. Consequences of rising atmospheric carbon dioxide levels for the belowground microbiota associated with the white oak. *Journal of Environmental Quality* 26:495-503.

Robertson, G.P., K.M. Klingensmith, M.J. Klug, E.A. Paul, J.R. Crum, B.G. Ellis. 1997. Soil resources, microbial activity, and primary production across an agricultural ecosystem. *Ecological Applications* 7:158-170.

Rønn, R., B.S. Griffiths, F. Ekelund, S. Christensen. 1996. Spatial distribution and successional pattern of microbial activity and micro-faunal populations on decomposing barley roots. *Journal of Applied Ecology* 33:662-667.

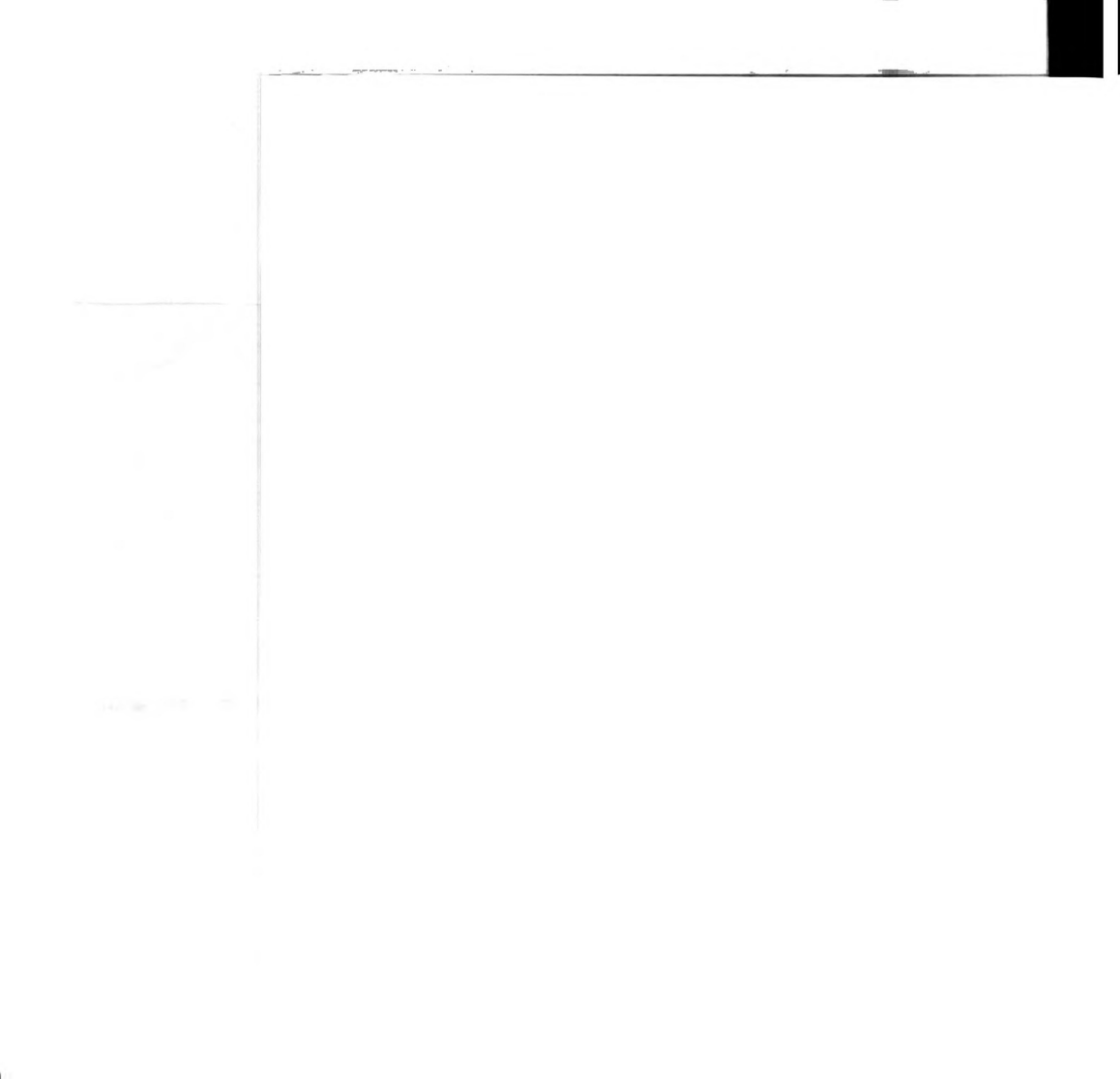
Rouatt, J.W., H. Katznelson, T.M.B. Payne. 1960. Statistical evaluation of the rhizosphere effect. *Soil Science Society of America Proceedings* 24:271-273.

Sandaa, R.A., V. Torsvik, Ø. Enger, F.L. Daac, T. Castberg, D. Hahn. 1999. Analysis of bacterial communities in heavy metal-contaminated soils at different levels of resolution. *FEMS Microbiology Ecology* 30:237-251.

Sengeløv, G., G.A. Kowalchuk, S.J. Sørensen. 2000. Influence of fungal-bacterial interactions on bacterial conjugation in the residuesphere. *FEMS Microbiology Ecology* 31:39-45.

Smith, J.L., E.A. Paul. 1990. The significance of soil microbial biomass estimations. In *Soil Biochemistry*, edited by J. Bollag and G. Stotzky. New York: Marcel Dekker.

Söderberg, K.H., E. Bååth. 1998. Bacterial activity along a young barley root measured by the thymidine and leucine incorporation techniques. *Soil Biology and Biochemistry* 30:1259-1268.



- Staricka, J.A., R.R. Allmaras, W.W. Nelson. 1991. Spatial variation of crop residue incorporated by tillage. *Soil Science Society of America Journal* 55:1668-1674.
- Thom, C. 1935. Micropopulations correlated to decomposition processes. *Transactions of the Third International Congress of Soil Science* 1:160-163.
- Tilman, D. 1982. *Resource Competition and Community Structure*. Princeton, NJ: Princeton University Press.
- Torsvik, V., J. Goksoyr, F.L. Daae. 1990. High diversity of DNA of soil bacteria. *Applied and Environmental Microbiology* 56:782-787.
- Tunlid, A., B.H. Baird, M.B. Trexler, S. Olsson, R.H. Findlay, G. Odham, D.C. White. 1985. Determination of phospholipid ester-linked fatty acids and poly B-hydroxybutyrate for the estimation of bacterial biomass and activity in the rhizosphere of the rape plant *Brassica napus* (L.). *Canadian Journal of Microbiology* 31:1113-1119.
- Willson, T.C., E.A. Paul, R.R. Harwood. 2001. Biologically active soil organic matter fractions in sustainable cropping systems. *Applied Soil Ecology* 16:63-76.
- Yakovchenko, V.P., L.J. Sikora, P.D. Millner. 1998. Carbon and nitrogen mineralization of added particulate and macroorganic matter. *Soil Biology and Biochemistry* 30:2139-2146.
- Zelles, L., R. Rackwitz, Q.Y. Bai, T. Beck, F. Beese. 1995. Discrimination of microbial diversity by fatty acid profiles of phospholipids and lipopolysaccharides in differently cultivated soils. *Plant and Soil* 170:115-122.



Table 1: Biogeochemical characteristics of soil fractions. P-values indicate the significance of the effect of cropping system within the fraction in a one-way ANOVA. NS implies cropping system not significant at P=0.05 level. Values in parentheses are standard deviations; N=4.

Fraction	Cropping System	% soil by weight	% C	% N	% of total soil C	% of total soil N	C:N
Roots/ Rhizosphere	Alfalfa	0.22 (0.06)	10.2 (1.4)	0.6 (0.06)	1.7 (0.4)	1.1 (0.3)	17 (1)
	Cont. Corn	0.45 (0.12)	6.4 (1.2)	0.4 (0.06)	2.8 (0.7)	1.7 (0.5)	18 (1)
	Org. Corn	0.42 (0.07)	5.6 (0.9)	0.3 (0.05)	1.7 (0.4)	1.2 (0.3)	16 (1)
	P	0.0078	0.0008	0.0002	0.0260	NS	NS
Shoot Residue >2 mm	Alfalfa	0.13 (0.07)	21.7 (6.1)	1.2 (0.3)	2.1 (0.9)	1.3 (0.8)	18 (3)
	Cont. Corn	0.37 (0.12)	14.4 (0.7)	0.7 (0.07)	5.2 (1.7)	2.6 (0.8)	22 (2)
	Org. Corn	0.33 (0.04)	17.0 (2.2)	0.9 (0.1)	4.0 (1.0)	2.5 (0.5)	18 (3)
	P	0.0069	NS	0.0086	0.0217	NS	NS
LF-1	Alfalfa	0.05 (0.01)	27.3 (3.1)	1.6 (0.09)	1.0 (0.3)	0.6 (0.1)	18 (1)
	Cont. Corn	0.13 (0.03)	21.5 (2.0)	1.2 (0.06)	2.7 (0.5)	1.7 (0.4)	18 (2)
	Org. Corn	0.10 (0.01)	23.8 (0.9)	1.4 (0.1)	1.7 (0.2)	1.1 (0.2)	18 (1)
	P	0.0005	0.0145	0.0021	0.0003	0.0008	NS
HF-1	Alfalfa	99.6 (0.1)	1.2 (0.1)	0.1 (0.01)	95 (1.4)	97 (1.1)	10 (1)
	Cont. Corn	99.0 (0.1)	0.9 (0.03)	0.09 (0.004)	89 (1.6)	94 (1.0)	11 (1)
	Org. Corn	99.1 (0.06)	1.3 (0.1)	0.1 (0.004)	93 (0.9)	95 (0.1)	11 (1)
	P	<0.0001	0.0003	0.0015	0.0007	0.0037	NS
LF-1.7	Alfalfa	0.40 (0.07)	21.4 (1.8)	1.3 (0.2)	7.1 (1.2)	3.4 (2.4)	18 (1)
	Cont. Corn	0.69 (0.08)	17.6 (3.0)	1.1 (0.2)	11.3 (3.4)	5.9 (4.2)	18 (2)
	Org. Corn	1.02 (0.2)	20.2 (1.7)	1.3 (0.2)	14.4 (2.4)	10.6 (3.0)	18 (1)
	P	0.0031	NS	NS	0.0142	0.0341	NS



Table 2: Numbers of bacterial cells and percent of cells in different cell size classes. P-values indicate the significance of the effect of cropping system within the fraction in a one-way ANOVA. NS implies cropping system not significant at P=0.05 level. Values in parentheses are standard deviations; N=4. * - see text for description of significant two-way ANOVA results.

Fraction	Cropping System	Bacterial cells/ $\mu\text{g C}$ $\times 10^5$ *	% of total soil bacteria	% cells $> 0.18 \mu\text{m}^3$ *	% cells $< 0.065 \mu\text{m}^3$ *
Roots/ Rhizosphere	Alfalfa	2.6 (1.4)	0.7 (0.3)	13.5 (2.2)	65.2 (0.8)
	Cont. Corn	4.5 (1.3)	2.1 (1.1)	14.0 (0.8)	62.5 (2.7)
	Org. Corn	4.8 (1.6)	2.0 (0.4)	13.3 (2.0)	65.3 (2.1)
	P	NS	0.0327	NS	NS
Shoot Residue >2 mm	Alfalfa	2.1 (0.5)	0.6 (0.3)	17.7 (2.8)	57.8 (5.8)
	Cont. Corn	2.9 (0.1)	2.5 (1.3)	15.8 (2.8)	61.1 (4.9)
	Org. Corn	2.5 (1.4)	2.3 (0.9)	15.0 (1.6)	61.1 (3.5)
	P	NS	0.0340	NS	NS
LF-1	Alfalfa	3.9 (2.9)	0.5 (0.3)	19.6 (2.4)	59.1 (4.6)
	Cont. Corn	3.0 (0.5)	1.3 (0.2)	16.7 (1.0)	57.2 (3.9)
	Org. Corn	2.7 (0.7)	1.2 (0.4)	17.3 (1.5)	57.3 (2.9)
	P	NS	0.0166	NS	NS
HF-1	Alfalfa	7.2 (2.0)	98.1 (0.5)	14.6 (1.1)	64.1 (2.5)
	Cont. Corn	6.7 (1.6)	94.1 (2.2)	13.3 (2.0)	65.3 (4.3)
	Org. Corn	4.0 (0.6)	94.6 (0.8)	14.5 (1.4)	60.9 (3.1)
	P	0.0374	0.0054	NS	NS

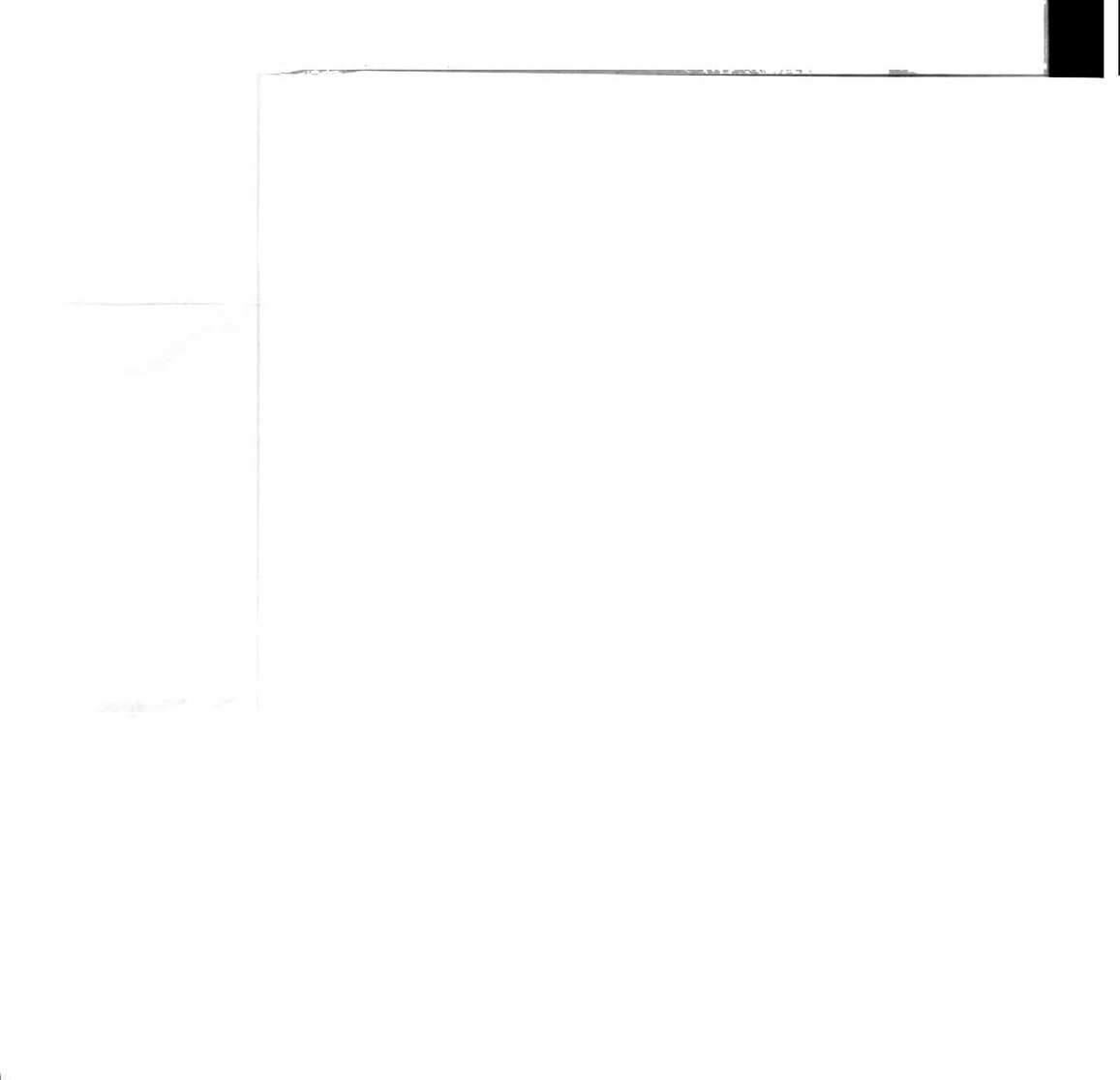


Table 3: Redundancy analysis testing treatment effects on T-RFLP profiles derived from differing soil fractions and cropping systems. P-values were generated by 9999 random permutations of the data; N=4 except MspI where N=3.

		Soil Fraction	Cropping System	Interaction	Sum
Hellinger Distance					
1998 RsaI	P	0.0001	0.0001	0.0001	
	% of total variance	16.6	16.2	14.8	47.6
1998 MspI	P	0.0001	0.0001	0.0037	
	% of total variance	22.3	18.5	14	54.8
1999 RsaI	P	0.0001	0.0001	0.0001	
	% of total variance	16.4	15.6	14.2	46.2
1999 MspI	P	0.0001	0.0001	0.0001	
	% of total variance	17.2	10.3	13.7	41.2
Jaccard Distance					
1998 RsaI	P	0.0001	0.0001	0.0001	
	% of total variance	10.9	11.6	15.3	37.8
1998 MspI	P	0.0001	0.0001	0.0055	
	% of total variance	16.8	14.6	15.2	36.6
1999 RsaI	P	0.0001	0.0001	0.0001	
	% of total variance	10.5	11.5	13.6	35.6
1999 MspI	P	0.0001	0.0001	0.0001	
	% of total variance	12.5	9.5	13.9	35.9

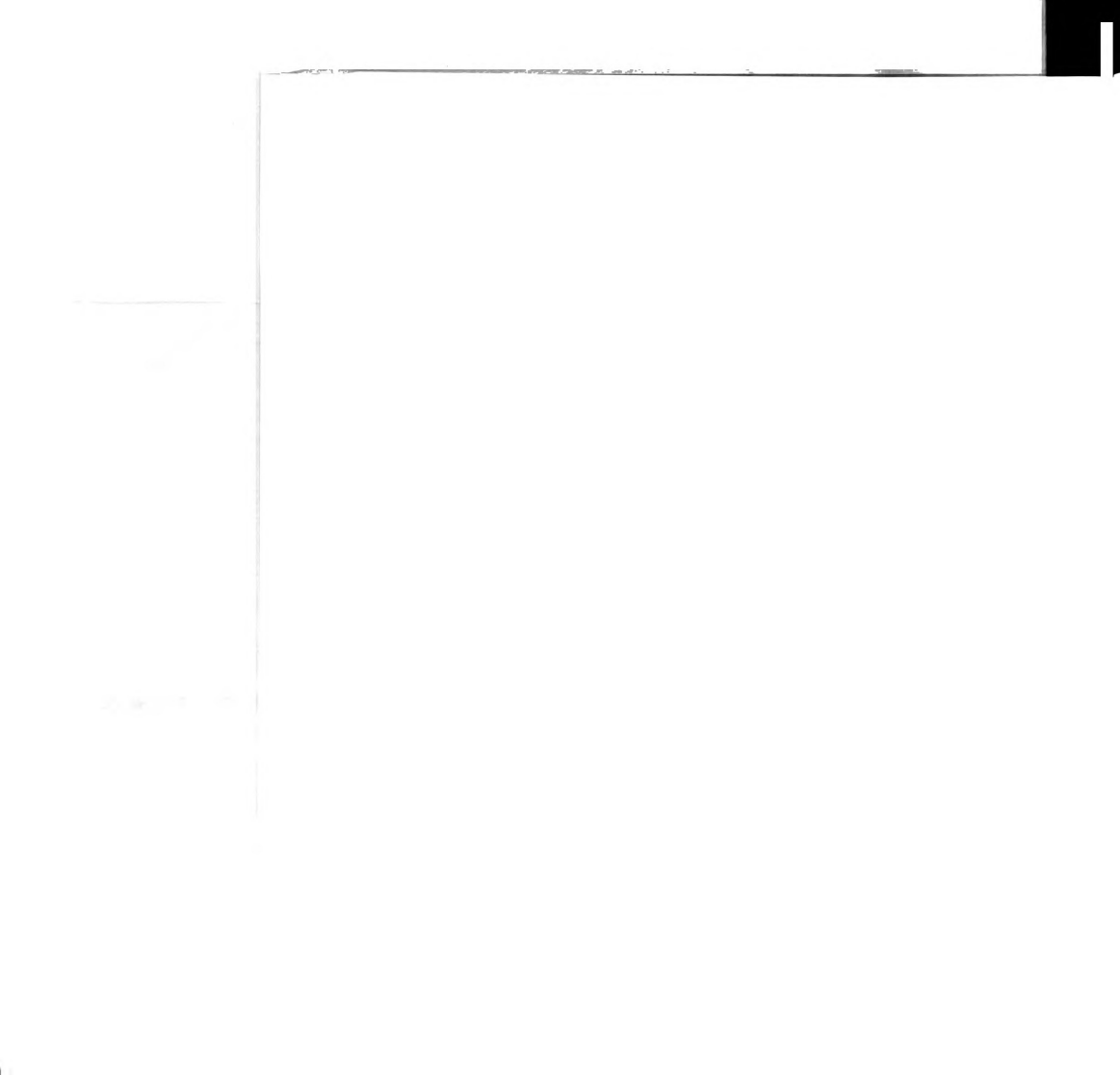


Table 4: Terminal restriction fragments (T-RFs) associated with the same treatment in 1998 and 1999. Note that this table does not include all the T-RFs important within a given year, or necessarily the most important T-RFs in a given year. The # of genera matching a T-RF size in the database may be due to as few as one sequence per genera, with many sequences from the same genera resulting in T-RFs of different sizes; hence the genera found for different T-RFs are not mutually-exclusive. HF-1=heavy fraction, LF-1=light fraction, S=shoot residue >2 mm, R=rhizosphere, C=conventional corn, A=alfalfa, O=organic corn

Restriction Enzyme	T-RF size, bp	Treatment	% variation	# of genera	Select Genera with sequences in RDP 8.1 corresponding to T-RFs
RsaI	55-58	HF-1	31-35	9	<i>Enterococcus, Lactobacillus, Flexibacter</i>
	76-80	LF-1	31-55	15	<i>Mycobacterium, Rhodococcus, Saccharothrix, Actinoplanes</i>
	83-85	C	34-35	4	<i>Propionigenium, Corynebacterium, Deferribacter, Flexistipes</i>
	90-93	C	32-45	3	<i>Capnocytophaga, Weeksella, Chryseobacterium</i>
	121-124	C	26-33	5	<i>Azoarcus, Clostridium, Kingella, Dechlorisoma, Treponema</i>
	176-178	S	29-38	3	<i>Clostridium, Eubacterium, Spirochaeta</i>
	296-303	A	26-38	2	<i>Spirochaeta, Flexibacter</i>
	311-314	HF-1	36-59	7	<i>Cytophaga, Persicobacter, Sporocytophaga, Psychroserpens</i>
	438-441	C	34-41	5	<i>Clostridium, Selenomonas, Ehrlichia, Leptospira</i>
	456-459	HF-1	20-36	37	<i>Bacillus, Clostridium, Fibrobacter, Microbacterium</i>
	466-469	O	21-39	16	<i>Clostridium, Sulfobacillus, Cytophaga, Arthrobacter</i>
	491-494	HF-1	41-66	10	<i>Bacillus, Lactobacillus, Paenibacillus, Desulfovibrio</i>
MspI	74-75	O	21	3	<i>Enterococcus, Desulfohalobium, Epifagus</i>
	77-80	LF-1 and not A	20-24	8	<i>Polyangium, Methanobrevibacter, Geobacter, Thermus</i>
	88-90	not A and not HF-1	28-67	13	<i>Neisseria, Spirochaeta, Eikenella, Polaribacter</i>
	125-128	A	20-45	8	<i>Agrobacterium, Streptomyces, Rhizobium, Mesorhizobium</i>
	129-131	HF-1	22-37	11	<i>Rhodobacter, Paracoccus, Saccharothrix, Fibrobacter</i>
	155-158	HF-1 and not O	28-41	12	<i>Staphylococcus, Bacillus, Azospirillum, Kineosporia</i>
	198-200	HF-1 and A	70-71	2	<i>Mobiluncus, Propioniferax</i>
	200-202	not C	21-42	1	<i>Chryseobacterium</i>
	290-292	HF-1 and A	24-45	5	<i>Mycoplasma, Bdellovibrio, Clostridium, Acetonea</i>
	356-358	LF-1 and C	49-50	0	
	405-408	R	20-35	2	<i>Bartonella</i>
	456-459	R and O	39-67	3	<i>Clostridium, Comamonas, Ehrlichia</i>

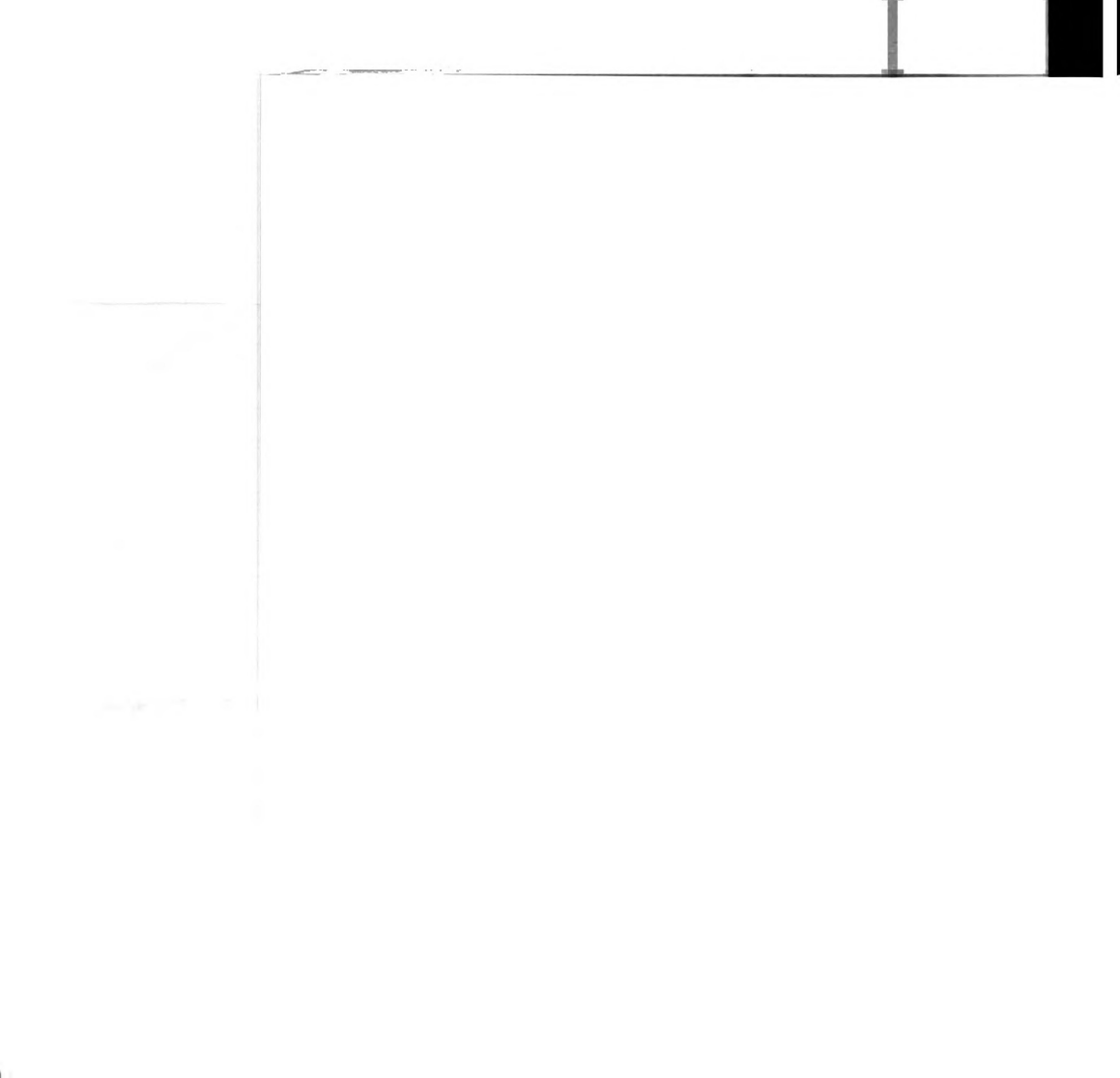
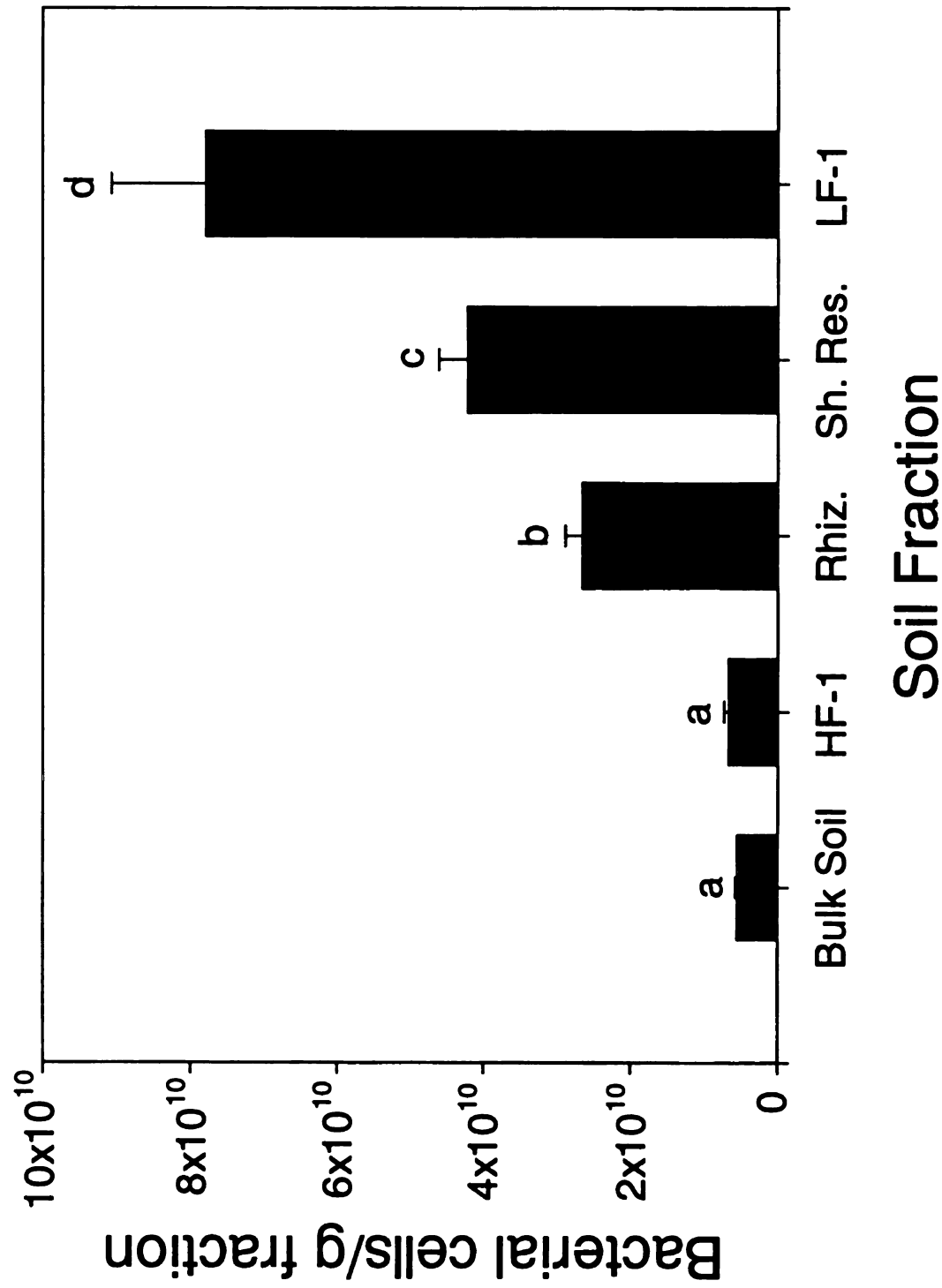


Figure 1: Number of DTAF-stained cells counted per g of soil fraction. Bars with different letters are significantly different via the Student-Neuman-Keuls test ($p<0.0001$). $N=12$ per soil fraction, error bars represent standard error.



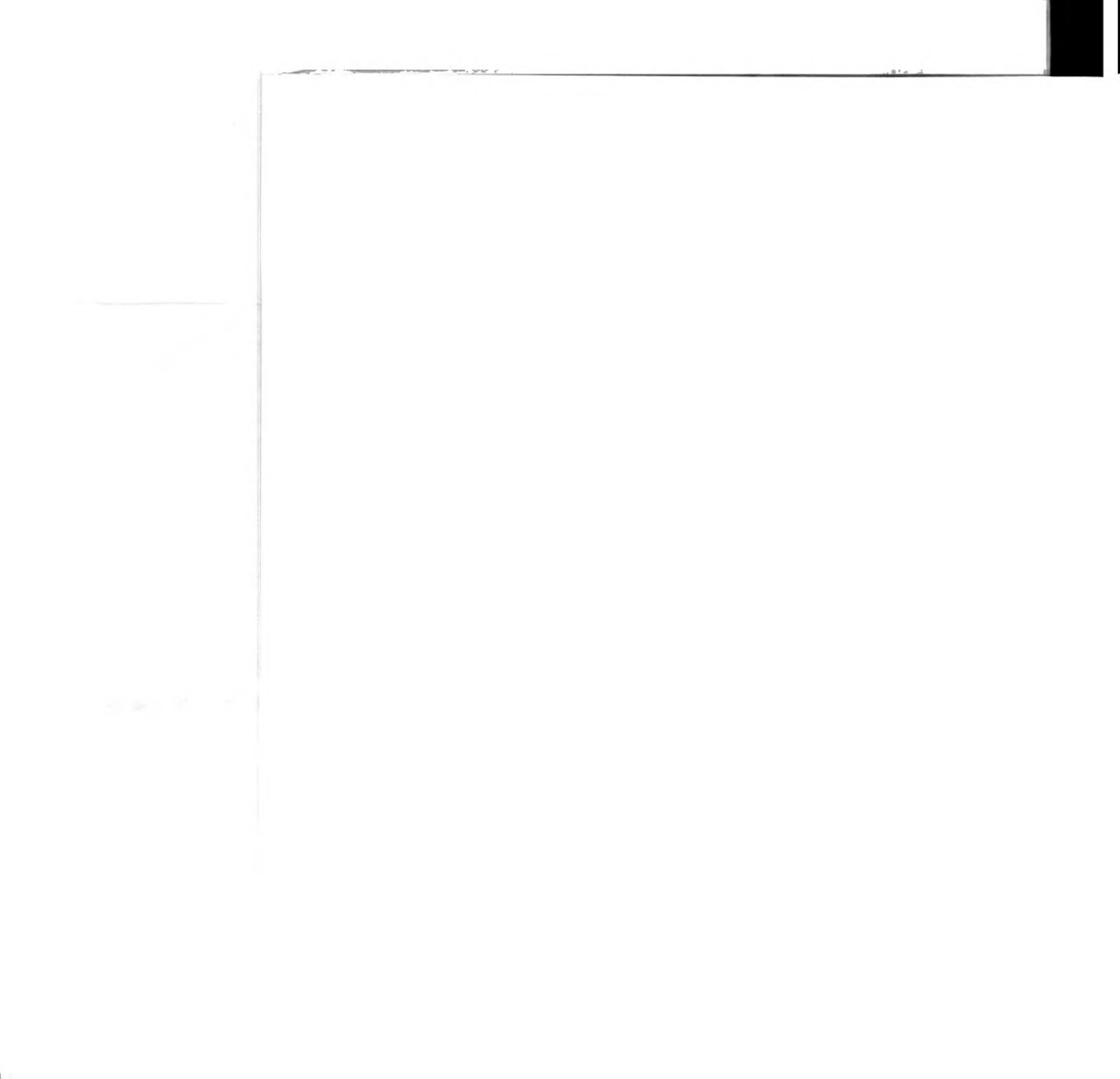


Figure 2: Regression of bacterial cells per g of soil fraction against percent C of soil fraction. The regression is significant at the 0.0001 significance level; $R^2=0.61$. H=HF-1, L=LF-1, S=shoot residue, R=rhizosphere, B=bulk soil. N=60.

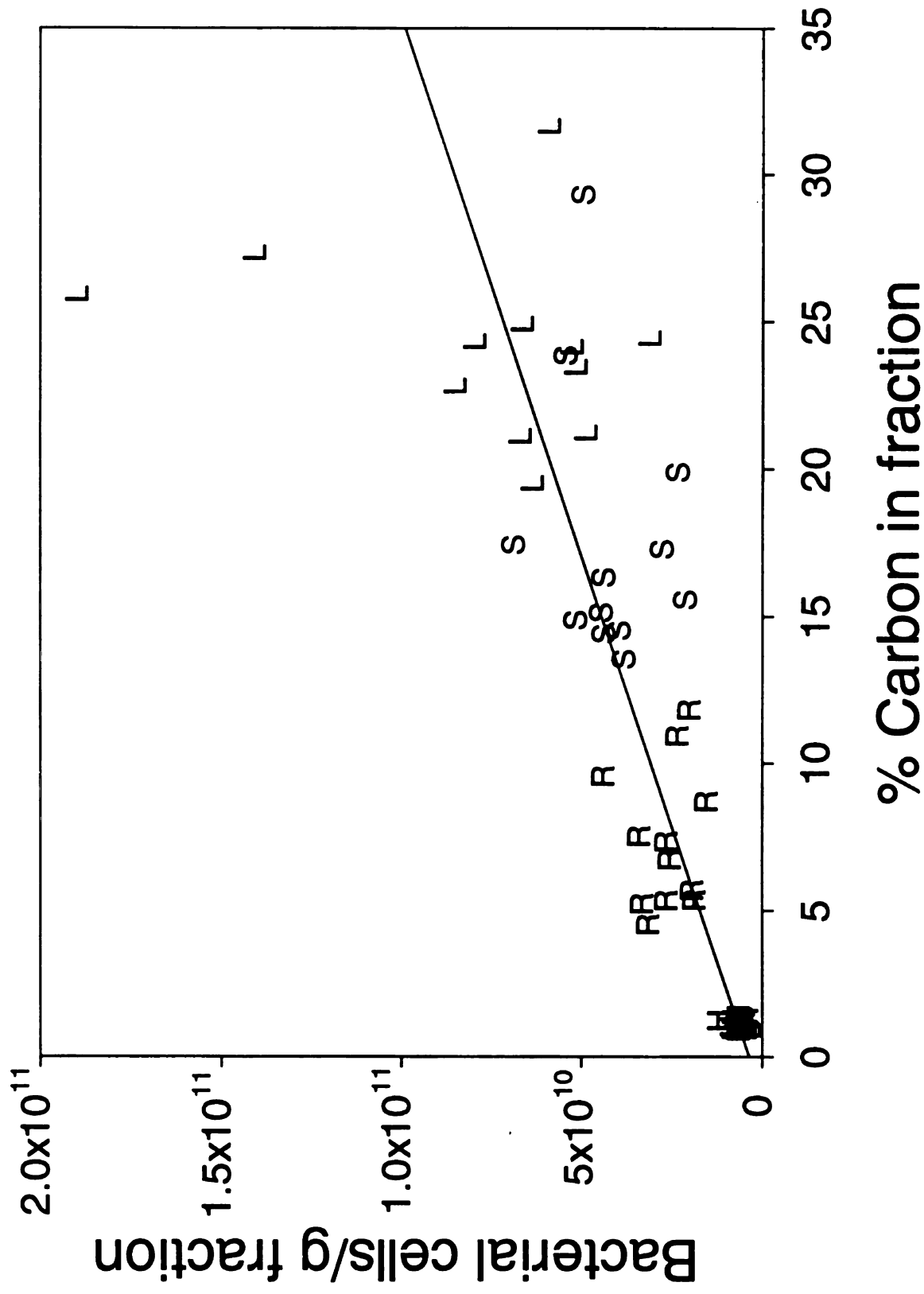
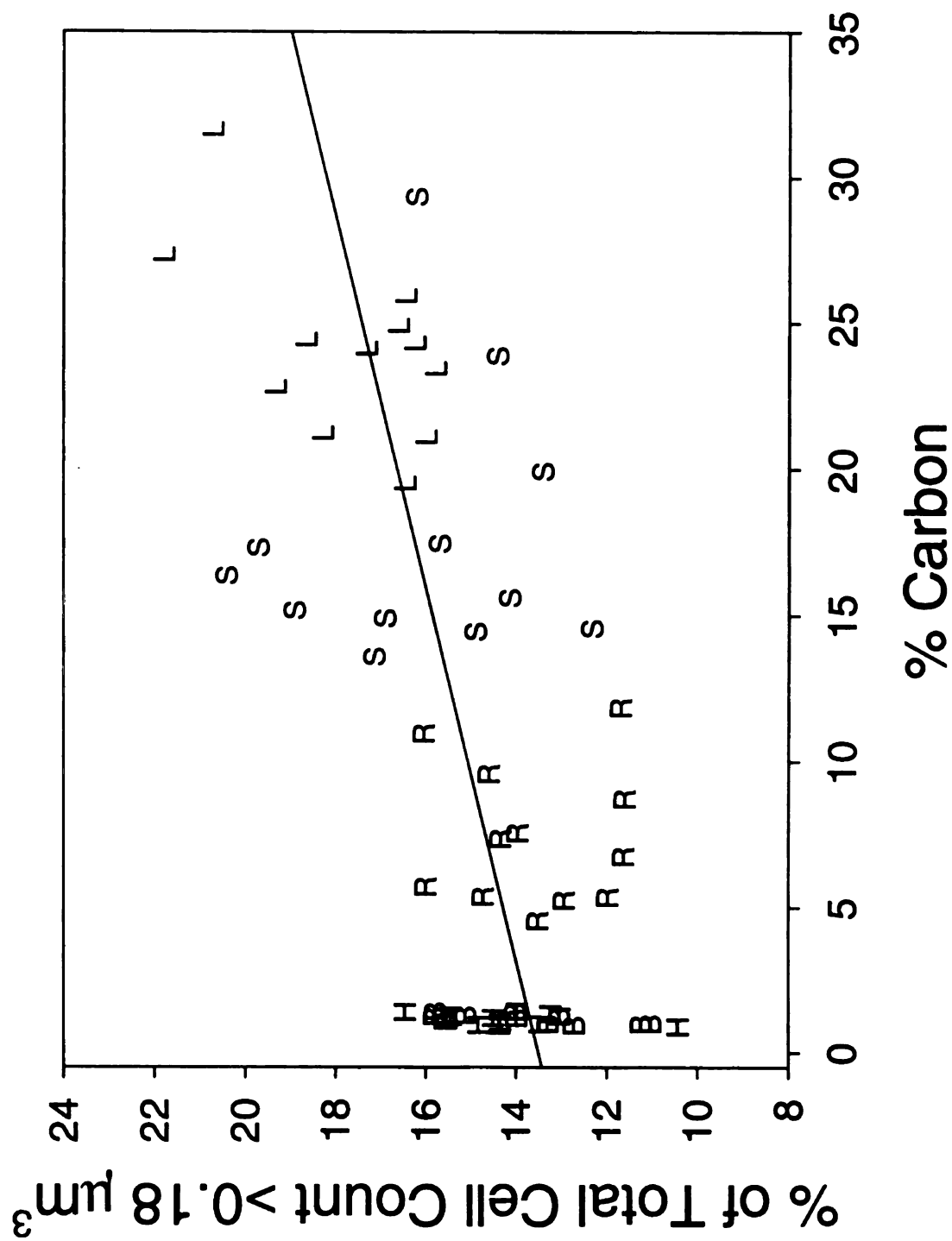


Figure 3: Regression of percent of cells in the largest cell size class ($>0.18 \mu\text{m}^3$) against percent C of the sample. The regression is significant at the 0.0001 level; $R^2=0.37$. H=HF-1, L=LF-1, S=shoot residue, R=rhizosphere, B=bulk soil. N=60.



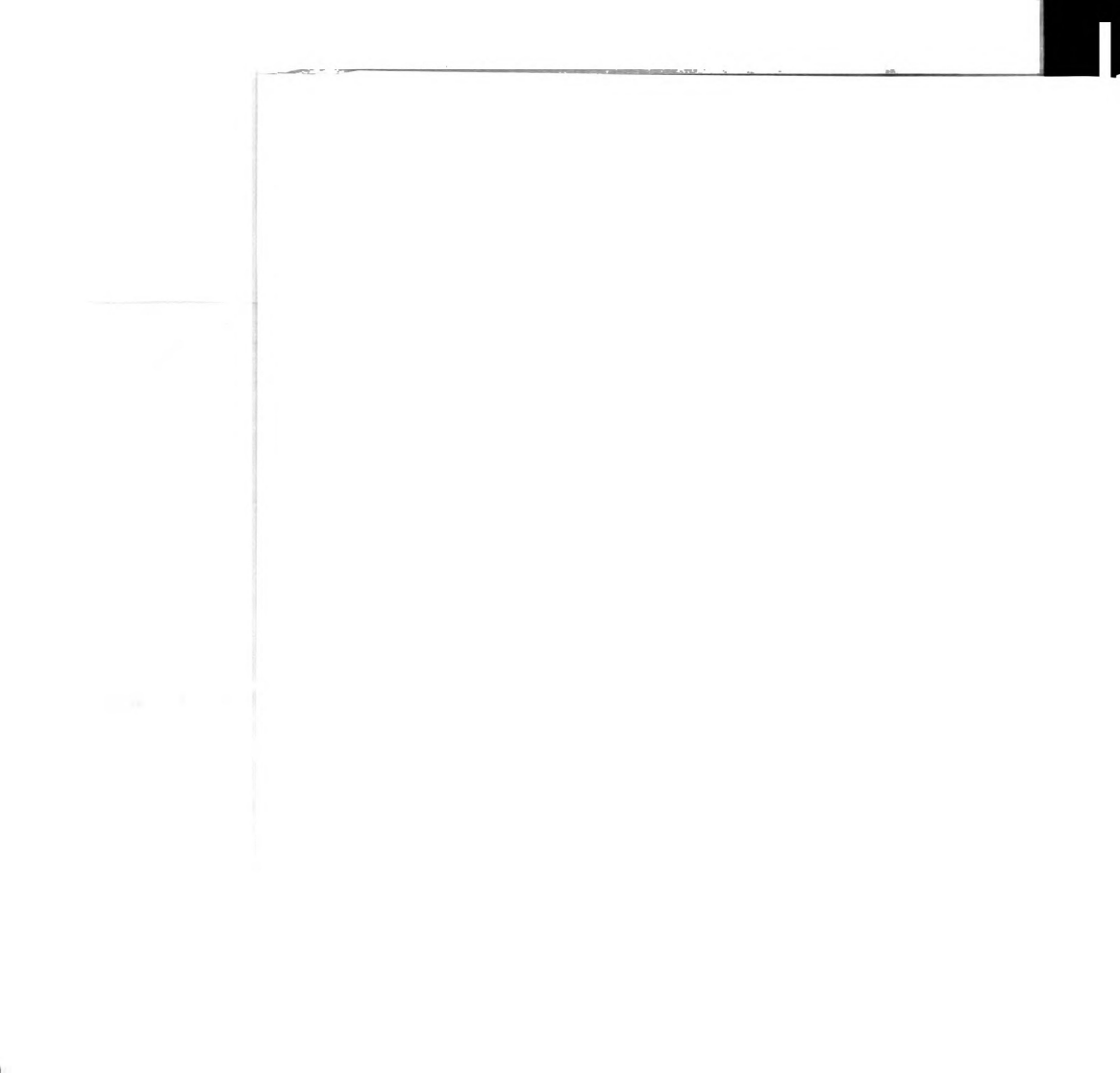


Figure 4: Partial canonical principal components plots derived from redundancy analysis of 1998 RsaI T-RFLP profiles. Circles=HF-1, triangles up=LF-1, triangles down=shoot residue, squares=rhizosphere, white=alfalfa, black=conventional corn, grey=organic corn.

Figure 4a: Soil fraction axes (2 of 3) with cropping system and interaction effects partialled out.

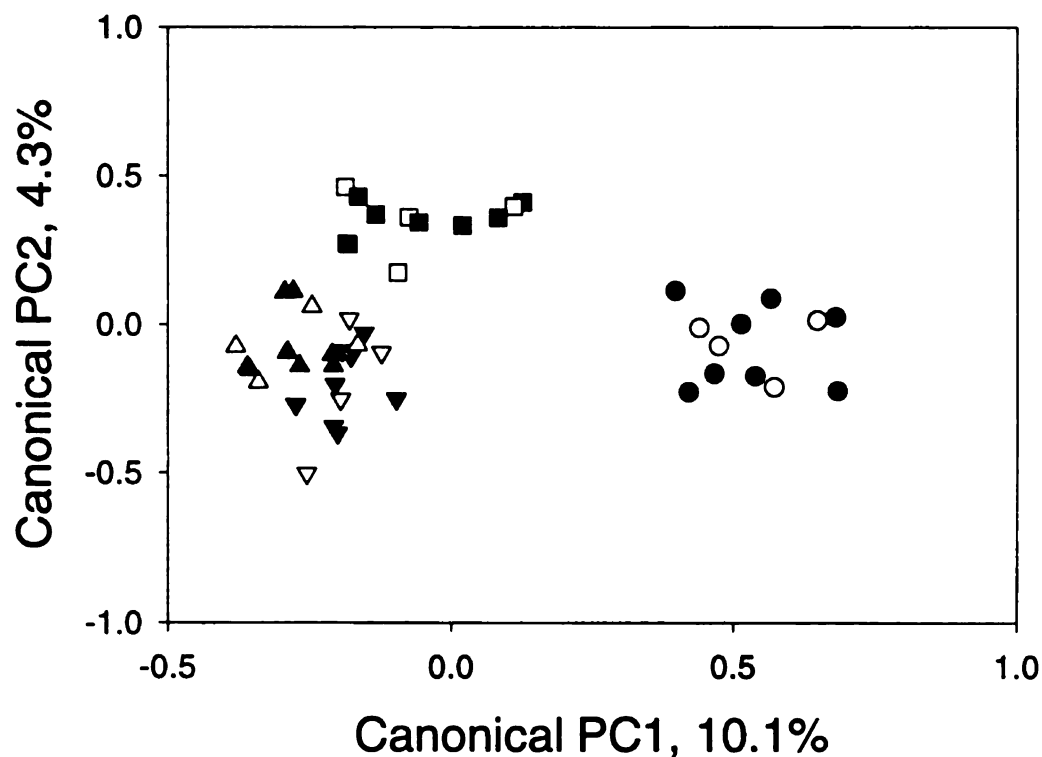
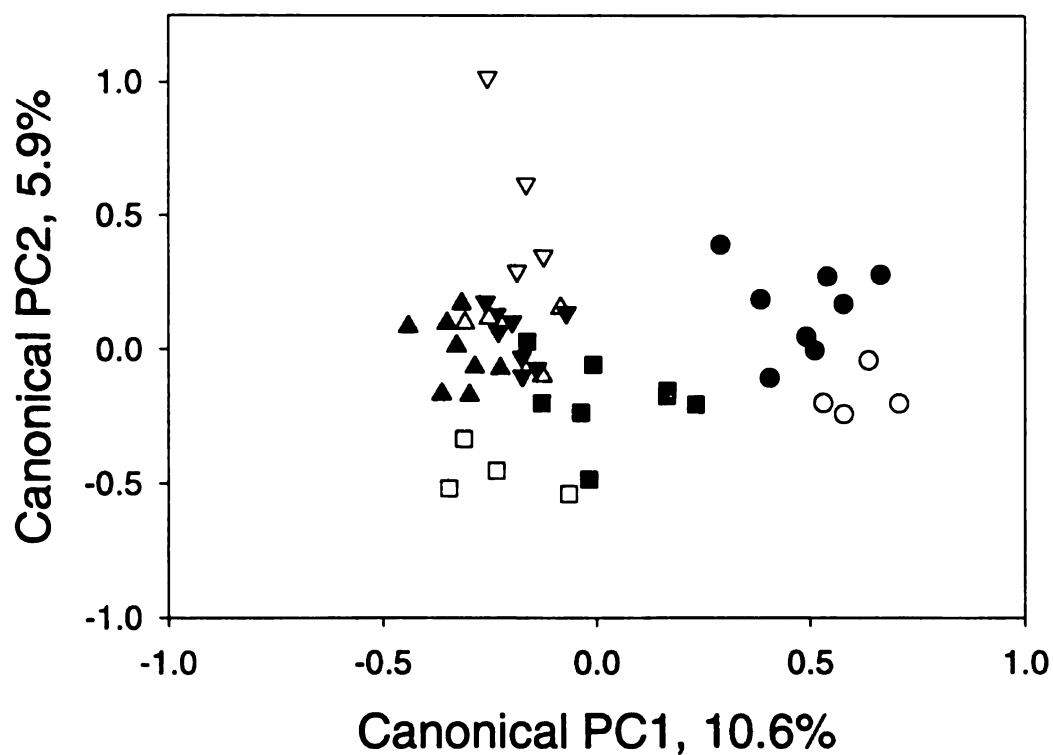


Figure 4b: Soil fraction and interaction axes (2 of 9) with cropping systems effects partialled out.



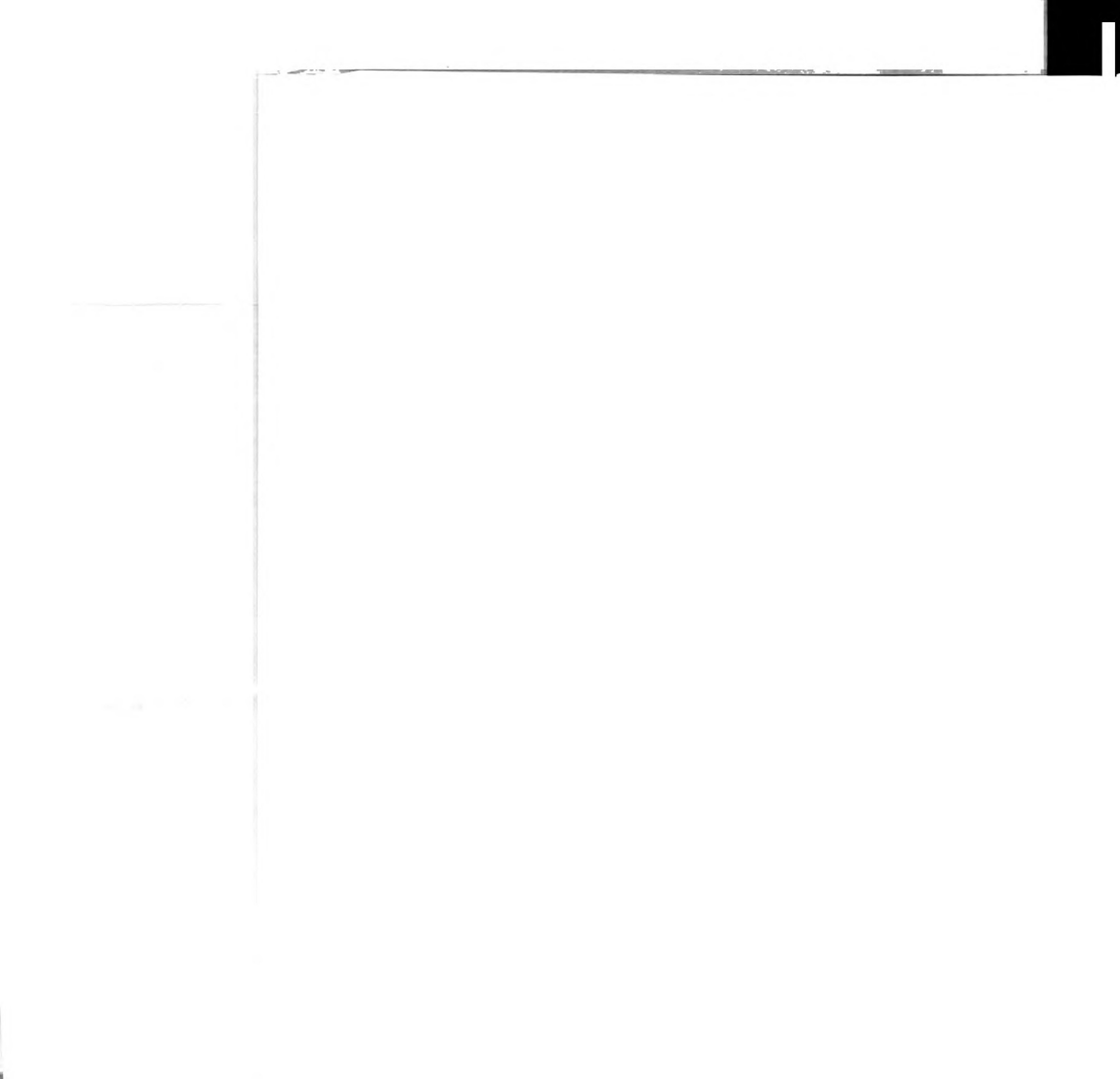


Figure 4, continued

Figure 4c: Cropping system axes (2 of 2) with effects of soil fraction and interactions partialled out.

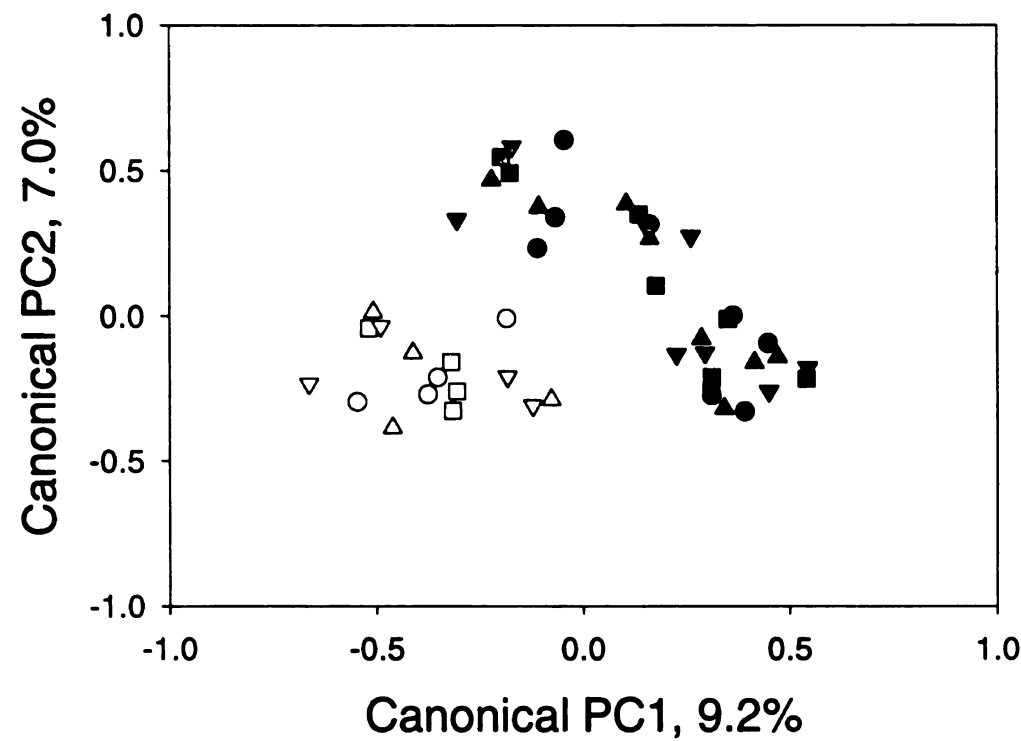
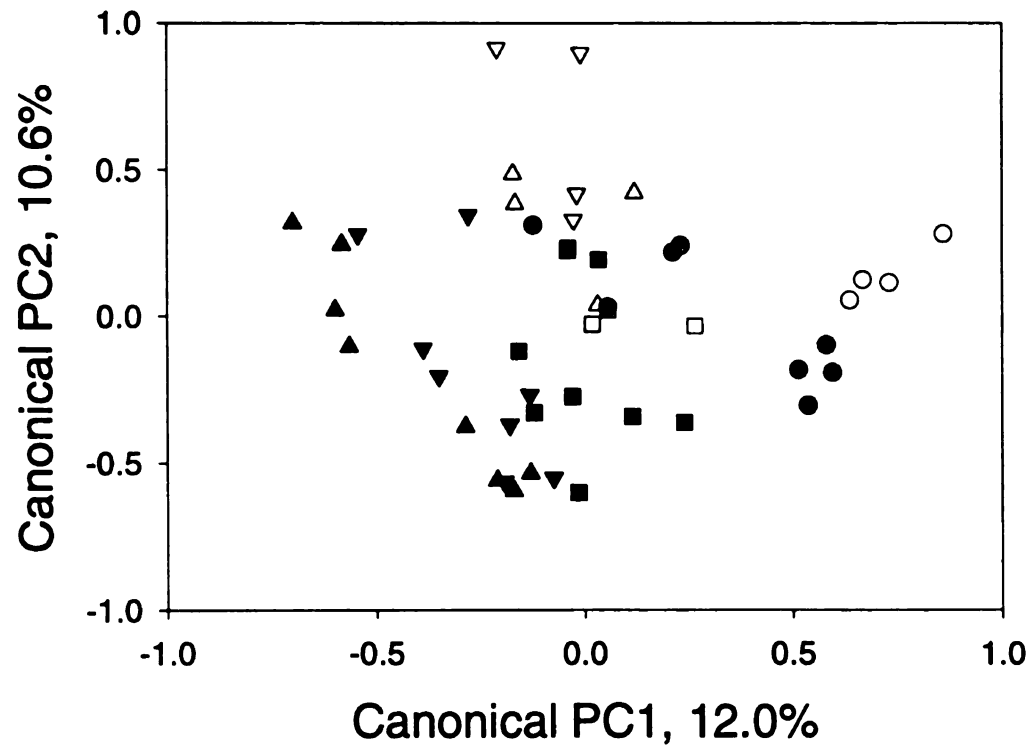


Figure 4d: All-treatment axes (2 of 11).



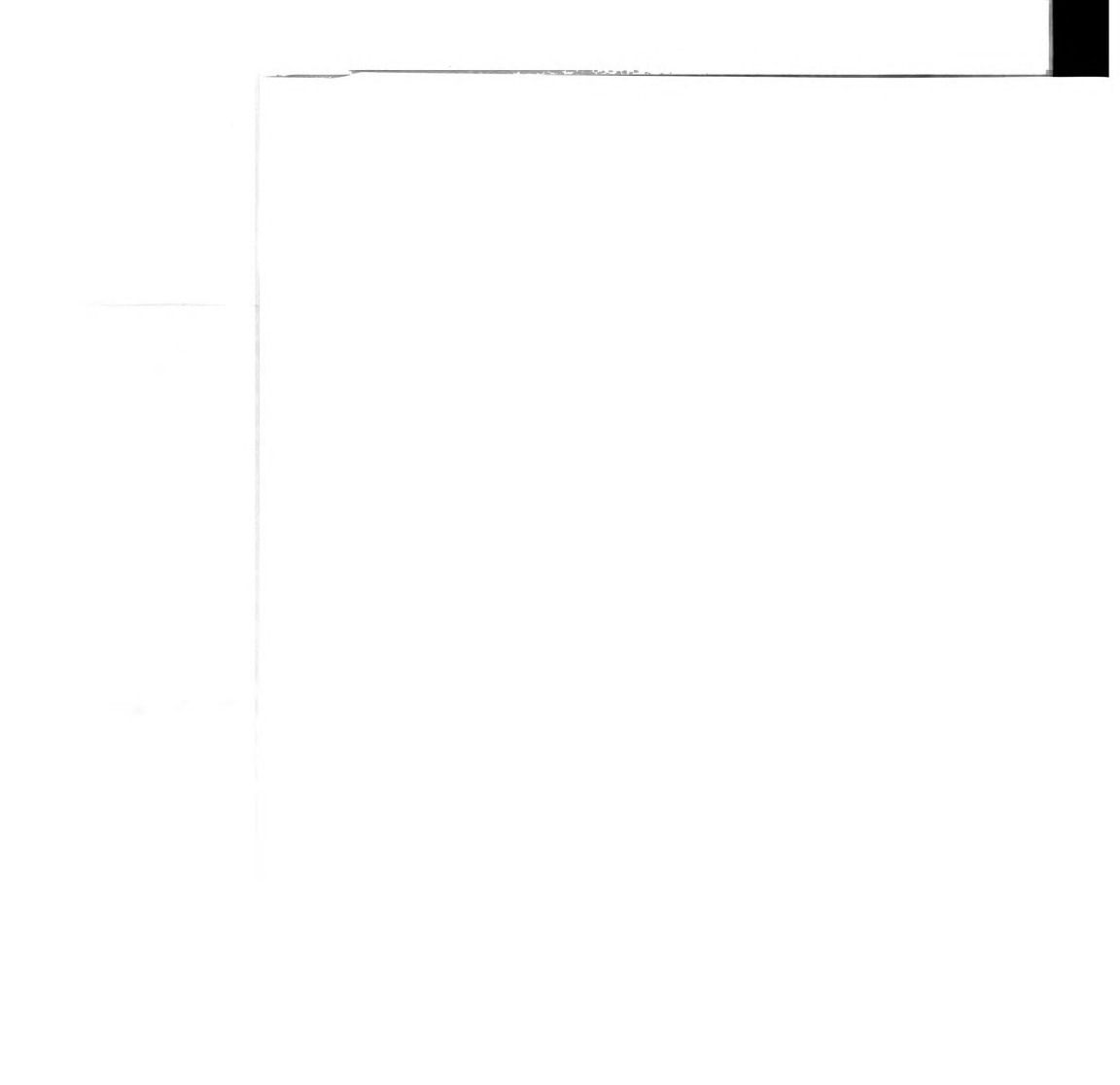


Figure 5: Dendrogram generated by Ward's method of hierarchical cluster analysis on 1999 Rsa1 T-RFLP profiles using Hellingier distance between profiles. Sample identities indicated by the following: First row, C=conventional corn, A=alfalfa, O=organic corn; Second row, 4=4-6.3 mm aggregates, 2=2-4 mm aggregates, 0=0-2 mm aggregates; Third row, H=HF-1, L=LF-1, S=shoot residue, R=rhizosphere, W=whole soil; Fourth row=replicate number.

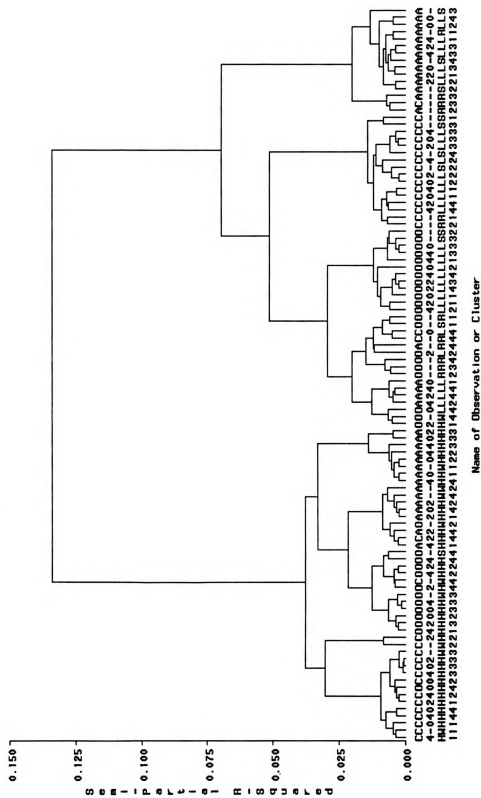
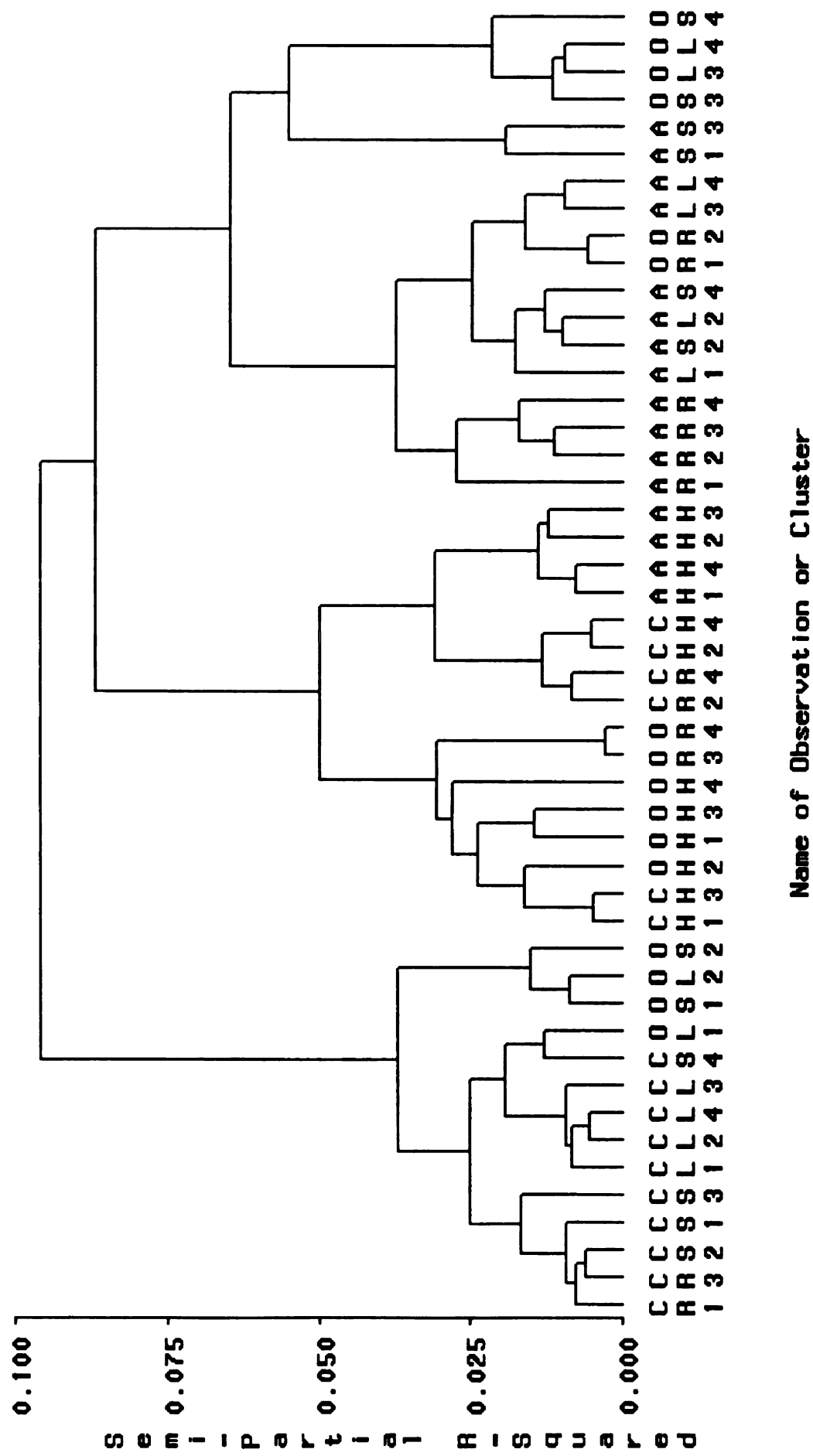


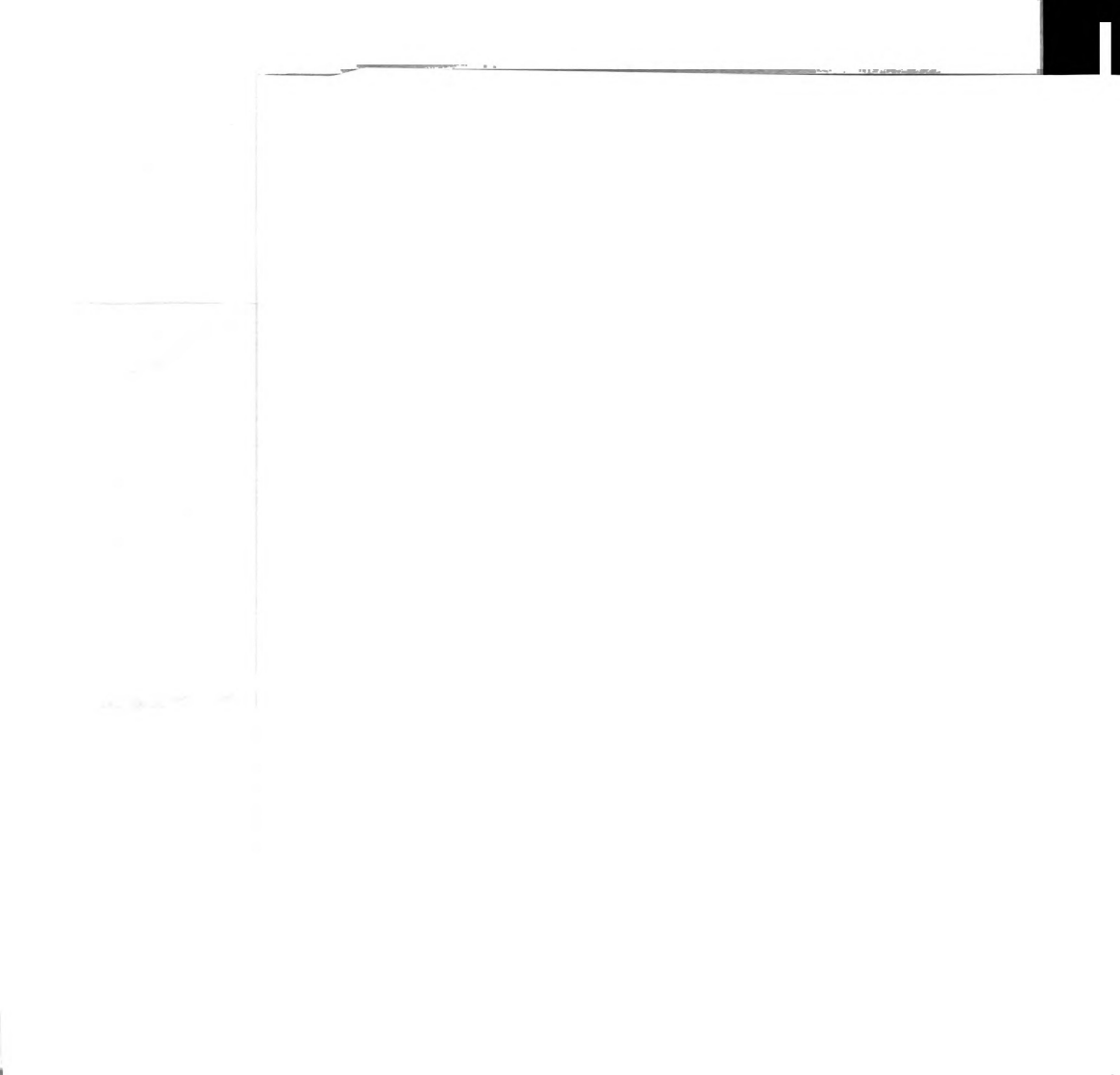
Figure 6: Dendrogram generated by Ward's method of hierarchical cluster analysis on 1998 RsaI T-RFLP profiles using Hellinger distance between profiles. Sample identities indicated by the following: Top row, C=conventional corn, A=alfalfa, O=organic corn; Second row, H=HF-1, L=LF-1, S=shoot residue, R=rhizosphere; Third row=replicate number.





Chapter 4

Eubacterial Community Response to Position within Soil Macroaggregates and Soil Management

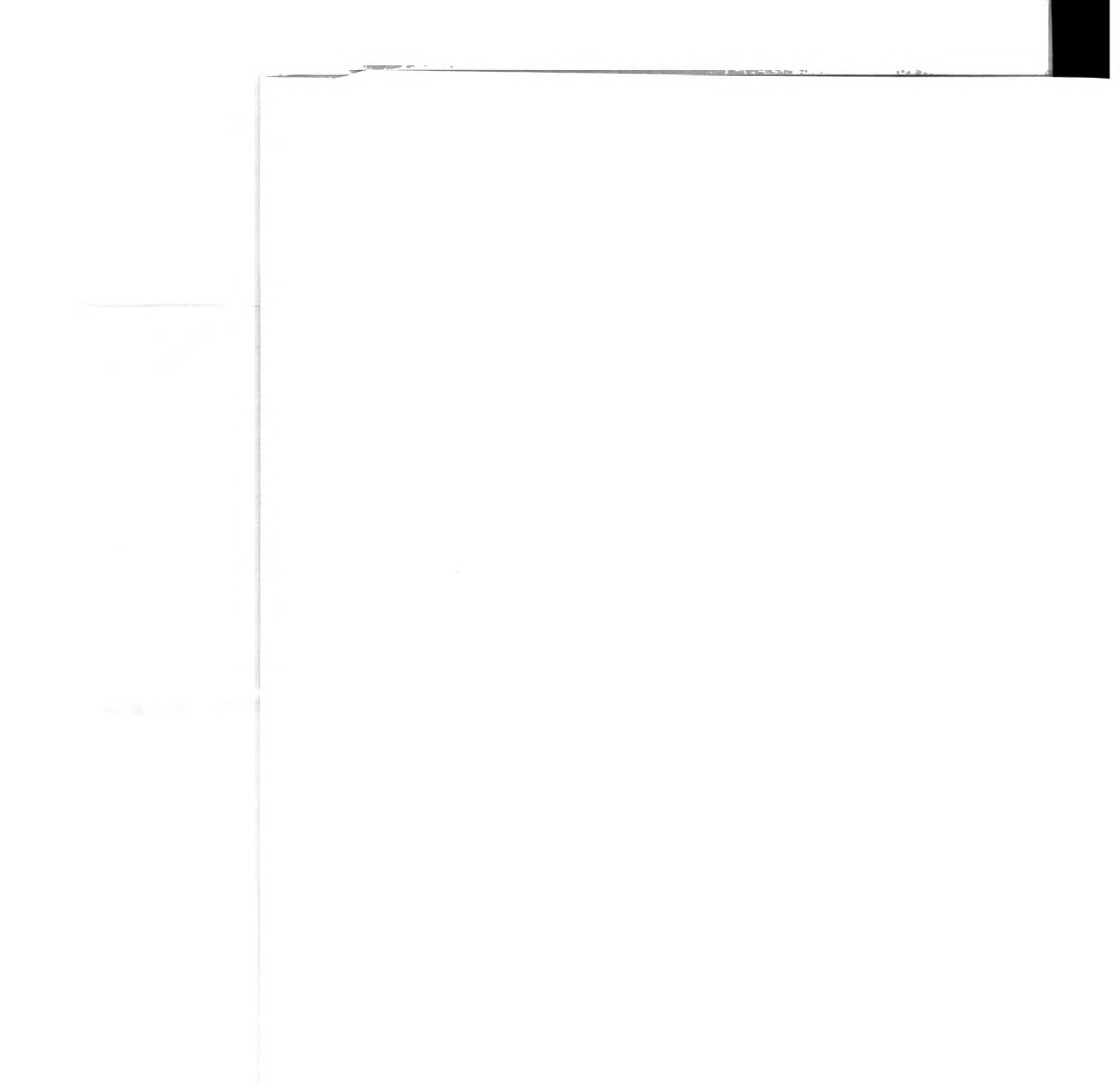


Abstract

Hierarchical aggregate structure is currently the dominant model of soil structure and has been shown to be useful in the study of organic matter turnover in soils. The hypotheses that 1. aggregates of different sizes and 2. layers within aggregates contain different bacterial communities were tested using terminal restriction fragment length polymorphism (T-RFLP) of the 16S ribosomal gene of eubacteria. Soil aggregate erosion was used to isolate layers of aggregates with their resident bacteria, resulting in knowledge of the precise location of the sample within the aggregate. Analysis of individual aggregates using a split-plot design was found to be the most satisfactory approach for investigating whether the communities in different aggregate layers were different. Marginally significant differences between eubacterial T-RFLP profiles of different aggregate layers were found. Aggregate-to-aggregate variability was large. Effects of macroaggregate size on eubacterial T-RFLP profiles were not detected. The major factor affecting T-RFLP profiles was cropping system (continuous conventional corn, organic corn in a crop rotation, and continuous alfalfa) or land management (conventional or no-till corn and successional vegetation) at field experiments in Michigan and Ohio, respectively. Organization by the tertiary structure of the soil (arrangement of aggregates in relation to shoot residue, roots, macropores, etc.) is hypothesized to be more important than aggregate layer or size in the determination of the types of microbial communities present in aggregates.

Introduction

The most common model of the spatial structure of soil particles at millimeter and



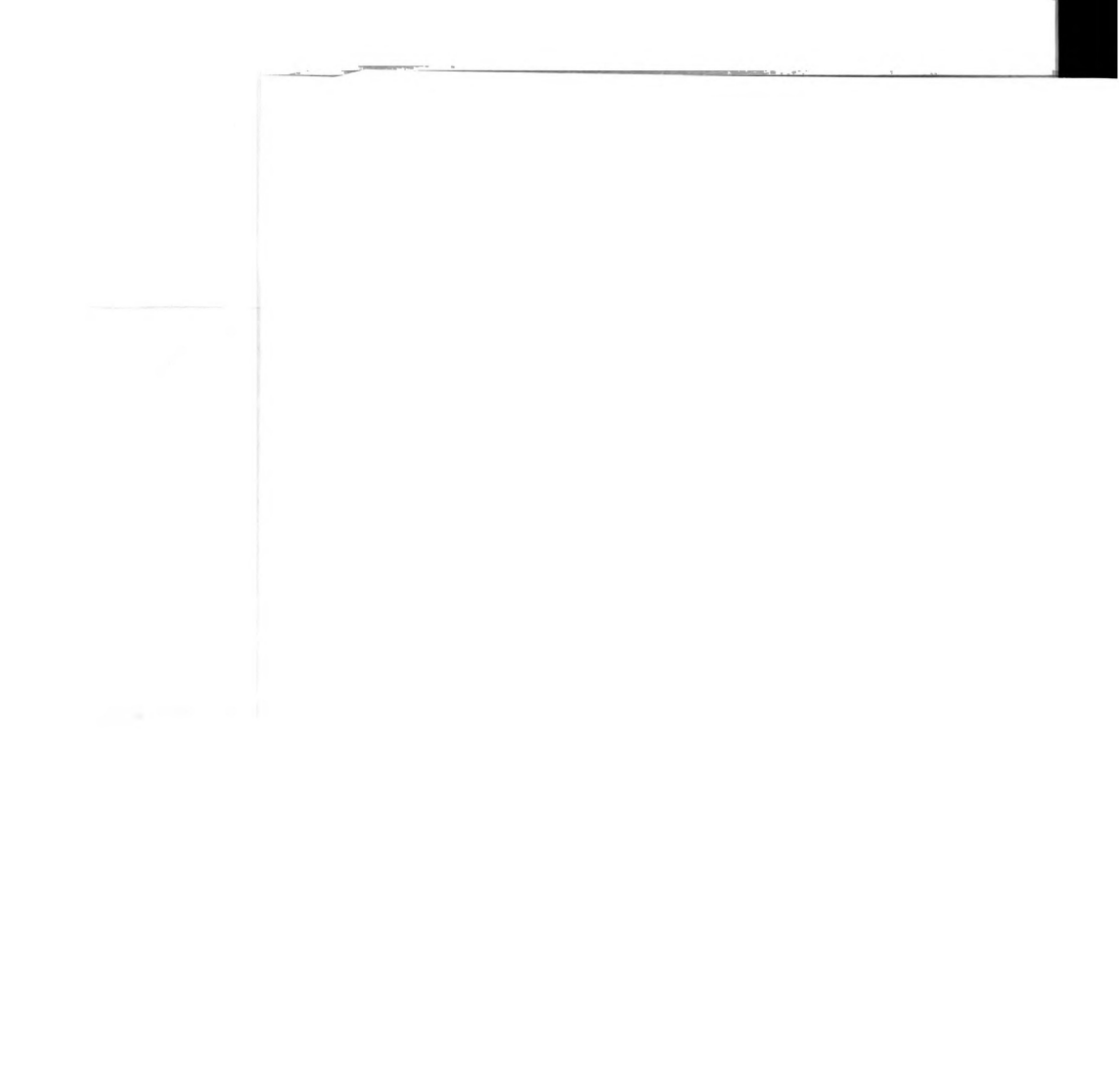
smaller scales is that of a hierarchical arrangement of soil aggregates (Edwards and Bremner 1967, Tisdall and Oades 1982, Elliott and Coleman 1988, Ladd et al. 1996, Christensen 1996). The process of aggregation is dynamic, with microaggregates being bound together by plant roots, fungi, and plant residues to form macroaggregates, defined as $>250\text{ }\mu\text{m}$ in diameter (Elliott 1986, Miller and Jastrow 1990). These organic particles decompose, leading to formation of new microaggregates and disintegration of the macroaggregates (Beare et al. 1994b, Golchin et al. 1994). Larger macroaggregates generally contain more labile organic matter (Beare et al. 1994a, Elliott 1986, Gupta and Germida 1988) with a more rapid turnover time (Buyanovsky et al. 1994, Monreal et al. 1997).

Numerous studies have been conducted to determine the effects of aggregate size class on soil microorganisms, with varying results. These studies generally involve initial dispersion steps designed to isolate microaggregates. Using various combinations of chloroform incubation, plate-counting, ATP determination, and enzyme assays, microbial populations were found to be greatest in $< 0.05\text{ mm}$ aggregates by Kanazawa and Filip (1986), $0.05\text{-}0.25\text{ mm}$ aggregates by Monreal and Kodama (1997), and $> 0.25\text{ mm}$ aggregates by Gupta and Germida (1988). Mendes et al. (1999, 1998) found the trends in microbial biomass and number of *Rhizobium leguminosarum* across aggregate size classes were not consistent between sampling dates, although number of bacterial cells was consistent. Differentiation of the microbial community in different aggregate size classes was not detected in phospholipid fatty acid profiles by Peterson et al. (1997), or in archaeal 16S ribosomal terminal restriction fragment length polymorphism (T-RFLP) profiles by Ramakrishnan et al. (2000). Poly et al. (2000) found some differences in

restriction fragment patterns of PCR-amplified *nifH* gene sequences from different aggregate size classes, but the significance of the results is difficult to assess because the soil fraction data presented is not replicated.

Another common model of intra-aggregate structure is the division of aggregates into central or internal portions and external portions. Macroaggregates can develop anaerobic cores due to microbial respiration (Lefelaar 1993, Priesack and Kisser-Priesack 1993, Zausig et al. 1993), resulting in denitrification (Hojberg et al. 1994, Sexstone et al. 1985). Exterior and interior layers of macroaggregates have also been found to differ in age of organic matter, and in contents of organic C and N, phosphorus, cations, and inorganic N (Santos et al. 1997, Smucker, in preparation). It is also thought that there may be protection of soil microbes from predators such as nematodes and protozoans in the centers of aggregates (Elliott et al. 1980, Elliott and Coleman 1988).

Several studies have addressed the question of whether there are changes in the microbial community due to the differences in the environments in the external and internal layers of soil aggregates. Hattori's (1988) washing-sonication method involves suspension of soil aggregates in water to separate bacteria located on the outer portions of aggregates, followed by sonication to isolate those bacteria in the inner portion. Hattori (1988) showed that bacteria in the outer portions of soil aggregates isolated by this method were more sensitive to air-drying, HgCl_2 , ethylene dibromide, and protozoan predation, and were more responsive to addition of substrate. Bacteria introduced into sterile aggregates accumulated more rapidly in the outer portion. Populations of Gram negative bacteria were greater than Gram positives in the inner portion of the aggregates, whereas the reverse was true for the outer portions. Drazkiewicz (1994) found most



types of cultivable bacteria had increased populations in the internal portion of aggregates in a heavy loam, but only a few had significantly increased populations in a silt loam. Dabek-Szreniawska (1993) examined the effects of keratin-carbamide fertilization on cultivable bacterial populations, and found no consistent trends in the effects due to location within the aggregate. Ribosomal intergenic spacer analysis was used by Ranjard et al. (2000b) to examine the eubacterial community response to Hg(II) contamination in outer and inner portions of soil aggregates; however it is difficult to assess the significance of the results with respect to soil fraction because replicated data were not presented. Ranjard et al. (2000a) have identified two ribosomal intergenic spacer sequences that are only present in the external portion of aggregates and the $< 2 \mu\text{m}$ soil particle fractions after incubation with Hg(II).

The drawback of the washing-sonication method used in previous studies is that differential adhesion of bacteria to soil particles and the number and length of washes will affect which cells are washed out of the soil and counted as being in the outer portions of the aggregate. It is not clear if this method could be standardized such that the locations of the communities isolated are less vague. A different method of dividing the community of an aggregate into internal and external portions is used in the study presented here. The method is based on the physical erosion of individual aggregates and has been proven useful in studies of the location of soil organic matter and nutrients (Santos et al. 1997). Erosion is stopped when the desired proportion of the total aggregate has been isolated. It has the additional advantage that the soil environment is isolated with the community, so other aspects such as chemical characteristics can be studied.



In this study we test the hypothesis that eubacterial communities differ based on their position within macroaggregates using both layers from individual aggregates and pooled aggregate layer samples. The hypothesis that communities differ based on macroaggregate size class is also tested. T-RFLP of the 16S ribosomal gene is used to test these hypotheses with respect to the entire eubacterial community. The use of molecular methods avoids many of the biases and random variability associated with cultivation-based techniques (Madsen 1996, Muyzer 1998). The finding that eubacterial communities differ between physical soil fractions would imply that these fractions comprise spatially-distinct habitats, with implications for the ecology and diversity of soil microorganisms as discussed in chapter 3.

Methods

Field Sites and Sample Collection

Samples were collected in 1999 from three field treatments at the Kellogg Biological Station (KBS) as described in chapter 3. Soils at the site are Typic Hapludalfs and approximately 43% sand and 40% silt (Robertson et al. 1997). Field treatments included: conventionally-managed continuous corn, organically-managed first-year corn (from the Living Field Laboratory, established in 1993), and continuous alfalfa (from the Long Term Ecological Research site, established in 1988). See chapter 3, Jones et al. (1998) and <http://lter.kbs.msu.edu/Agronomics> for descriptions of the management of these field treatments. The organically-managed first-year corn is in a corn-corn-soybean-wheat rotation, with cover crops planted after corn and wheat. Samples were collected from within rows, between plants, in corn fields, and nearby permanent

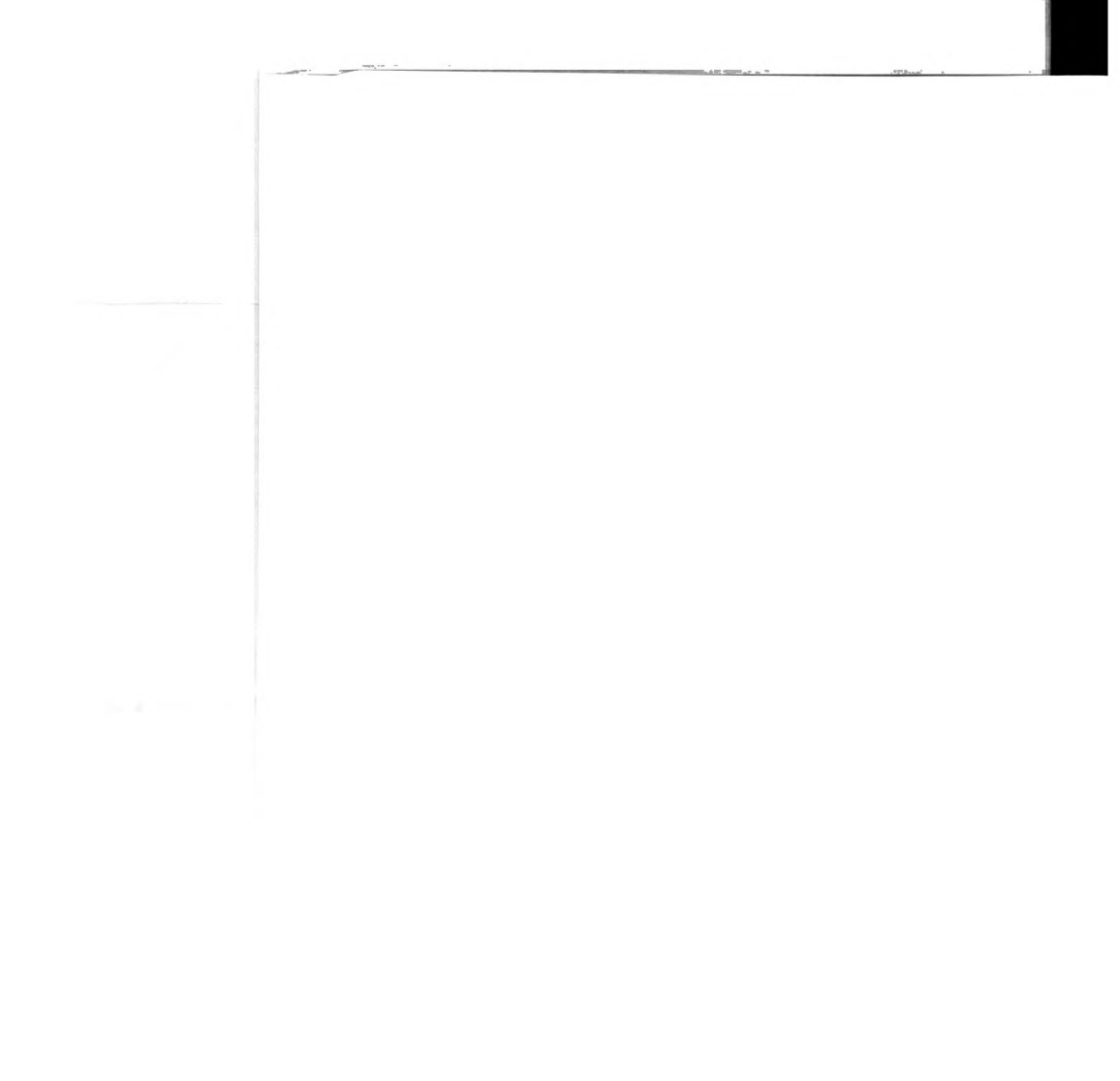
sampling stations in alfalfa fields. Four replicate fields per treatment were sampled. Three 350 g soil blocks 10 cm deep were excavated per field, and were transferred intact to glass jars for transportation. Samples were stored at 4°C until fractionation was complete.

Samples were collected from three field treatments in Wooster, OH, in 2000. Treatments included no-till continuous corn, conventionally-tilled continuous corn, and native successional vegetation. Treatments were started in 1962. Corn plots have been managed using standard agronomic practices in the region. Soils at the site are silt-loam. Three replicate plots per treatment were sampled by excavating a soil block 10 cm deep and storing in a plastic container at 4°C until fractionation was complete.

Soil Fractionation

Whole soil blocks from KBS were gently separated along planes of weakness over a nest of sieves with mesh sizes of 6.3, 4, and 2 mm, and roots and shoot residue >2 mm were removed. Soil aggregates were separated until they fit through the 6.3 mm sieve, following recommendations by Jastrow and Miller (1991). The nest of sieves was then shaken by hand until only stable aggregates that would not fit through the mesh were left on the 4 and 2 mm sieves. This resulted in isolation of aggregates of sizes 4-6.3, 2-4, and 0-2 mm. The 4-6.3 and 2-4 mm macroaggregate fractions were subsampled for analysis of aggregate layers. Density separation was performed on all KBS aggregate size classes with water, resulting in the isolation of a heavy fraction (HF-1) and light fraction (LF-1) as described in chapter 3.

Soil samples from Wooster were allowed to air dry completely before fractionation. Soil blocks were then gently separated along planes of weakness over a



nest of sieves with mesh sizes of 9.5, 6.3, 4, and 2 mm, and roots and shoot residue were removed. The sieves were shaken by hand, and 4-6.3 and 2-4 mm aggregates were isolated for this study.

Four 4-6.3 mm aggregates and four (KBS) or eight (Wooster) 2-4 mm aggregates from each plot were weighed and placed individually in the upper compartments of meso-soil aggregate erosion chambers (A. Smucker, personal communication). The removable upper compartments have textured walls and a screen bottom. Material that is eroded due to rubbing of the aggregate against the walls falls through the screen and is trapped in a lower compartment. Chambers were shaken on a horizontal rotary shaker and upper compartments with aggregates were weighed periodically to determine the proportion of the aggregate that had been eroded. Weighing was performed as frequently as every 10 minutes and shaking was at 150 to 250 rpm, depending on the rate of erosion. After the weight of the aggregate had decreased by 33%, the material trapped in the bottom of the chamber (the exterior layer of the aggregate) was removed. Erosion was continued until the weight of the aggregate was reduced by another 33%. The uneroded portion of the aggregate in the upper part of the erosion chamber (the aggregate interior) was then isolated. Aggregates that broke into multiple large fragments during erosion were replaced.

The layers of four 4-6.3 mm aggregates from one plot (replicate 4) of each KBS treatment were analyzed individually. Aggregate replicates from the remaining plots and for all 2-4 mm aggregates were pooled for analysis. Samples were divided into three subsamples. These were 1. frozen for DNA extraction 2. stored in 4.9% formaldehyde 3. weighed before and after drying at 65°C.



Fractionation of the 4-6.3 mm KBS aggregates from field replicate 4, to be analyzed individually without pooling of aggregate layers from the same treatment, was completed 7 weeks after sampling. Fractionation of the remainder of the KBS aggregates was completed approximately 17 weeks after sampling. To test for an effect of storage over an extended period, heavy fraction samples were isolated using water for density separation (HF-1) from whole aggregates after 20 weeks of storage, for comparison to those isolated after 8 weeks described in chapter 3. Fractionation of Wooster aggregates was completed within three weeks after sampling.

T-RFLP Analysis

T-RFLP was performed essentially as described in Liu (1997) and in chapter 2. Community DNA was extracted from samples using the standard Ultraclean Soil DNA extraction kit (Mo Bio Laboratories, Solana Beach, CA). Genomic DNA was found to be of sufficient purity to be used directly in PCR reactions. PCR was performed using a standard reaction mixture of 160 μ M of each deoxynucleoside triphosphate, 3 mM $MgCl_2$, 0.05 U/ μ L Taq DNA polymerase and the appropriate volume of accompanying 10X PCR buffer (Gibco BRL, Gaithersburg, MD), and 0.2 μ g/mL bovine serum albumin (Boehringer Mannheim Biochemicals, Indianapolis, IN). PCR mastermix, without primers, and PCR reaction tubes were sterilized for 14 minutes with direct ultraviolet radiation in a Cleanspot PCR/UV workstation. Primers used were the general eubacterial primer 8-27F (AGAGTTTGATCCTGGCTCAG, E. coli numbering, Amann et al. 1995, Integrated DNA Technologies, Coralville, IA) and the universal primer 1392-1406R (ACGGGCGGTGTGTACA). PCR reactions were optimized for each sample of genomic DNA using a master mix with primer concentrations of 0.4 μ M. Optimizations

were performed by adjusting the amount of genomic DNA extract used (0.4 to 7.5 μL /50 μL reaction) and the number of PCR cycles run (28 to 33) to obtain a strong band without visible non-specific product. PCR was performed in a Perkin-Elmer 9600 thermocycler using an initial denaturation step of 95°C followed by 28-33 cycles of the following program: denaturation at 94°C for 30 sec., primer annealing at 55°C for 30 sec., and extension at 72°C for 30 sec. A modified hot start procedure was used where PCR tubes were not placed in the thermocycler until the block temperature had reached 80°C. A final extension at 72°C for 7 min. was performed after the programmed number of cycles was complete. PCR product concentration and specificity was checked by electrophoresis on a 1% agarose gel, followed by staining with ethidium bromide.

PCR reactions (50-75 μL) were performed in triplicate for each sample using the optimal conditions found previously. These reactions were performed using the same PCR master mix and program described above except that the forward primer was 0.6 μM hexachlorofluorescein (hex)-labeled 8-27F (Integrated DNA Technologies). PCR replicates were pooled. The PCR product from aggregates analyzed individually was purified by washing three times with sterile water in Microcon 100 concentrators, and then isolated in 17 μL sterile water. PCR product from pooled aggregates samples was purified using the Promega PCR Preps Wizard Kit as directed by the supplier, except that elution was performed with 19 μL of sterile water heated to 55-65°C. Five μL of purified PCR product was mixed with 5 μL of restriction enzyme master mix containing 1.5 U/ μL of restriction enzyme and one μL of the accompanying reaction buffer (Gibco). Restriction reactions were incubated for three hours at 37°C, followed by 16 min. at 65°C to denature the restriction enzyme. Three μL of the restricted PCR product was mixed



with one μL of 2500 TAMRA size standard (Applied Biosystems Instruments, Foster City, CA). DNA fragments were separated by size by electrophoresis at 1800 V for 14 hours on an ABI 373 automated DNA sequencer at Michigan State University's DNA Sequencing Facility. The 5' terminal fragments (T-RFs) were visualized by excitation of the hex molecule attached to the forward primer. The gel image was captured and analyzed using Genescan Analysis Software 3.1. A peak height threshold of 50 fluorescence units was used in the initial analysis of the electropherogram. T-RFLP profiles for all samples were generated using the restriction enzyme *RsaI*. *MspI* was used to generate additional profiles for two replicates of each cropping system/aggregate layer/aggregate size class combination for the pooled KBS samples. Negative controls (no genomic DNA) were conducted with every PCR and run on several Genescan gels. Contamination in PCR reactions was not detected. Small peaks occasionally appeared in negative control lanes on Genescan gels, but the cumulative peak height was always below 1000 units. Samples were re-run if the cumulative peak height was below 9500 fluorescence units, except as noted.

Direct Microscopy

Cells were dispersed in formaldehyde-fixed individual aggregate layer samples by diluting to 2 mL with water and vortexing for 5 min. with 0.5 mL of 1 mm glass beads. Bacterial cell numbers were quantified in the individual aggregate samples following the procedure of Paul et al. (1999). Briefly, 4 μL of diluted fraction that had been fixed with formaldehyde was placed in each of five 6 mm diameter wells of an analytical microscope slide (Cel-Line Associates, Newfield, NJ) and allowed to dry overnight. Dried sample smears were then stained with 5-(4,6-dichlorotriazin-2-yl)

aminofluorescein (DTAF) for 40 minutes, followed by rinsing in phosphate buffer (30 minutes X 3 rinses) and water (30 minutes). Wells were flooded with type FF immersion oil and then a coverslip was glued in place. Bacteria were observed at 100X magnification using a 63X objective and 1.6X zoom with a Leitz Orthoplan 2 microscope. Digital images of bacteria were obtained using a Princeton Instruments digital microscope camera. Cells were counted and measured by a script written in the image analysis program IPLab (Princeton Instruments, Trenton, NJ).

Carbon and Nitrogen Analyses

Carbon and nitrogen contents of dried, ground samples were obtained using a Carlo-Erba NA1500 series 2 Nitrogen-Carbon-Sulfur Analyzer.

Statistical Analysis

Statistical analyses were performed using SAS version 8 (Stat and IML components) and Canoco. All analyses were performed taking into account blocking of replicates in the field and lab, which was not found to be significant.

Percent C and N of pooled aggregate layers was analyzed using three-way analysis of variance (ANOVA) to test for significant effects of aggregate layer, aggregate size class, cropping system, and interaction effects. Percent C and N and microscopic cell counts in individual aggregate layers were analyzed as a split-plot experimental design, with each aggregate as a whole plot and aggregate layer as the split plot. Regression analysis was used to test for an effect of percent C and N on bacterial cell counts.

T-RLFP profiles were aligned against a database of T-RFs with sample identities concealed. Cumulative peak height was standardized to 10,000 fluorescence units, with

peaks deleted if their height was less than 50 after standardization. Relationships between T-RFLP profiles were examined using Hellinger distance and Jaccard distance (see chapter 2 for a complete discussion of data analysis of T-RFLP profiles).

Differentiation of eubacterial T-RFLP profiles was tested using redundancy analysis (or distance-based redundancy analysis in the case of Jaccard's distance) with dummy variables coding for cropping system, soil fraction, and interaction terms. Coding followed the method described in (Legendre and Anderson 1999). Distributions of partial pseudo-F statistics were generated with 9999 random permutations of the identities of profiles in the software Canoco. To test for aggregate layer effects on individual aggregates, profiles were permuted within individual aggregates as in a split-plot experimental design. This method was also compared to unrestricted permutation for pooled aggregate layer profiles since layers of only 4 to 8 aggregates were pooled together.

Adequately strong T-RFLP profiles were not obtained for the following samples: an alfalfa whole soil sample, an organic corn whole soil sample, an organic corn 0-2 mm HF sample, and a conventional corn 2-4 mm LF sample, from KBS, and one successional vegetation 4-6.3 mm internal aggregate sample from Wooster. Where necessary these were replaced by the mean vector generated from the other three replicates of the respective treatment, following the method of Legendre and Anderson (1999). In other datasets some treatments could not simultaneously tested due to presence of other weak profiles (see Results).

Relationships between profiles were also examined using Ward's method of hierarchical cluster analysis, principal components analysis (with Hellinger distance),

principal coordinates analysis (with Jaccard distance), and canonical principal components plots obtained from the redundancy analyses. Percent C and N were tested for significant effects on T-RFLP profiles using redundancy analysis.

Results

KBS Aggregate Size Classes and Density Fractions

One aggregate size class made up approximately 38% of the soil mass, but this was different for each cropping system. In organic corn, 0-2 mm aggregates made up 38% of the soil weight, in conventional corn it was the 2-4 mm aggregates, and in alfalfa it was the 4-6.3 mm aggregates. Mean proportion of the total soil for other size class-cropping system combinations was 29-33%. These differences were significant in the 2-4 mm size class, where alfalfa had significantly increased mass ($F=12.6$, d.o.f=2,9, $p=0.002$).

Aggregate size class did not have a significant effect on T-RFLP profiles in redundancy analysis of either LF-1 or HF-1, but cropping system was significant (see Table 1). HF-1 samples were analyzed with whole soil samples to test the hypothesis that whole soil sample T-RFLP profiles are equivalent to HF profiles. This was hypothesized because HF bacteria make up greater than 90% of the bacteria in the soil (see chapter 3). Results were consistent in analyses performed including whole soil profiles with HF aggregate size classes, without whole soils (data not shown), and with only the 2-4 and 4-6.3 mm macroaggregate size classes. Interaction terms were significant when whole soils were analyzed with aggregate HF-1 samples using Jaccard distance. Examination of the first four canonical principal components showed that this was primarily due to increased

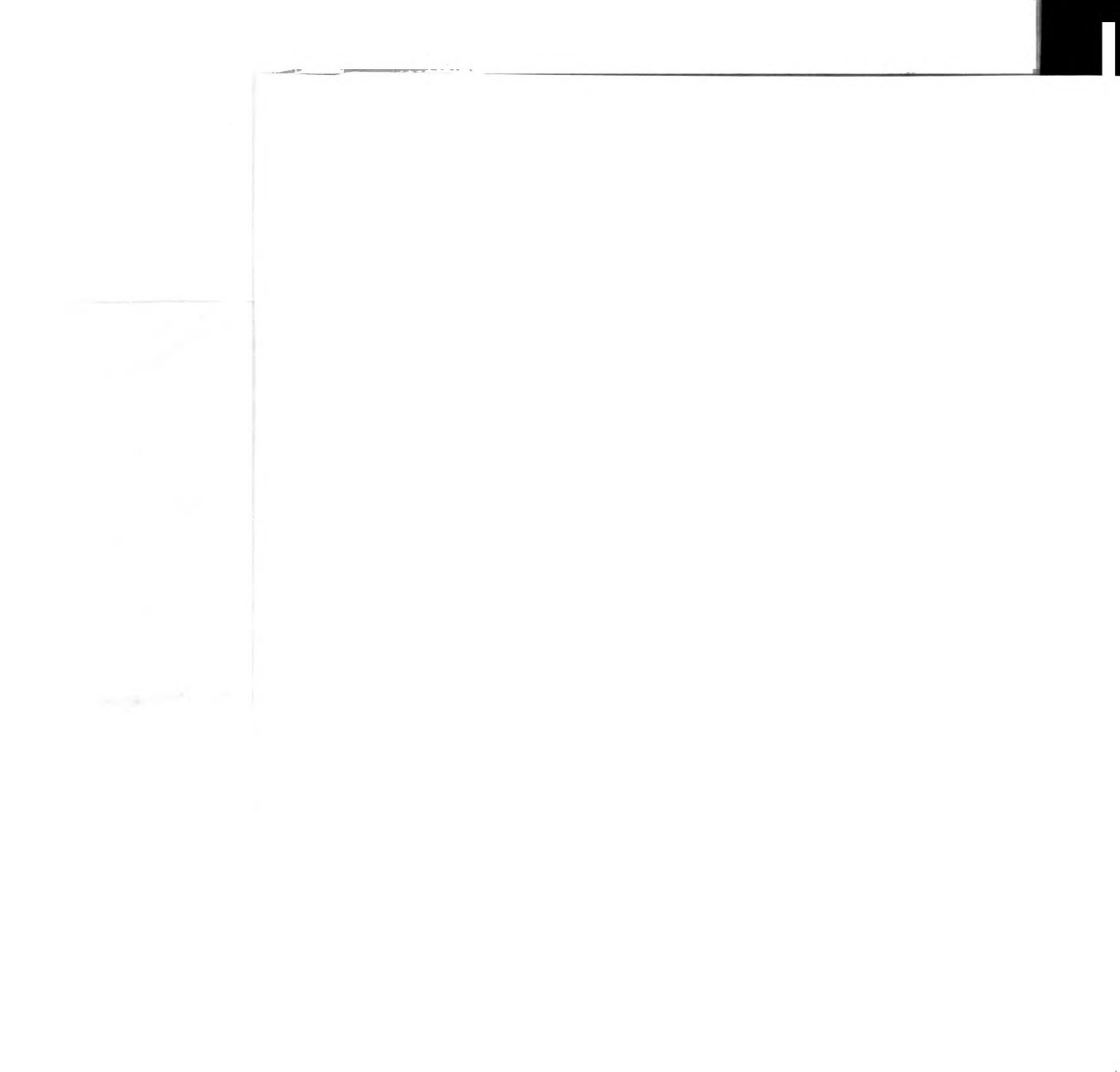


separation of cropping systems in the whole soil and 0-2 mm aggregate HF-1 profiles (data not shown).

Redundancy analysis of HF-1 profiles from samples that had and had not been stored at 4°C for an additional 12 weeks showed a marginally significant storage effect when analyzed with Hellinger distance ($p=0.0556$), accounting for a small amount of the total variance in the dataset (5.8%). Two T-RFs (114-115 bp and 443-446 bp) had greater than 20% of the variation in their Hellinger-transformed abundance explained by storage, after accounting for effects of cropping system. The variation that storage accounted for when analyzing Jaccard distance (4.7%) was not significant ($p=0.2700$). The twentieth principal coordinate had 19% of its variance explained by storage, which was the only principal coordinate with greater than 12% explained, after accounting for cropping system effects. Further analyses of aggregate layer T-RFLP profiles from KBS were conducted after deletion of the two T-RFs identified as being affected by storage in the analysis of Hellinger distance.

Layers of Individual KBS Aggregates

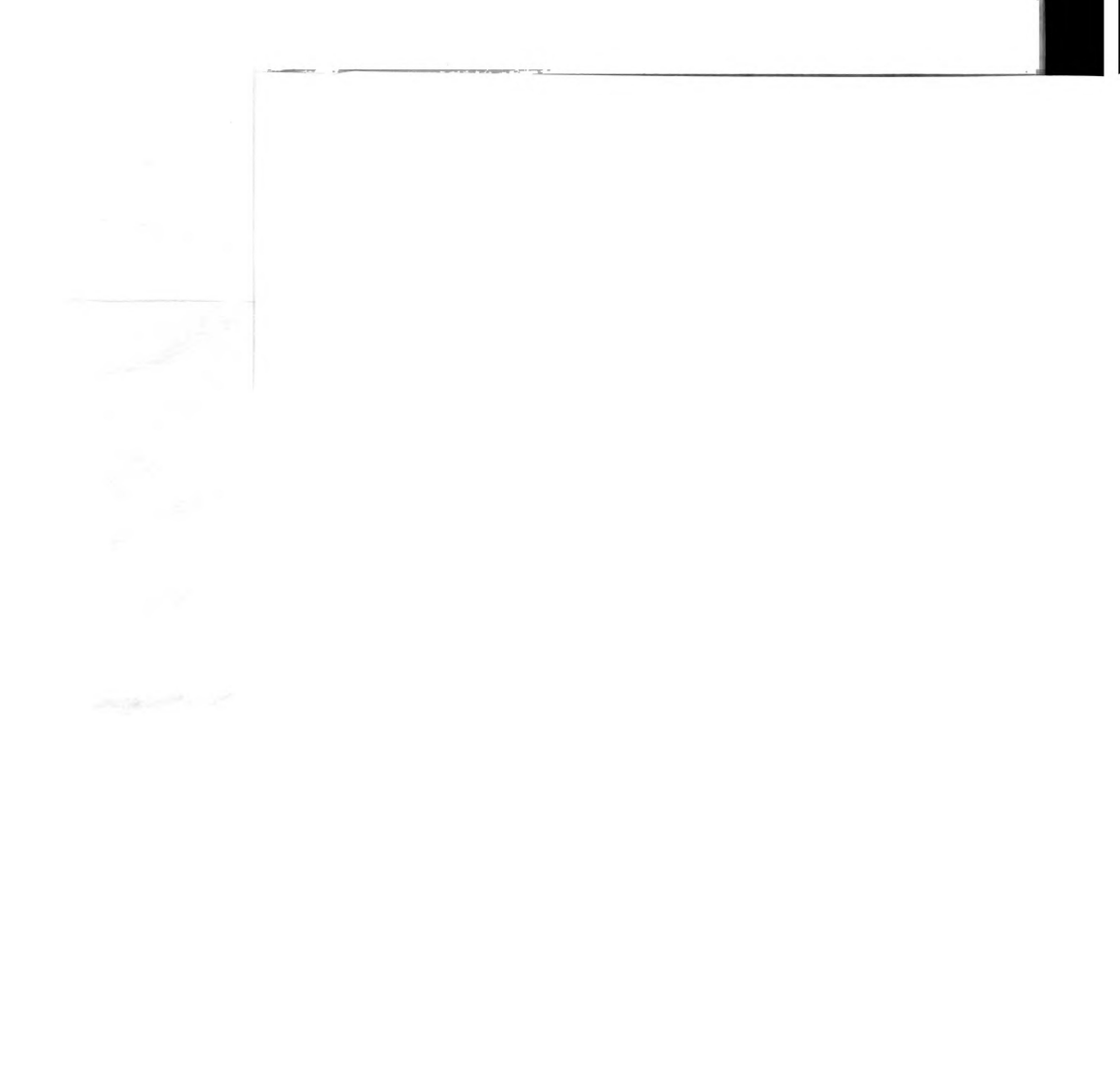
Several individual 4-6.3 mm aggregate layers did not produce adequately strong T-RFLP profiles for analysis. Limiting samples to those with a cumulative T-RF peak height greater than 7500 fluorescence units resulted in 18 profiles, with 7 aggregates fully represented by both layers. Three of these were from alfalfa soil, three were from organic corn, and one was from conventional corn. Redundancy analysis on Hellinger distance, using each aggregate as a block for purposes of permutation as in a split-plot design, found that aggregate layer was marginally significant ($p=0.0771$) and accounted for 12.5% of the variation in the dataset. Greater than 20% of the variability in Hellinger-



transformed abundance was explained by aggregate layer for 12 T-RFs. Divergences in profiles due to the individual aggregate of origin accounted for a large proportion of the variance in the dataset (47%), but this was not statistically significant due to the large number of parameters involved ($p=0.3583$).

Limiting samples to those with cumulative peak height greater than 10,000 fluorescence units for analysis by Jaccard distance (see chapter 2) resulted in 13 acceptable profiles. The set was heavily weighted toward alfalfa samples, and only 4 aggregates were represented by both layers, so exploratory data analysis of Jaccard distance was used. Figure 1 shows the Ward's clustering dendrogram based on Jaccard distance between these 13 samples. While clustering based on cropping system (or plot in the case of this set of aggregates) is not evident, four of six external-layer samples are separated from the other samples, accounting for 23% of the variance in the dataset. The same four external-layer samples are "grouped" on the upper and right edges of the data cloud in the plot of the first two principal coordinates (see Figure 2a). They are grouped much more clearly, and with an additional external-layer sample, in the upper-left of the plot of the third and fourth principal coordinates (which account for 23% of the variance in the dataset, see Figure 2b). The external-layer sample that never groups with the other external-layer samples is consistently grouped with its complementary internal-layer sample of the same aggregate. Other samples are not grouped by aggregate.

There were no significant effects of aggregate layer or cropping system on percent C or N, bacterial cells per g fraction, or percentage of cells in the smallest ($<0.065 \mu\text{m}^3$) size class in the individual 4-6.3 mm aggregates at the 0.05 significance level (data not shown). The effects of aggregate layer were significant for the percentage of cells in the



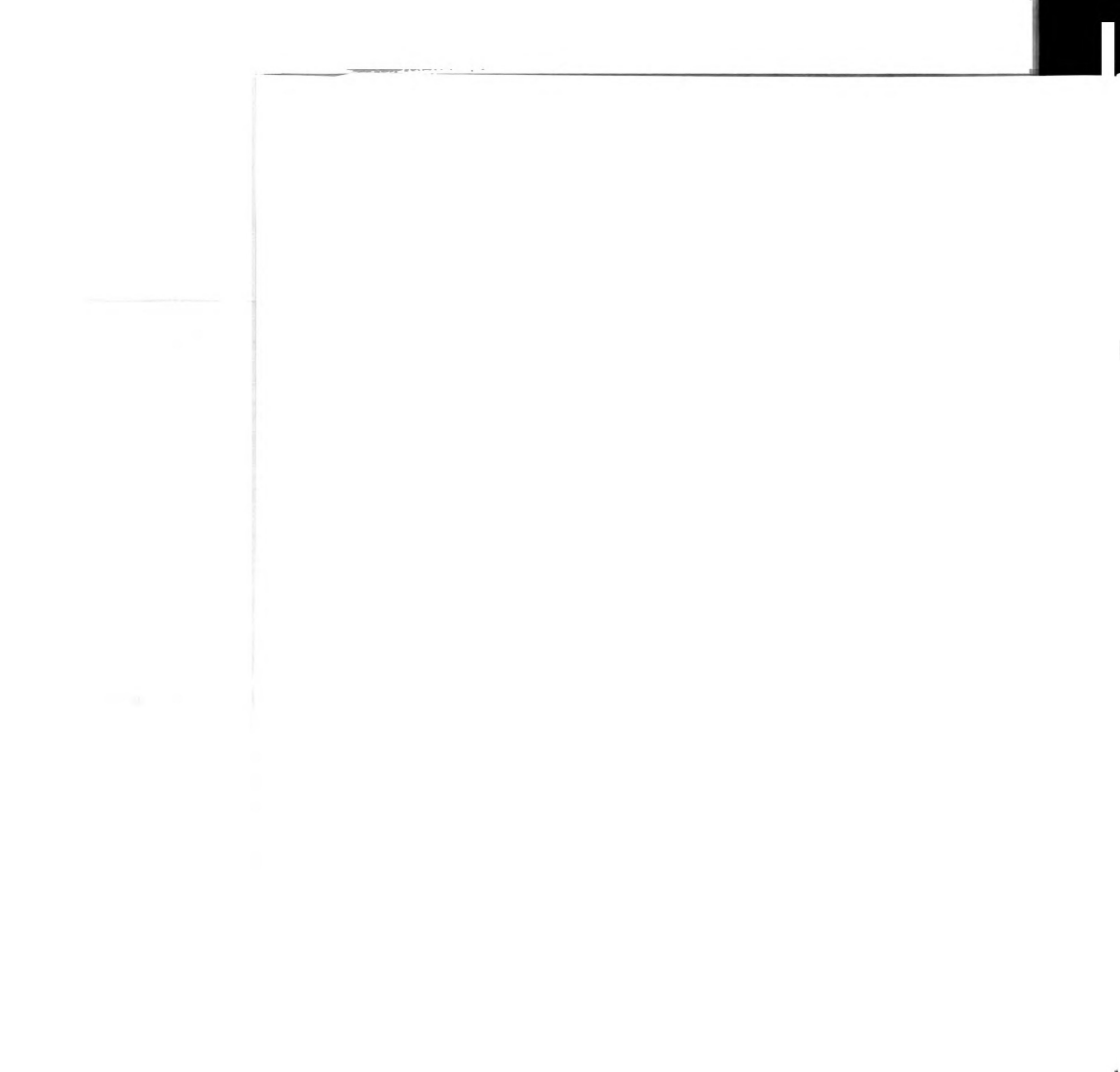


largest size class ($>0.18 \mu\text{m}^3$, $F=5.3$, $\text{d.o.f.}=1,9$, $p=0.047$). Proportion of cells $>0.18 \mu\text{m}^3$ was 15.4% in aggregate exteriors and 16.7% in interiors. Cropping system had a significant effect on percentage of cells in the largest size class in the aggregate interiors ($F=4.29$, $\text{d.o.f.}=2,9$, $p=0.049$), with 13.9% of cells in this class in conventional corn aggregate interiors, 17.9% in organic corn, and 18.2% in alfalfa. Cropping system effects were not significant in the aggregate exteriors (mean=15.4%) or overall between aggregates.

Regression analysis showed that the relationship between percent of cells in the largest size class and percent organic C in the sample was significant ($F=6.8$, $\text{d.o.f.}=1,22$, $p=0.016$, $R^2=24\%$). The regression of total numbers of bacterial cells on percent C was not significant ($F=1.56$, $\text{d.o.f.}=1,22$, $p=0.225$). Percent C and N did not explain a significant amount of the variation in the T-RFLP profiles of the individual 4-6.3 mm aggregates ($p=0.3494$).

KBS Pooled Aggregate Layers

Effects of aggregate layer and cropping system were tested using all T-RFLP profiles generated from pooled aggregate layers from KBS. The effect of aggregate size class was tested after reducing the number of replicates in the 2-4 mm size class to three, to be balanced with the 4-6.3 mm size class, where the layers of aggregates of one field replicate were not pooled. Aggregate layer was found to have a significant effect on MspI T-RFLP profiles using Jaccard distance if permutations were restricted to the layers of corresponding aggregate samples, as in a split-plot design. The variability explained by aggregate layer was 5.5% of the total variability in Jaccard distances (see Table 2). The effect of aggregate layer was also marginally significant in the case of Hellinger

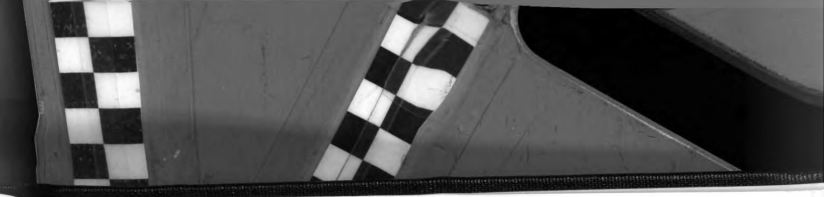


distances between MspI profiles using the same permutation scheme, but was not significant for RsaI profiles. Three T-RFs had greater than 20% of the variability in their Hellinger-transformed abundance explained by aggregate layer in the MspI profiles after accounting for effects of aggregate size, cropping system, and treatment interactions: 435-437 bp (23% explained, found only in external layers from corn soil), 439-442 bp (43%, found only in external layers), and 450-452 bp (25%, found in six internal layer samples and two alfalfa external layer samples).

Aggregate size class and cropping system were consistently found significant in both RsaI and MspI profiles in pooled aggregate layer samples, while interaction effects were only significant in MspI profiles (see Table 2). Clustering by treatments was weak in dendrograms such as Figure 3. Figure 4 shows the separation of samples by aggregate size class and cropping system in the canonical principal components ordination from the RsaI Hellinger distance redundancy analysis. While cropping systems are completely separated in the canonical cropping systems ordination (see Figure 4a), there is some overlap of aggregate size classes in the size class ordination (see Figure 4b). Treatment explained greater than 20% of the variation in 21 T-RFs. Their relationships to the treatments are shown by plotting their canonical principal component scores with the sample scores in Figure 4.

Percent C in pooled KBS aggregate layers was not significantly affected by aggregate layer, size class, or interaction effects, as indicated three-way ANOVA. The ANOVA model was significant overall due to cropping system effects ($F=8.3$, $d.o.f.=4,37$, $p<0.0001$). Percent C was 1.8% in organic corn, 1.3% in alfalfa, and 0.9% in conventional corn aggregate layers. Treatment effects on percent N were also significant





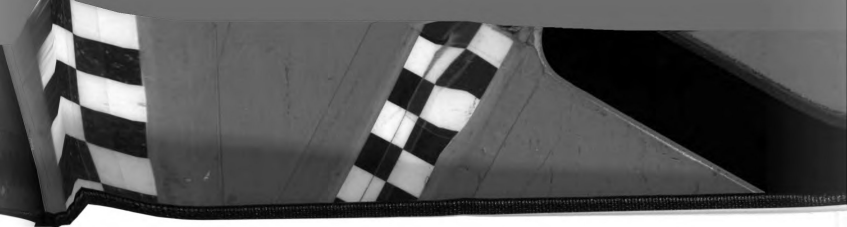
overall ($F=3.5$, d.o.f.=4,37, $p=0.016$), with trends due to cropping system following the same trend as for percent C ($p=0.049$). Percent N was also significantly increased in the 2-4 mm (0.24%) compared to 4-6.3 mm aggregates (0.11%, $p=0.017$).

Percent C explained a small but significant proportion of the total variability in T-RFLP profiles of the pooled aggregate layers from KBS in both RsaI ($p=0.0004$, variability explained=6%) and MspI ($p=0.0087$, variability explained=9%) profiles. Percent C was not significant if treatment effects were first partialled out. Effects of percent N were not significant ($p=0.727$ for RsaI and 0.4279 for MspI).

Wooster Pooled Aggregate Layers

To achieve balanced replicate numbers of profiles between treatments, two datasets were used to test different treatment effects on T-RFLP profiles with redundancy analysis. The 4-6.3 mm aggregate size class was used to test the effects of aggregate layer and soil management. Aggregate layer (with or without restricted permutations) and interaction effects were significant when analyzing principal coordinates of Jaccard distance between profiles, and soil management was marginally-significant (see Table 3). The effects of aggregate layer (using restricted permutation) was the only significant treatment effect when analyzing Hellinger distance between the same profiles. The significant effects can be seen in the canonical principal components plot derived from the redundancy analysis of aggregate layer and treatment interaction effects in Figure 5. The aggregate layers are separated, and all successional vegetation samples are separated from the continuous corn samples. In plots of non-canonical analyses, such as the Jaccard distance principal coordinates plot in Figure 6, separation of samples due to management is not evident. Two-thirds of the aggregate interiors group apart from the





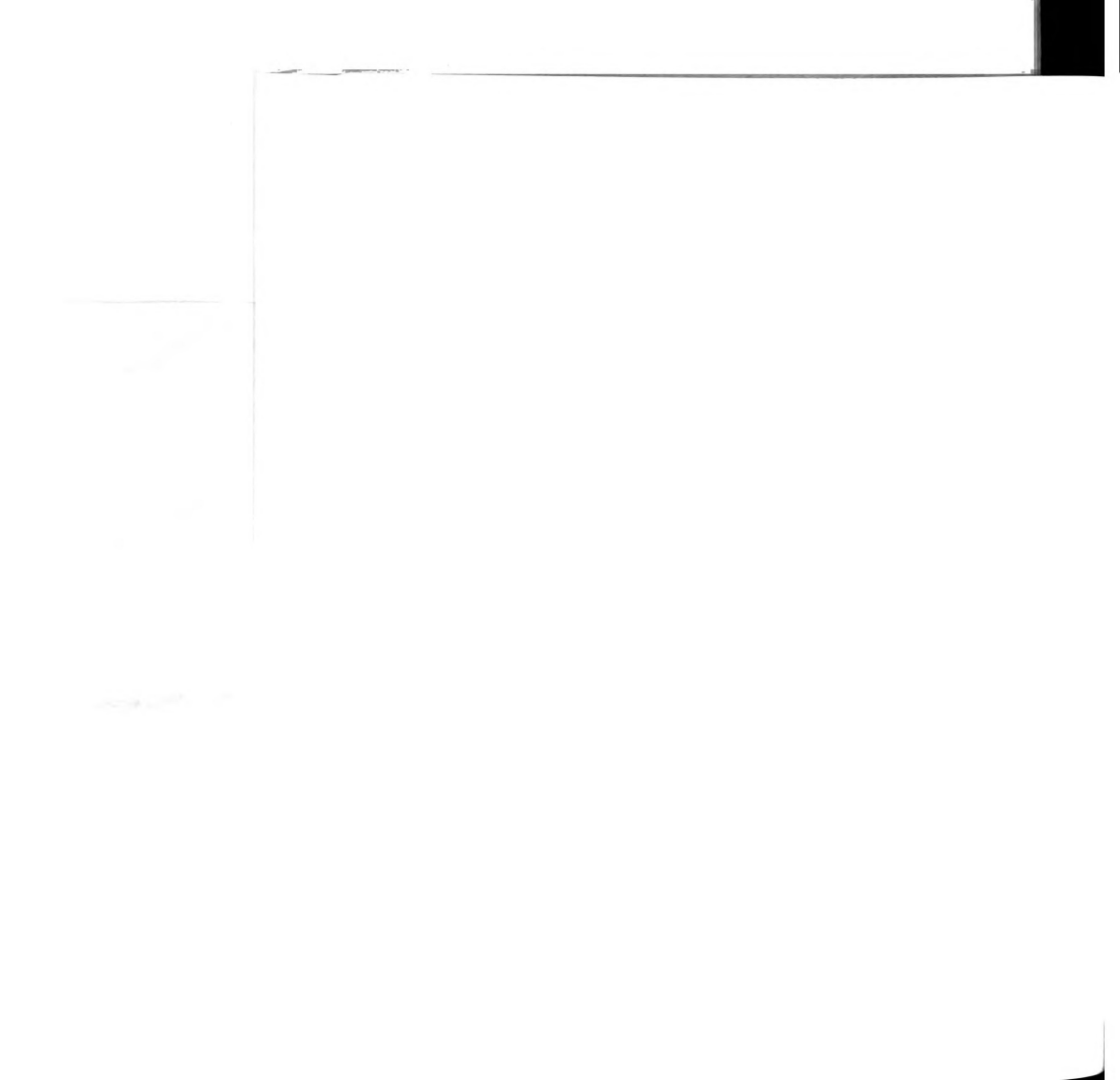
aggregate exteriors. Less structure is evident in Figure 6, the Ward's clustering dendrogram of Jaccard distances, the main feature of which is a successional vegetation aggregate interior as an outlier.

The significance of aggregate size on Wooster T-RFLP profiles was tested with no-till and successional vegetation aggregate layers. Significant treatment effects were only observed when analyzing Jaccard distance. Soil management and treatment interaction effects were significant and aggregate size was marginally significant (see Table 3). The absence of any aggregate layer effect implies that 2-4 mm aggregates are much more uniform than the 4-6.3 mm aggregates.

Discussion

The strongest influence on the T-RFLP profiles detected in this study was from land management regimes, accounting for from 10 to 40% of the variance in patterns of T-RF abundance, depending on the dataset and method of analysis. This is in agreement with the analyses of other of soil fractions described in chapter 3.

Significant effects of aggregate size at KBS were detected in pooled aggregate layer profiles, but not in profiles from HF-1 or LF-1 from differing aggregate size classes from subsamples of the same soil. Different communities in aggregate layers may confound effects of aggregate size in the HF-1 and LF-1, where aggregate layers are combined by default. It cannot be discounted that the differences in T-RFLP profiles due to aggregate size class in the pooled aggregate layer samples may be due to differential effects of storage and erosion on aggregate size class since 1. the effects of aggregate layer were relatively weak, 2. grouping by layer was not observed in the canonical

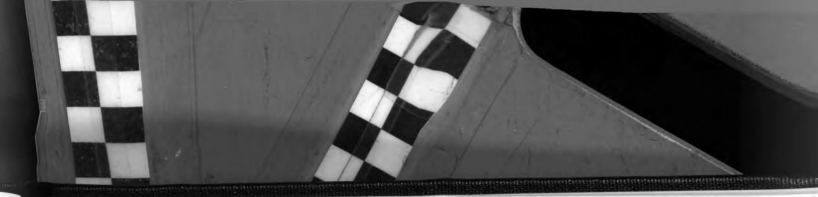


ordination plots, and 3. the overall variability accounted for by size class was only 5%. A small but significant storage effect was detected in HF-1 profiles from samples that had and had not been stored an additional 12 weeks, and the RsaI T-RFs involved were deleted in other analyses. Aggregate size class was not found to be a significant factor in profiles from Wooster aggregate layer samples, where length of storage of aggregates was not as great.

Effects of aggregate layer were detected in RsaI profiles from layers of individual KBS aggregates using exploratory data analysis of strong profiles (see Chapter 2 for a discussion of exploratory data analysis of T-RFLP profiles). Within pooled aggregate layers, effects of aggregate layer on T-RFLP profiles were detected only in MspI digests, which were not corrected for storage. The proportion of the total variability accounted for by layer in the MspI digests was similar to the amount accounted for by the storage effect. Therefore the effects of aggregate layer were probably not significant for these samples, as indicated by the pooled aggregate layer RsaI profiles.

Aggregate layer effects may have been detected in individual aggregate layers and not pooled aggregate layers due to high aggregate-to-aggregate variability. Aggregate-to-aggregate variability was taken into account in the significance testing of individual aggregate layers by permuting layers only within individual aggregates. This form of permutation was also required because aggregate layer was nested within cropping system treatment for individual aggregates. Pooling of aggregate layers was an attempt to average out this variability. Success in the ability to average out the variability, however, depends on its strength. If very strong aggregate-to-aggregate variability exists, pooling of layers from only four aggregates may confound any differences between





layers, rather than enhancing the ability to detect them. While permuting within field replicate of pooled aggregate layers is not strictly correct, it is probable that not enough aggregates were pooled to average out the aggregate-to-aggregate variability or result in independence of aggregate layer and cropping system treatments. Note that while the split-plot design alters the permutation procedure it does not alter the assumption of redundancy analysis of a linear relationship between T-RFs and treatment. Hence the effects of aggregate layer must still be consistent across aggregates (corrected for other treatment and interaction effects) for significant differences to be found.

Permuting using the split-plot design resulted in significant differences between aggregate layers for the 4-6.3 mm Wooster aggregates, but not when 2-4 mm aggregates were included in the analysis. This is not surprising since it is likely that differences in the environments of external and internal aggregate layers are greater when aggregates are larger. Differences between aggregate profiles based on tillage were not found at Wooster, although the T-RFLP profiles from successional vegetation were quite different from those of the continuous corn fields. This result is not consistent with the differences between profiles due to cropping system at KBS presented here and in chapter 3. The cropping systems studied at KBS may be more divergent than the tilled and no-till continuous corn plots at Wooster because many agronomic variables at KBS are varied besides tillage, including the type and diversity of crops and addition of fertilizers and compost.

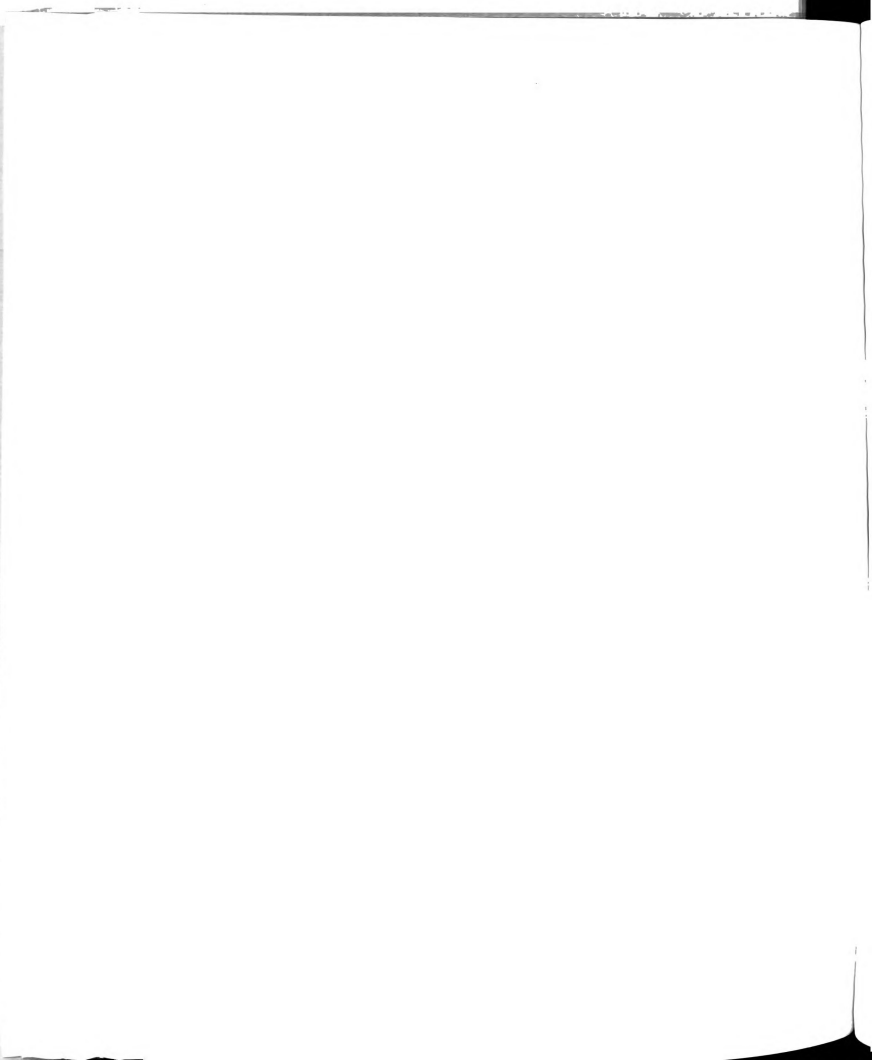
Conclusions

There is high variability in the literature concerning which aggregate size class contains the greatest numbers and activities of soil microorganisms, as noted in the

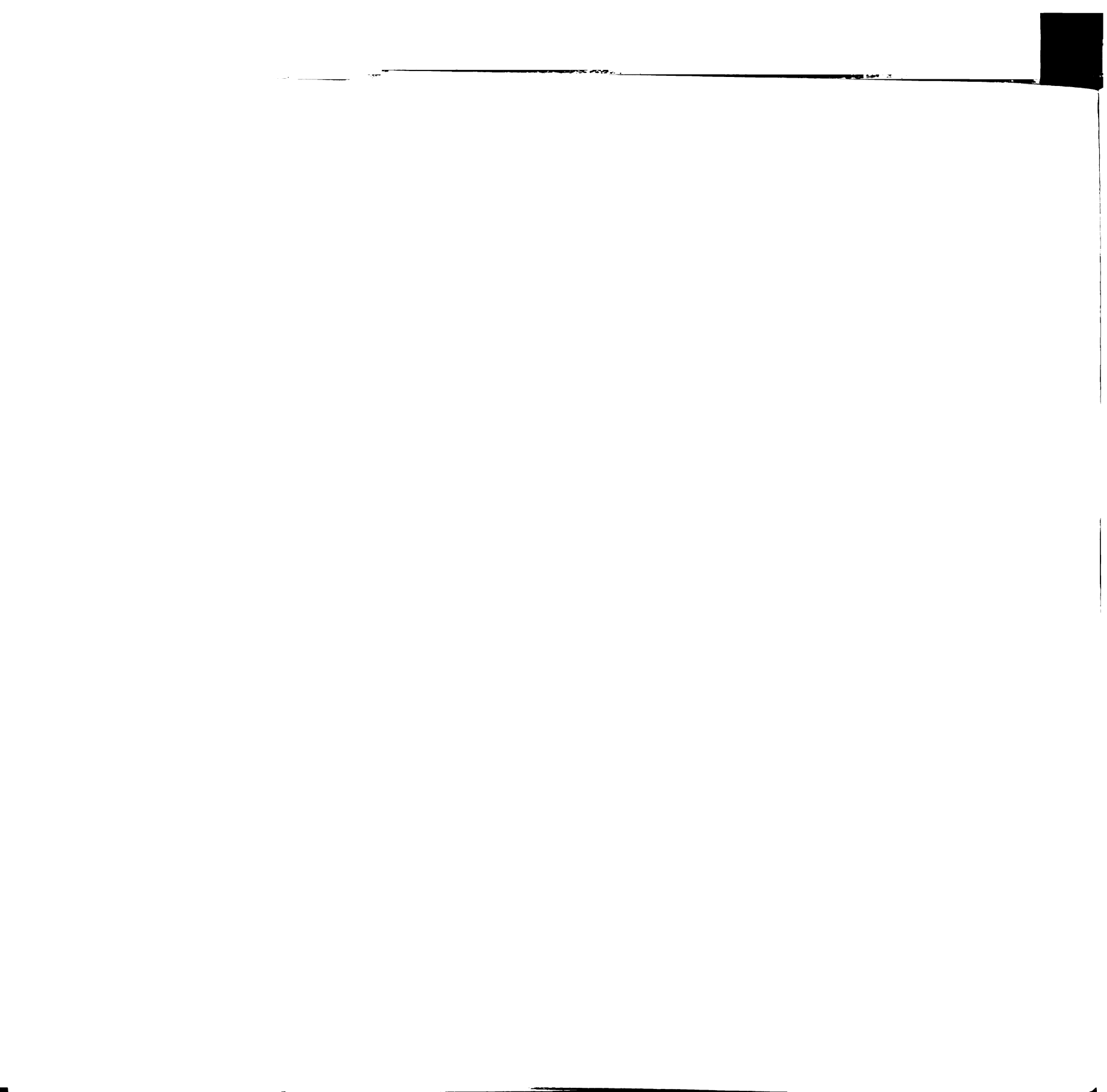


Introduction. Soil aggregate dynamics are dependent on particular site characteristics such as clay and organic matter content and soil management (Ladd et al. 1996). Seasonal variability in soil aggregation is also likely important in the field (Mendes et al. 1999, Mendes and Bottomley 1998), and variability in methods of soil fractionation are likely the cause of many differences between studies (Christensen 1996, Jastrow and Miller 1991). The results obtained here agree in general with other culture-independent studies which have found that aggregate size class has small effects on microbial communities, if any (Peterson et al. 1997, Ramakrishnan et al. 2000).

The effects of the position of a community within a soil aggregate may be greater than size class, but is dependent on statistical comparisons within individual aggregates. Tertiary soil structure, such as proximity of sites to macropores or decomposing shoot residue, may be essential in determining the composition and activity of microbial communities within different aggregates and sites within aggregates (Parkin 1993, Young and Ritz 2000). While some consistent environmental differences may exist between macroaggregate size classes and layers within aggregates, their turnover time of up to 10 years (Buyanovsky et al. 1994, Monreal et al. 1997) may be too rapid relative to the low rates of microbial growth in soil to allow much differentiation of communities to occur (approximately 3 generations per year, Harris and Paul 1994). More rapid growth in the rhizosphere, LF, and shoot residue, on the other hand, allows for extensive changes in the makeup of the community due to differential success of species under different conditions (see Chapter 3). Dispersal rates relative to rates of habitat turnover and growth will also affect the differentiation of communities in different soil fractions. Microbial dispersal is generally viewed as passive and dependent on the soil water status,

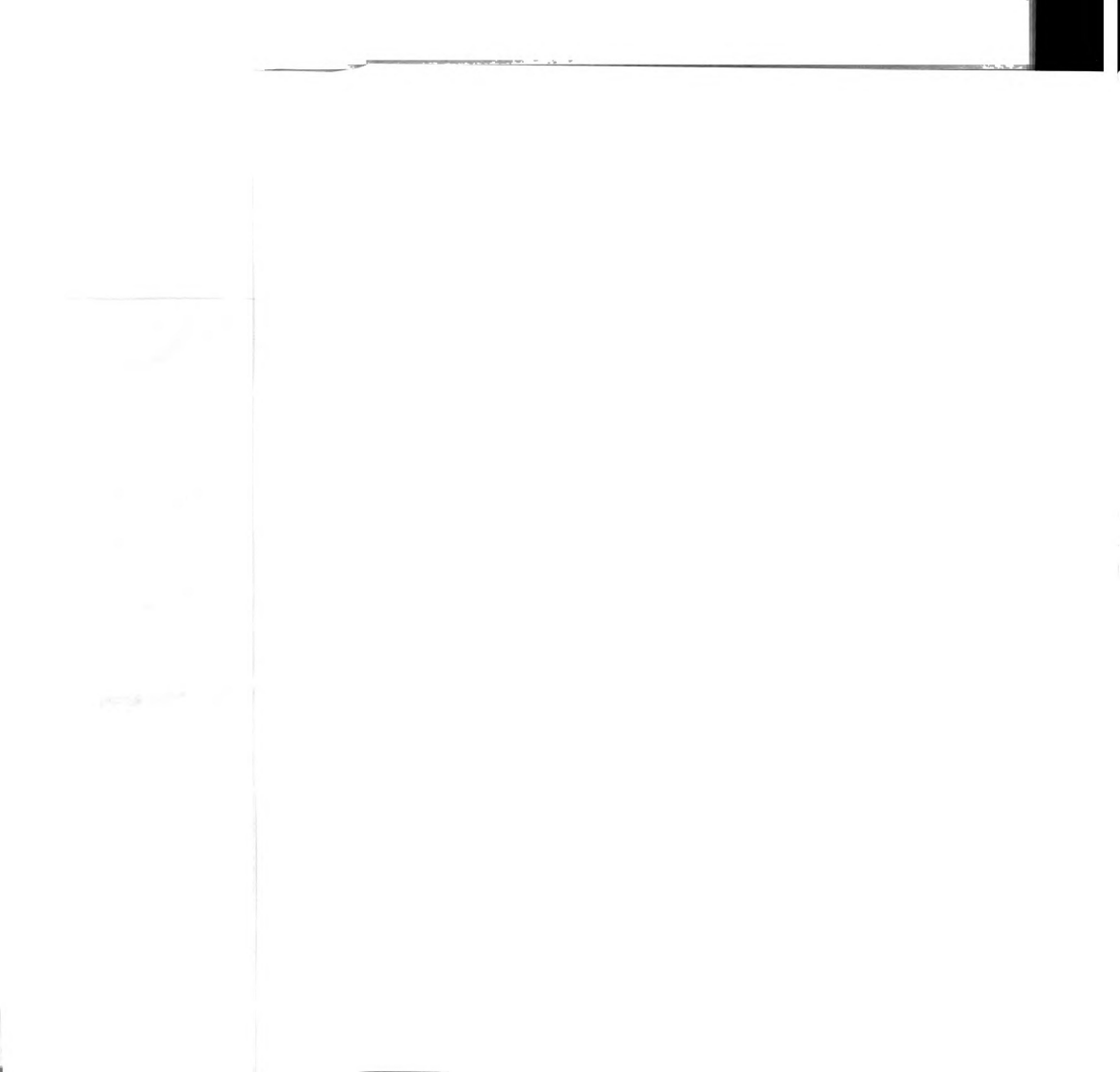


although more study of this phenomenon is greatly needed (Murphy and Tate 1996). If the structure of soil aggregates is truly hierarchical, differences between microaggregate size classes, which turn over much more slowly than macroaggregates, may also be important in determining community composition. Environmental heterogeneity at a broader scale was found to be important since communities were consistently differentiated by cropping system or soil management. This shows that the numerically dominant bacterial community in agricultural soil, those in heavy fraction or aggregates, is sensitive to long term changes in their environment.

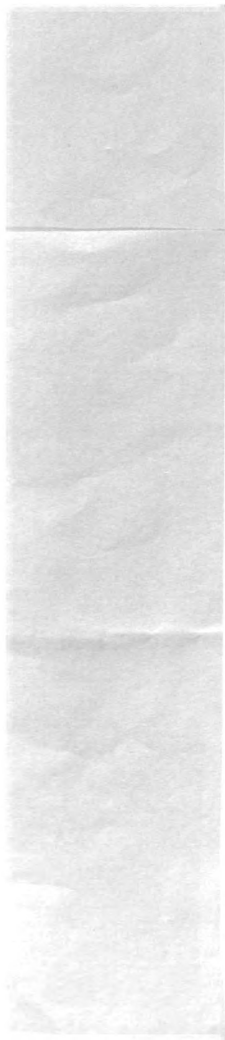


References

- Beare, M.H., M.L. Cabrera, P.F. Hendrix, D.C. Coleman. 1994a. Aggregate-protected and unprotected organic matter pools in conventional and no-tillage soils. *Soil Science Society of America Journal* 58:787-795.
- Beare, M.H., P.F. Hendrix, D.C. Coleman. 1994b. Water-stable aggregates and organic matter fractions in conventional- and no-tillage soils. *Soil Science Society of America Journal* 58:777-786.
- Buyanovsky, G.A., M. Aslam, G.H. Wagner. 1994. Carbon turnover in soil physical fractions. *Soil Science Society of America Journal* 58:1167-1173.
- Christensen, B.T. 1996. Carbon in primary and secondary organomineral complexes. In *Structure and Organic Matter Storage in Agricultural Soils*, edited by M. R. Carter and B. A. Stewart. Boca Raton: CRC Press.
- Dabek-Szreniawska, M. 1993. Effect of keratin-carbamide fertilization on microorganisms in soil aggregates. *Polish Journal of Soil Science* 26:49-57.
- Drazkiewicz, M. 1994. Distribution of microorganisms in soil aggregates: effect of aggregate size. *Folia Microbiologica* 39:276-282.
- Edwards, A.P., J.P. Bremner. 1967. Microaggregates in soils. *Journal of Soil Science* 18:64-73.
- Elliott, E.T. 1986. Aggregate structure and carbon, nitrogen, and phosphorus in native and cultivated soils. *Soil Science Society of America Journal* 50:627-633.
- Elliott, E.T., R.V. Anderson, D.C. Coleman, C.V. Cole. 1980. Habitable pore space and microbial trophic interactions. *Oikos* 35:327-335.
- Elliott, E.T., D.C. Coleman. 1988. Let the soil work for us. *Ecological Bulletins* 39:23-32.
- Golchin, A., J.M. Oades, J.O. Skjemstad, P. Clarke. 1994. Soil structure and carbon cycling. *Australian Journal of Soil Research* 32:1043-1068.
- Gupta, V.V.S.R., J.J. Germida. 1988. Distribution of microbial biomass and its activity in different soil aggregate size classes as affected by cultivation. *Soil Biology and Biochemistry* 20:777-786.
- Harris, D., E.A. Paul. 1994. Measurement of bacterial growth rates in soil. *Applied Soil Ecology* 1:277-290.



- Hattori, T. 1988. Soil aggregates as microhabitats of microorganisms. *Report of the Institute for Agricultural Research, Tohoku University* 37:23-36.
- Hojberg, O., N.P. Revsbech, J.M. Tiedje. 1994. Denitrification in soil aggregates analyzed with microsensors for nitrous oxide and oxygen. *Soil Science Society of America Journal* 58:1691-1698.
- Jastrow, J.D., R.M. Miller. 1991. Methods assessing the effects of biota on soil structure. *Agriculture, Ecosystems and Environment* 34:279-303.
- Jones, M.E., R.R. Harwood, N.C. Dehne, J. Smeenk, E. Parker. 1998. Enhancing soil nitrogen mineralization and corn yield with overseeded cover crops. *Soil and Water Conservation* 53:245-249.
- Kanazawa, S., Z. Filip. 1986. Distribution of microorganisms, total biomass, and enzyme activities in different particles of brown soil. *Microbial Ecology* 12:205-215.
- Ladd, J.N., R.C. Foster, P. Nannipieri, J.M. Oades. 1996. Soil structure and biological activity. In *Soil Biochemistry*, edited by G. Stotzky and J. Bollag. New York: Marcel Dekker.
- Lefelaar, P.A. 1993. Water movement, oxygen supply and biological processes at the aggregate scale. *Geoderma* 57:143-165.
- Legendre, P., M.J. Anderson. 1999. Distance-based redundancy analysis: testing multispecies responses in multifactorial ecological experiments. *Ecological Monographs* 69:1-24.
- Madsen, E.L. 1996. A critical analysis of methods for determining the composition and biogeochemical activities of soil microbial communities in situ. In *Soil Biochemistry*, edited by G. Stotzky and J. Bollag. New York: Marcel Dekker.
- Mendes, I.C., A.K. Bandick, R.P. Dick, P.J. Bottomley. 1999. Microbial biomass and activities in soil aggregates affected by winter cover crops. *Soil Science Society of America Journal* 63:873-881.
- Mendes, I.C., P.J. Bottomley. 1998. Distribution of a population of *Rhizobium leguminosarum* bv. trifolii among different size classes of soil aggregates. *Applied and Environmental Microbiology* 64:970-975.
- Miller, R.M., J.D. Jastrow. 1990. Hierarchy of root and mycorrhizal fungal interactions with soil aggregation. *Soil Biology and Biochemistry* 22:579-584.
- Monreal, C.M., H. Kodoma. 1997. Influence of aggregate architecture and minerals on living habitats and soil organic matter. *Canadian Journal of Soil Science* 77:367-377.



Monreal, C.M., H.-R. Schulten, H. Kodoma. 1997. Age, turnover and molecular diversity of soil organic matter in aggregates of a Gleysol. *Canadian Journal of Soil Science* 77:379-388.

Murphy, S.L., R.L. Tate, III. 1996. Bacterial movement through soil. In *Soil Biochemistry*, edited by G. Stotzky and J. Bollag. New York: Marcel Dekker.

Muyzer, G. 1998. Structure, function and dynamics of microbial communities: the molecular biological approach. In *Advances in Molecular Ecology*, edited by G. R. Carvalho: IOS Press.

Parkin, T.B. 1993. Spatial variability of microbial processes in soil - a review. *Journal of Environmental Quality* 22:409-417.

Paul, E.A., D. Harris, M.J. Klug, R.W. Ruess. 1999. The determination of microbial biomass. In *Standard Soil Methods for Long Term Ecological Research*, edited by G. P. Robertson, D. C. Coleman, C. S. Bledsoe and P. Sollins. New York: Oxford University Press.

Peterson, S.O., K. Debosz, P. Schojoning, B.T. Christensen, S. Elmholt. 1997. Phospholipid fatty acid profiles and C availability in wet-stable macroaggregates from conventionally and organically farmed soils. *Geoderma* 78:181-196.

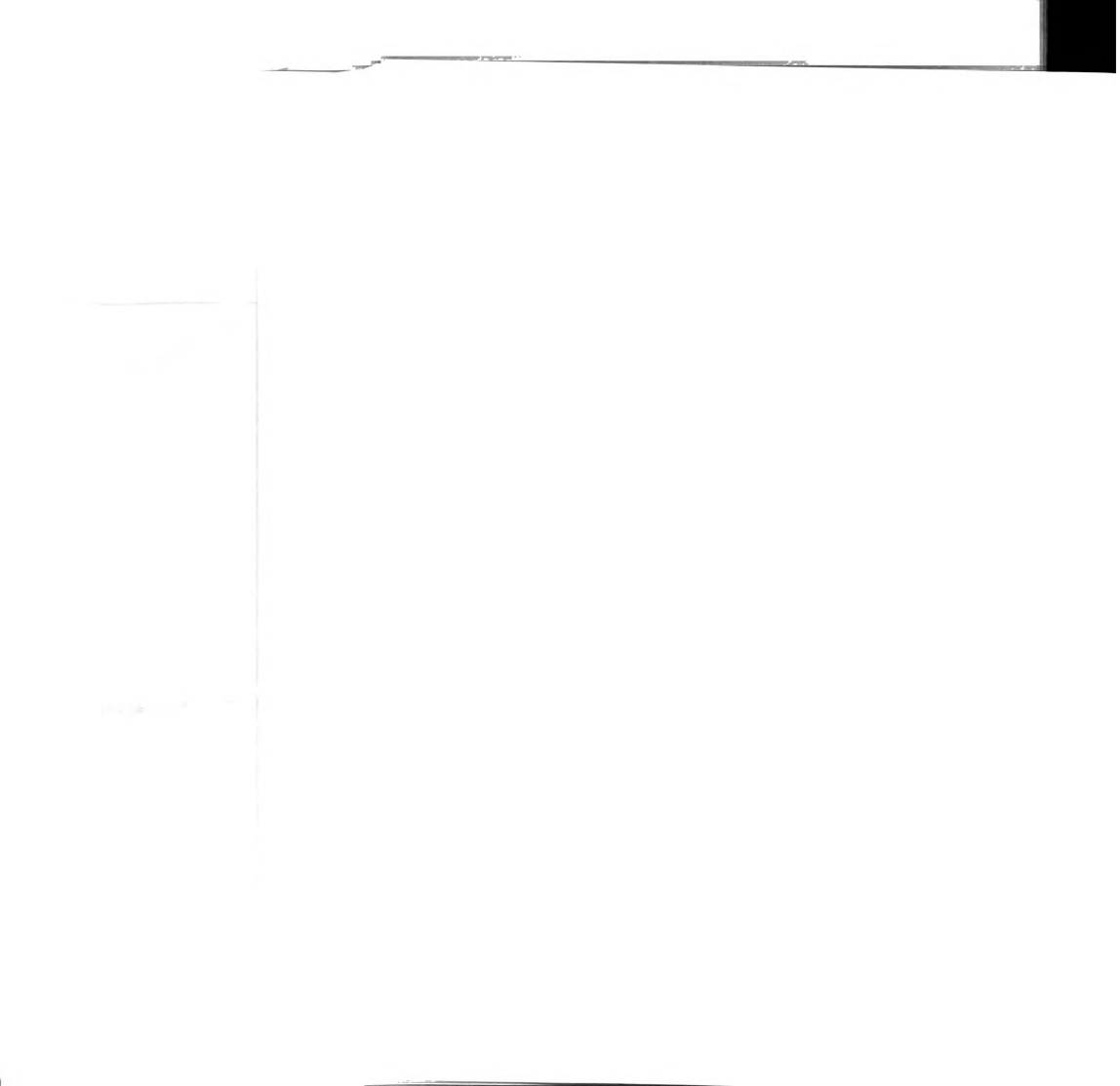
Poly, F., L. Ranjard, S. Nazaret, F. Gourbière, L.J. Monrozier. 2000. Comparison of *nifH* gene pools in soils and soil microenvironments with contrasting properties. *Applied and Environmental Microbiology* 67:2255-2262.

Priesack, E., G.M. Kisser-Priesack. 1993. Modelling diffusion and microbial uptake of ¹³C-glucose in soil aggregates. *Geoderma* 56:561-573.

Ramakrishnan, B., T. Lueders, R. Conrad, M. Friedrich. 2000. Effect of soil aggregate size on methanogenesis and archaeal community structure in anoxic rice field soil. *FEMS Microbiology Ecology* 32:261-270.

Ranjard, L., E. Brothier, S. Nazaret. 2000a. Sequencing bands of ribosomal intergenic spacer analysis fingerprints for characterization and microscale distribution of soil bacterium populations responding to mercury spiking. *Applied and Environmental Microbiology* 66:5334-5339.

Ranjard, L., S. Nazaret, F. Gourbière, J. Thioulouse, P. Linet, A. Richaume. 2000b. A soil microscale study to reveal the heterogeneity of Hg(II) impact on indigenous bacteria by quantification of adapted phenotypes and analysis of community DNA fingerprints. *FEMS Microbiology Ecology* 31:107-115.



Robertson, G.P., K.M. Klingensmith, M.J. Klug, E.A. Paul, J.R. Crum, B.G. Ellis. 1997. Soil resources, microbial activity, and primary production across an agricultural ecosystem. *Ecological Applications* 7:158-170.

Santos, D., S.L.S. Murphy, H. Taubner, A.J.M. Smucker, R. Horn. 1997. Uniform separation of concentric surface layers from soil aggregates. *Soil Science Society of America Journal* 61:720-724.

Sexstone, A.J., N.P. Revsbech, T.B. Parkin, J.M. Tiedje. 1985. Direct measurement of oxygen profiles and denitrification rates in soil aggregates. *Soil Science Society of America Journal* 49:645.

Tisdall, J.M., J.M. Oades. 1982. Organic matter and water-stable aggregates in soils. *Journal of Soil Science* 33:141-163.

Young, I.M., K. Ritz. 2000. Tillage, habitat space and function of soil microbes. *Soil & Tillage Research* 53:201-213.

Zausig, J., W. Stepniewski, R. Horn. 1993. Oxygen concentration and redox potential gradients in unsaturated model soil aggregates. *Soil Science Society of America Journal* 57:908-916.

Table 1: Redundancy analysis of HF-1 and LF-1 isolated from different aggregate size classes at KBS. Analyses of “all” fractions included 0-2 mm HF-1 and whole soil samples for HF-1 analysis, and 0-2 mm LF-1 for LF-1 analysis. N=4 replicates per fractionXcropping system treatment.

		Soil Fraction	Cropping System	Interaction	Sum
Hellinger distance					
HF-1, all	P	0.4731	0.0001	0.1348	
	% of total variance		20.6		20.6
HF-1, 2-4 and 4-6.3	P	0.5893	0.0001	0.8249	
	% of total variance		23.8		23.8
LF-1, all	P	0.6239	0.0001	0.4269	
	% of total variance		31.4		31.4
LF-1, 2-4 and 4-6.3	P	0.4445	0.0001	0.3449	
	% of total variance		34.7		34.7
Jaccard distance					
HF-1, all	P	0.2697	0.0001	0.0116	
	% of total variance		15.4	12.7	28.1
HF-1, 2-4 and 4-6.3	P	0.7966	0.0081	0.9512	
	% of total variance		10.5		10.5

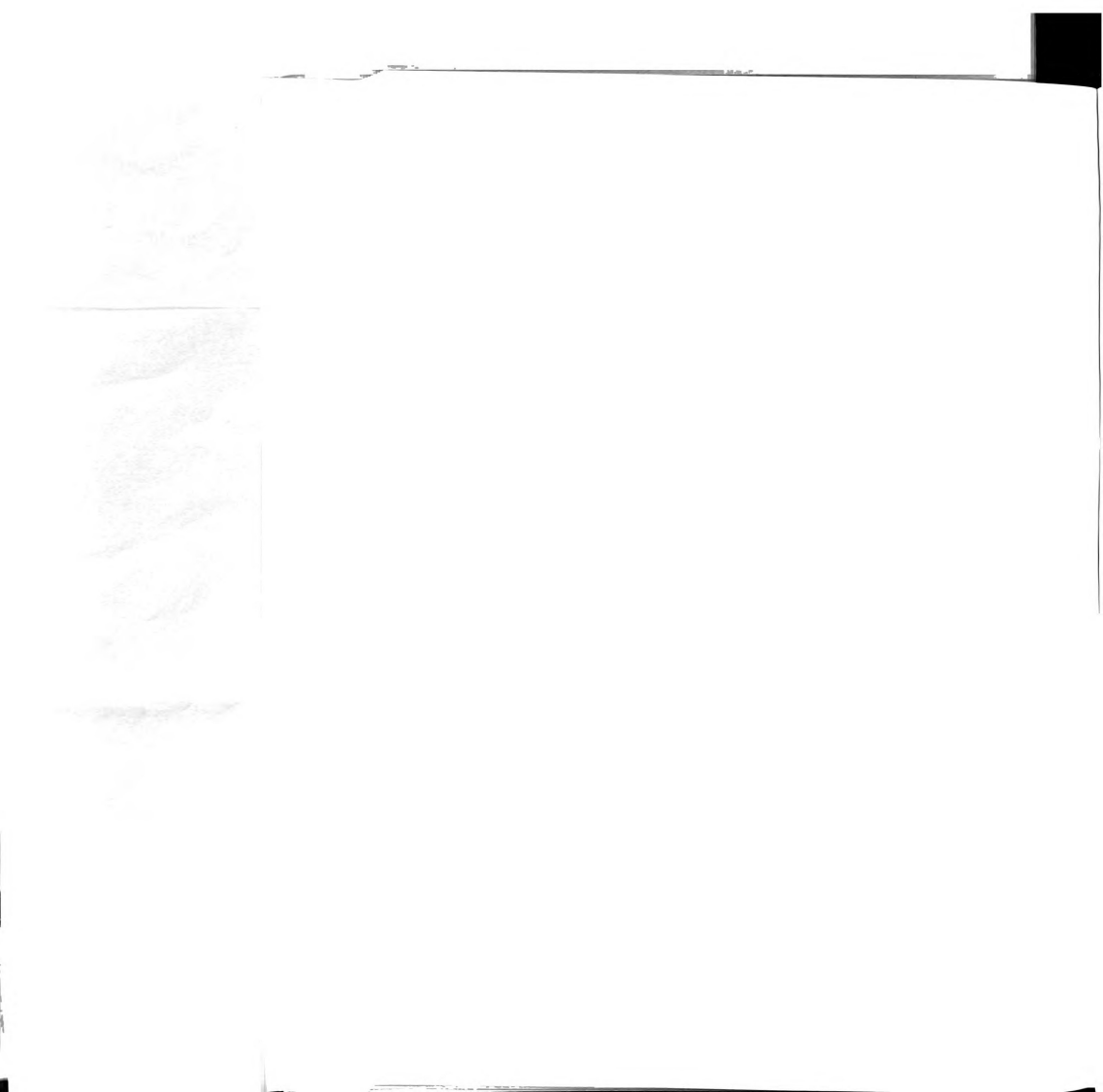


Table 2: Redundancy analysis of pooled aggregate layer samples from KBS. P-values generated by 9999 random permutations of sample identity. N=3 replicates per layerXaggregate sizeXcrop treatment in testing cropping effects and N=4 replicates per treatment when testing other effects on RsaI profiles. N=2 replicates per treatment for MspI profiles.

		Layer	Size	Crop	Interaction	Sum
Hellinger Distance						
RsaI	P (unrestricted)	0.1893	0.0003	0.0001	0.0563	
	P (split-plot)	0.1998				
	% of total variability		5	14.1		19.1
MspI	P (unrestricted)	0.5300	0.0004	0.0001	0.0338	
	P (split-plot)	0.0648				
	% of total variability		9.2	18.5	10.9	38.6
Jaccard Distance						
RsaI	P (unrestricted)	0.5203	0.0046	0.0001	0.0800	
	P (split-plot)	0.1417				
	% of total variability		4.4	10.2		14.2
MspI	P (unrestricted)	0.2254	0.0317	0.0006	0.0358	
	P (split-plot)	0.0096				
	% of total variability	5.5	6.3	13.3	11.3	36.3

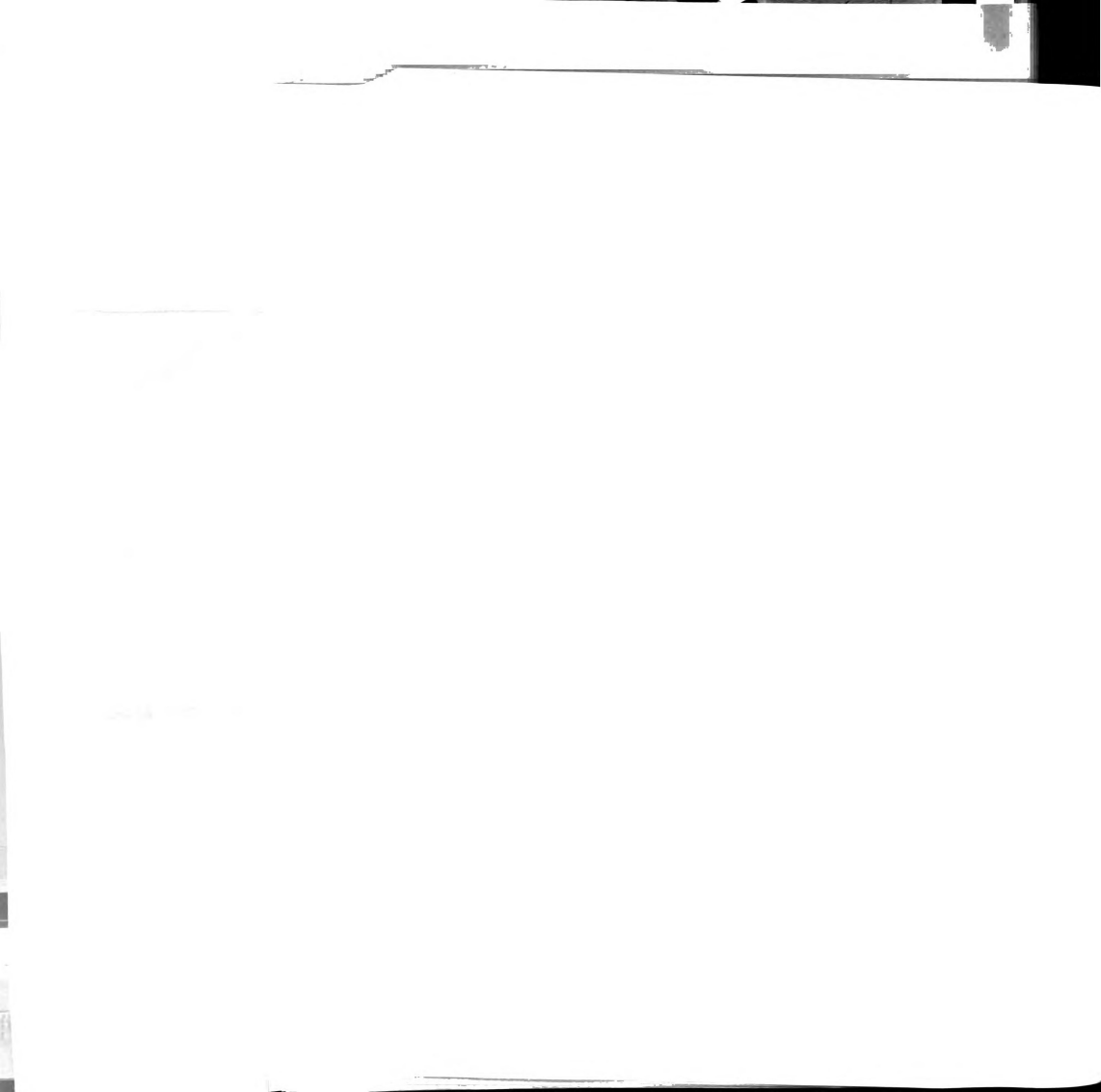


Table 3: Redundancy analysis of pooled aggregate layer samples from Wooster. P-values generated by 9999 random permutations of sample identity. N=3 replicates per layerXaggregate sizeXmanagement treatment.

	Layer	Size	Management	Interaction	Sum
4-6.3 mm aggregates					
Hellinger Distance	P (unrestricted)	0.4380	NA	0.4390	0.4615
	P (split-plot)	0.0274			
	% of total variability	7.1			7.1
Jaccard Distance	P (unrestricted)	0.0165	NA	0.0552	0.0221
	P (split-plot)	0.0089			
	% of total variability	9.2		14.9	24.1
No-till corn and successional vegetation					
Hellinger Distance	P (unrestricted)	0.4183	0.3331	0.3342	0.3742
	P (split-plot)	0.4412			
	% of total variability				
Jaccard Distance	P (unrestricted)	0.6340	0.0723	0.0201	0.0154
	P (split-plot)	0.3819			
	% of total variability		6.5	16.1	22.6

Figure 1: Dendrogram of cluster analysis by Ward's method of RsaI T-RFLP profiles from aggregate layers of individual 4-6.3 mm KBS aggregates. Samples are named according to the following: plot number (T6R4 is alfalfa, 419 is conventional corn, 407 is organic corn)-aggregate identification number-aggregate layer (E=external, I=internal).

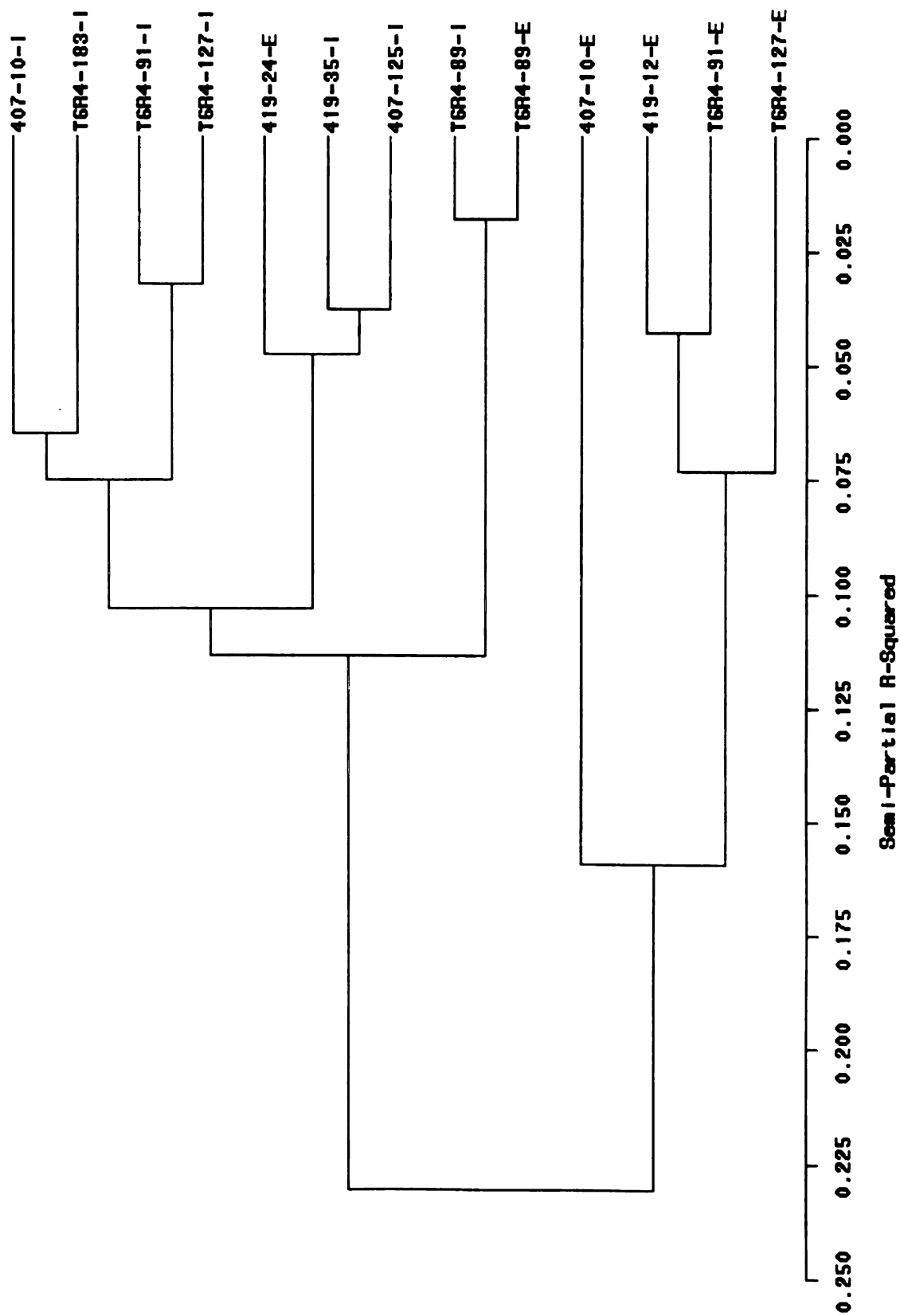


Figure 2: Plots of principal coordinates of Jaccard distance between T-RFLP profiles of layers of individual 4-6.3 mm KBS aggregates. Lines connect layers of the same aggregate. Circles=internal layer, Triangles=external layer, White=alfalfa, Black=conventional corn, Grey=organic corn

Figure 2a: First and second principal coordinates

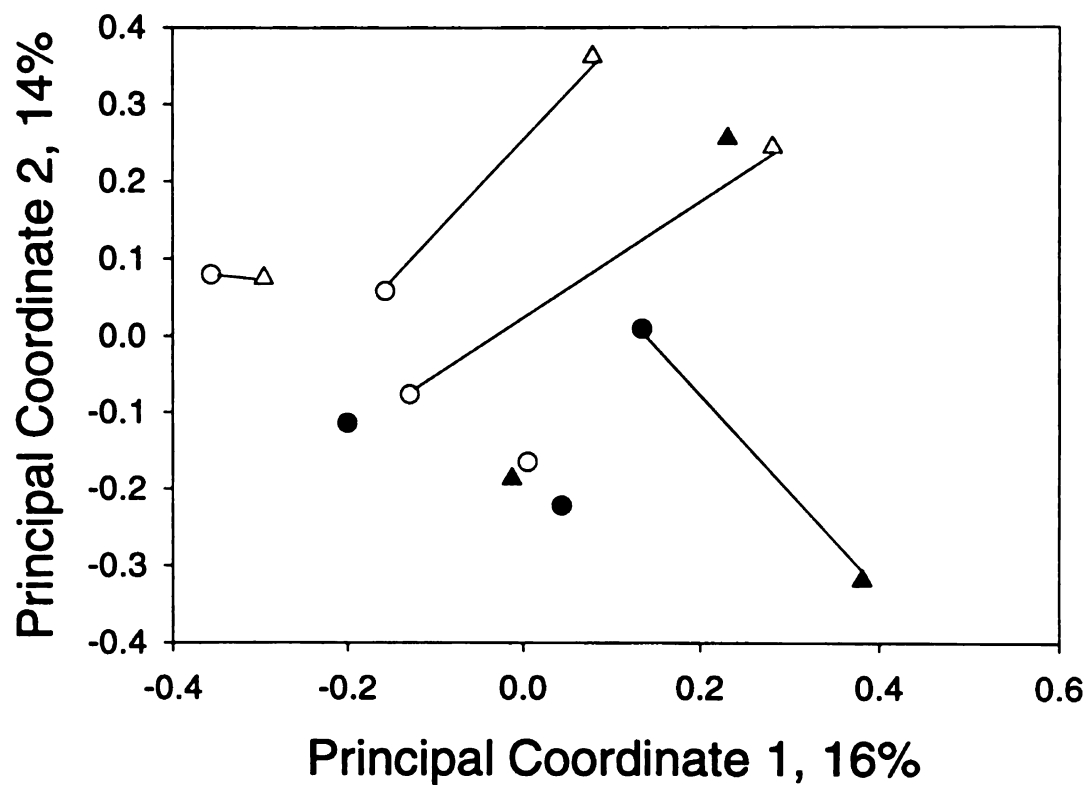
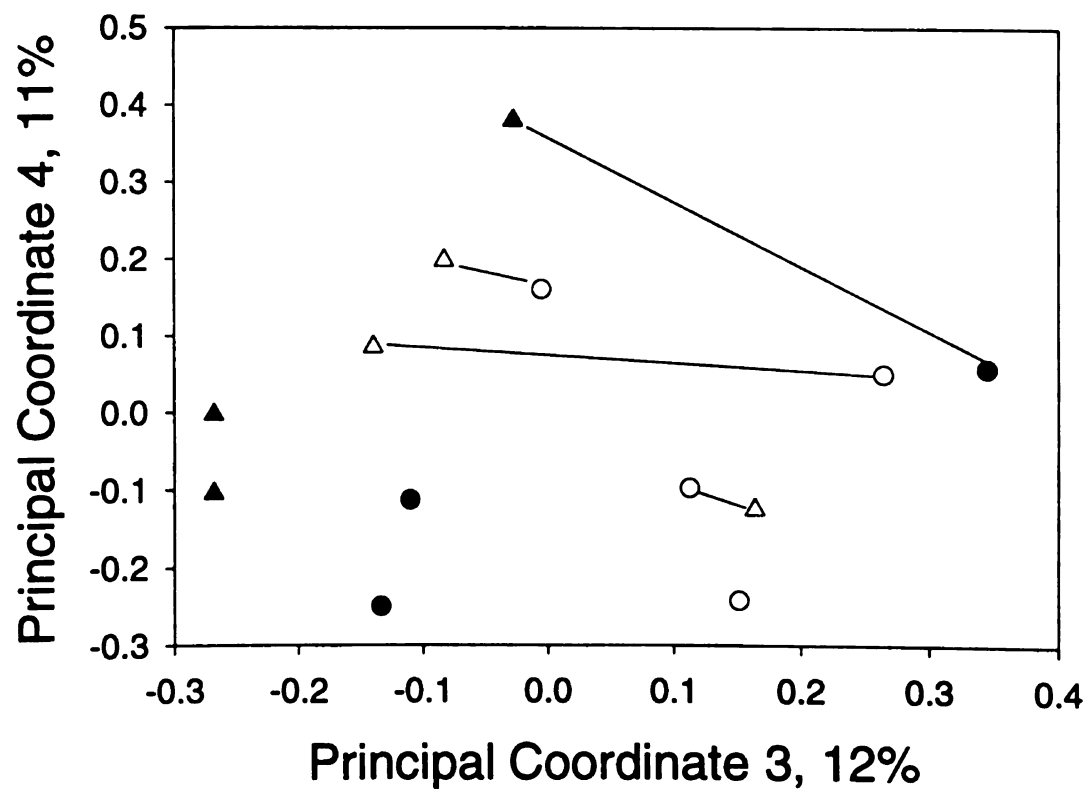


Figure 2b: Third and fourth principal coordinates



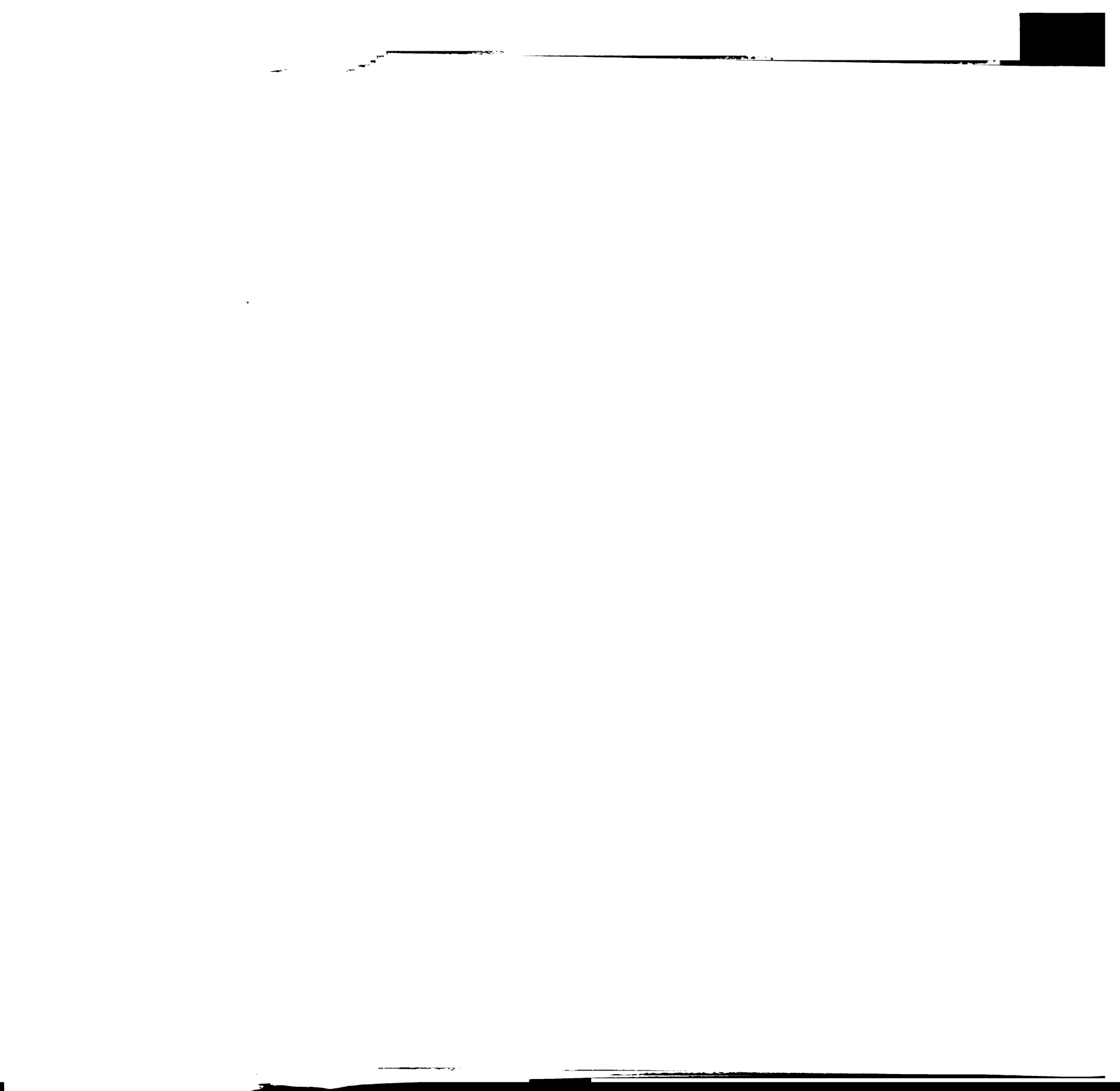
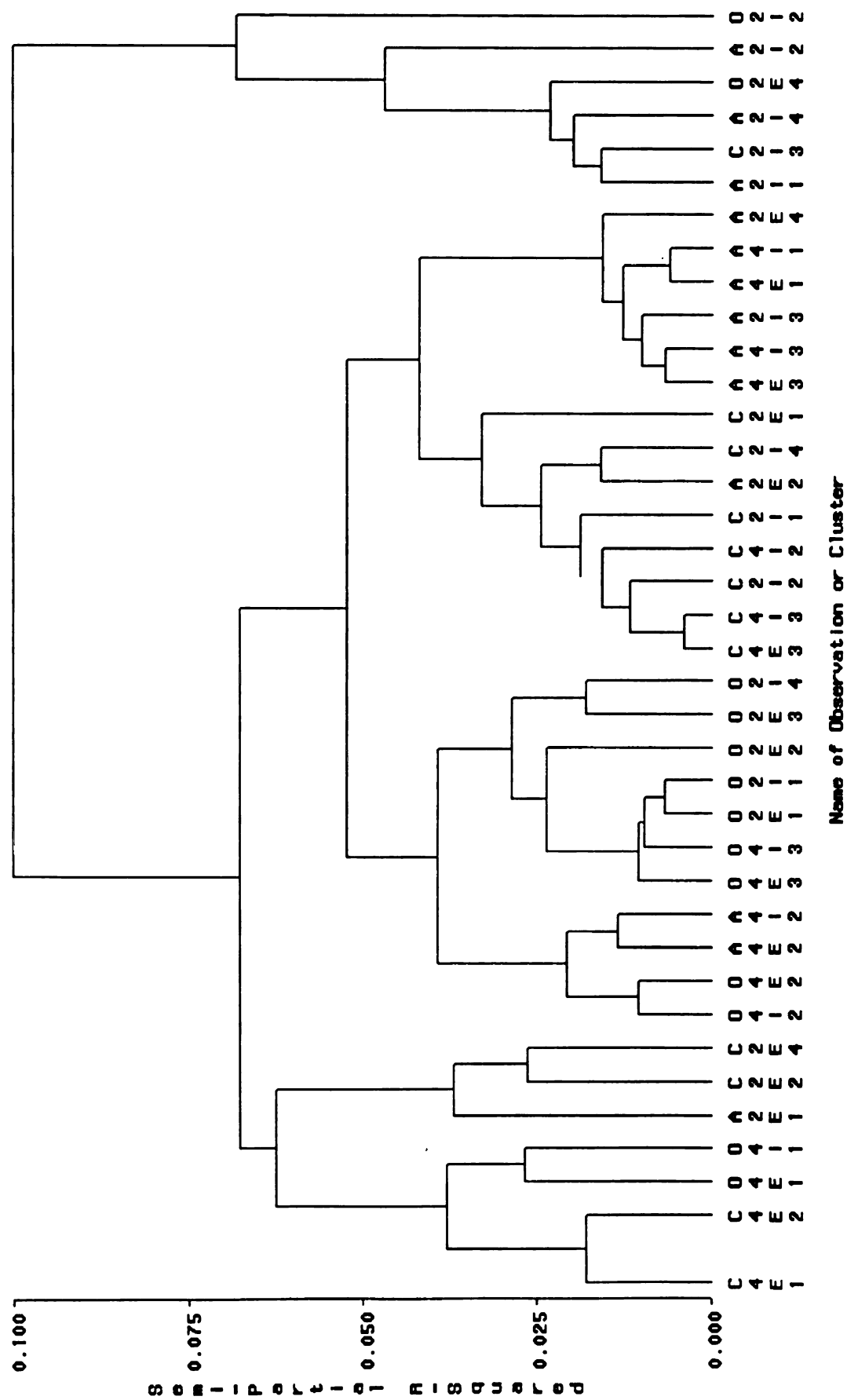


Figure 3: Dendrogram of cluster analysis by Ward's method of Rsa1 T-RFLP profiles from pooled KBS aggregate layers using Hellinger distance. First row, C=conventional corn, A=alfalfa, O=organic corn; Second row, 4=4-6.3 mm aggregates, 2=2-4 mm aggregates; Third row, E=external, I=internal.



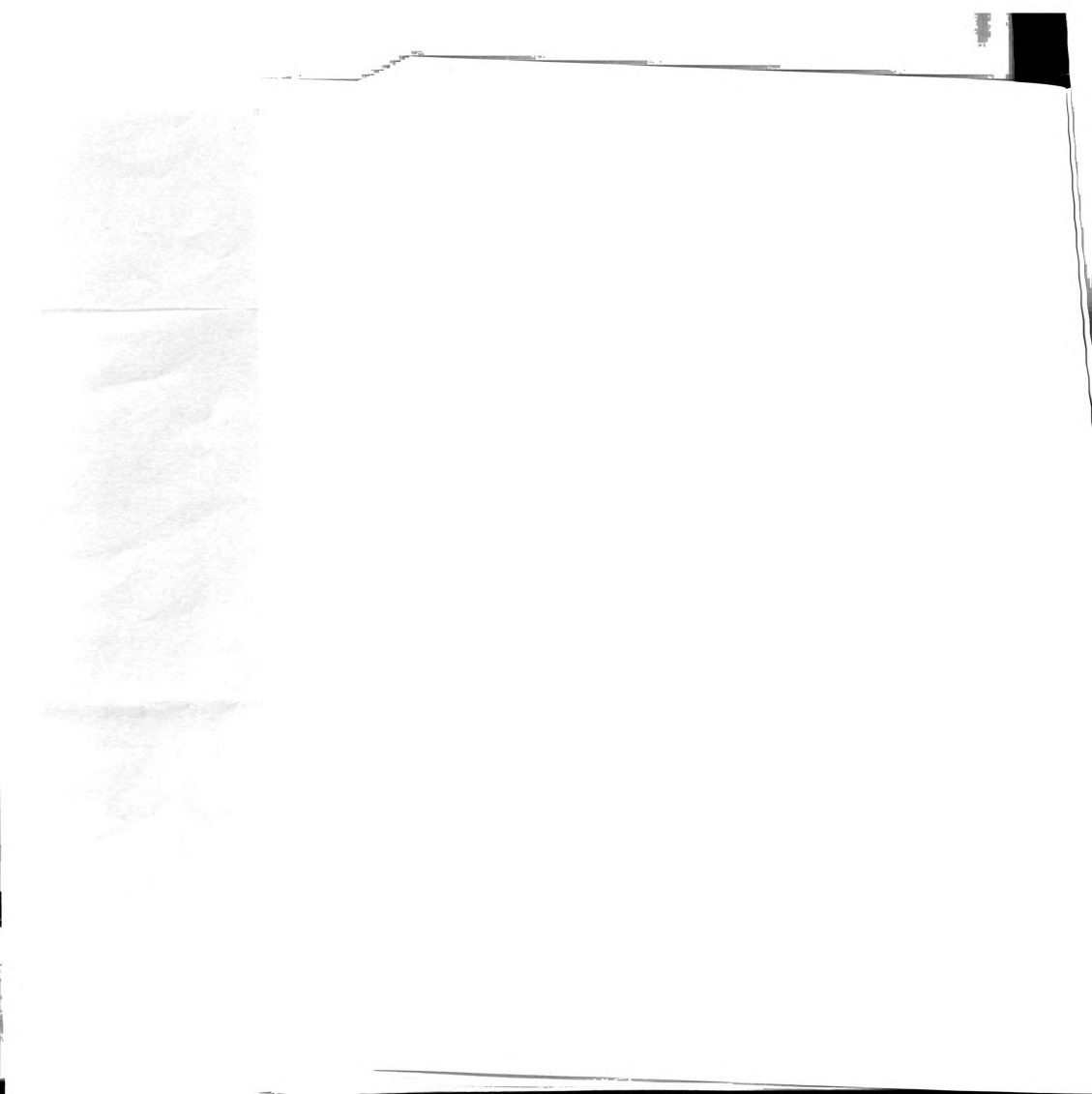
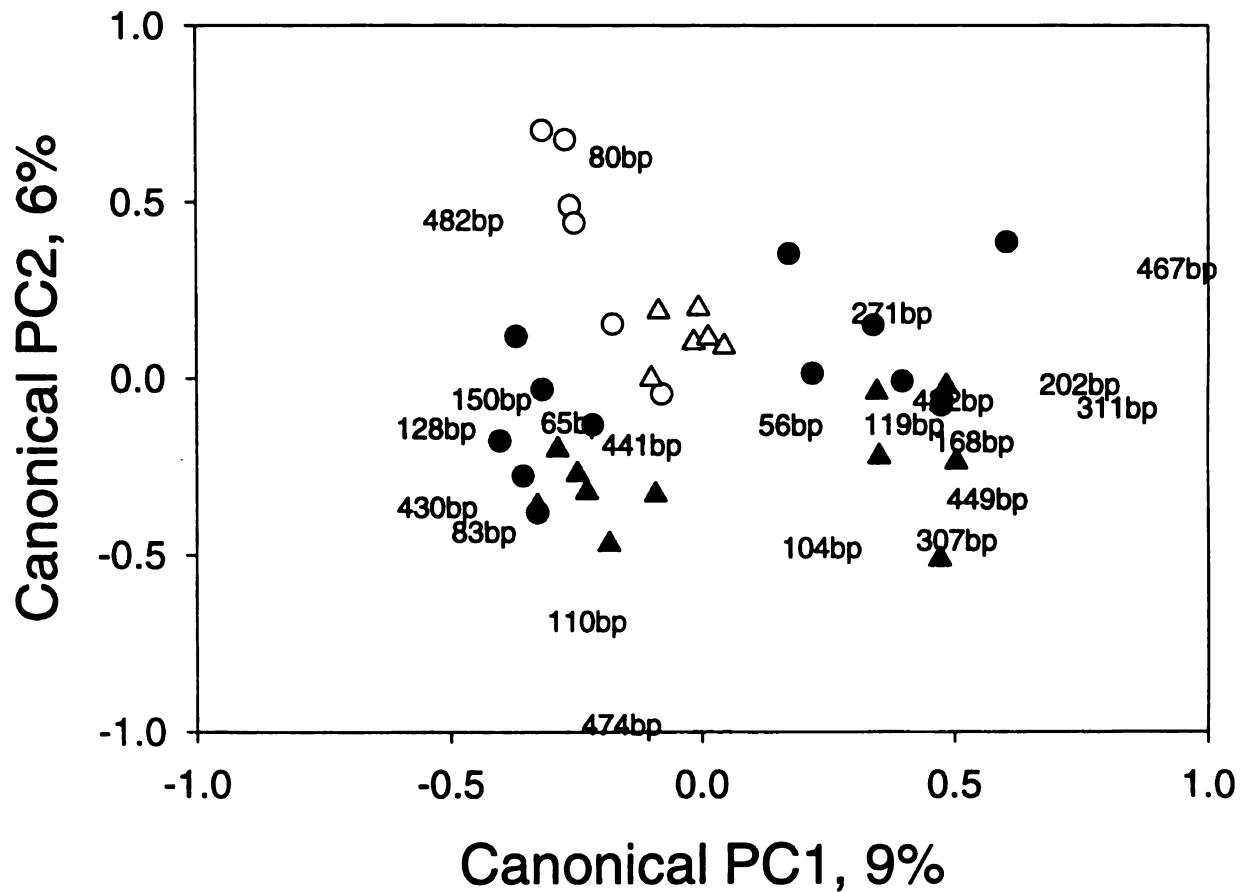


Figure 4: Biplots of sample and T-RF scores for the three canonical principal components (PCs) derived from redundancy analysis of Hellinger distance between pooled aggregate layers from KBS. T-RFs shown had 20-76% of variability explained by canonical ordination. Axes are constrained to maximize variation due to cropping system and aggregate size. Circles=2-4 mm aggregates, Triangles=4-6.3 mm aggregates, White=alfalfa, Black=conventional corn, Grey=organic corn.

Figure 4a: Aggregate layer/cropping system axes 1 and 2.



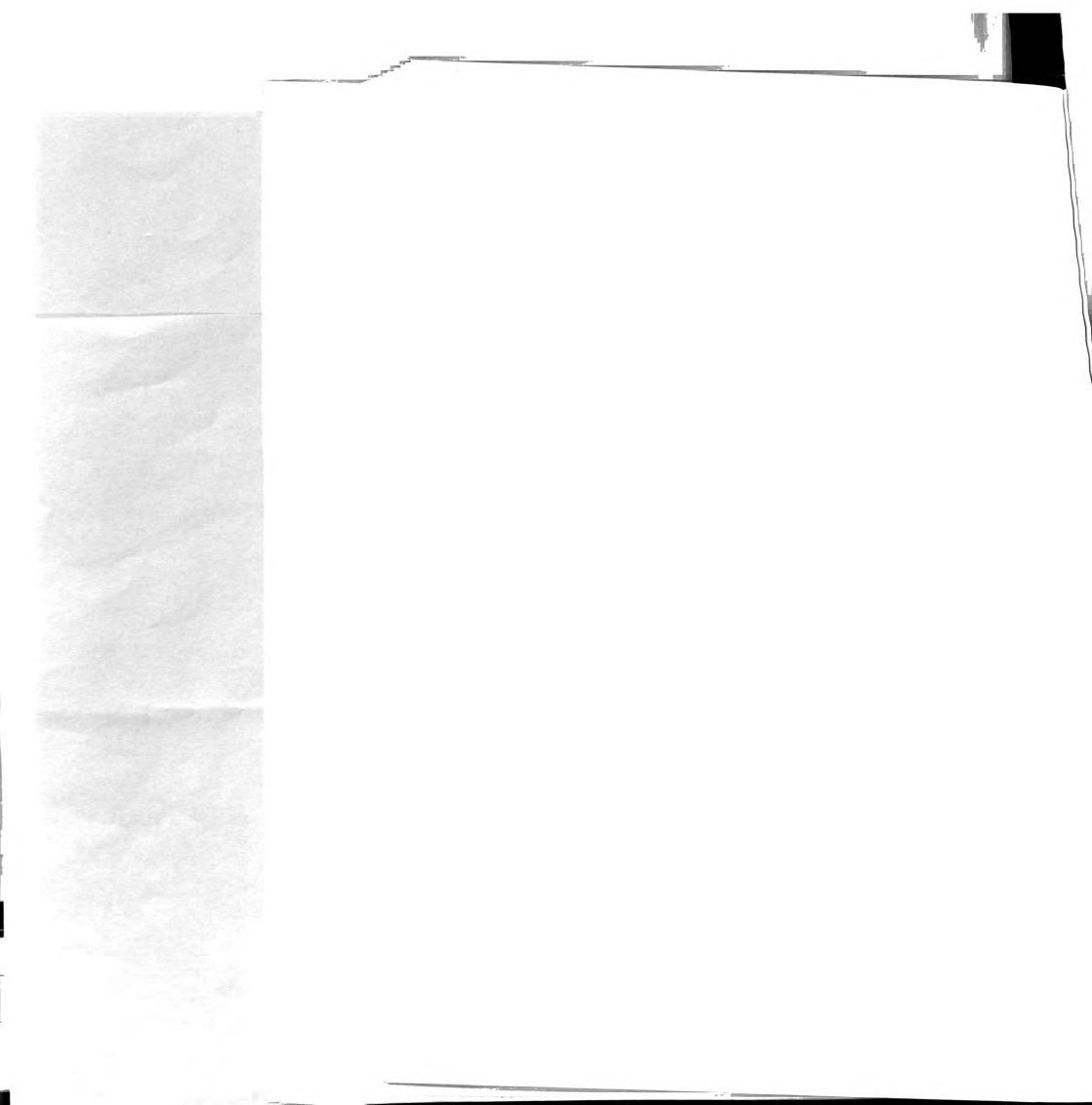
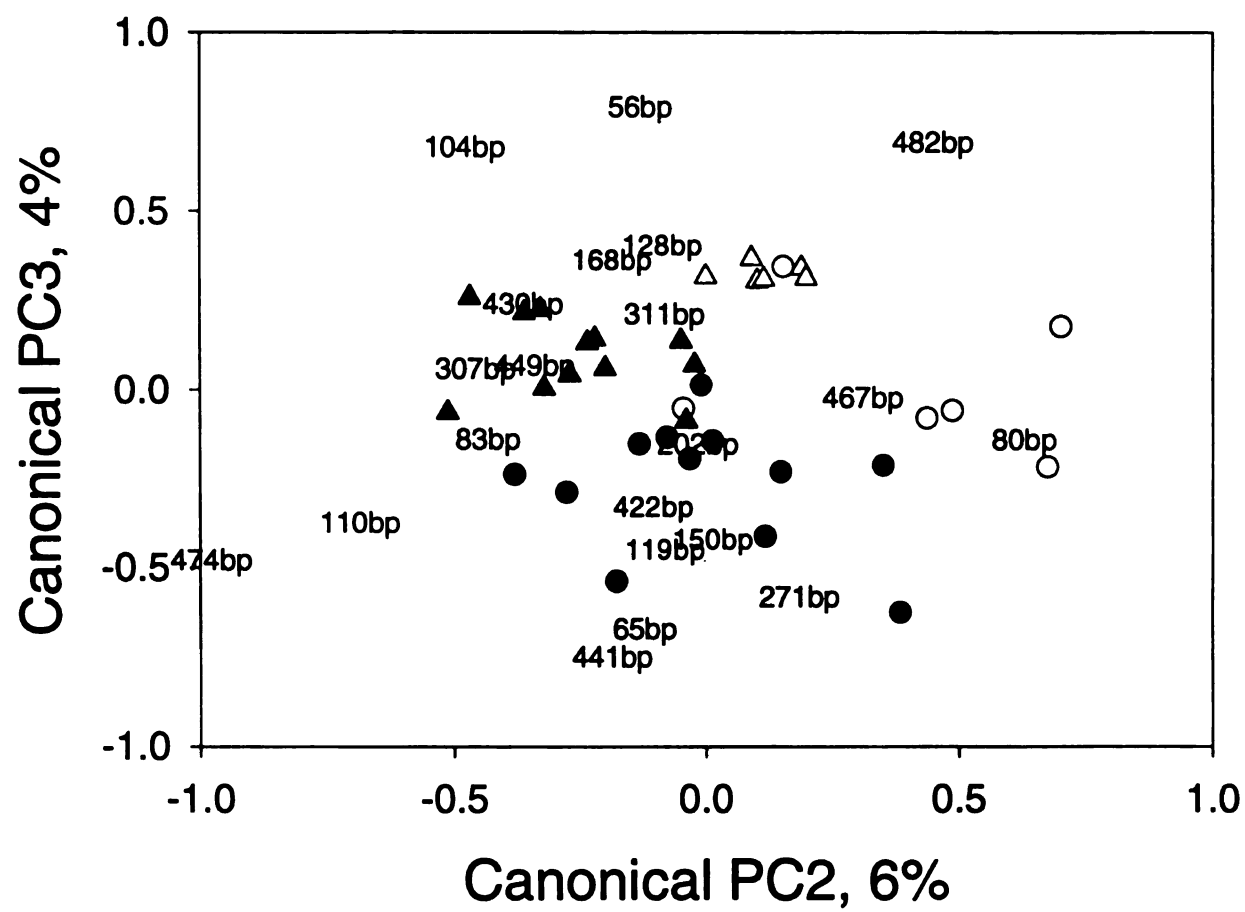


Figure 4, continued

Figure 4b: Aggregate layer/cropping system axes 2 and 3.



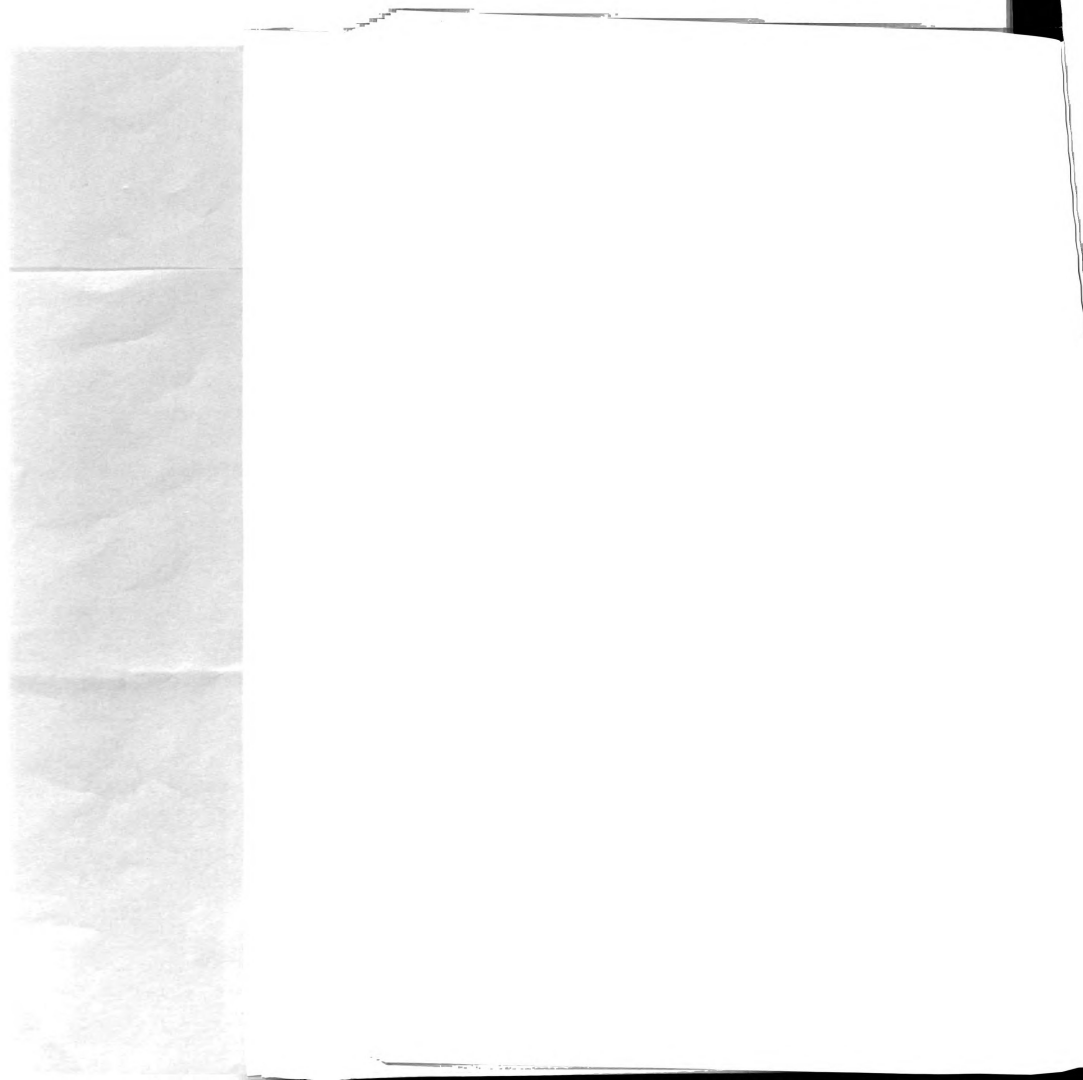


Figure 5: Aggregate layer and treatment interaction axes of canonical principal components derived from distance-based redundancy analysis of Jaccard distance between Wooster aggregate layer RsaI T-RFLP profiles. Circles=aggregate interior, Triangles=aggregate exterior, White=successional vegetation, Black=conventional-tillage corn, Grey=no-till corn.

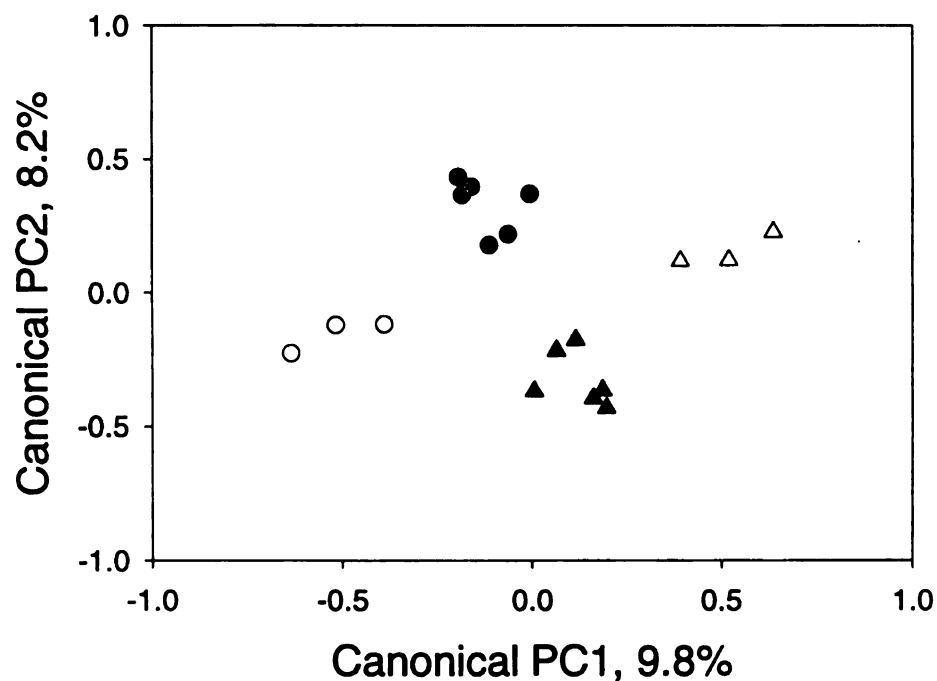
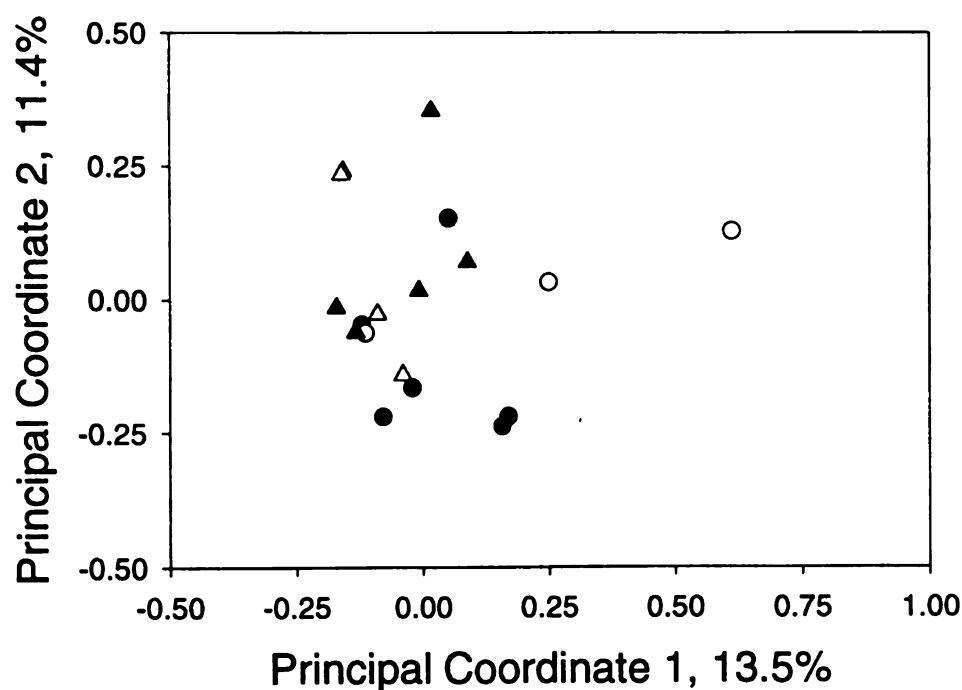


Figure 6: Principal coordinates derived from Jaccard distance between Wooster aggregate layer RsaI T-RFLP profiles. Circles=aggregate interior, Triangles=aggregate exterior, White=successional vegetation, Black=conventional-tillage corn, Grey=no-till corn.



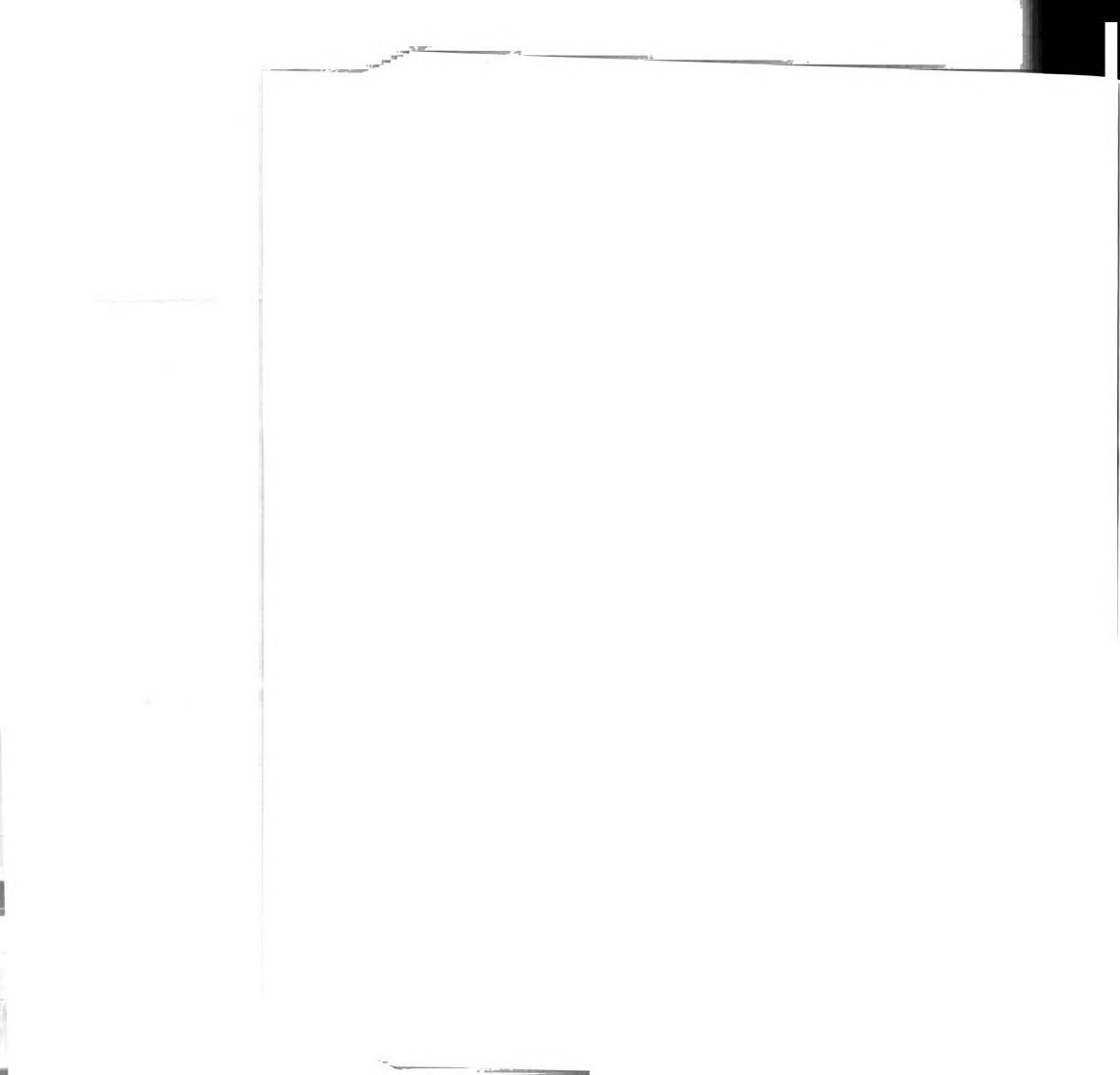
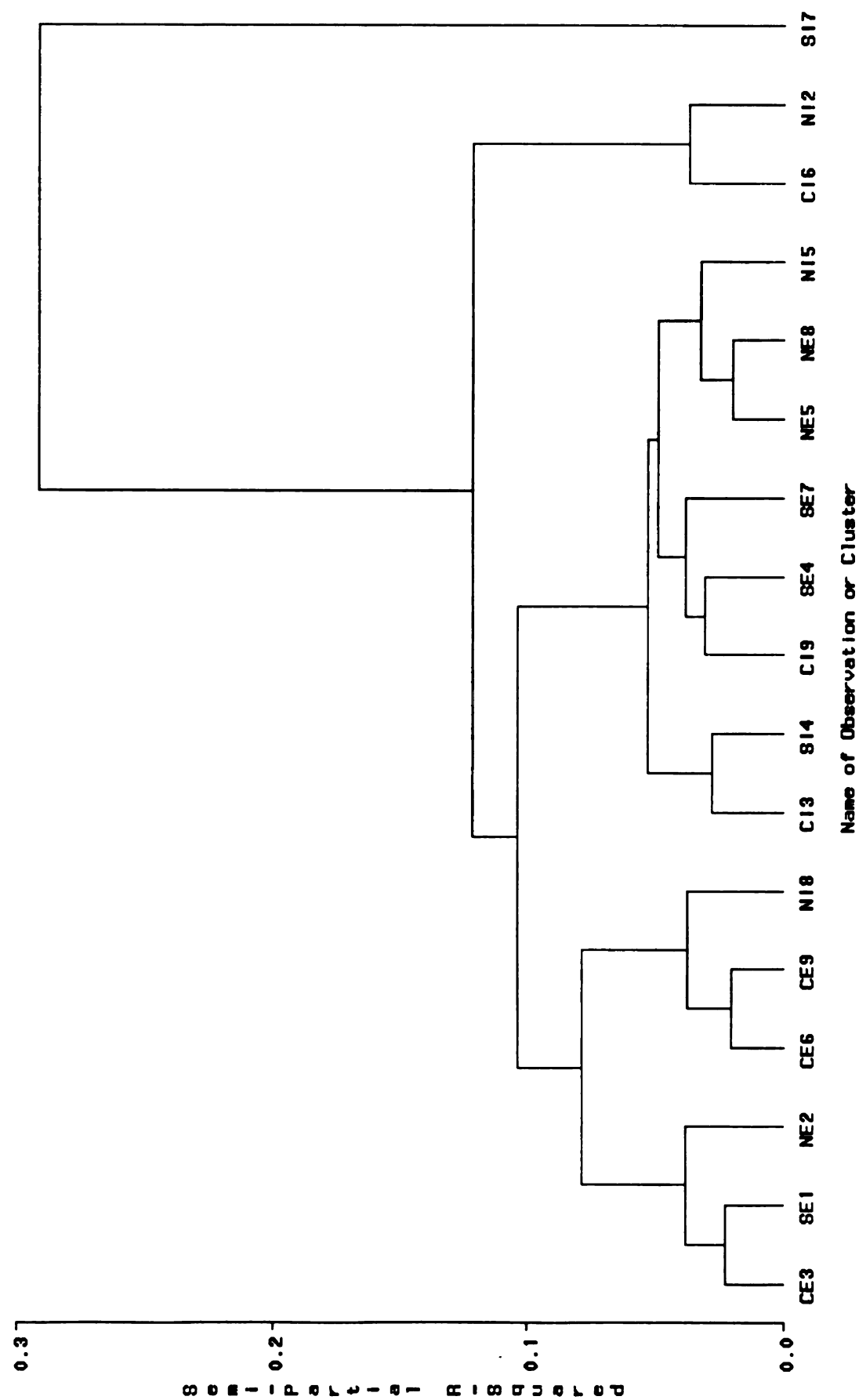


Figure 7: Dendrogram of cluster analysis by Ward's method of RsaI T-RFLP profiles from Wooster aggregate layers using Jaccard distance. C=conventional-tillage corn, S=successional vegetation, N=no-till corn, E=external, I=internal, the final number in each sample name identifies a field replicate.



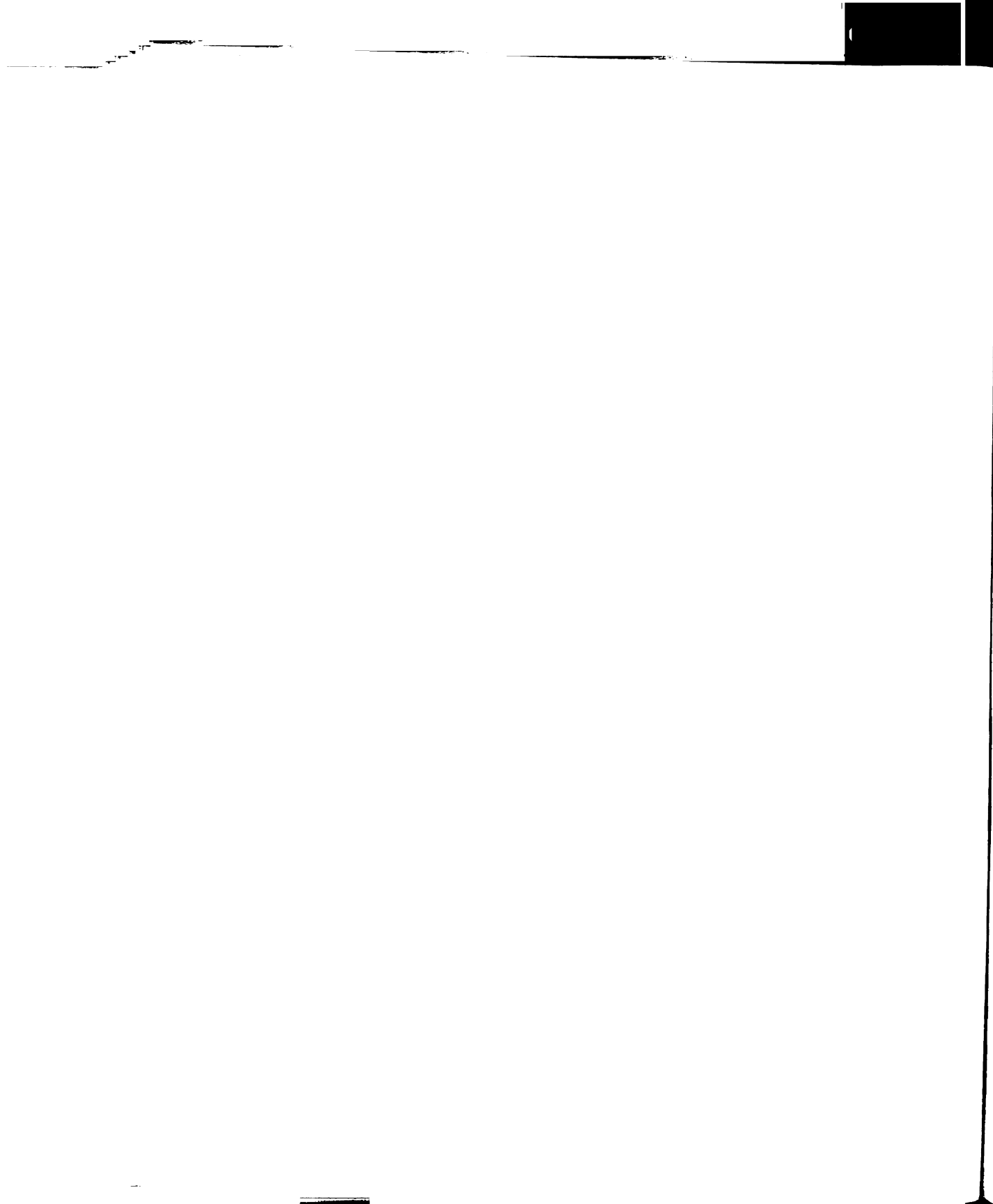


Chapter 5

Use of Multivariate Spatial Statistics to Test Hierarchical Structure within a Soil Eubacterial Community Analyzed by T-RFLP

Abstract

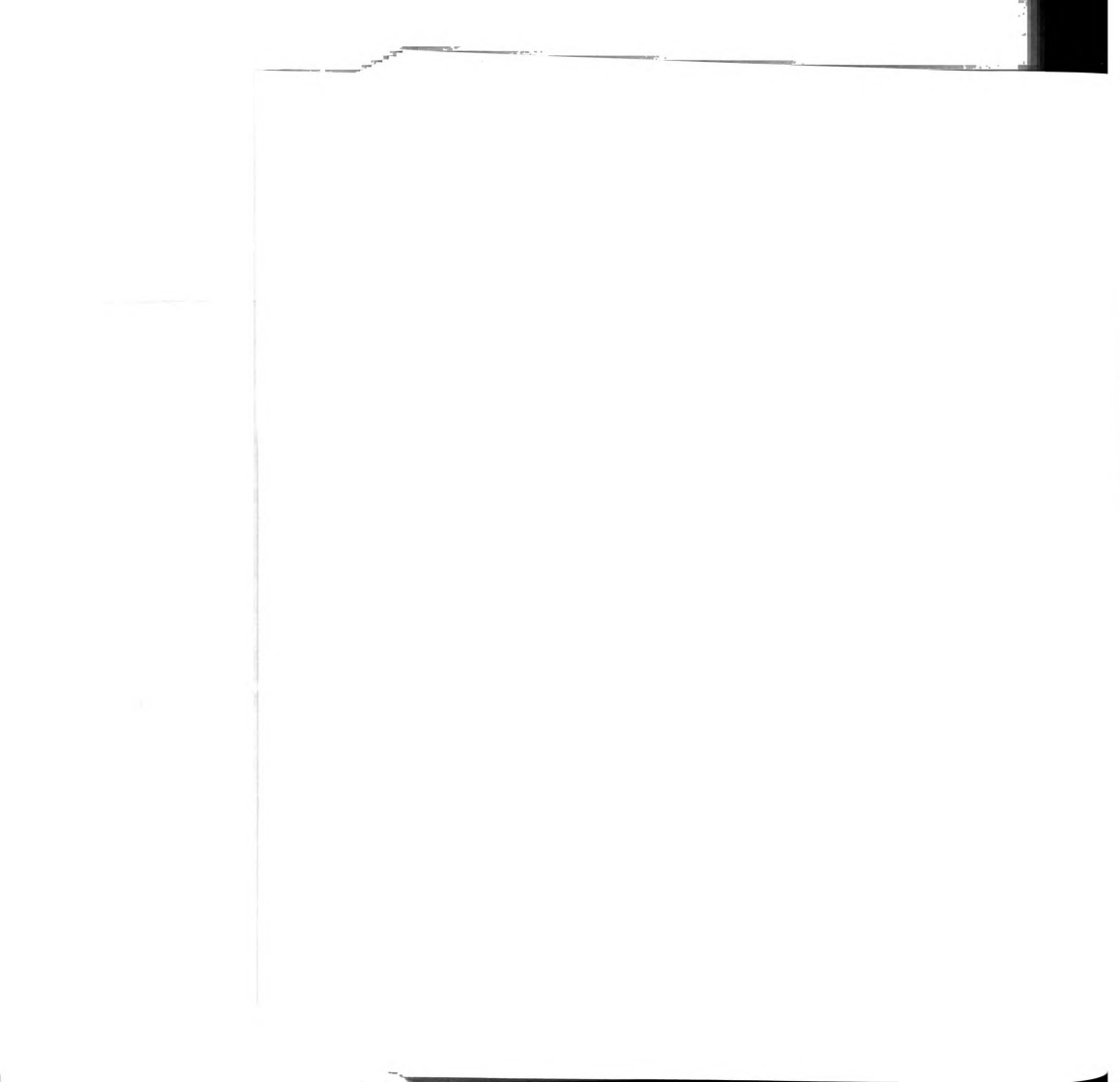
The presence of hierarchical spatial organization was investigated in soil eubacterial communities within three 1.5x2 meter plots. Hierarchical spatial structure is indicated by changes in spatial organization with changes in scale of sampling. Ten samples of various sizes, or sampling grains, were collected from each plot, with a minimum weight of approximately 10 mg. Fifty 10 g samples were also taken in each plot. Eubacterial community composition was assayed using terminal restriction fragment length polymorphism (T-RFLP) of the 16S ribosomal gene. Paired-quadrat analysis and semivariance analysis were adapted to multivariate problems in a generalized method called variability-scale analysis, where the changes in variability statistics or community distance metrics due to spatial scale is examined. Analyses based on changes in sampling grain and extent were integrated. Three hierarchical levels of organization in soil eubacterial communities were separated by phase shifts in spatial organization, where there were significant changes in the slope of the relationship between variability statistics and spatial scale. These included one level, operating at a scale of 10 to 100 g or 2 to 25 cm, with minimal change in community variability with spatial scale. Experimental designs with treatments blocked within these scales should not violate assumptions of standard (non-spatial) statistics. The extent-based scale-variability analysis of spatial structure in soil microbial communities was also compared to Mantel methods and spatially-constrained ordination, with similar results. A method of examining the variability in covariance structure across spatial scales is proposed called the correlation super-matrix, based on the correlation between covariance matrices constructed from samples at different scales. Changes in covariance structure due to



spatial scale are then investigated using principal coordinates analysis and cluster analysis of the correlation super-matrix. This method verified conclusions based on the extent-based analyses of other methods, but was not as useful in the grain-based analysis because the covariance structures of communities sampled at different grain sizes was extremely diverse. Soil eubacterial communities displayed significant hierarchical spatial structure, suggesting they are regulated by mechanisms analogous to those for plant and animal communities.

Introduction

The complexity of soil microbial communities is reflected in the enormous amount of microbial diversity that can be detected in soil (Hugenholtz et al. 1998, Torsvik et al. 1990). Biological, chemical, and physical properties are generally heterogeneous in soil (Harris 1994, Parkin 1993, Stark 1994). A key question for our understanding of soil microbial communities is: How much of the heterogeneity in microbial community composition has a mechanistic ecological basis, and how much is truly random variability that is historical artifact? More generally, this can be seen as “the central question of community ecology,” (Roughgarden 1989). There are strong arguments to be made for either hypothesis. Hrabar and Milne (1997) found that the manifestation of community assembly rules is dependent on the rate of colonization by new species relative to the rate of operation of the rules. Random variability in soil bacterial community structure may be likely because it has been shown that bacterial growth (Harris and Paul 1994, Smith and Paul 1990) and dispersal (Murphy and Tate 1996) are generally low in soil. The major determinant of soil bacterial community



structure may be the environments serving as sources for bacterial colonizers. However even this signal could be rapidly diluted since the time frame for a soil bacterial community to reach equilibrium number of species is less than 200 years (Nüsslein and Tiedje 1998), while the lifespan of initial colonizers, as well as subsequent arrivals, may extend to millions of years (Greenblatt et al. 1999). On the other hand, numerous mechanisms, or assembly rules, can be hypothesized to affect soil bacterial community composition and diversity in a predictable fashion. Traditional ecology provides a plethora of potential ecological mechanisms, including competition (Leibold 1995, MacArthur and Levins 1967), trophic interaction (Holt 1984, Schmitt 1987), disturbance (Bormann and Likens 1979, Connell 1978), and resource distribution (Grime 1994, Harrison 1997). In controlled experiments, these mechanisms have all been shown to have the potential to organize soil microbial communities (Minamisawa and Mitsui 2000, Griffiths and Bardgett 1997, Beare et al. 1992, and chapters 3 and 4, respectively). It is unknown, however, how strongly these mechanisms act in the field, or, if they do have significant impact in the field, whether their interactions result in a general coherent structure. This lack of basic knowledge is due to the inadequacy of our understanding of the spatial structure of soil microbial communities, which is a direct reflection of those mechanisms, if any, organizing a community.

Recently the heterogeneity of soils has been highlighted, and the spatial structure quantified, through the use of semivariance analyses of soil nutrients (Boerner et al. 1998, Dobermann et al. 1995, Schlesinger et al. 1996), potential rates of biological processes (Robertson et al. 1993, 1997, Stoyan et al. 2000) and numbers of soil organisms (Klironomos et al. 1999, Morris 1999, Robertson and Freckman 1995, Rossi et al. 1997).

Cavigelli et al. (1995) used semivariance analysis to quantify spatial structure of 56 microbial fatty acids across separation distances from 2 cm to 80 m. They found no spatial autocorrelation of microbial fatty acids at ranges greater than 20 cm, and for most fatty acids found no spatial autocorrelation at any scale at all. At the other extreme, Felske and Akkermans (1998) concluded that 16S rDNA DGGE patterns were qualitatively homogeneous over ranges of 1 to 40 m.

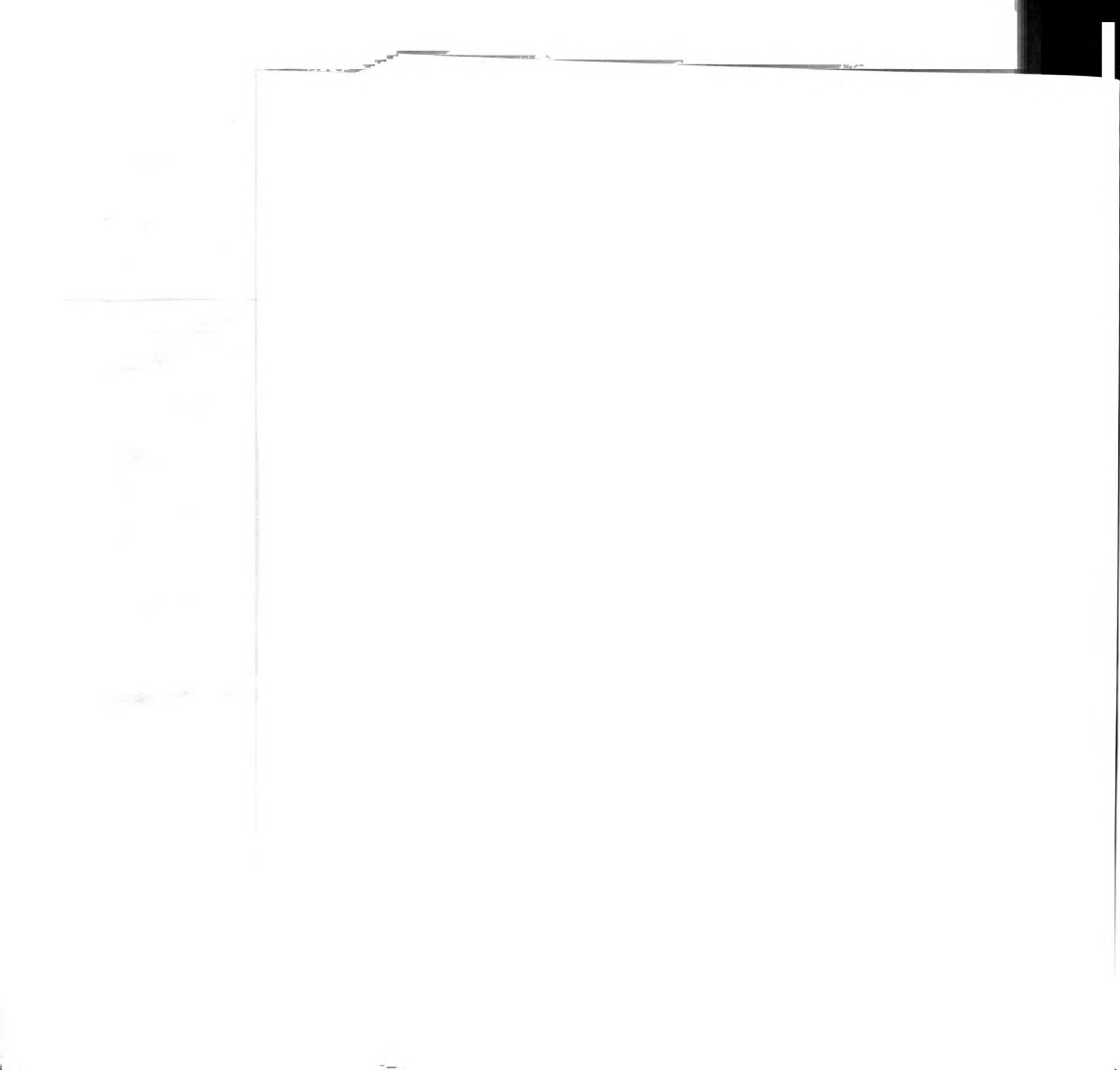
A complete understanding of the spatial structure of ecological phenomena must involve consideration of both spatial pattern and scale (Levin 1992). Spatial patterns in community composition are an outcome of the interactions between organisms and their abiotic and biotic environment. Spatial scale can be used to denote both spatial extent (maximum size) and grain or resolution (minimum size) of any object or phenomenon (Schneider 1994). Variability of an environmental characteristic, and patterns caused by it, will normally be found at some spatial scales but not at others. Hence the spatial scale of observation will affect which mechanisms regulating community structure are detected (Levin 1992, Schneider 1994). Note that scientific observation itself is a biological phenomenon with a particular spatial scale which will often not coincide with the scale of the object or phenomena under study (i.e. the scale of a soil core is equal to the *measurement* grain; it need not be the characteristic scale of a forest, microbial population, or any natural phenomenon).

An important distinction must be drawn between a spatial scale, defined above, and a level of organization, which is a range of conditions, including spatial scales, over which phenomena affecting the parameter of interest are homogeneous. To deal with the complexity generated through the interaction of many phenomena operating across a



wide variety of spatial scales, it has been suggested that mechanisms regulating communities may form a hierarchy, resulting in spatially nested levels of organization that operate at particular scales (Allen and Starr 1982, O'Neill et al. 1986). In formal hierarchy theory, hierarchical structure was attributed to the separation of ecological processes by their rates, and the constraining of dynamics at lower levels in the hierarchy by higher levels. Other treatments of the topic have stressed the separation of ecological processes by effects on species (Parker and Pickett 1998), or spatial extent (Wu and Loucks 1995). The detection of such organization would be a powerful method of summarizing the outcomes of complex phenomena. This approach has proven to be successful in several communities (see next section).

Ecological studies are often described as global, regional, landscape, or local. These terms connote both particular spatial scales (i.e. the “regional scale” is about the size of a large state) and levels of organization (community structure at the “regional level” is organized by climate and geology). The design of ecological studies around pre-conceived hierarchies without reference to patterns intrinsic to the organisms is now under question (Hoekstra et al. 1991, O'Neill et al. 1986). The hierarchy described above has been shown to be useful in understanding species endemism in some soil bacterial culture collections (Cho and Tiedje 2000, Fulthorpe et al. 1998), but not for genetic structure in *Rhizobium leguminosarum* (Hagen and Hamrick 1996, Strain et al. 1995, but see also Souza et al. 1994). For microbial communities, it seems likely that there are levels of organization that operate at spatial scales smaller than what is normally considered the local (field or plot) scale (see Beare et al. 1995), but this has not been explicitly tested.

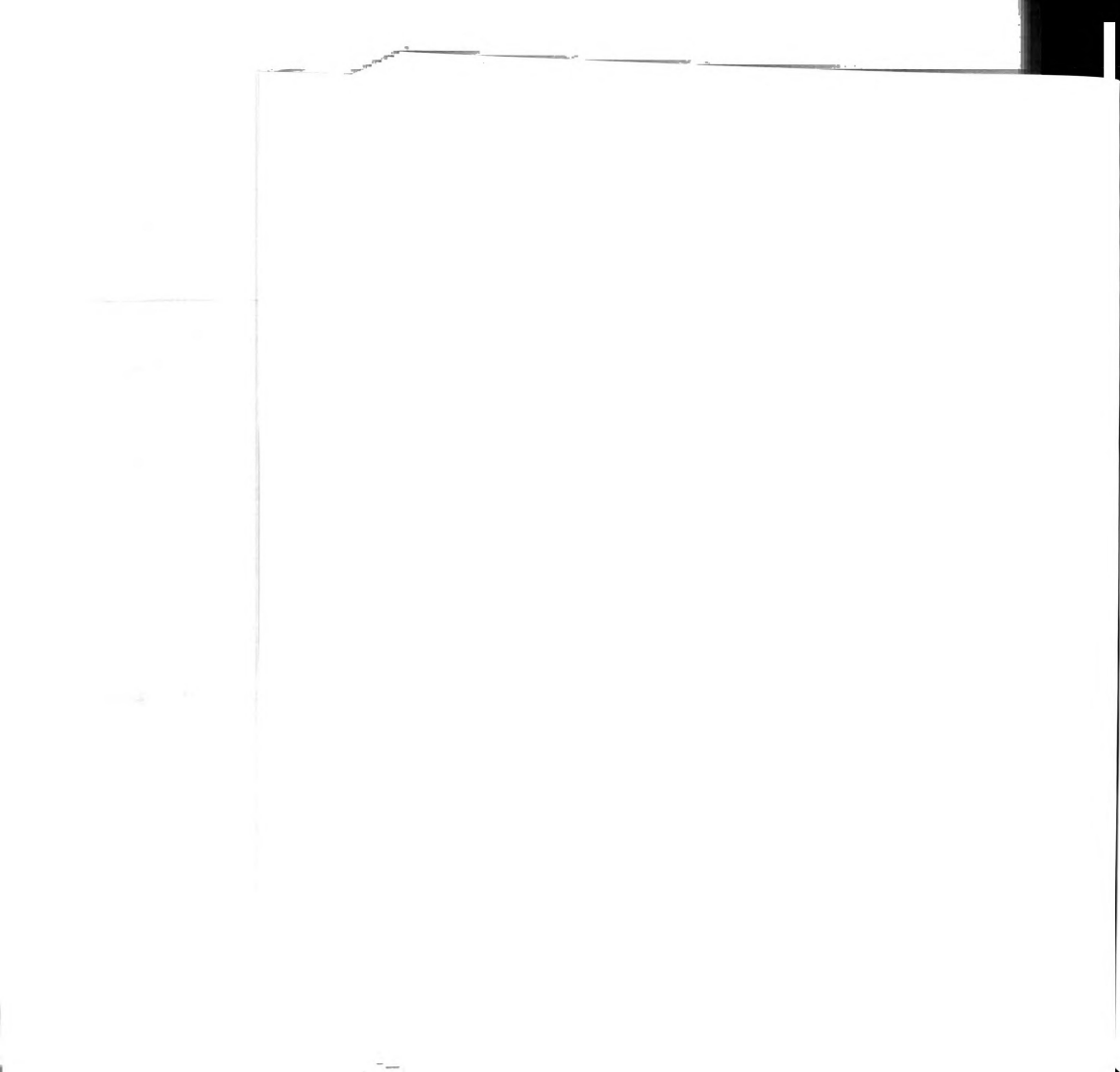


The goal of the current study is to explicitly and quantitatively consider scale and test for hierarchical structure in an investigation of spatial structure of soil bacterial communities. This was accomplished using multivariate spatial statistics coupled with community-level terminal restriction fragment length polymorphism (T-RFLP) of the 16S ribosomal gene. Molecular genetic techniques such as T-RFLP have become well-established methods to assay *in situ* community structure of soil bacteria, avoiding the problems associated with elective enrichment culture (Muyzer 1998, Tiedje et al. 1999). The specific hypothesis tested is that a soil microbial community is structured by levels of organization operating at different spatial scales. This is a holistic method of testing the overall importance of ecological phenomena in community assembly, as opposed to random assortment as discussed previously. Several new approaches to multivariate spatial statistics were developed in conjunction with this study, so the theoretical and historical framework of hierarchy theory and multivariate spatial statistics are briefly presented prior to a description of the experiment.

Detection of Levels of Ecological Organization: Statistical Approaches

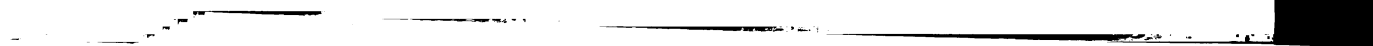
Grain-Based Analysis of Spatial Structure in Community Ecology

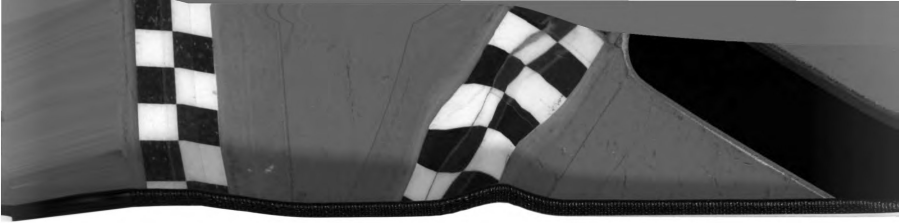
Hierarchy theory is one of the few conceptual approaches in ecology that fully incorporates the concept of scale (Peterson and Parker 1998). This results in an intuitive method of recognizing organization in the face of complexity and heterogeneity. As such it has proved useful as a conceptual basis for ecological mapping (O'Connor et al. 1996), modeling (Maurer 1990, Palmer 1992), new research methods (Johnson and Gage 1997, Quinones 1994), and strategies of land management (Eswaran et al. 2000, Hoekstra and Flather 1987, Jennings and Reganold 1991, Lee and Grant 1995, Palik et al. 2000). In



these contexts hierarchy theory is normally used as justification for assuming that one structure or process is constrained by another (usually spatially-constrained). Empirical tests of hierarchy theory have focused exclusively on structural components of ecosystems, namely abundances of species. Several studies have looked for hierarchical structure among traits of species in a community. These have tested predictions from hierarchy theory using empirically-suggested (Waltho and Kolasa 1994) or pre-conceived (Gaedke 1998) levels of organization among aquatic species.

Other studies have investigated the presence of hierarchical spatial structure, and therefore distinct levels of organization regulating species abundance, in plant communities. The hierarchical spatial structure is detected by discontinuities in spatial pattern across a range of spatial scales. The changes in spatial pattern have most often been detected using variance analysis. If a quantity is randomly distributed, a plot of log variance versus log sampling grain has a slope of -1 (Levin 1992, Wiens 1989). If there is spatial structure, however, the slope will be greater than -1 , and will depend on the particular pattern and strength of autocorrelation. Discontinuities in this slope indicate phase shifts in spatial structure, and hence changes in organization. O'Neill et al. (1991a) calculated the variance in percent cover of vegetation across 32 transects radiating from a single position. Using this method they were able to detect hierarchical structure of varying degrees in all six landscapes examined. Several other studies have looked at distributions of single species within communities (Cullinan et al. 1997, Kotliar 1996, O'Neill et al. 1991b). Where abundance of more than one species was recorded, these were simply analyzed separately. In these studies, various forms of blocked-quadrat-variance analysis (BQV) were used to examine effects of sampling grain on spatial





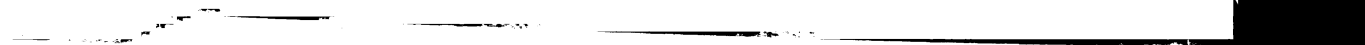
structure. The BQV approach is basically the same as in O'Neill (1991a), except that only contiguous blocks of quadrats within a single transect or grid are compared. This method of generating quadrats of different scales confounds sampling grain with separation distance between quadrat centers, resulting in an initial increase in variance with scale rather than a continuous decrease. The BQV methods have a long history in plant ecology and differ based on how quadrats are blocked and paired for estimation of variance (Grieg-Smith 1952, Hill 1973, Galiano 1983). The placement of this line of research into the conceptual context of hierarchy theory represents a leap forward in our ability to interpret the spatial patterns that have been investigated by ecologists for so long.

Multivariate studies have been conducted to examine spatial structure encompassing the entire community. Community structure is dependent on the existence of non-random associations between species. The debate over causes of such associations has a long history, ranging from common responses of species to the environment (Gleason 1939) to the existence of coevolved species complexes (Clements 1936). It is probable that many phenomena are involved (Ricklefs 1987, Roughgarden 1989, Belyea and Lancaster 1999, Wilson 1999); hence holistic methods such as the study of spatial structure and hierarchy theory are particularly useful.

The simplest form of multivariate analysis of community spatial structure has consisted of an ordination to derive new variables (ordination axes) that summarize the majority of the variance in species distributions. Site scores of the first few variables are then plotted along the length of a transect (Bouxin and Gautier 1982, Shmida and Whittaker 1981). The variance of these derived variables has also been examined using

techniques related to BQV (Galiano 1983, Milne 1991). Multiscale ordination is another method that has been proposed as a way to partition variance of an ordination between scales (Hoef and Glenn-Lewin 1989, Noy-Meir and Anderson 1971). Covariance matrices derived from different plot sizes are summed, followed by a principal components analysis. The variation of each eigenvector can then be partitioned into the contributions from each scale. However, Wackernagel (1998) writes that if principal components analysis is performed on a covariance matrix that incorporates dynamics of mechanisms operating at different scales, the analysis will be invalid because the orthogonality of principal components will be scale-dependent (i.e. they will be correlated at some scales). Hence multiple scales of spatial pattern and other sources of variation may interact to confound the ordination, obscuring dynamics present at any given scale. In addition, it is assumed that spatial structure will be the primary source of variation in the dataset and will therefore be reflected in the first few ordination axes. Depending on the ordination, the majority of the variability in the dataset may be left unexamined, and weaker spatial patterns will be missed. This problem arises because the null hypothesis of no spatial structure is not explicitly tested on the entire dataset. Finally, the ordination axes analyzed are dependent on a particular dataset. This causes difficulty in the comparison with other samples since it requires the assumption that the same phenomena are affecting both datasets in the same way, and hence would result in identical ordinations and comparable axes.

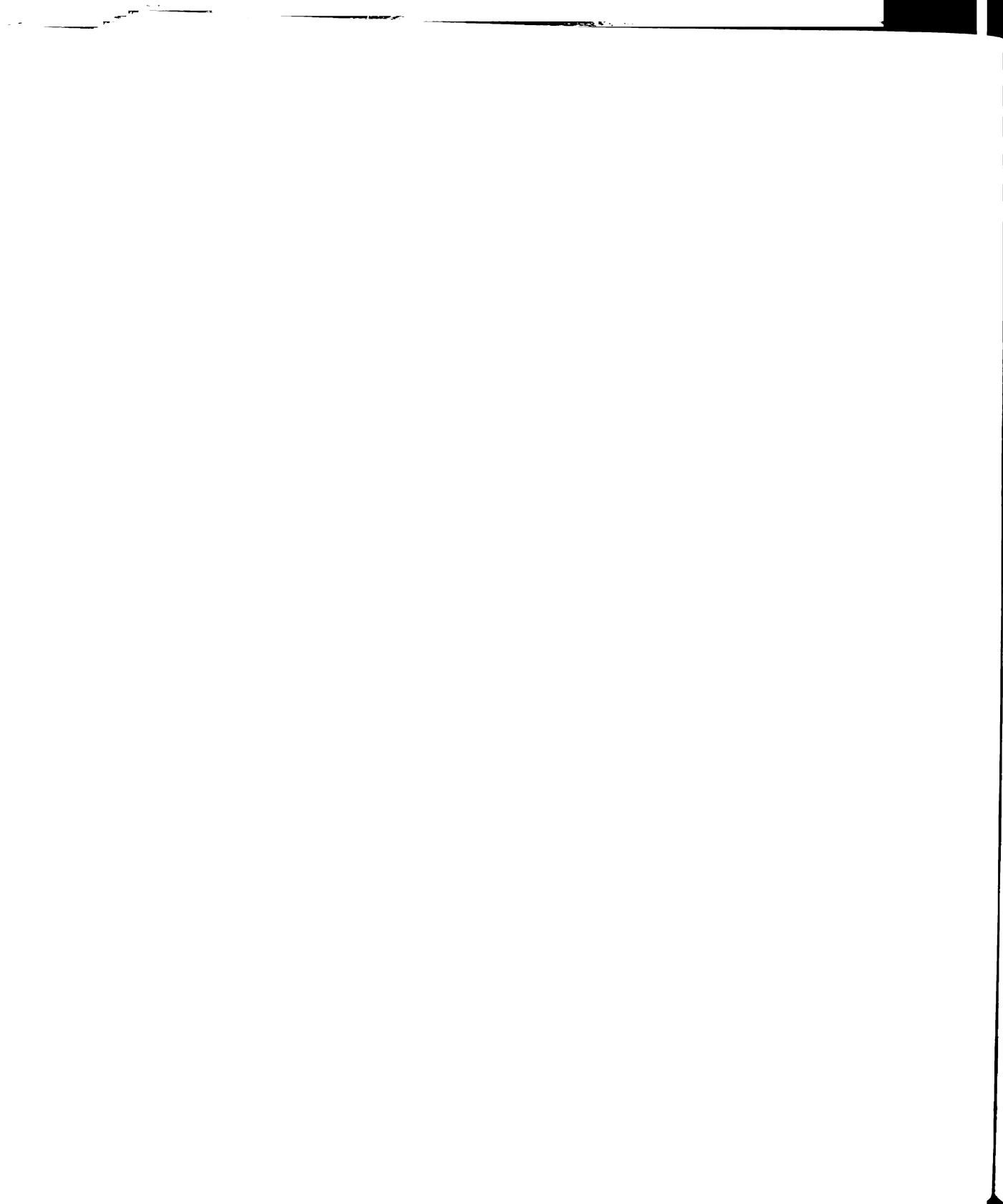
The variance test of Schluter (1984) tests for non-random associations between species by comparing the variance of total numbers of individuals within samples to the sum of the variances of each species. If these variances are not equal, then the sum of the





covariances between species must be different from zero, implying there is some overall pattern present in the species associations. Yoshioka and Yoshioka (1989) adapted this by computing variances for each block size (sampling grain) separately. The departure from random association between species was tested for each scale using nested ANOVA. This test is invalid if the species abundance data are transformed to relative abundances prior to analysis, as is often recommended for ecological data and is required if the variance in total numbers of individuals is not meaningful (i.e. due to analytical variability or sampling effort). However, the interpretation of the variance and covariance statistics after transformation is dependent only on variability in community composition, having removed the variability due strictly to site productivity. Hence plotting the sum (or mean) of the species variances against sampling grain will reflect how the heterogeneity in relative abundance across all species (i.e. the heterogeneity in community composition) changes with spatial scale. The sum of species covariances measures the same property of the dataset as the sum of the species variances after transformation to relative abundances, namely heterogeneity of community composition. Other methods are required to examine the overall homogeneity of elements within the covariance matrix across spatial scales (see next section).

The utility of mean variance in describing multivariate patterns becomes obvious if it is considered that the mean species variance is equal to one half of the mean pairwise Euclidean distance between samples, which is commonly used as the basis for community ordination, clustering, and classification methods. Euclidean distance itself has been recognized as inappropriate for these applications (Legendre and Legendre 1998), but alternative distance metrics can be derived by using an appropriate



transformation prior to calculating Euclidean distance. The transformation to relative abundances is an improvement, but several further transformations have been shown to be superior by Legendre and Gallagher (in press). In this paper we use the Hellinger distance because it does not heavily weight rare species and is simple to calculate, being equal to the Euclidean distance between the square-root of relative abundances. The use of ecologically-appropriate data transformations and the focus on mean distance (or mean variance) greatly enhances the flexibility of the types of data and analyses that can be performed in grain-based approaches to assessing spatial structure. Significance tests can still be performed using randomization procedures (see below). The generalized concept of comparing a variability statistic to spatial scale is further developed below, and will be referred to as variability-scale analysis.

Extent-Based Analysis of Spatial Structure in Geostatistics

A rich set of methods for analyzing spatial structure based on separation distance between samples rather than sample grain has been developed within the field of geostatistics. Examination of the change in variance due to changes in separation distance is known as semivariance analysis or variography. It is equivalent systematically varying sampling extent at all locations. Inferences about sampling grain are also possible (Bellehumeur et al. 1997, Schneider 1994). Identical methods were independently discovered in community ecology and were known as paired-quadrat-variance analysis (PQV, Goodall 1974). Comparisons of the extent-based versus grain-based methods have generally found that the extent-based methods are more sensitive, at least in part because the BQV variants that have been tested confound extent with grain (Carpenter and Chaney 1983, Ludwig and Goodall 1979), although this was also noted by



Schneider (1994). In geostatistics it is standard to fit semivariance to combinations of variogram functions (Robertson and Gross 1994, Rossi et al. 1992). Typically these include an intercept called nugget variance. Nugget variance is due to analytical variability and variability at scales smaller than the sampling grain and minimum separation distance. Other variance functions of separation distance may increase unbounded (e.g. the linear model) or reach an asymptote or sill (e.g. the exponential model). The separation distance at which a sill is reached is the range of influence of the particular phenomenon causing pattern at the scale. While not often recognized as such, semivariance analyses are tests of hierarchy theory. Hierarchical patterns are often found and modeled in the form of nested functions, where variance reaches a sill but then starts to increase again with further increases in separation distance.

Attempts at combining extent-based methods with multivariate analysis often involve semivariance analysis of the first few axes of an ordination (Cash and Breen 1992, Jonsson and Moen 1998, Rossi et al. 1997) or the equivalent multiscale ordination (Schaefer and Messier 1994). This approach has the same shortcomings as when used with BQV. Multivariate factorial kriging analysis (FKA) is another procedure that has been developed by geostatisticians to incorporate spatial structure into principal components analysis (Wackernagel 1998). This involves fitting each variance and covariance (or cross-variogram in geostatistical jargon) in a multivariate dataset to a common basic variogram model, which would include the same functions and ranges. The fitted model coefficients (nugget, sills) are then used to construct a variance-covariance matrix, or coregionalization matrix, for each function/range modeled. Hence a coregionalization matrix represents the complete dynamics, at a given spatial scale, of a

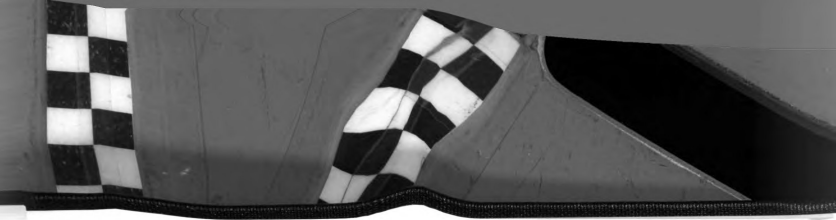
a covariation matrix represents the complete phenomena, at a given spatial scale, of a covariance matrix, or conditionalization modelled. Hence the fitted model coefficients (nugget, sill) are then used to construct a variance-covariance (or cross-variogram) in a multivariate dataset to a components analysis (Wackernagel 1988). This involves fitting each variance and been developed by geostatisticians to incorporate spatial autocorrelation into principal with BQV. Multivariate factor loading analysis (FVA) is another procedure that has (Schneider and Massini 1994). This approach has the same shortcomings as when used (1992, Jonsson and Møller 1994, Jonsson et al. 1997) in the equivalent multivariate ordination. Attempts to combine with a fixed number of multivariate analysis often to increase again with further distances with each analysis and modelled in the form of a conditionalization model. However, patterns are often found covariance analysis and the same conditionalization model. The separation between the model (The separation between the model and the data is often not clear, but the model is often unbounded (e.g. the form model) in conditionalization, and a separation distance. Conditionalization is often used to model spatial phenomena, but it includes an intercept coefficient, which is often not a spatial phenomenon. variogram functions (Robertson 1994) are often used to model spatial phenomena. Schneider (1994). In geostatistics, the model is often used to model spatial phenomena.

set of variables, independent of dynamics at other scales. Principal components analysis can then be performed on coregionalization matrices for different scales separately. The goal of the analysis is to assess relationships between complex sets of variables without averaging over multiple spatial scales. Such averaging causes samples to not be independent, resulting in principal components that are correlated at some scales (Wackernagel 1998). It is not unusual to find that variables important in ordination at one scale are unimportant at another, or that relationships between variables are reversed at different scales (e.g. Dobermann et al. 1995, Goovaerts 1994, Monestiez et al. 1994).

Multivariate factorial kriging analysis is a highly reductionistic approach to assessing the degree of spatial organization in communities. First the importance of spatial scale is examined variable by variable (or species by species) and covariance by covariance. Then the overall importance to the entire community is built up from each of these individual analyses, finally expressed as qualitative differences between principal components analyses. On the other hand, use of a multivariate distance coefficient in a variability-scale analysis is a holistic method of accomplishing the same goal.

Variability-scale analysis can easily be extended to the extent-based sampling design; samples at the same grain are taken at varying distances apart, and mean distance coefficients are calculated over pairs of samples in each category of separation distance. Again, the approach is not limited to Euclidean distance since transformations can be performed to result in more ecologically-relevant distances. The choice of distance coefficient is even more flexible than previously mentioned since any ecological distance coefficient can be calculated and plotted as a function of sampling grain or extent.

Whittaker (1960) plotted Jaccard's coefficient as a function of separation distance and



found that similarity of communities decreased at a steady rate as separation distance increased until a threshold was reached, at which point the similarity between communities declined precipitously. The relationship to hierarchy theory is clear: two levels of organization operated simultaneously but at different spatial scales to organize the communities. Each distance coefficient has unique advantages and disadvantages (Legendre and Legendre 1998); in this study we use both Hellinger distance and one minus Jaccard's similarity coefficient (hereafter referred to as Jaccard's distance).

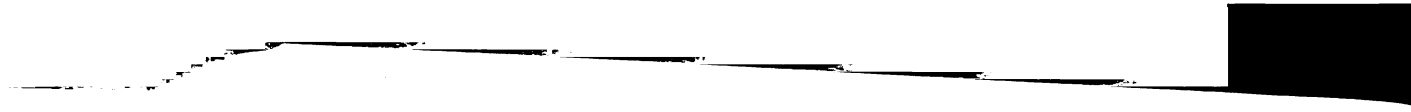
While it may be desirable to use FKA to examine the homogeneity of structure within the covariance matrix, across spatial scales, instead of the overall strength of covariance, in many ecological applications it is not practical. Ecological communities normally contain many species, sometimes numbering in the hundreds. Hundreds to thousands of variances and covariances would therefore have to be separately modeled using nonlinear regression to construct the coregionalization matrices of FKA. It is also unlikely that the majority of these would be adequately fit by a common model, as required in FKA. We propose a new method, called the correlation super-matrix, to adapt the goals of FKA to large ecological datasets. As in FKA, variance and cross-variograms are calculated for all variables (species) for each distance class separately. Hence a different variance-covariance matrix can be constructed from empirical data for each distance class. Rather than model each element of these matrices, however, the matrices can also be compared using a correlation coefficient. This method of comparing distance or similarity matrices is known as the cophenetic correlation (Jobson 1992) or "normalized" Mantel statistic (Legendre and Legendre 1998). By calculating the correlation for each pair of covariance matrices, a new "super"-matrix can be constructed

found that similarity of response (PCA) increased until a threshold was reached, after which it declined. The communities declined from the threshold level, and the level of organization decreased. The communities (Lévesque and Legendre 1998) and Legendre's similarity (Legendre 1993) are used to measure the similarity of response (PCA). While it may be possible to use the covariance matrix within the covariance matrix, it is not possible to use the covariance matrix in many situations. The covariance matrix normally contains many zeros, and the covariance matrix is normally modeled thousands of variables and variables. Legendre's similarity is used to model the covariance matrix of PCA. It is also using nonlinear regression to model the covariance matrix of PCA. It is also unlikely that the majority of these would be adequately fit by a common model, as required in PCA. We propose a new method, called the correlation super-matrix, to adapt the goals of PCA to large ecological datasets. As in PCA, variance and cross-variance are calculated for all variables (species) for each distance class separately. Hence a different variance-covariance matrix can be constructed from empirical data for each distance class. Rather than model each element of these matrices, however, the matrices can also be compared using a correlation coefficient. This method of comparing distance or similarity matrices is known as the coproduct correlation (Legendre 1993) or "normalized" Mantel statistic (Legendre and Legendre 1998). By calculating the correlation for each pair of covariance matrices, a new "super"-matrix can be constructed

containing the similarities of the species covariance structures for each pair of distance classes. The method can be applied to the grain-based methods as well. The significance of these pairwise correlations could each be tested using permutation or a normal distribution approximation, although this could easily result in an excessive number of pairwise tests. Structure within the correlation matrix could also be investigated using multivariate exploratory data analysis techniques such as cluster analysis or principal coordinates analysis. The results would summarize the similarities in species covariances across the different spatial scales, albeit without explicit hypothesis-testing. An additional advantage of the correlation super-matrix approach is that it does allow the differences in relationships to be quantitatively assessed in a single analysis, rather than qualitatively in separate principal components analyses as in FKA. The correlation super-matrix approach does not result in the ability to attribute differences between scales to particular variables; however this can easily be accomplished by carrying out a principal components analysis on the individual covariance matrix for any particular scale of interest.

Mantel Procedures and Constrained Ordination

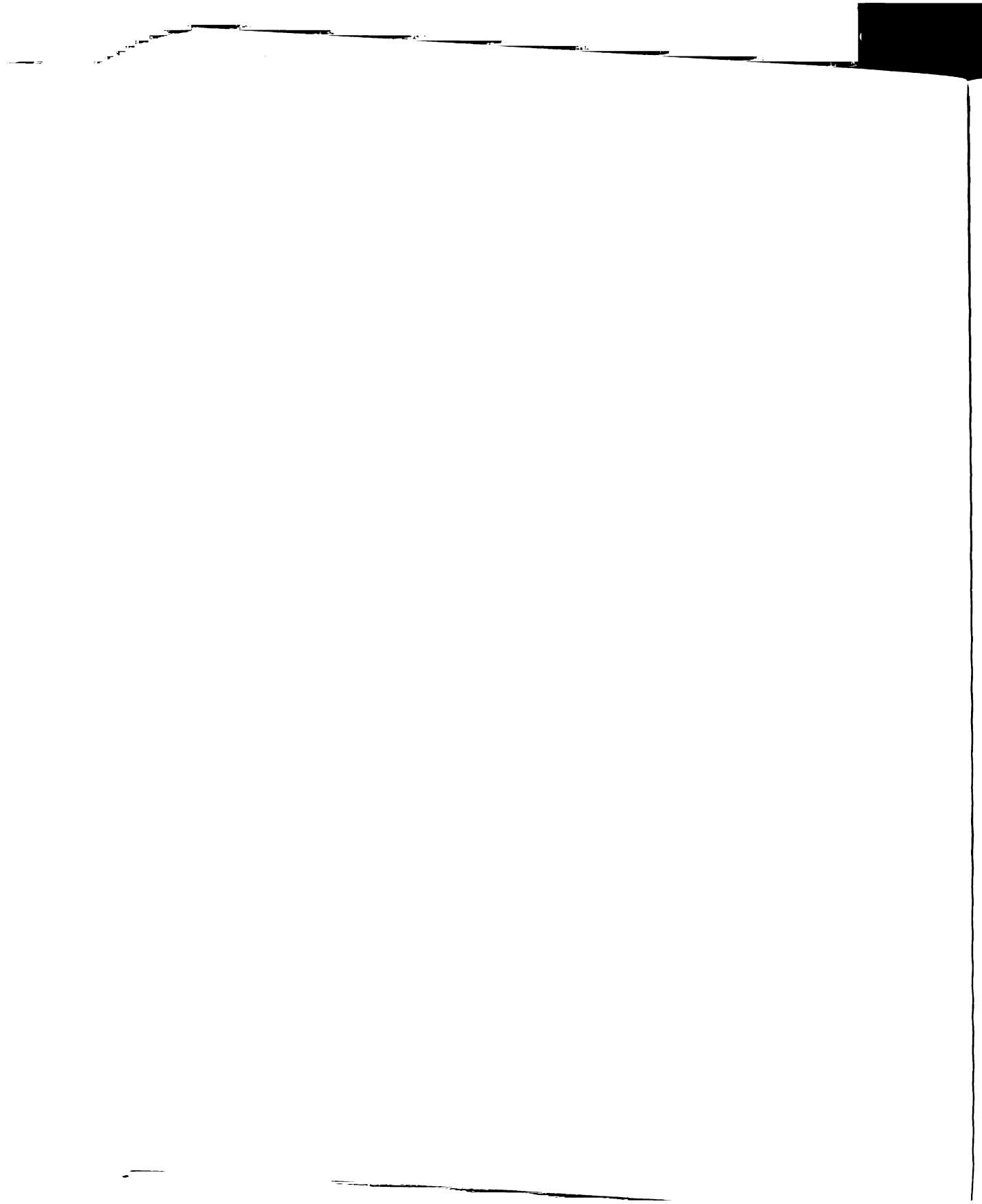
Other holistic methods of assessing the significance of spatial pattern in community composition include the Mantel test and constrained ordination. These are both based on separation distance between samples (extent). The Mantel test can be used to determine whether two distance matrices, one containing spatial distance and the other calculated using a community distance coefficient, are significantly correlated (Legendre and Fortin 1989). A positive result implies that communities are more different the farther apart they are. The normalized Mantel statistic (r_M) can also be calculated using a



series of matrices indicating which sample pairs belong to different separation distance classes. Plotted against separation distance, this Mantel statistic indicates regions of positive or negative spatial autocorrelation. It can be interpreted in much the same way as the semivariogram, where changes in slope represent a change in the spatial pattern detected. One complicating factor is that the value of r_M for each distance class is relative to the contrasting structure in the remaining distance classes; i.e. changing a value outside the distance class will change r_M .

Community ordination procedures are commonly used to extract major gradients within community composition from a group of sites. The amount of variability in community composition that can be correlated with independent measurements or treatments at the same sites can be determined by constraining the ordination axes to be linear combinations of environmental variables. If the environmental variables consist of geographical coordinates, and other polynomial terms derived from them, then the influence of spatial position on community composition can be determined (Borcard et al. 1992). If redundancy analysis, the constrained version of principal components analysis, is used then the procedure is analogous to a multivariate trend-surface-analysis. Another approach is the use of canonical correspondence analysis. The constrained ordination approach is limited by the ability of the geographical variables to capture the spatial patterns present. The extrapolation to other scales of sampling grain is also more difficult.

In presentations of Mantel procedures and constrained ordination, several characteristics of the procedures have been stressed: the null hypothesis of no spatial pattern can be explicitly tested using randomization tests, any community distance or



similarity metric can be used, and the analyses can be used to partition variability in community composition among various sources (Borcard et al. 1992, Legendre and Anderson 1999, Legendre and Fortin 1989). The other methods of spatial analysis described share these characteristics, if adapted in the same way that Mantel procedures and constrained ordination have been.

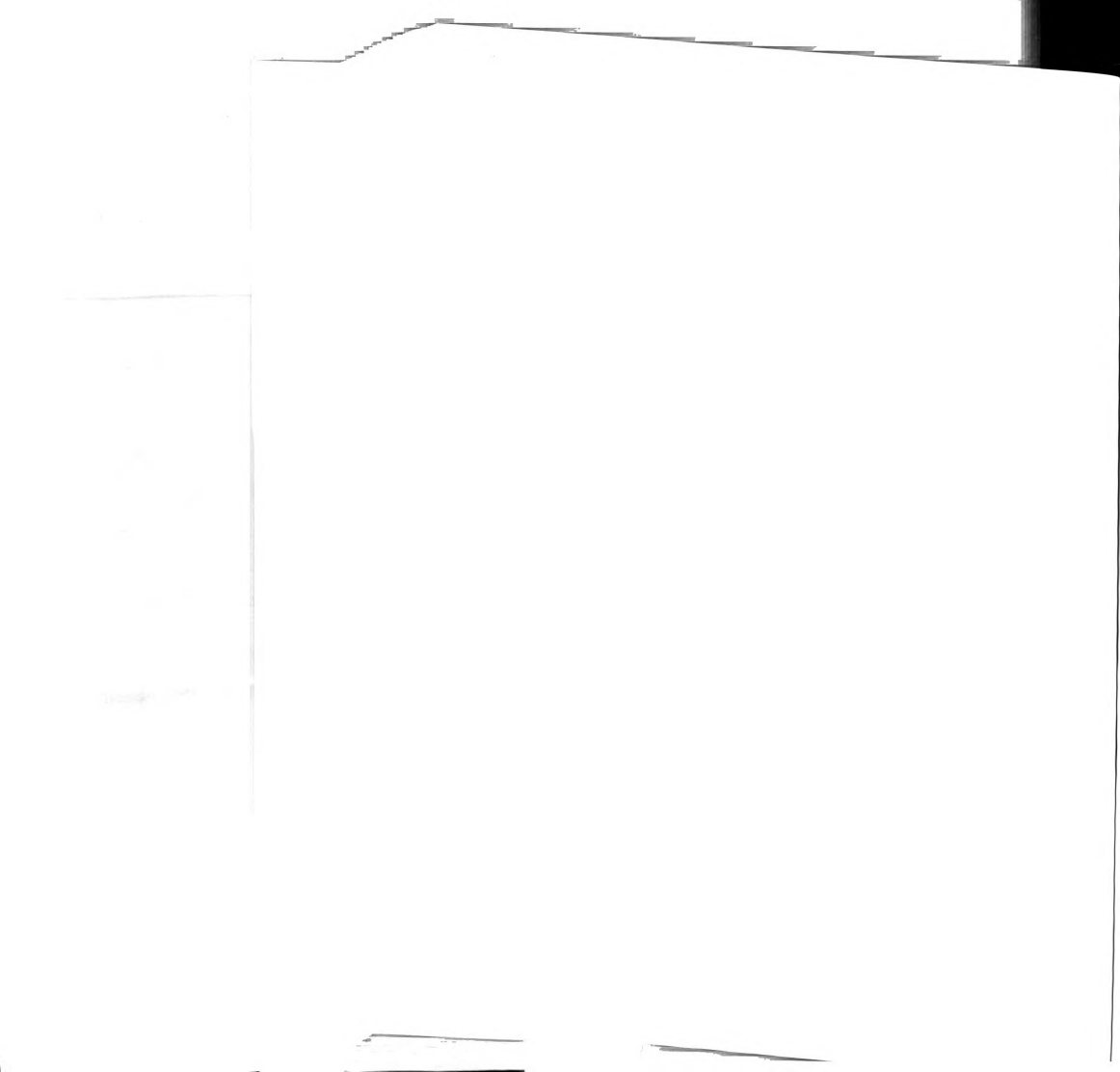
Materials and Methods

Sampling Design

Sampling was performed in three 1 ha alfalfa field replicates at the W.K. Kellogg Biological Station Long Term Ecological Research Site in June of 1999. Plots had been in agronomically-managed perennial alfalfa for 10 years at time of sampling. Alfalfa was killed with herbicide every five years and resown to maintain stand vigor.

Approximately two months prior to sampling, 5 year-old stands of alfalfa had been killed with 3.5 L/ha of the herbicide glyphosphate (Roundup). Plots were then fertilized with 2.9 Mg/ha dolomitic lime and re-planted to alfalfa at a rate of 10 kg/ha for each of two perpendicular passes. Details of the management of this site can be found elsewhere (<http://lter.kbs.msu.edu/Agronomics>).

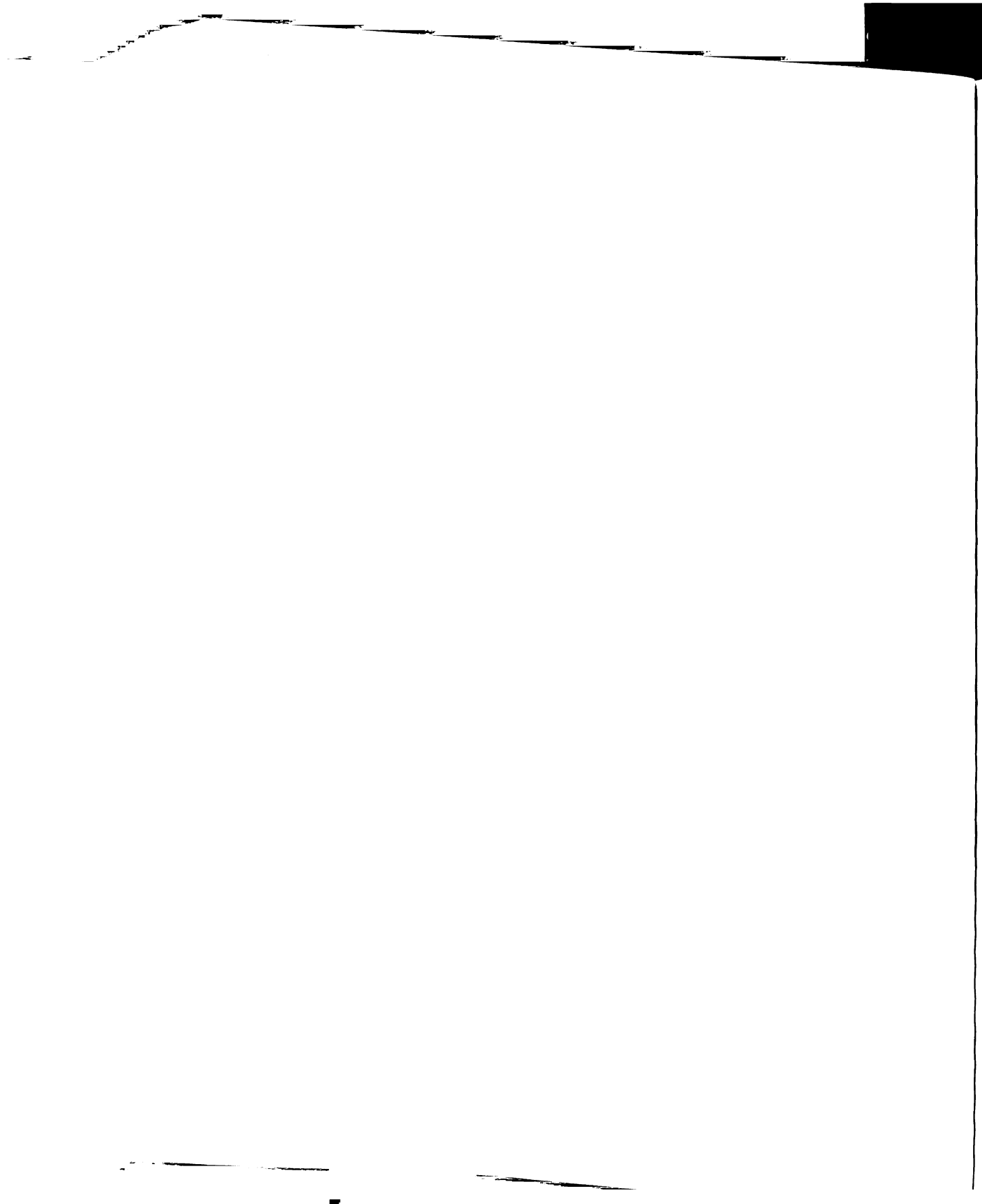
Within each of the three field replicates, a sampling grid with adjacent samples being 39.6 cm apart was placed over an approximately 1.6 x 2 m area. Ten locations within each grid were randomly chosen for multiple-grain sampling (see Figure 1). Five soil samples differing in soil weight were collected at each of these locations to obtain a set of samples representing a wide range of sampling scales. Approximately 1 and 10 g samples were collected by pushing sterile sample tubes (5 mL Falcon specimen tubes and



50 mL Corning centrifuge tubes, respectively) into the soil. Approximately 100 g samples were collected by pushing the tip of a 6.4 cm hydraulic Giddens tube (soaked in bleach between samples) into the soil and then excavating the sample with a sterile laboratory weighing spatula. 100 g samples were then placed in sterile Whirlpack specimen bags. Smaller samples (10 and 100 mg) were collected using sterile weighing spatulas and placed in sterile 1.5 mL microcentrifuge tubes. All samples were from the layer of soil 2–4 cm deep to avoid increased variability at the soil surface.

Two additional 10 g samples were taken 8.5 cm from each of the ten multiple-grain sampling locations in each grid described above. These were on opposite sides of the multiple-grain sampling locations. The orientation of these samples within the artificial coordinate system was determined randomly. If the multiple-grain sampling location was at the edge of a grid and the orientation of the additional samples was such that one of them would be placed outside of the grid, this sample was instead located within the grid 8.5 cm from the other additional sample for that location (see Figure 1). Twenty additional 10 g samples were collected at each field site to fill in the sampling grids described above. All 10 g samples were collected as described above for the multiple-grain sampling locations. The location of the center of each sample was recorded with respect to the artificial coordinate system constructed.

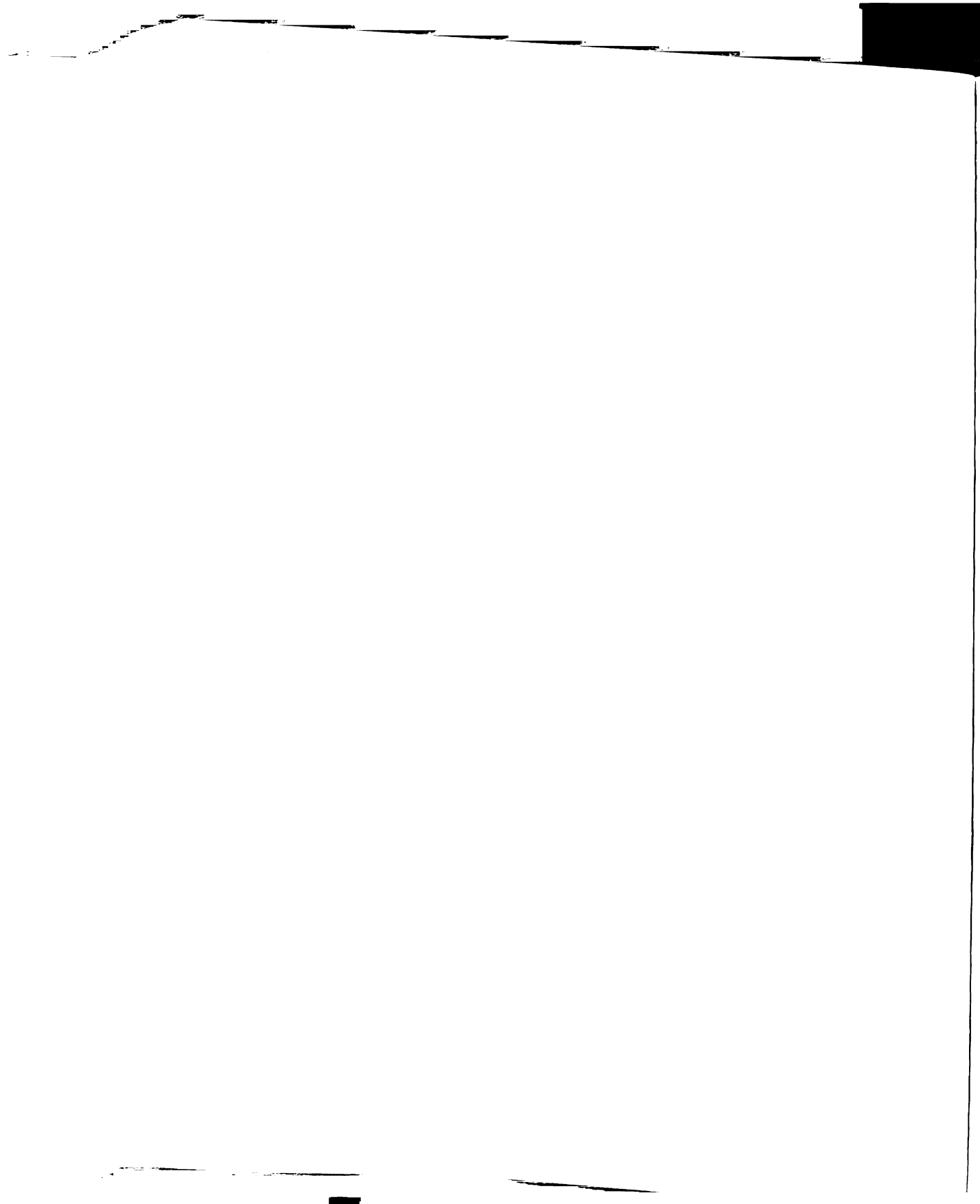
This sampling scheme resulted in each of the three 1.6 x 2 m sampling grids being characterized by two sets of samples: 1. ten samples at each of five sampling scales (10 mg to 100 g), 2. fifty 10 g samples spaced 8.5 to 200 cm apart. All samples were immediately frozen and stored with dry ice while being transported to the laboratory, where they were transferred to –20°C storage. The actual wet weight of all samples was



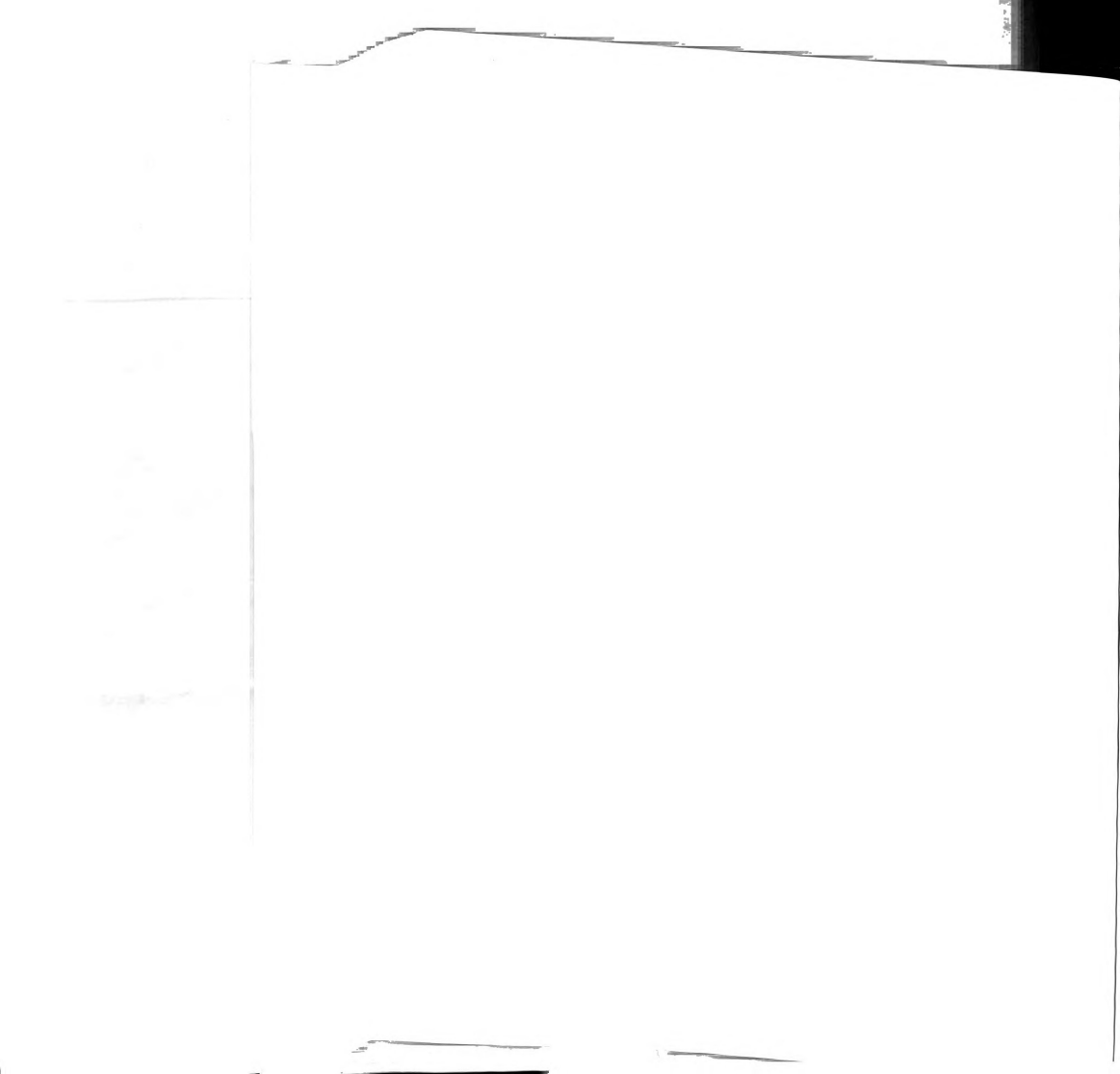
recorded in the laboratory and used in statistical analyses. References made hereafter to sampling scales such as the "10 mg" scale are for convenience.

Eubacterial Community Characterization by T-RFLP

T-RFLP was performed essentially as described in Liu (1997) and in chapter 1. Community DNA was extracted from 10 mg to 1 g soil samples using the standard Ultraclean Soil DNA extraction kit (Mo Bio Laboratories, Solana Beach, CA). Preliminary experiments were performed to determine whether slurring and homogenizing 10 and 100 g samples with sterile water had any effect on the variability of T-RFLP profiles of a set of samples: 1. Eight 10 g samples were slurried with 10 mL of sterile water and then homogenized by shaking on a vortexer. DNA was then extracted from 0.5 mL subsamples (approximately 5% of sample) using the standard Ultraclean Soil DNA extraction kit, and from the remainder of each sample using the Large-Scale Ultraclean kit. 2. Seven 100 g samples were slurried and homogenized with 50 mL sterile water. DNA was extracted from 0.5 mL subsamples (approximately 1% of sample) using the standard Ultraclean kit, from 15 mL subsamples (approximately 20% of sample) using the Large-scale Ultraclean kit, and from the remainder of each sample using four large-scale Ultraclean kits which were then pooled together. T-RFLP was performed and the variability of T-RFLP profiles for each set of samples was assessed as described below. Based on the results of this experiment (see Results below), remaining 100 g samples were slurried and DNA was extracted from 15 mL subsamples, DNA was extracted from entire 10 g samples at multiple-grain sampling locations, and 10 g samples at the remaining 40 locations per grid were slurried and DNA was extracted from 0.5 mL subsamples.



Genomic DNA was found to be of sufficient purity to be used directly in PCR reactions. PCR was performed using a standard reaction mixture of 160 μ M of each deoxynucleoside triphosphate, 3 mM MgCl_2 , 0.05 U/ μ L Taq DNA polymerase and the appropriate volume of accompanying 10X PCR buffer (Gibco BRL, Gaithersburg, MD), and 0.2 μ g/mL bovine serum albumin (Boehringer Mannheim Biochemicals, Indianapolis, IN). PCR mastermix, without primers, and PCR reaction tubes were sterilized for 14 minutes with direct ultraviolet radiation in a Cleanspot PCR/UV workstation. Primers used were the general eubacterial primer 8-27F (AGAGTTTGATCCTGGCTCAG, E. coli numbering, Amann et al. 1995, Integrated DNA Technologies, Coralville, IA) and the universal primer 1392-1406R (ACGGGCGGTGTGTACA). PCR reactions were optimized for each sample of genomic DNA using a master mix with primer concentrations of 0.4 μ M. Optimizations were performed by adjusting the amount of genomic DNA extract used (0.4 to 15 μ L/50 μ L reaction) and the number of PCR cycles run (18, 22, 28, or 33) to obtain a strong band without visible non-specific product. PCR was performed in a Perkin-Elmer 9600 thermocycler using an initial denaturation step of 95°C followed by 18-33 cycles of the following program: denaturation at 94°C for 30 sec., primer annealing at 55°C for 30 sec., and extension at 72°C for 30 sec. A modified hot start procedure was used where PCR tubes were not placed in the thermocycler until the block temperature had reached 80°C. A final extension at 72°C for 7 min. was performed after the programmed number of cycles was complete. PCR product was checked by electrophoresis on a 1% agarose gel stained with ethidium bromide.





PCR reactions (50-75 μL) were performed in triplicate for each sample using the optimal conditions found previously. These reactions were performed using the same PCR master mix and program described above except that the forward primer was 0.6 μM hexachlorofluorescein (hex)-labeled 8-27F (Integrated DNA Technologies). Negative controls (no genomic DNA) were conducted with every PCR and run on several Genescan gels. Contamination in PCR reactions was not detected. Small peaks occasionally appeared in negative control lanes on Genescan gels, but the cumulative peak height was always below 1000 units. Samples were re-run if the cumulative peak height was below 9500 fluorescence units.

PCR replicates were pooled and purified using the Promega PCR Preps Wizard Kit as directed by the supplier, except that elution was performed with 19 μL of sterile water heated to 55-65°C. Five μL of purified PCR product was mixed with 5 μL of restriction enzyme master mix containing 1.5 U/ μL of restriction enzyme and one μL of the accompanying reaction buffer (Gibco). Restriction reactions were incubated for three hours at 37°C, followed by 16 min. at 65°C to denature the restriction enzyme. Three μL of the restricted PCR product was mixed with one μL of 2500 TAMRA size standard (Applied Biosystems Instruments, Foster City, CA). DNA fragments were separated by size by electrophoresis at 1800 V for 14 hours on an ABI 373 automated DNA sequencer at Michigan State University's DNA Sequencing Facility. The 5' terminal fragments (T-RFs) were visualized by excitation of the hex molecule attached to the forward primer. The gel image was captured and analyzed using Genescan Analysis Software 3.1. A peak height threshold of 50 fluorescence units was used in the initial analysis of the electropherogram. T-RFLP profiles for all samples were generated using the restriction



enzyme *RsaI*. *MspI* was used to generate additional profiles for all samples in grid 2, and *HhaI* and *HaeIII* profiles were also generated for several samples in grid 2.

The effect of the number of cycles of PCR on variability of the T-RFLP profiles was assessed using five samples for which optimal PCR conditions had been determined as 22 PCR cycles and 1.2 μL genomic DNA per 75 μL reaction. Optimal PCR conditions for 1:6 dilutions of these samples was determined as 28 cycles and 0.6 μL genomic DNA per 75 μL reaction. When 1:6 diluted samples were PCR-amplified using 22 cycles and 0.6 μL genomic DNA per 75 μL reaction, the PCR product was approximately 1/8 the strength of an optimal reaction. Three analytical PCR replications were then performed for each of these diluted samples at 28 cycles and 24 replications were performed at 22 cycles using the same master mix. The pooled replicates then had equivalent amounts of DNA in each sample, differing only by the number of cycles and analytical replicates used. The 24-replicate pooled samples were concentrated using a Speed-Vac centrifuge. These test samples were then analyzed by T-RFLP as described above. Variability was compared between the sets of samples run at different numbers of PCR cycles.

Data Analysis Methods

The details of T-RFLP data processing have been described elsewhere (chapter 2). Briefly, all T-RFLP profiles were standardized to a cumulative peak height of 10,000 fluorescence units, except for the few profiles that were used that had a cumulative peak height less than 10,000 fluorescence units. T-RFs with a peak height of less than 50 fluorescence units after standardization were thrown out. This is equivalent to using relative abundance of T-RFs that were strong enough to have been detected if the



1

cumulative peak height had equaled 10,000 fluorescence units in all samples. T-RFs were aligned in an Excel spreadsheet against a set of categories previously defined for profiles of the particular restriction enzyme used. Sample identities were concealed during alignment.

All data analyses were performed using the computer software Microsoft Excel or SAS version 8 (principally IML and Stat software components) except as otherwise noted.

Variability Statistics

Statistical analyses were based on several scores designed to describe the variability or heterogeneity of a set of T-RFLP profiles. Mean variance, or one half of mean Euclidean distance, was calculated from relative abundances because of its precedence in studies on spatial structure. Other statistics were used because they have been shown to be superior to mean variance in comparison of profiles of multi-species communities. Mean Hellinger variance (HV) was adopted based on the recommendation of Hellinger distance in Legendre and Gallagher (in press) for use in analysis of species abundances. Mean Hellinger variance was determined by calculating the mean variance after a Hellinger-transformation, resulting in:

$$HV = \frac{1}{p} \sum_{j=1}^p \left(\frac{1}{n-1} \sum_{i=1}^n \left(\sqrt{\frac{y_{ij}}{y_{i+}}} - \bar{y}_{Hj} \right)^2 \right), \quad \bar{y}_{Hj} = \frac{1}{n} \sum_{k=1}^n \sqrt{\frac{y_{kj}}{y_{k+}}}$$

where p is the total number of T-RFs, n is the number of profiles in a set, y is T-RF peak height, and y_{i+} is the sum of all peak heights in profile i. This is also equivalent to one half of the mean Hellinger distance among samples, which is determined by calculating



mean Euclidean distance after Hellinger-transformation (Legendre and Gallagher in press).

The Jaccard similarity coefficient takes into account presence-absence data and only uses information from a variable (T-RF) when it is present in at least one of the two profiles being compared. It is calculated:

$$S_j = \frac{a}{a + b + c}$$

where a is the number of T-RFs present in both profiles being compared, and b and c are the number unique to each profile. The distance complement of the Jaccard coefficient ($JD=1-S_j$) was calculated and will be referred to here as Jaccard distance. Mean Jaccard distance is simply the mean value from a set of pairwise comparisons.

Heterogeneity among T-RFLP profiles was also compared using the mean absolute deviation of standardized t-scores (MAD-t scores), an index derived from recommendations in Edgington (1995), and calculated:

$$MAD-t = \frac{1}{p} \sum_{j=1}^p \left(\frac{1}{n} \sum_{i=1}^n \left| \frac{y_{ij} - \bar{y}_j}{s_j} \right| \right)$$

where \bar{y}_j is the mean peak height and s_j is the standard deviation of peak height for T-RF j in the n profiles being compared. A MAD-t score equals the mean number of standard deviations any given peak height is from the mean height for that T-RF. The overall MAD-t score is calculated by averaging MAD-t scores calculated for each T-RF. Hence rare and common T-RFs are equally weighted and it is a true index of data “evenness”. Unlike HV and JD, calculation of MAD-t scores must be based on an entire set of samples, and not sets of sample pairs.



DNA Extraction Experiment

For the preliminary DNA extraction experiment conducted on 10 and 100 g soil samples, mean variance, HV, mean JD, and MAD-t scores were calculated for each set of DNA extractions. The significance of the differences found in MAD-t scores were determined using distribution-free random permutation tests as described by Edgington (1995). The null hypothesis was that the difference in MAD-t scores for a pair of DNA extraction treatments was not different from that which would be found if the profiles were randomly associated with the treatments. Empirical differences in MAD-t scores were compared to a distribution of differences generated by 9999 random permutations of profiles with respect to their identities in the two treatments being compared. The p-value for such a test is the proportion of all values, including the empirical value, that are equal to or greater than the empirical value.

Multiple-Grain Analysis

Variability-scale analysis was performed by calculating mean JD, log HV, and MAD-t scores for each set of T-RFLP profiles representing samples taken at a given scale from a given grid. Scores were plotted as a function of log mean soil weight, which represents the sampling grain. Least-squares regression models of the variability statistics as a function of log soil weight were generated. MAD-t scores for the *MspI* profiles were shifted above scores for the *RsaI* profiles; therefore residuals about the means of *MspI* and *RsaI* MAD-t scores were used in regression. The fit of simple linear regression (without hierarchical structure) was compared to more complex hybrid models (indicating hierarchical structure) using partial F-tests.



T-RF covariance matrices were also constructed for each set of samples from the Hellinger-transformed peak heights. These were then compared by calculating the Pearson correlation coefficient between elements of the matrices (also called the normalized Mantel statistic or cophenetic correlation). A correlation super-matrix was constructed by pairwise comparison of all covariance matrices. This was then analyzed by principal coordinates analysis and cluster analysis using average linkage (UPGMA) and Ward's linkage methods.

Extent-Based or Separation Distance Analysis

For each set of fifty 10 g samples, the significance of differences in T-RFLP profiles due to subsets being run on different gels was tested using redundancy analysis in the software Canoco (Microcomputer Power, Ithaca, NY). This test compares the amount of variability in the profiles that can be accounted for by external data (such as gel identity) to a distribution generated by random permutations of the profile identities (Legendre and Legendre 1998). To perform redundancy analysis on JD, principal coordinates analysis was first used to derive new variables from the pairwise JD matrix (Legendre and Anderson 1999). Euclidean distance calculated from these variables preserves the Jaccard distances of the original matrix. The proportion of variability that could be accounted for in the T-RFLP profiles was significant for several grids ($p=0.0001$ to 0.37 , 9999 random permutations). Therefore all further extent-based analyses of the 10 g samples were performed on residuals from multiple linear regression accounting for the gel-effect. Regressions were performed directly on Hellinger-transformed peak height or on JD principal coordinates. For some grids this had a large effect on the



analysis, and for some it did not (usually accounting for approximately 10% of the total variance in the datasets, but for as low as 4% and as high as 22%).

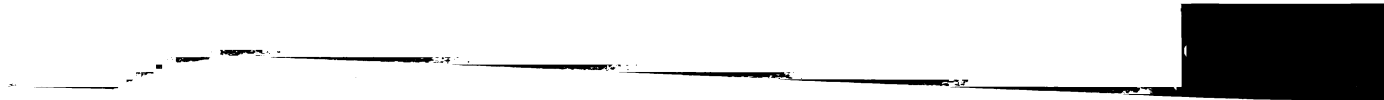
Various different sizes of distance classes (lag distances) were investigated for grouping pairs of samples. A lag distance of 20 cm was chosen so that there would be greater than 30 pairs of samples in all distance classes. The distance classes with the two greatest lag distances were excluded from analyses to avoid edge effects from classes containing only pairs where both samples were from the edges of the grid. Variability-scale analysis was conducted by calculating HV and mean JD values for each distance class and plotting as a function of mean geographic distance. Both isotropic and anisotropic pairings of samples were used to look for directional differences. Isotropic values were used in subsequent analyses.

The significance of the spatial autocorrelation within each distance class was tested by comparison of HV and mean JD to distributions created by 9999 random permutations of the geographic coordinates of samples. The specific null hypothesis tested was that the statistic from a distance class was not more different from the mean value over all sample pairs than would be expected due to chance (i.e. no spatial autocorrelation, Legendre and Legendre 1998).

Exponential or linear models, with nugget effects, were then fitted to the distance plots using weighted least-squares regression (Cressie 1985). The forms of these models are, respectively:

$$V = C_0 + C_{1(\text{exp})}(1 - e^{(-h/a)}) \quad \text{and} \quad V = C_0 + C_{1(\text{lin})}h$$

where V is HV or mean JD, h is the distance between samples, a is one-third of the “practical” range of spatial autocorrelation for exponential models, C_0 is the nugget (or



unaccounted for variability), and C_1 is the sill (or variability associated with spatial structure) in the exponential model and the change in variability with separation distance between samples in the linear model.

New distance functions for HV were constructed for alternative sampling grains from the fitted exponential models using the principals described in Bellehumeur et al. (1997). Briefly, a theoretical point model was formed by assuming: $a_p = (3a - L)/3$ and $C_{1(\text{exp})p} = C_1/(1 - F)$, where L is the distance that the edges of samples were brought closer together by taking real samples instead of “point samples” (i.e. the diameter of the samples), and F is the proportion of the structural variability that is masked by taking real samples. F is calculated by stochastic integration of an exponential model (without nugget) with sill equal to one and range equal to a_p . The integration was accomplished by generating 100,000 random lags (h) between zero and L , constraining the distribution by the geometry of the sampling area. The exponential portion of the distance model for an alternative sampling grain was then constructed by finding L and F for the new grain and rearranging the above equations to solve for C_1 and a . The unexplained variability C_0 was not discounted as a function of the ratio between the new and original sampling grains since this procedure assumes that there is no analytical variability contributing to C_0 ; in fact, preliminary experiments showed analytical variability may be equal to C_0 (data not shown), so the C_0 was not adjusted with sampling grain.

The distance functions for alternative sampling grains were used to estimate HV of the set of multiple-grain sample locations had they been sampled at the alternative grains. This was done by finding the number of pairs of samples within this set that fell into each of the 20 cm lag distance classes. The mean separation distance within each



class was used to calculate an HV for that class using the new distance function, and the overall HV for the entire set of multiple-grain samples was calculated by finding the weighted mean HV of all classes. These estimates were then plotted as a function of log sampling grain with the empirical multiple-grain location data described above.

T-RF covariance matrices were calculated from Hellinger-transformed peak heights for each lag distance class. A correlation super-matrix was constructed and analyzed using principal coordinates analysis and cluster analysis, as described above.

Redundancy analysis was also used to perform multivariate trend-surface analysis using the computer software Canoco. The external data used were the geographical x,y coordinates of each sample, and combinations of the coordinates to the third power (x^2 , y^2 , xy , x^3 , y^3 , x^2y , xy^2) as suggested by Legendre and Legendre (1998). The significance of the variability explained by these geographical variables was tested with 9999 random permutations. Forward selection of external variables was also used to check the significance of each geographical term after accounting for the terms that explained more variability.


Mantel correlograms were constructed from pairwise T-RFLP distance matrices and a series of similarity matrices indicating presence of pairs in the distance classes (Legendre and Fortin 1989, Legendre and Legendre 1998). Therefore a negative normalized Mantel statistic for a distance class indicates positive spatial autocorrelation at that scale. The normalized Mantel statistic was also calculated between the T-RFLP and geographic distance matrices to test for an overall effect of separation distance across all scales (with the opposite interpretation of the sign of the statistic). Mantel statistics were tested for significance using 9999 random permutations of the geographic



1

2

3



coordinates of the samples. The null hypothesis tested is therefore that the empirical Mantel statistics are not more different from zero than would be expected by random arrangement of the samples (i.e. no spatial structure).

Results

DNA Extraction Experiment

In the DNA extraction experiment, HV, mean JD (data not shown) and MAD-t scores (Figure 2) were higher for the set of DNA extractions derived from 5% subsamples of the slurried 10 g samples when compared to the set of 95% subsample extracts. Random permutation testing of the significance of the difference in MAD-t scores resulted in a marginally-significant p-value (0.089). It was therefore decided to extract DNA from whole samples for the 10 g samples from multiple-grain locations. There were ten such samples from each of the three sampling grids. The remaining forty 10 g samples from each grid were slurried and DNA was extracted from 5% subsamples to reduce the cost of DNA extraction. It was felt this was justifiable due to the increased number of samples in this analysis and the relatively weak effect of subsampling.

For the 100 g samples, variability statistics decreased in the order of 1%, 80%, and 20% subsamples (see Figure 2). Random permutation testing found that the difference in MAD-t scores between the 1% and 20% DNA extracts were marginally-significant ($p=0.069$), while neither score was significantly different from that for the set of 80% DNA extracts. These somewhat contradictory results led to the decision that 100 g samples would be slurried and DNA would be extracted from 20% subsamples.

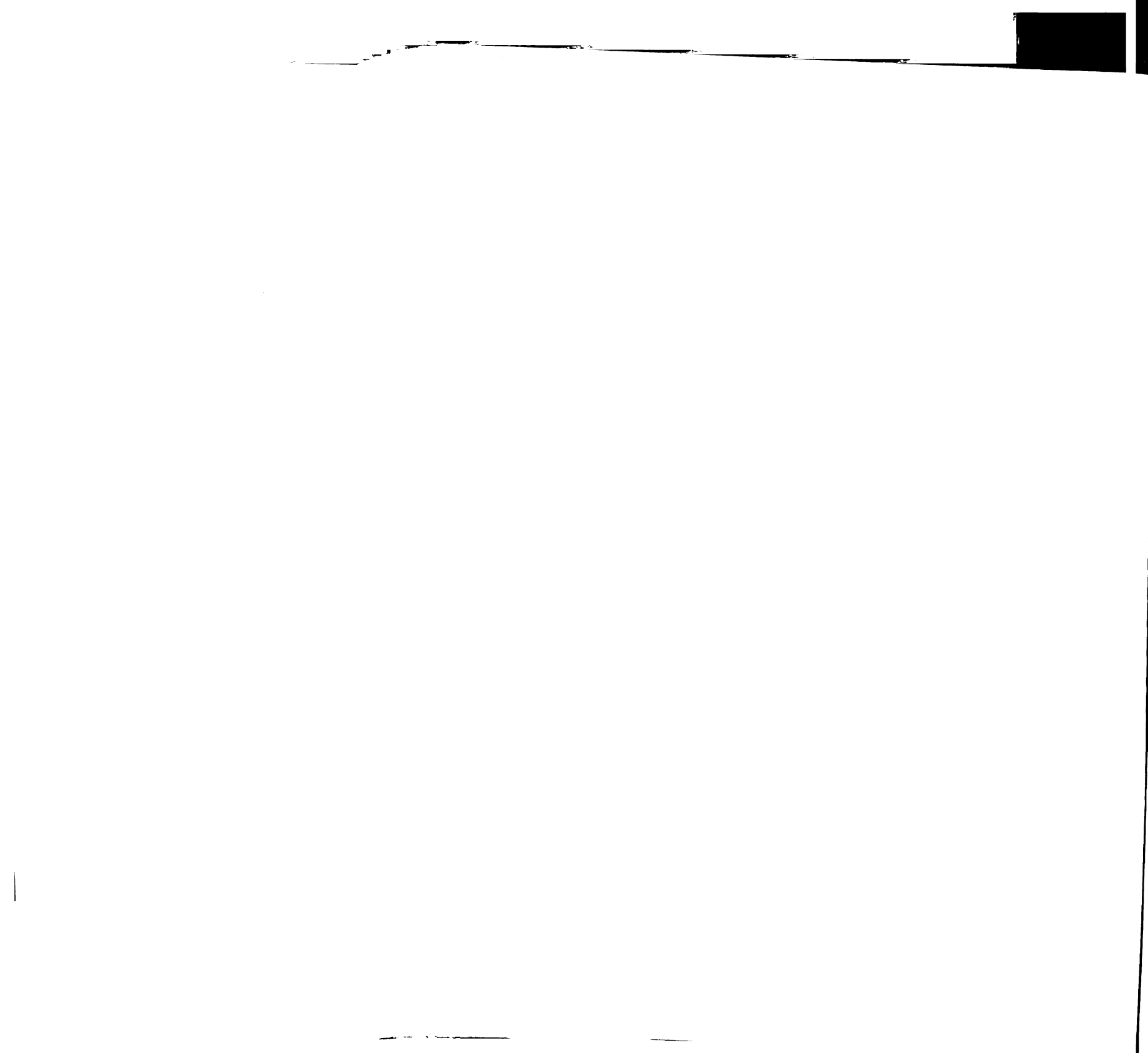


PCR Cycles Experiment

The effect of number of cycles on heterogeneity of a set of samples was contradictory to the hypothesis based on the theory that increased numbers of PCR cycles increases the number of nucleotide mismatches due to random polymerase mistakes. The HV was higher for the set of samples amplified using 22 PCR cycles, diluted genomic DNA and 24 PCR replicates than either the set from 28 PCR cycles, diluted genomic DNA and 3 PCR replicates or the set from 22 PCR cycles, undiluted genomic DNA, and 3 PCR replicates. The HV of the latter two sets were approximately equal (data not shown). Pooling of PCR replicates is performed to reduce the significance of PCR artifacts; however these results indicate that this may also increase the overall heterogeneity of PCR amplicons.

Grain-Based Analyses

The overall trend for all variability statistics was a decrease with increasing scale of sampling grain (see Figure 3). The slope of a simple linear regression of log HV on log soil weight is much closer to zero than -1 (although it is also significantly different from zero, $p=0.00005$). The slope for variance is almost the same as for HV (data not shown). While this could be taken to imply that there is strong autocorrelation in the peak heights themselves (i.e. a small-grain sample profile is almost the same as its corresponding larger-grain sample profile from the same location), that is not the case for this set of T-RFLP profiles. Based on the fairly noisy profiles we obtained, we suggest that instead this result implies that there are self-similar (or fractal) patterns across these scales. However, the fact that there is a significantly negative slope for HV as well as mean JD and MAD-t implies that pattern from some phenomena (and its accompanying



variability) are not completely fractal and are not being detected at the larger sampling grains.

While simple linear regression explained a significant portion of the relationship between the variability statistics and sampling grain, distinct zones which are characterized by unique slopes are apparent from the data plots, indicating hierarchical structure. Partial F-tests indicated that models which include a change in slope (which will be referred to as hierarchical models) had significantly reduced residual sums of squares for HV and MAD-t when compared to simple linear regression (see Table 1 and Figure 3). The hierarchical models were constructed by separate linear regressions in regions where the slopes appeared to differ. The slope of a regression was discarded from the model if it was not significantly different from zero. The phase-shift region where the slope changes is undefined in these models since there is no data describing the relationship there. The hierarchical model for mean JD was not significantly superior to the linear model, although it did have a lower residual sum of squares. The HV and mean JD plots had changes in slope between sampling scales different from where the slope changed for MAD-t scores. This is not overly surprising since MAD-t scores weight rare T-RFs much more heavily than HV or JD. Potential outliers were not removed in the testing of these models. Removal of outliers would cause the hierarchical model to fit the data significantly better than the linear model for mean JD, remove the hierarchical relationship for MAD-t, and have no effect on HV.

The correlation between Hellinger covariance matrices from different sampling grains was uniformly low (ranging from -0.03 to 0.31 , mean 0.08), resulting in uninformative principal coordinates and cluster analyses of the correlation super-matrix.


In general, comparison of covariance structures was not as useful as mean variability of T-RF peak heights for this dataset.

Extent-Based Analyses

As expected, HV and mean JD increase as separation distance between samples increases, as shown for HV in Figure 4. Mean JD plots looked almost identical to HV plots, except for the scale of the y-axis (data not shown). Hellinger variance for grids 2 (RsaI and MspI digests) and 3 (RsaI) reach an asymptote between approximately 50 and 75 cm, while the HV plot for grid 1 (RsaI) rises linearly across the entire range of separation distances. Permutation testing indicated that one or two of the first few distance classes had HV significantly below the mean HV, indicating significantly positive spatial autocorrelation at that scale (see Figure 4).

Exponential models were fit to HV plots for grids 2 and 3 and a linear model was fit for grid 1 (see Figure 4 and Table 2). Spatial structure accounted for 18 to 23% of the total variance in each grid dataset. Estimates of HV for the multiple-grain sampling locations based on the fitted exponential models are shown in Figure 5. The range over which the estimation was made overlaps with two sampling grains for which samples are available (10 and 100 g). The 10 g samples at multiple-grain locations went into construction of the models, along with the forty other 10 g samples per grid, and the empirical HV values are very close to the estimated values. The model estimates for the 100 g samples are quite close to the empirical values for grid 2 digests, but are well-above the empirical value for grid 3. This may be due to noise within the empirical values, which are based on fewer samples than the sets from which the models were constructed (10 versus 50 samples). Between 10 and 1000 g the HV estimates are

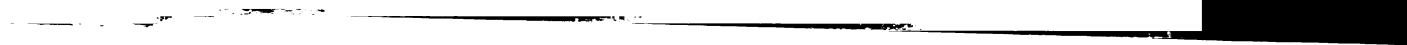




relatively flat, in agreement with the hierarchical least-squares model fitted to the empirical values in the grain-based analysis (see Figure 3). At scales greater than 1000 g the slopes change, becoming noticeably steeper. There may be some flattening of the curve again as soil weight approaches 10^5 g, although this transition is not completely represented within the range shown.

Inferences from the extent-based models to other sampling grains outside the range estimated over in Figure 5 cannot be made since they would involve either 1. smaller sampling grains than that which the model was based on or 2. sampling grains larger than the area sampled. It should be noted that the estimates for samples larger than 10^4 g are theoretical since samples taken at such a scale would overlap. However, the spatial structure reflected in HV estimates, even over theoretical sampling grains, is certainly real, being based on a model derived from empirical extent-based data. The construction of estimates and theoretical samples is a convenient way to integrate the grain-based and extent-based analyses. Hierarchical spatial structure is evident from the HV estimates since there are two well-defined regions with differing slopes. Hierarchical structure is not evident and estimates cannot be made, however, from the grid 1 extent-based analysis since the relationship between HV and separation distance for grid 1 is linear.

Analysis of the correlation super-matrix describing the relationship between Hellinger covariance matrices defined by distance classes found that the first distance class (0 to 20 cm separation distance) had a unique T-RF covariance structure in all four grids (see Figures 6 and 7 for examples). Cluster analysis also resulted in distance classes 8, 9, and 10 being clustered separately from classes 2 through 6, with distance





class 7 being in either cluster depending on the grid. Principal coordinate analysis showed distance classes 2 through 10 in a gradient without strong hierarchical structure, although classes 9 and 10 were always somewhat separate from the rest of the gradient. When covariance matrices from the grain-based analysis were included with those derived from distance classes, matrices derived from samples taken at alternative sampling grains were identified as outliers (data not shown).

Redundancy analysis found linear combinations of geographical terms did account for a significant portion of the variability in Hellinger and Jaccard distances in all cases except one (see Table 3). When the analysis was limited to those two or three geographical terms found to be statistically significant using forward selection of variables, the amount of variation explained dropped from 20-25% to 5-13%. Geographical terms consistently explained a greater portion of the variability in Hellinger distances than in Jaccard distances.

Global Mantel tests found weak but significant correlation between geographic distance and Hellinger distance between T-RFLP profiles for all grids (see Table 3). The same trend was present but not as strong for Jaccard distance. Mantel correlograms (where negative values imply positive spatial autocorrelation within a distance class, relative to the rest of the dataset) indicated that the statistically significant spatial structure was short-range autocorrelation (<50 cm; see Figure 8). The relationship between r_M and separation distance is essentially linear for the HD-based Mantel correlograms, as well as the grid 1 JD-based Mantel correlogram. Jaccard distance-based Mantel correlograms for the other grids reach an asymptote after approximately 70 cm.

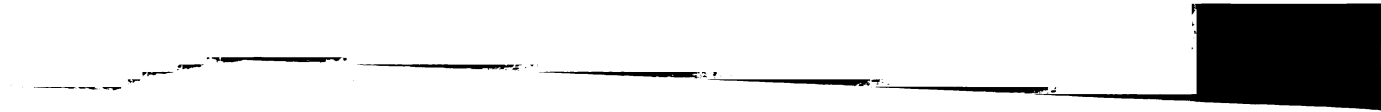



Discussion

Hierarchical Spatial Structure Detected within the Soil Microbial Community

The soil bacterial community was shown to have significant spatial structure in an area that is relatively small and homogenous from the perspective of the plant community: the layer of soil at a depth of from 2 to 4 cm, over a 1.5 x 2 m area of soil, under perennial alfalfa. Furthermore, this spatial structure was shown to be organized by at least three hierarchical levels. The levels of organization are hierarchical since they operate within distinct ranges of spatial scale, or scale domains (Wiens 1989), and hence variability within the lower levels are affected by higher levels, but not vice versa. Note that while mechanisms operating at low levels within the hierarchy will not affect variability at scales larger than the level's scale domain, this does not imply that those mechanisms will not affect other aspects of phenomena at larger scales. In particular, mechanisms causing patchiness in T-RF abundance at lower levels may determine mean abundance in samples taken at larger scales.

While this study was not designed to determine the causes of the hierarchical spatial structure, it is possible to hypothesize what they may be. The level operating at smaller scales, 10 mg to 1 g, or 1 to 13 mm, may be regulated by resource heterogeneity at that scale, such as proximity of a site to individual roots, pieces of decomposing shoot residue, or macropores. These create gradients of water, organic matter, terminal electron acceptors, and other organisms (see chapter 3). Aggregate structure and disturbance history (such as by soil fauna or aggregate disintegration) may also affect communities at this scale (see chapter 4). The scale domain of the highest level detected (1000 to 10⁵ g or 25 to 220 cm) has been intensively investigated recently (e.g. Boerner et al. 1998,





Schlesinger et al. 1996, Stoyan et al. 2000). Therefore it is well known that there is considerable resource heterogeneity at these scales, a large portion of which is generated by the plants themselves. We suspect heterogeneity of plant density, organic matter, phosphorus, pH, etc. regulates eubacterial community structure at this level.

The intermediate level (10 to 1000 g or 2 to 25 cm) is interesting because there is virtually no change in variance with scale. This implies that there are few important mechanisms regulating eubacterial community structure that operate at these scales. If strong mechanisms did exist at these scales, variance would decrease with increasing sampling grain since the spatial patterns generated by the mechanisms would become increasingly diluted. Instead it appears that the scale is not yet large enough to begin to decrease the variability due to spatial structure generated at the higher level, but it is large enough to mask all variability due to spatial structure generated at the lower level. The implications of this for designing future sampling is discussed below.

Results of this study indicate greater spatial structure in the soil microbial community than was found previously by Cavigelli et al. (1995) or Felske and Akkermans (1998). One difference is that sampling in this study was extended to much smaller spatial scales. This has also been advocated for more detailed analyses in soil microbial diversity studies (Grundmann and Gourbière 1999). The above studies also skipped quantitative comparison of community profiles altogether (Felske and Akkermans 1998) or used univariate geostatistics without testing for structure within the community as a whole (Cavigelli et al. 1995). Hopefully the statistical methods outlined here will contribute to the ability to perform true tests of the hypothesis of spatial structure within a community, microbial or otherwise.



Comparison of Statistical Methods

The hierarchical structure was detected by extending previous work on univariate spatial structure to the use of community distance coefficients under the general name of variability-scale analysis. It was shown that extent- and grain-based approaches can be fully integrated if they are based on the same statistic. This was accomplished by modeling the spatial structure of the statistic in the extent-based approach and then using the method of Bellehumeur et al. (1997) to derive new models at different sampling grains. The new models are then applied to the same locations that were sampled using the grain-based approach. This integration of methods is an important development because grain- and extent-based methods have the same goal but are practical over different spatial scales. For example, it would have been unrealistic to use the grain-based approach at scales much larger than 100 g because of the difficulties in obtaining a representative DNA extract from large samples. Likewise, using the extent-based approach to try to examine small-scale structure would have either resulted in an unmanageable number of samples or much less sensitivity at all scales.


The approach taken here of testing for changes in slope of the variability-scale plots using regression and partial F-statistics may be questioned since the datapoints are derived from essentially the same sets of locations and are therefore not independent. However, as pointed out by O'Neill et al. (1991a), this bias will make the analysis conservative since successive points will tend to be similar and reduce the likelihood of finding changes in slope.

Several other extent-based approaches were also used for comparison to the extent-based variability-scale analysis. Redundancy analysis found that 20-25% of the



variability in the 10 g samples was due to spatial structure, in agreement with the extent-based variability-scale analysis (see Tables 2 and 3). A disadvantage of redundancy analysis is that it requires many geographical terms to detect complex spatial structures, causing over-parameterization of the analysis and inflating p-values. However, forward selection of a few terms resulted in a subset that was not adequate to account for as much variability as the extent-based variability-scale analysis. Maps of the sampling area could be constructed from canonical principal components scores derived from the redundancy analysis; however these must be interpreted with caution since they are “best-case” scenarios, dependent on the geographical terms present, and each map would show only the portion of the total spatial structure present that its principal component had captured. Hence the form of the spatial structure is more difficult to ascertain for complex datasets when using redundancy analysis. Global Mantel tests also showed there was a significant correlation between geographic distance and Hellinger distance (see Table 3). As has been pointed out in the past (Legendre and Fortin 1989), this test is most sensitive to gradients across the sampled area or other simple structures. Mantel correlograms showed similar forms of spatial structure to those found by extent-based variability-scale analysis, as well as significant spatial autocorrelation in the same distance classes (see Figure 8). The strength of this spatial structure (i.e. the amount of variability accounted for), however, is not readily apparent from the Mantel correlograms for reasons discussed previously. Neither Mantel correlograms nor redundancy analysis can be fully integrated with a grain-based approach.

Another statistical method proposed here that can integrate extent- and grain-based approaches is the exploratory data analysis of a correlation super-matrix. This



method is loosely based on Mantel procedures since correlation coefficients between matrices are used. The pairwise correlations from a set of matrices are used to create a correlation super-matrix which summarizes the relationships between all matrices. The matrices used here were T-RF covariance matrices. Cluster analysis and principal coordinates analysis were then performed on the correlation super-matrix to summarize these relationships. The result is an analysis of the similarities in the covariance structures for each scale separately analyzed. Scales from both extent- and grain-based approaches can be used. Analysis of the correlation super-matrix from the extent-based approach reinforced the general results found in variability-scale analysis. These results are more general, however, implying not only that communities are more similar when they are closer together, but also that the interactions between T-RFs are organized differently at different spatial scales. This was particularly true for the transition between the 0-20 cm separation distance scale and other scales, but also true for the 140-200 cm scale compared to other scales (see Figures 6 and 7). The former transition between covariance structures is at the same scale as the transition between levels of organization detected by variance-scale analysis at approximately 1000 g soil.

The attempt to integrate the extent- and grain-based approaches using the correlation super-matrix analysis was not fruitful for the current dataset. This was because the covariance matrices from different sampling grains were widely different from one another and from the covariance matrices from the extent-based approach (except for the 10 g samples). It may be that dynamics at the sampling grains used were so diverse that the covariance structures were completely different, or that there was



1



significantly greater noise in the covariance matrices from the grain-based approach, being based on fewer samples.

Interpretation of Molecular Community Fingerprint Data

Structure detected using MAD-t scores was somewhat different from what was detected using HV, with a phase transition between 10 and 100 mg. MAD-t scores analyze the T-RFLP profiles from a different perspective, weighting rare (i.e. less-frequently occurring) T-RFs equally with common ones, unlike either HV or mean JD. With each transition between sampling grains, higher MAD-t scores were obtained, indicating more variability and more rare T-RFs being detected. The jump in MAD-t scores between 10 and 100 mg was disproportionate, however, to the increases between all other scales (see Figure 3). It could be hypothesized that the size of many micro-habitats that support populations of specialized eubacteria are approximately 10 mg in weight, or a mm in diameter. However, it must be noted that T-RFLP shares with all other PCR-based techniques the potential problems of methodological artifacts such as chimera formation and point mutations (Wintzingerode et al. 1997). Artifacts are known to increase with PCR cycle number, although variability actually decreased with cycle number in a preliminary experiment presented here.

Mean JD, based on presence of T-RFs only and containing no information from the peak heights, portrayed the same trends as HV but generally evidence of structure was weaker. Utilization of peak height data enhanced the detail with which the community could be viewed using T-RFLP.

Molecular methods were used to avoid the severe biases in community composition known to occur with culture-based methods. DNA extraction and PCR

composition known to occur with culture-based methods. DNA extraction and PCR methods were used to avoid the severe biases in community composition that could be viewed using T-RFLP.

was weaker. Utilization of peak height data enhanced the detail with which the peak heights portrayed the same trends as HV but generally evidence of structure was weaker. Mean JD, based on presence of T-RFs only and containing no information from number in a preliminary experiment presented here.

to increase with PCR cycle number, although variability actually increased with cycle chimera formation and point mutations (Wernegreen et al. 1993). Variants are known other PCR-based techniques the potential problems of methodological artifacts such as weight, or a mm in diameter. However, it must be noted that T-RFLP shares with all habitats that support populations of microbial biodiversity are approximately 10 ng in all other scales (see Table 2). It should be noted that the increase in the size of many micro scores between 10 and 100 ng, whereas the increase between the two increases between indicating more variability and more variability. The range in MAD is

With each transition between habitats, the MAD score was not significantly different. (frequently occurring) T-RFs could be identified in the same way as in the other habitats. analyze the T-RFLP profiles in the same way as in the other habitats. detected using HV, with a few exceptions. Significant differences between the two detected using HV, with a few exceptions. Interpretation of Molecular Data is being based on fewer samples significantly greater noise in the data.

methods have their own biases, and so the structure detected in this study does not include those organisms not amenable to DNA extraction and PCR amplification using our methods. Great precaution was taken to ensure that biases would not occur due to the scale or position of samples.

Conclusions

This study is a snapshot of the microbial community structure, which is dynamic due to the seasonality of root growth, alfalfa harvests, and abiotic factors such as temperature, moisture, etc. It is a holistic snapshot, both from the viewpoint that the strength of many ecological phenomena were tested simultaneously, and that the structure was detected from the distributions of all T-RFs and their interactions. While significant random variability did exist (not associated with the spatial structure), the results strengthen the theory that soil eubacterial communities are not simply random assemblages formed by historical events. They display structure that suggests that at least some species are regulated by mechanisms analogous to those for macroorganism distributions.

The appropriate scale of sampling will depend on the goals of the analysis. Often the goal is to assess the effects of some field treatment. If the hypothesized effect is on variability or spatial structure, a multiple-scale approach such as the one here should be taken. If, on the other hand, the goal is to test for changes in the average community composition without regard to spatial structure, the sort of “null level” detected in this study (between 10 and 1000 g) presents a unique opportunity. If treatments are blocked within the scale domain of such a level, and samples are also taken at a grain within the

scale domain, then increased variability, decreased sensitivity, and non-independence of replicates due to spatial structure is avoided. Otherwise, many samples must be taken in order to characterize the spatial variability, or they can be composited in an attempt (probably in vain) to overcome the spatial variability. Likewise, we do not feel there is a unique "scale of a community", in part because communities are affected in some way by mechanisms operating at all scales from molecular to global. Community composition is ultimately affected by which species the ecologist chooses to include, and the particular scales chosen for investigation. Therefore it is more useful to focus efforts on examining how organization changes with scale than on finding "the scale" (Levin 1992).

References

- Allen, T.F.H., T.B. Starr. 1982. *Hierarchy: Perspectives for Ecological Complexity*. Chicago: University of Chicago Press.
- Amann, R.L., W. Ludwig, K. Schleifer. 1995. Phylogenetic identification and in situ detection of individual microbial cells without cultivation. *Microbiological Reviews* 59:143-169.
- Beare, M.H., D.C. Coleman, D.A. Crossley Jr, P.F. Hendrix, E.P. Odum. 1995. A hierarchical approach to evaluating the significance of soil biodiversity to biogeochemical cycling. In *The Significance and Regulation of Soil Biodiversity*, edited by H. P. Collins, G. P. Robertson and M. J. Klug. Netherlands: Kluwer Academic Publishers.
- Beare, M.H., R.W. Parmelee, P.F. Hendrix, W. Cheng. 1992. Microbial and faunal interactions and effects on litter nitrogen and decomposition in agroecosystems. *Ecological Monographs* 62:569-591.
- Bellehumeur, C., P. Legendre, D. Marcotte. 1997. Variance and sampling scales in a tropical rain forest: changing the size of sampling units. *Plant Ecology* 130:89-98.
- Belyea, L.R., J. Lancaster. 1999. Assembly rules within a contingent ecology. *Oikos* 86:402-416.
- Boerner, R.E.J., A.J. Scherzer, J.A. Brinkman. 1998. Spatial patterns of inorganic N, P availability, and organic C in relation to soil disturbance: a chronosequence analysis. *Applied Soil Ecology* 7:159-177.
- Borcard, D., P. Legendre, P. Drapeau. 1992. Partialling out the spatial component of ecological variation. *Ecology* 73:1045-1055.
- Bormann, F.H., G.E. Likens. 1979. Catastrophic disturbance and the steady state in northern hardwood forests. *American Scientist* 67:660-669.
- Bouxin, G., N. Gautier. 1982. Pattern analysis in Belgian limestone grasslands. *Vegetatio* 49:65-83.
- Carpenter, S.R., J.E. Chaney. 1983. Scale of spatial pattern: four methods compared. *Vegetatio* 53:153-160.
- Cash, G.G., J.J. Breen. 1992. Principal component analysis and spatial correlation: environmental analytical software tools. *Chemosphere* 24:1607-1623.



- Cavigelli, M.A., G.P. Robertson, M.J. Klug. 1995. Fatty acid methyl ester (FAME) profiles as measures of soil microbial community structure. *Plant and Soil* 170:99-113.
- Cho, J., J.M. Tiedje. 2000. Biogeography and degree of endemism of fluorescent *Pseudomonas* strains in soil. *Applied and Environmental Microbiology* 66:5448-5456.
- Clements, F.E. 1936. Nature and structure of the climax. *Journal of Ecology* 24:252-284.
- Connell, J.H. 1978. Diversity in tropical rain forests and coral reefs. *Science* 199:1302-1310.
- Cressie, N. 1985. Fitting variogram models by weighted least squares. *Mathematical Geology* 17:563-586.
- Cullinan, V.I., M.A. Simmons, J.M. Thomas. 1997. A Bayesian test of hierarchy theory: scaling up variability in plant cover from field to remotely sensed data. *Landscape Ecology* 12:273-285.
- Dobermann, A., P. Goovaerts, T. George. 1995. Sources of soil variation in an acid Ultisol of the Philippines. *Geoderma* 68:173-191.
- Edgington, E.S. 1995. *Randomization Tests*, 3 ed. New York: Marcel Dekker.
- Eswaran, H., F.H. Beinroth, S.M. Virmani. 2000. Resource management domains: A biophysical unit for assessing and monitoring land quality. *Agriculture Ecosystems and Environment* 81:155-162.
- Felske, A., A.D.L. Akkermans. 1998. Spatial homogeneity of abundant bacterial 16S rRNA molecules in grassland soils. *Microbial Ecology* 36:31-36.
- Fulthorpe, R.R., A.N. Rhodes, J.M. Tiedje. 1998. High levels of endemism of 3-chlorobenzoate-degrading soil bacteria. *Applied and Environmental Microbiology* 64:1620-1627.
- Gaedke, U. 1998. The response of the pelagic food web to re-oligotrophication of a large and deep lake (L. Constance): evidence for scale-dependent hierarchical patterns? *Ergebnisse der Limnologie* 53:317-333.
- Galiano, E.F. 1983. Detection of multi-species patterns in plant populations. *Vegetatio* 53:129-138.
- Gleason, H.A. 1939. The individualistic concept of the plant association. *American Midland Naturalist* 21:92-110.
- Goodall, D.W. 1974. A new method for the analysis of spatial pattern by random pairing of quadrats. *Vegetatio* 29:135-146.

Goovaerts, P. 1994. Study of the relationships between two sets of variables using multivariate geostatistics. *Geoderma* 62:93-107.

Greenblatt, C.L., A. Davis, B.G. Clement, C.L. Kitts, T. Cox, R.J. Cano. 1999. Diversity of microorganisms isolated from amber. *Microbial Ecology* 38:58-68.

Grieg-Smith, P. 1952. The use of random and contiguous quadrats in the study of the structure of plant communities. *Annals of Botany New Series* 16:293-316.

Griffiths, B.S., R.D. Bardgett. 1997. Interactions between microbe-feeding invertebrates and soil microorganisms. In *Modern Soil Microbiology*, edited by J. D. v. Elsas, J. T. Trevors and E. M. H. Wellington. New York: Marcel Dekker.

Grime, J.P. 1994. The role of plasticity in exploiting environmental heterogeneity. In *Exploitation of Environmental Heterogeneity by Plants: Ecophysiological Processes Above- and Belowground*, edited by M. M. Caldwell and R. W. Pearcy. San Diego: Academic Press.

Grundmann, L.G., F. Gourbière. 1999. A micro-sampling approach to improve the inventory of bacterial diversity in soil. *Applied Soil Ecology* 13:123-126.

Hagen, M.J., J.L. Hamrick. 1996. A hierarchical analysis of population genetic structure in *Rhizobium leguminosarum* bv. *trifolii*. *Molecular Ecology* 5:177-186.

Harris, D., E.A. Paul. 1994. Measurement of bacterial growth rates in soil. *Applied Soil Ecology* 1:277-290.

Harris, P.J. 1994. Consequences of the spatial distribution of microbial communities in soil. In *Beyond the Biomass*, edited by K. Ritz, J. Dighton and K. E. Giller.

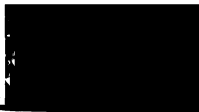
Harrison, S. 1997. How natural habitat patchiness affects the distribution of diversity in Californian serpentine chaparral. *Ecology* 78:1898-1906.

Hill, M.O. 1973. The intensity of spatial pattern in plant communities. *Journal of Ecology* 61:225-235.

Hoef, J.M.V., D.C. Glenn-Lewin. 1989. Multiscale ordination: a method for detecting pattern at several scales. *Vegetatio* 82:59-67.

Hoekstra, T.W., T.F.H. Allen, C.H. Flather. 1991. Implicit scaling in ecological research. *BioScience* 41:148-154.

Hoekstra, T.W., C.H. Flather. 1987. Theoretical basis for integrating wildlife in renewable resource inventories. *Journal of Environmental Management* 24:95-110.



- Holt, R.D. 1984. Spatial heterogeneity, indirect interactions, and the coexistence of prey species. *American Naturalist* 124:377-406.
- Hraber, P.T., B.T. Milne. 1997. Community assembly in a model ecosystem. *Ecological Modelling* 104:267-285.
- Hugenholtz, P., B.M. Goebel, N.R. Pace. 1998. Impact of culture-independent studies on the emerging phylogenetic view of bacterial diversity. *Journal of Bacteriology* 180:4765-4774.
- Jennings, M.D., J.P. Reganold. 1991. Hierarchy and subsidy-stress as a theoretical basis for managing environmentally sensitive areas. *Landscape and Urban Planning* 21:31-46.
- Jobson, J.D. 1992. *Applied Multivariate Data Analysis Volume II: Categorical and Multivariate Methods*. New York: Springer-Verlag.
- Johnson, L.B., S.H. Gage. 1997. Landscape approaches to the analysis of aquatic ecosystems. *Freshwater Biology* 37:113-132.
- Jonsson, B.G., J. Moen. 1998. Patterns in species associations in plant communities: the importance of scale. *Journal of Vegetation Science* 9:327-332.
- Klironomos, J.N., M.C. Rillig, M.F. Allen. 1999. Designing belowground field experiments with the help of semi-variance and power analyses. *Applied Soil Ecology* 12:227-238.
- Kotliar, N.B. 1996. Scale dependency and the expression of hierarchical structure in *Delphinium* patches. *Vegetatio* 127:117-128.
- Lee, D.C., W.E. Grant. 1995. A hierarchical approach to fisheries planning and modeling in the Columbia River basin. *Environmental Management* 19:17-25.
- Legendre, P., M.J. Anderson. 1999. Distance-based redundancy analysis: testing multispecies responses in multifactorial ecological experiments. *Ecological Monographs* 69:1-24.
- Legendre, P., M. Fortin. 1989. Spatial pattern and ecological analysis. *Vegetatio* 80:107-138.
- Legendre, P., E.D. Gallagher. in press. Ecologically meaningful transformations for ordination of species data. *Oecologia*.
- Legendre, P., L. Legendre. 1998. *Numerical Ecology*, 2 ed. Amsterdam: Elsevier.
- Leibold, M.A. 1995. The niche concept revisited: mechanistic models and community context. *Ecology* 76:1371-1382.

- Legendre, P., & Legendre, P. 1983. Spatial pattern and ecological analysis. *Vegetatio* 80:107-138.
- Legendre, P., & Legendre, P. 1988. *Statistical Ecology*. 2 ed. Amsterdam: Elsevier.
- Legendre, P., & Legendre, P. 1992. The metric concept revisited: mechanistic models and community context. *Ecology* 73:1371-1382.
- Legendre, P., & Legendre, P. 1993. Distance-based redundancy analysis: testing multiresponses in multivariate ecological experiments. *Ecological Monographs* 63:1-24.
- Legendre, P., & Legendre, P. 1994. Distance-based redundancy analysis: testing multiresponses in multivariate ecological experiments. *Ecological Monographs* 64:1-24.
- Legendre, P., & Legendre, P. 1995. A statistical approach to landscape planning and modeling in the Columbia River basin. *Environmental Management* 19:1-24.
- Legendre, P., & Legendre, P. 1996. Statistical analysis of spatial data. *Ecological Modelling* 12:1-24.
- Legendre, P., & Legendre, P. 1997. Statistical analysis of spatial data. *Ecological Modelling* 12:1-24.
- Legendre, P., & Legendre, P. 1998. Statistical analysis of spatial data. *Ecological Modelling* 12:1-24.
- Legendre, P., & Legendre, P. 1999. Statistical analysis of spatial data. *Ecological Modelling* 12:1-24.
- Legendre, P., & Legendre, P. 2000. Statistical analysis of spatial data. *Ecological Modelling* 12:1-24.
- Legendre, P., & Legendre, P. 2001. Statistical analysis of spatial data. *Ecological Modelling* 12:1-24.
- Legendre, P., & Legendre, P. 2002. Statistical analysis of spatial data. *Ecological Modelling* 12:1-24.
- Legendre, P., & Legendre, P. 2003. Statistical analysis of spatial data. *Ecological Modelling* 12:1-24.
- Legendre, P., & Legendre, P. 2004. Statistical analysis of spatial data. *Ecological Modelling* 12:1-24.
- Legendre, P., & Legendre, P. 2005. Statistical analysis of spatial data. *Ecological Modelling* 12:1-24.
- Legendre, P., & Legendre, P. 2006. Statistical analysis of spatial data. *Ecological Modelling* 12:1-24.
- Legendre, P., & Legendre, P. 2007. Statistical analysis of spatial data. *Ecological Modelling* 12:1-24.
- Legendre, P., & Legendre, P. 2008. Statistical analysis of spatial data. *Ecological Modelling* 12:1-24.
- Legendre, P., & Legendre, P. 2009. Statistical analysis of spatial data. *Ecological Modelling* 12:1-24.
- Legendre, P., & Legendre, P. 2010. Statistical analysis of spatial data. *Ecological Modelling* 12:1-24.
- Legendre, P., & Legendre, P. 2011. Statistical analysis of spatial data. *Ecological Modelling* 12:1-24.
- Legendre, P., & Legendre, P. 2012. Statistical analysis of spatial data. *Ecological Modelling* 12:1-24.
- Legendre, P., & Legendre, P. 2013. Statistical analysis of spatial data. *Ecological Modelling* 12:1-24.
- Legendre, P., & Legendre, P. 2014. Statistical analysis of spatial data. *Ecological Modelling* 12:1-24.
- Legendre, P., & Legendre, P. 2015. Statistical analysis of spatial data. *Ecological Modelling* 12:1-24.
- Legendre, P., & Legendre, P. 2016. Statistical analysis of spatial data. *Ecological Modelling* 12:1-24.
- Legendre, P., & Legendre, P. 2017. Statistical analysis of spatial data. *Ecological Modelling* 12:1-24.
- Legendre, P., & Legendre, P. 2018. Statistical analysis of spatial data. *Ecological Modelling* 12:1-24.
- Legendre, P., & Legendre, P. 2019. Statistical analysis of spatial data. *Ecological Modelling* 12:1-24.
- Legendre, P., & Legendre, P. 2020. Statistical analysis of spatial data. *Ecological Modelling* 12:1-24.
- Legendre, P., & Legendre, P. 2021. Statistical analysis of spatial data. *Ecological Modelling* 12:1-24.
- Legendre, P., & Legendre, P. 2022. Statistical analysis of spatial data. *Ecological Modelling* 12:1-24.
- Legendre, P., & Legendre, P. 2023. Statistical analysis of spatial data. *Ecological Modelling* 12:1-24.
- Legendre, P., & Legendre, P. 2024. Statistical analysis of spatial data. *Ecological Modelling* 12:1-24.
- Legendre, P., & Legendre, P. 2025. Statistical analysis of spatial data. *Ecological Modelling* 12:1-24.

- Levin, S.A. 1992. The problem of pattern and scale in ecology. *Ecology* 73:1943-1967.
- Liu, W.-T., T.L. Marsh, H. Cheng, L.J. Forney. 1997. Characterization of microbial diversity by determining terminal restriction fragment length polymorphisms of genes encoding 1S rRNA. *Applied and Environmental Microbiology* 63:4516-4522.
- Ludwig, J.A., D.W. Goodall. 1979. A comparison of paired- with blocked-quadrat variance methods for the analysis of spatial pattern. *Vegetatio* 38:49-59.
- MacArthur, R., R. Levins. 1967. The limiting similarity, convergence, and divergence of coexisting species. *The American Naturalist* 101:377-385.
- Maurer, B.A. 1990. *Dipodomys* populations as energy-processing systems: regulation, competition, and hierarchical organization. *Ecological Modelling* 50:157-176.
- Milne, B.T. 1991. Heterogeneity as a multiscale characteristic of landscapes. In *Ecological Heterogeneity*, edited by J. Kolasa and S. T. A. Pickett. New York: Springer-Verlag.
- Minamisawa, K., H. Mitsui. 2000. Genetic ecology of soybean bradyrhizobia. In *Soil Biochemistry*, edited by J. Bollag and G. Stotzky. New York: Marcel Dekker.
- Monestiez, P., M. Goulard, G. Charmet. 1994. Geostatistics for spatial genetic structures: study of wild populations of perennial ryegrass. *Theoretical and Applied Genetics* 88:33-41.
- Morris. 1999. Spatial distribution of fungal and bacterial biomass in southern Ohio hardwood forest soils: fine scale variability and microscale patterns. *Soil Biology and Biochemistry* 31:1375-1386.
- Murphy, S.L., R.L. Tate, III. 1996. Bacterial movement through soil. In *Soil Biochemistry*, edited by G. Stotzky and J. Bollag. New York: Marcel Dekker.
- Muyzer, G. 1998. Structure, function and dynamics of microbial communities: the molecular biological approach. In *Advances in Molecular Ecology*, edited by G. R. Carvalho: IOS Press.
- Noy-Meir, I., D.J. Anderson. 1971. Multiple pattern analysis, or multiscale ordination: towards a vegetation hologram? In *Many Species Populations, Ecosystems, and Systems Analysis*, edited by G. P. Patil, E. C. Pielou and W. E. Waters. University Park PA: The Pennsylvania State University Press.
- Nüsslein, K., J.M. Tiedje. 1998. Characterization of the dominant and rare members of a young Hawaiian soil bacterial community with small-subunit ribosomal DNA amplified

from DNA fractionated on the basis of its guanine and cytosine composition. *Applied and Environmental Microbiology* 64:1283-1289.

O'Connor, R.J., M.T. Jones, D. White, C. Hunsaker, T. Loveland, B. Jones, E. Preston. 1996. Spatial partitioning of environmental correlates of avian biodiversity in the conterminous United States. *Biodiversity Letters* 3:97-110.

O'Neill, R.V., D.L. DeAngelis, J.B. Waide, T.F.H. Allen. 1986. *A Hierarchical Concept of Ecosystems*. Princeton, NJ: Princeton University Press.

O'Neill, R.V., R.H. Gardner, B.T. Milne, M.G. Turner, B. Jackson. 1991a. Heterogeneity and spatial hierarchies. In *Ecological Heterogeneity*, edited by J. Kolasa and S. T. A. Pickett. New York: Springer-Verlag.

O'Neill, R.V., S.J. Turner, V.I. Cullinan, D.P. Coffin, T. Cook, W. Conley, J. Brunt, J.M. Thomas, M.R. Conley, J. Gosz. 1991b. Multiple landscape scales: an intersite comparison. *Landscape Ecology* 5:137-144.

Palik, B.J., P.C. Goebel, L.K. Kirkman, L. West. 2000. Using landscape hierarchies to guide restoration of disturbed ecosystems. *Ecological Applications* 10:189-202.

Palmer, J.B. 1992. Hierarchical and concurrent individual based modeling. In *Individual-Based Models and Approaches in Ecology*, edited by D. L. DeAngelis and L. J. Gross. New York: Chapman & Hall.

Parker, V.T., S.T.A. Pickett. 1998. Historical contingency and multiple scales of dynamics within plant communities. In *Ecological Scale: Theory and Applications*, edited by D. L. Peterson and V. T. Parker. New York: Columbia University Press.

Parkin, T.B. 1993. Spatial variability of microbial processes in soil - a review. *Journal of Environmental Quality* 22:409-417.

Peterson, D.L., V.T. Parker. 1998. Dimensions of scale in ecology, resource management, and society. In *Ecological Scale: Theory and Applications*, edited by D. L. Peterson and V. T. Parker. New York: Columbia University Press.

Quinones, R.A. 1994. A comment on the use of allometry in the study of pelagic ecosystem processes. *Scientia Marina* 58:11-16.

Ricklefs, R.E. 1987. Community diversity: relative roles of local and regional processes. *Science* 235:167-171.

Robertson, G.P., J.R. Crum, B.G. Ellis. 1993. The spatial variability of soil resources following long-term disturbance. *Oecologia* 96:451-456.



- Robertson, G.P., D.W. Freckman. 1995. The spatial distribution of nematode trophic groups across a cultivated ecosystem. *Ecology* 76:1425-1432.
- Robertson, G.P., K.L. Gross. 1994. Assessing the heterogeneity of belowground resources: quantifying pattern and scale. In *Exploitation of Environmental Heterogeneity by Plants: Ecophysiological Processes Above- and Belowground*, edited by M. M. Caldwell and R. W. Pearcy. San Diego: Academic Press.
- Robertson, G.P., K.M. Klingensmith, M.J. Klug, E.A. Paul, J.R. Crum, B.G. Ellis. 1997. Soil resources, microbial activity, and primary production across an agricultural ecosystem. *Ecological Applications* 7:158-170.
- Rossi, J., P. Lavelle, A. Albrecht. 1997. Relationships between spatial pattern of the endogeic earthworm *Polypheretima elongata* and soil heterogeneity. *Soil Biology and Biochemistry* 29:485-488.
- Rossi, R.E., D.J. Mulla, A.G. Journel, E.H. Franz. 1992. Geostatistical tools for modeling and interpreting ecological spatial dependence. *Ecological Monographs* 62:277-314.
- Roughgarden, J. 1989. The structure and assembly of communities. In *Perspectives in Ecological Theory*, edited by J. Roughgarden, R. M. May and S. A. Levin. Princeton, NJ: Princeton University Press.
- Schaefer, J.A., F. Messier. 1994. A paired-quadrat method for use in multiscale ordination. *Vegetatio* 113:9-11.
- Schlesinger, W.H., J.A. Raikes, A.E. Hartley, A.F. Cross. 1996. On the spatial pattern of soil nutrients in desert ecosystems. *Ecology* 77:364-374.
- Schluter, D. 1984. A variance test for detecting species associations, with some example applications. *Ecology* 65:998-1005.
- Schmitt, R.J. 1987. Indirect interactions between prey: apparent competition, predator aggregation, and habitat segregation. *Ecology* 68:1887-1897.
- Schneider, D.C. 1994. *Quantitative Ecology*. San Diego, CA: Academic Press.
- Shmida, A., R.A. Whittaker. 1981. Pattern and biological microsite effects in two shrub communities, Southern California. *Ecology* 62:234-251.
- Smith, J.L., E.A. Paul. 1990. The significance of soil microbial biomass estimations. In *Soil Biochemistry*, edited by J. Bollag and G. Stotzky. New York: Marcel Dekker.
- Souza, V., L. Eguiarte, G. Avila, R. Capello, C. Gallardo, J. Montoya, D. Pinero. 1994. Genetic structure of *Rhizobium etli* biovar phaseoli associated with wild and cultivated





bean plants (*Phaseolus vulgaris* and *Phaseolus coccineus*) in Morelos, Mexico. *Applied and Environmental Microbiology* 60:1260-1268.

Stark, J.M. 1994. Causes of soil nutrient heterogeneity at different scales. In *Exploitation of Environmental Heterogeneity by Plants: Ecophysiological Processes Above- and Belowground*, edited by M. M. Caldwell and R. W. Pearcy. San Diego: Academic Press.

Stoyan, H., H. De-Polli, S. Böhm, G.P. Robertson, E.A. Paul. 2000. Spatial heterogeneity of soil respiration and related properties at the plant scale. *Plant and soil* 222:203-214.

Strain, S.R., T.S. Whittam, P.J. Bottomley. 1995. Analysis of genetic structure in soil populations of *Rhizobium leguminosarum* recovered from the USA and the UK. *Molecular Ecology* 4:105-114.

Tiedje, J.M., S. Asuming-Brempong, K. Nüsslein, T.L. Marsh, S.J. Flynn. 1999. Opening the black box of soil microbial diversity. *Applied Soil Ecology* 13:109-122.

Torsvik, V., J. Goksoyr, F.L. Daee. 1990. High diversity of DNA of soil bacteria. *Applied and Environmental Microbiology* 56:782-787.

Wackernagel, H. 1998. *Multivariate geostatistics: an introduction with applications*. Berlin: Springer.

Waltho, N., J. Kolasa. 1994. Organization of instabilities in multispecies systems, a test of hierarchy theory. *Proceedings of the National Academy of Sciences, USA* 91:1682-1685.

Whittaker, R.H. 1960. Vegetation of the Siskiyou Mountains, Oregon and California. *Ecological Monographs* 30:279-338.

Wiens, J.A. 1989. Spatial scaling in ecology. *Functional Ecology* 3:385-397.

Wilson, J.B. 1999. Assembly rules in plant communities. In *Ecological Assembly Rules: Perspectives, Advances, Retreats*, edited by E. Weiher and P. Keddy. Cambridge: Cambridge University Press.

Wintzingerode, F.v., U.B. Göbel, E. Stackebrandt. 1997. Determination of microbial diversity in environmental samples: pitfalls of PCR-based rRNA analysis. *FEMS Microbiology Reviews* 21:213-229.

Wu, J., O.L. Loucks. 1995. From balance of nature to hierarchical patch dynamics: a paradigm shift in ecology. *The Quarterly Review of Biology* 70:439-466.

Yoshioka, P.M., B.B. Yoshioka. 1989. A multispecies, multiscale analysis of spatial pattern and its application to a shallow-water gorgonian community. *Marine Ecology Progress Series* 54:257-264.

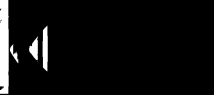


Table 1: Grain-based regression analysis of T-RFLP profile variability on mean log soil weight. The p-values listed under the two models are associated with the F-test of the overall fit each model. Direct comparison of the models is via partial F-test of the null hypothesis that the hierarchical model does not fit the data significantly better than the linear model. RSS is the residual sums of squares, df is the degrees of freedom associated with the F-tests.

Variability Statistic	Linear Model			Hierarchical Model			Direct Comparison				
	RSS	df	p	slope	RSS	df	p	Slopes	F	df	p
Hellinger Variance	0.081	1,18	5×10^{-5}	-0.05	0.065	2,17	5×10^{-5}	-0.03 0	4.4	1,17	0.05
Mean Jaccard Distance	0.046	1,18	0.001	-0.03	0.040	2,17	0.002	-0.05 0	2.4	1,17	0.14
MAD-t score	0.023	1,18	2×10^{-5}	-0.03	0.016	2,17	6×10^{-6}	0 -0.02	7.5	1,17	9×10^{-4}

Table 2: Distance function parameters fit with nonlinear least-squares to HV of 10 g sample T-RFLP profiles. Proportion is the proportion of total variability explained by the spatial structure detected, calculated by $C_H/(C_H+C_0)$ for the exponential models, and (maximum $HV-C_0$)/maximum HV for the linear model, 3a is the practical range of the spatial structure in the exponential model.

Grid	Model	Proportion	3a, cm	R^2 , %
1 RsaI	linear	0.18	-	92
2 RsaI	exponential	0.18	136	78
3 RsaI	exponential	0.23	91	74
2 MspI	exponential	0.23	67	61



Table 3: Redundancy analysis and global Mantel tests of all fifty 10 g sample T-RFLP profiles per grid. Select x-y terms were selected as significant in forward selection of variables ($p < 0.1$).

<i>Redundancy Analysis</i>		Grid 1	Rsal Grid 2	Grid 3	Mspl Grid 2
Hellinger Variance	All x-y terms	0.22	0.25	0.22	0.25
	% Variability explained				
	p	0.0191	0.0036	0.0318	0.0005
	Terms	x, x^2, y^3	x^2, xy^2	x, x^2, y	x^2, x^2y, xy^2
Jaccard Distance	Select x-y terms	0.12	0.12	0.10	0.13
	% Variability explained				
	p	0.24	0.21	0.19	0.22
	Terms	0.0003	0.0111	0.1817	0.0018
Global Mantel tests	All x-y terms	x, y^3	x, x^2	x^2, y^2	x^2, x^2y, xy^2
	Select x-y terms	0.09	0.09	0.05	0.10
	% Variability explained				
	p	0.12	0.10	0.10	0.14
Hellinger Distance	r_M	0.0274	0.0305	0.0338	0.0086
	p	0.13	0.08	0.05	0.09
Jaccard Distance	r_M	0.0135	0.0743	0.1462	0.0537
	p				

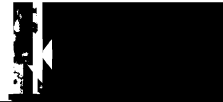
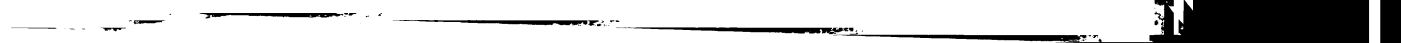


Figure 1: Sampling map for grid 1. 10 and 100 g samples at multiple grain sampling locations are white, other 10 g samples are black. Other sampling scales not shown were taken directly adjacent to the 10 and 100 g samples. Samples and distances are approximately to scale.

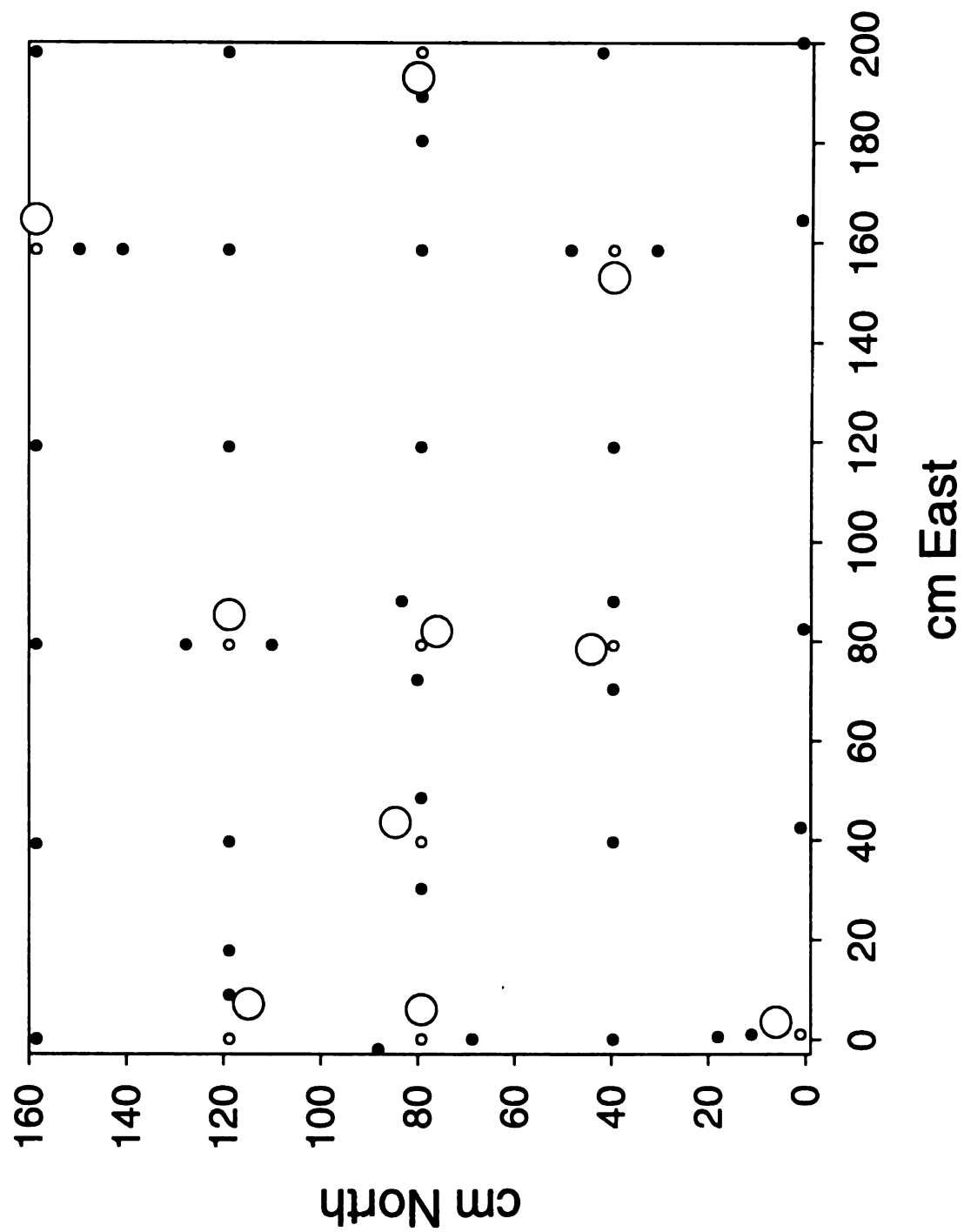


Figure 2: MAD-t scores derived from DNA extraction experiment. Bars with different letters within a weight category are significantly different at the $p=0.1$ significance level, $n=7$ for 100 g samples and 8 for 10 g samples.

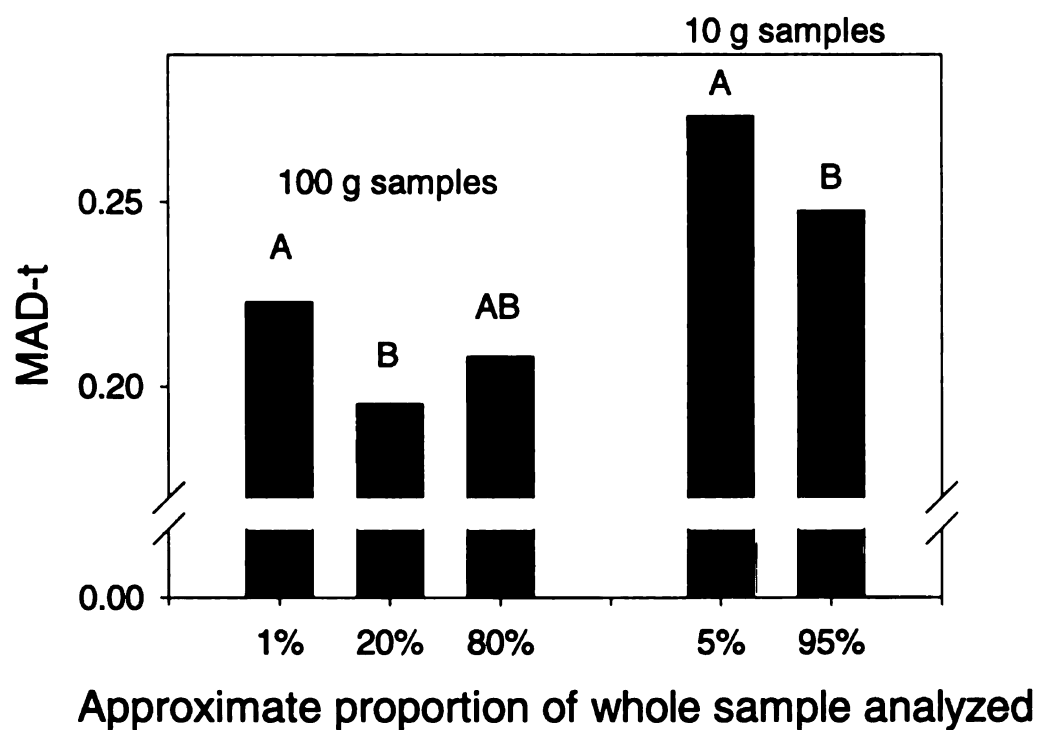


Figure 3: Grain-based analysis using three variability statistics. Colors indicate the three different grid replicates (red=grid 1, blue=grid 2, green=grid 3). Circles are sets of RsaI digests, triangles are sets of MspI digests. Lines represent the hierarchical models which fit the data significantly better than linear regression models, with undefined regions shown as dashed lines. *This figure is in color.*

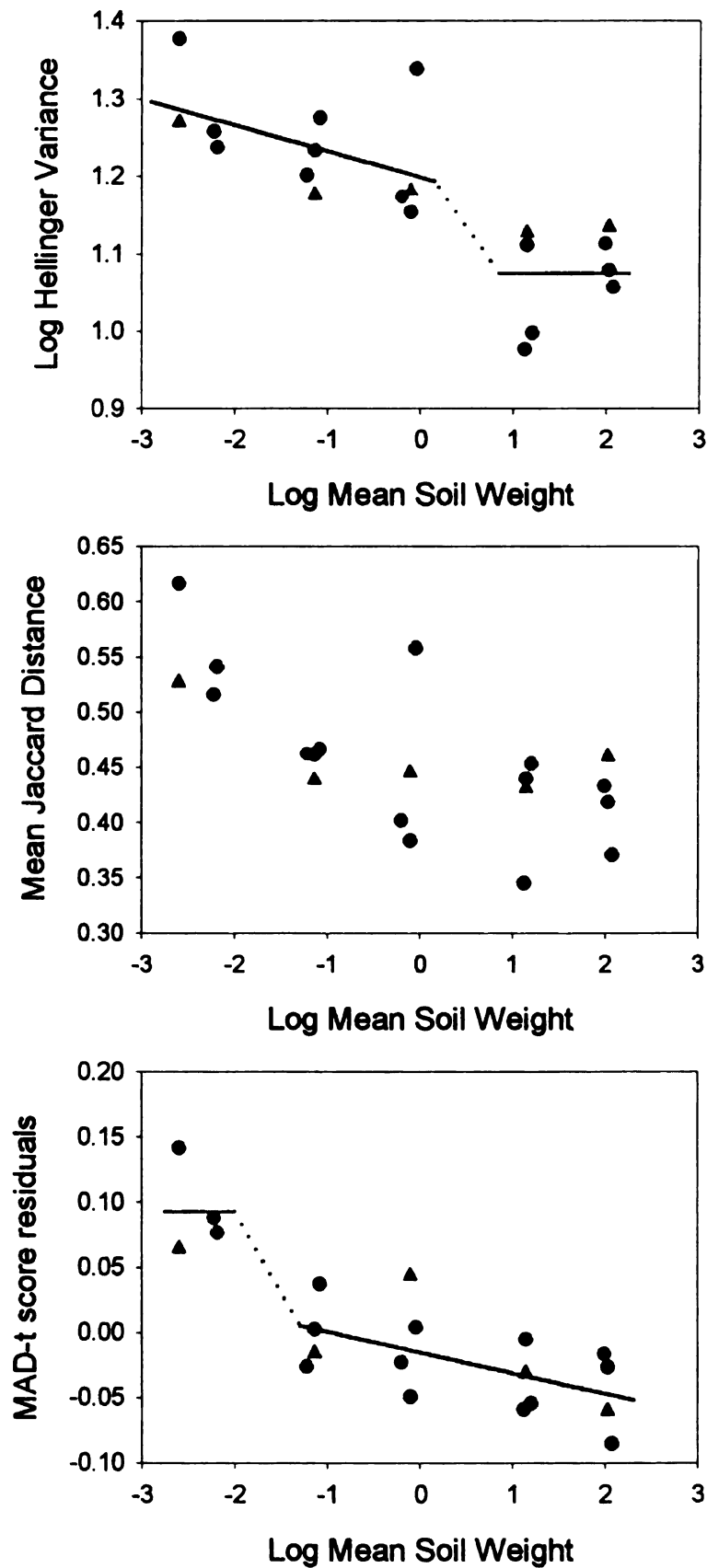
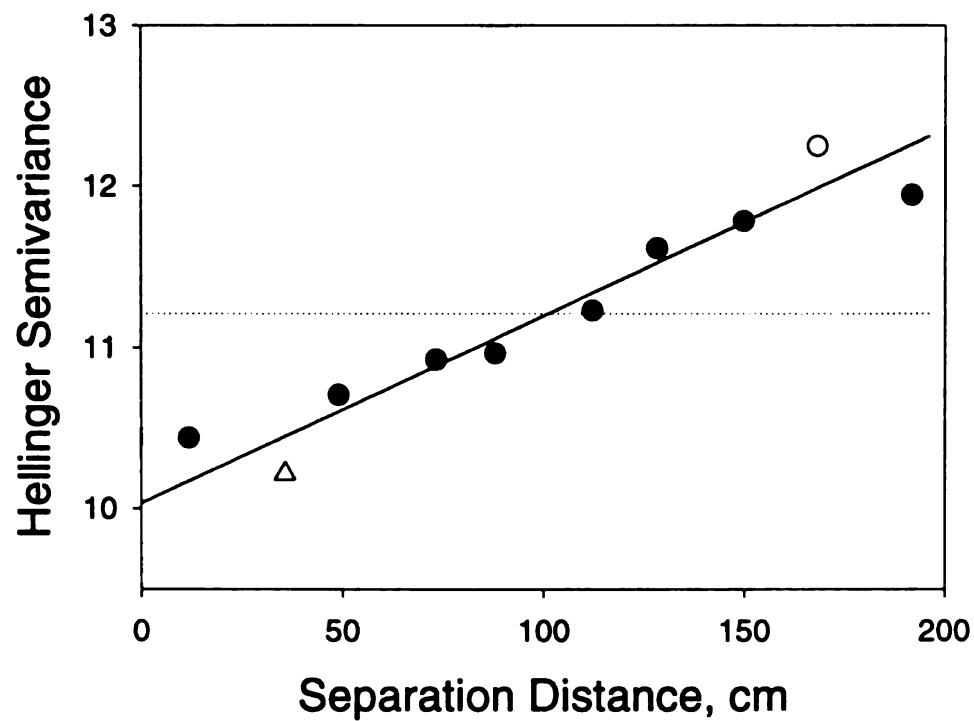




Figure 4: Hellinger variance as a function of separation distance. Hollow triangles indicate values significantly different from overall variance using the progressive Bonferroni correction for spatial analysis (initial significance value $p=0.05$). Hollow circle indicates a value significantly different from overall variance at the 0.05 level. Horizontal dashed lines indicate overall variance. Vertical dashed lines indicate the practical range of spatial structure found by weighted least squares modeling.

A. Grid 1, RsaI



B. Grid 2, RsaI

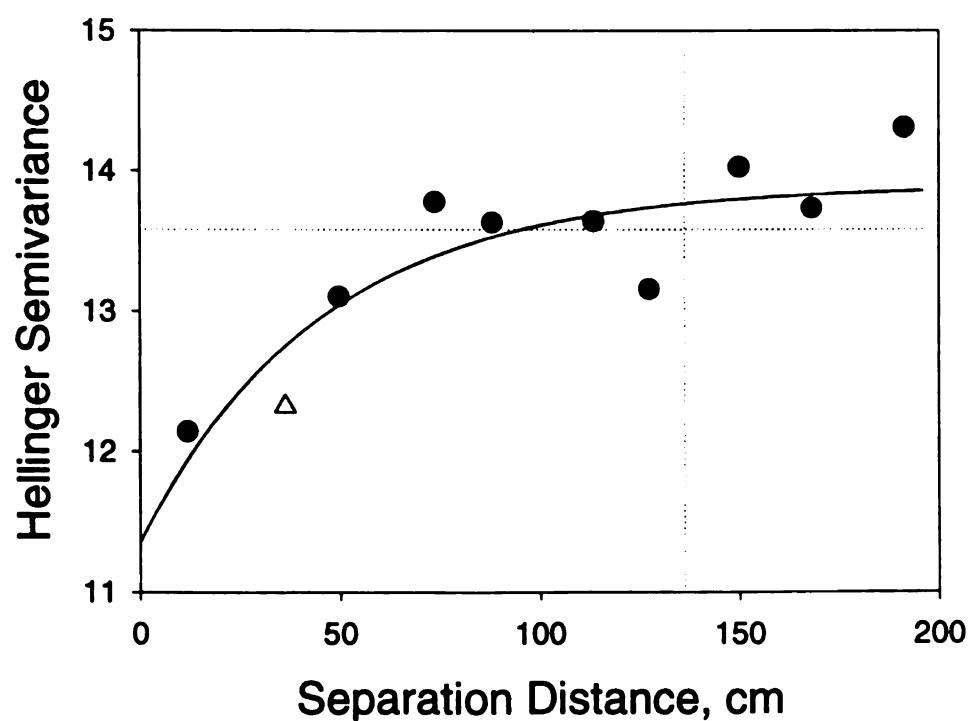
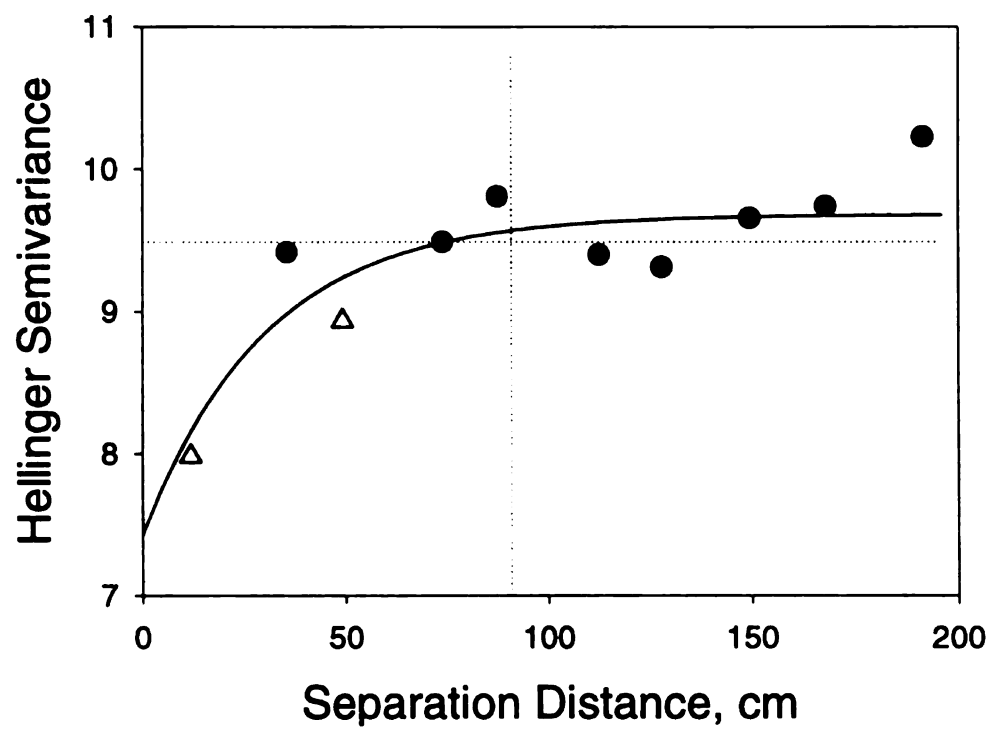


Figure 4, continued:

C. Grid 3, RsaI



D. Grid 2, MspI

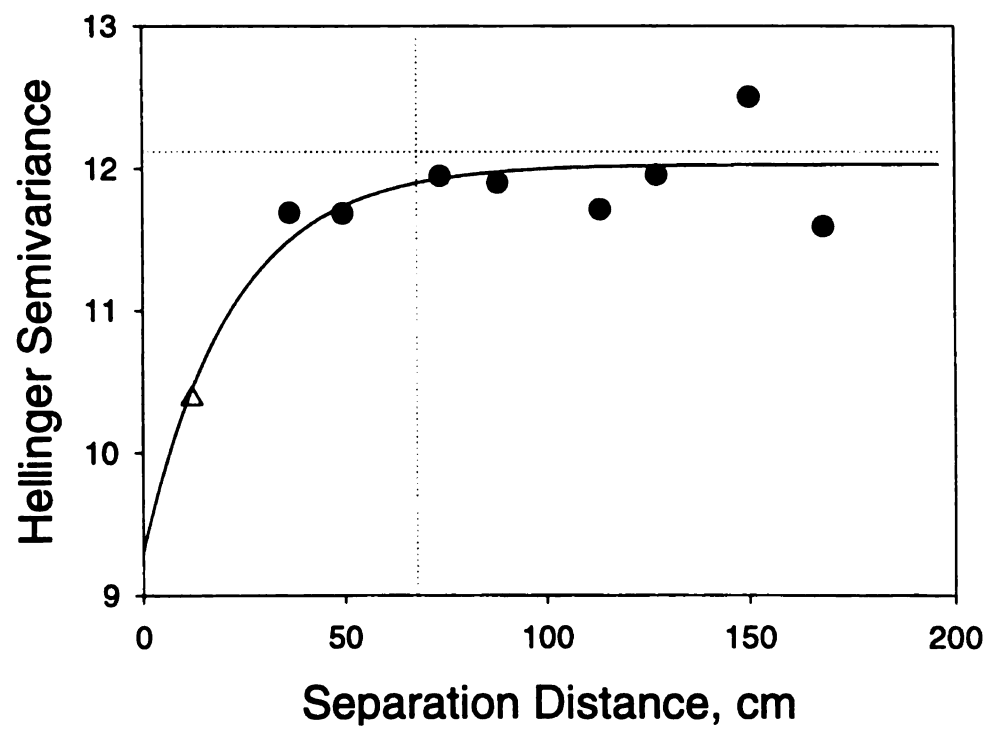
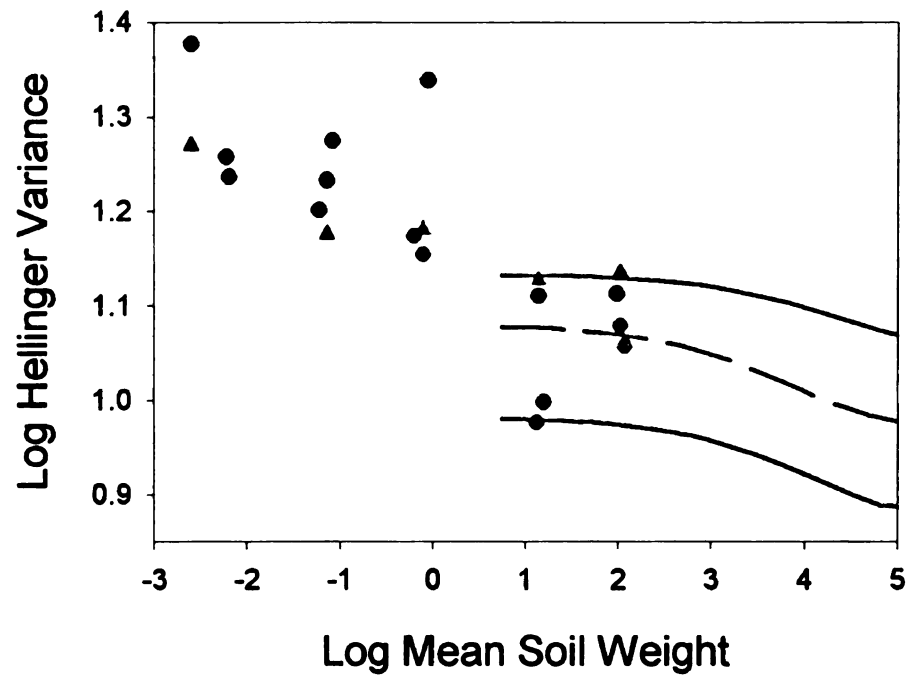


Figure 5: Integration of extent-based and grain-based analyses of Hellinger variance. Lines show estimates of log HV at larger grains based on application of the extent-based models to the multiple-grain sampling locations. Colors indicate the three different grid replicates (red=grid 1, blue=grid 2, green=grid 3). Solid lines and circles are sets of RsaI digests, dashed line and triangles are sets of MspI digests. *This figure is in color.*



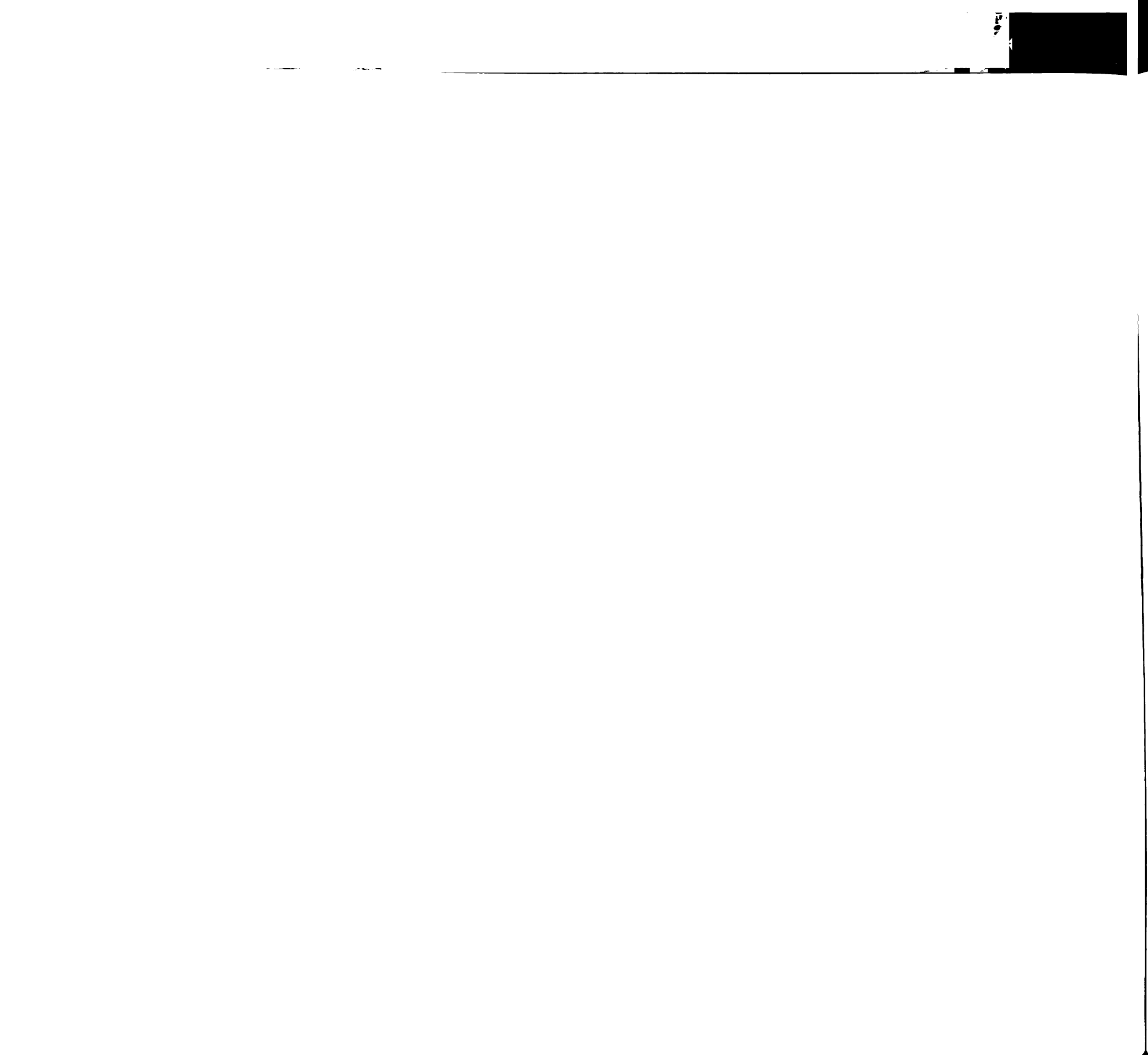


Figure 6: Principal coordinates analysis of correlation super-matrix of covariance matrices constructed from different distance classes in grid 2, RsaI digest. Numbers in the datapoint name represent the distance class from which each covariance matrix is derived (i.e. d1 is derived from distance class 1, 0-20 cm).

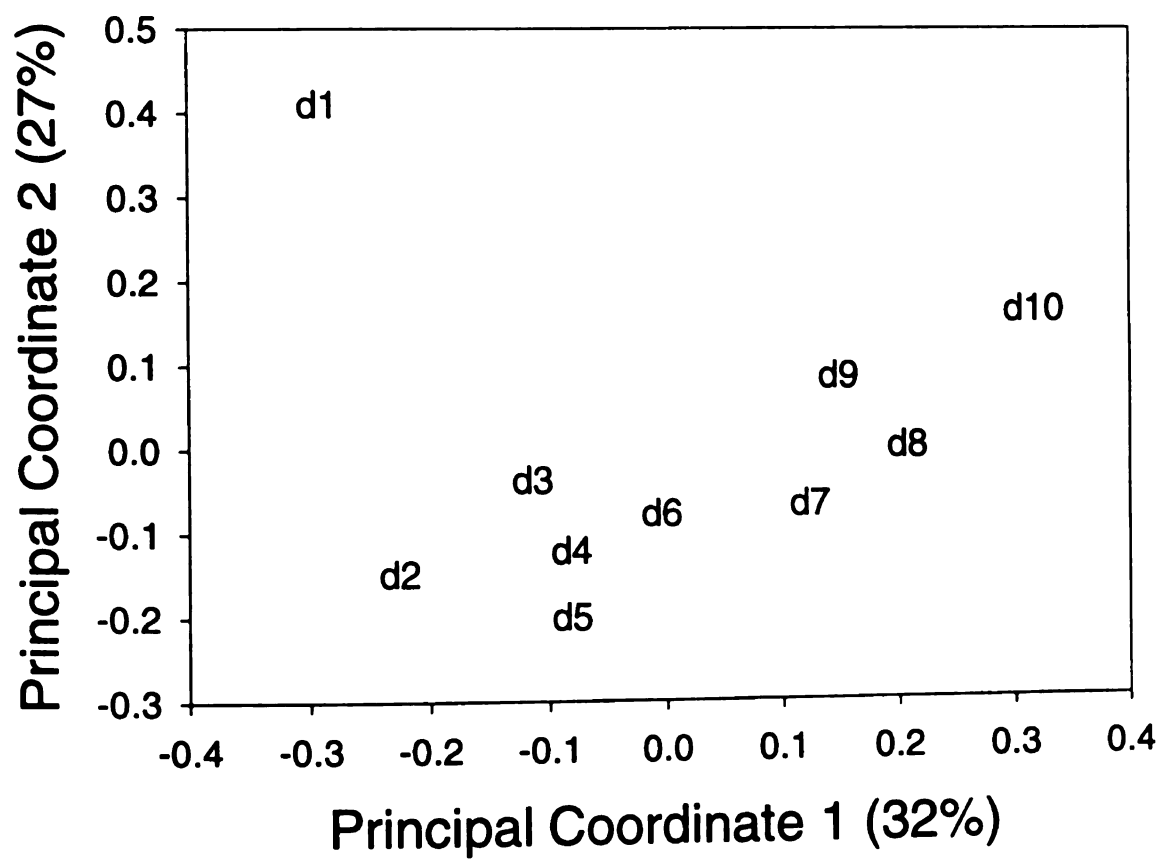




Figure 7: Cluster analysis correlation super-matrix describing covariance matrices constructed from different distance classes in grid 2, Rsa1 digest. Numbers in the datapoint name represent the distance class from which each covariance matrix is derived (i.e. OB1 is derived from distance class 1, 0-20 cm).

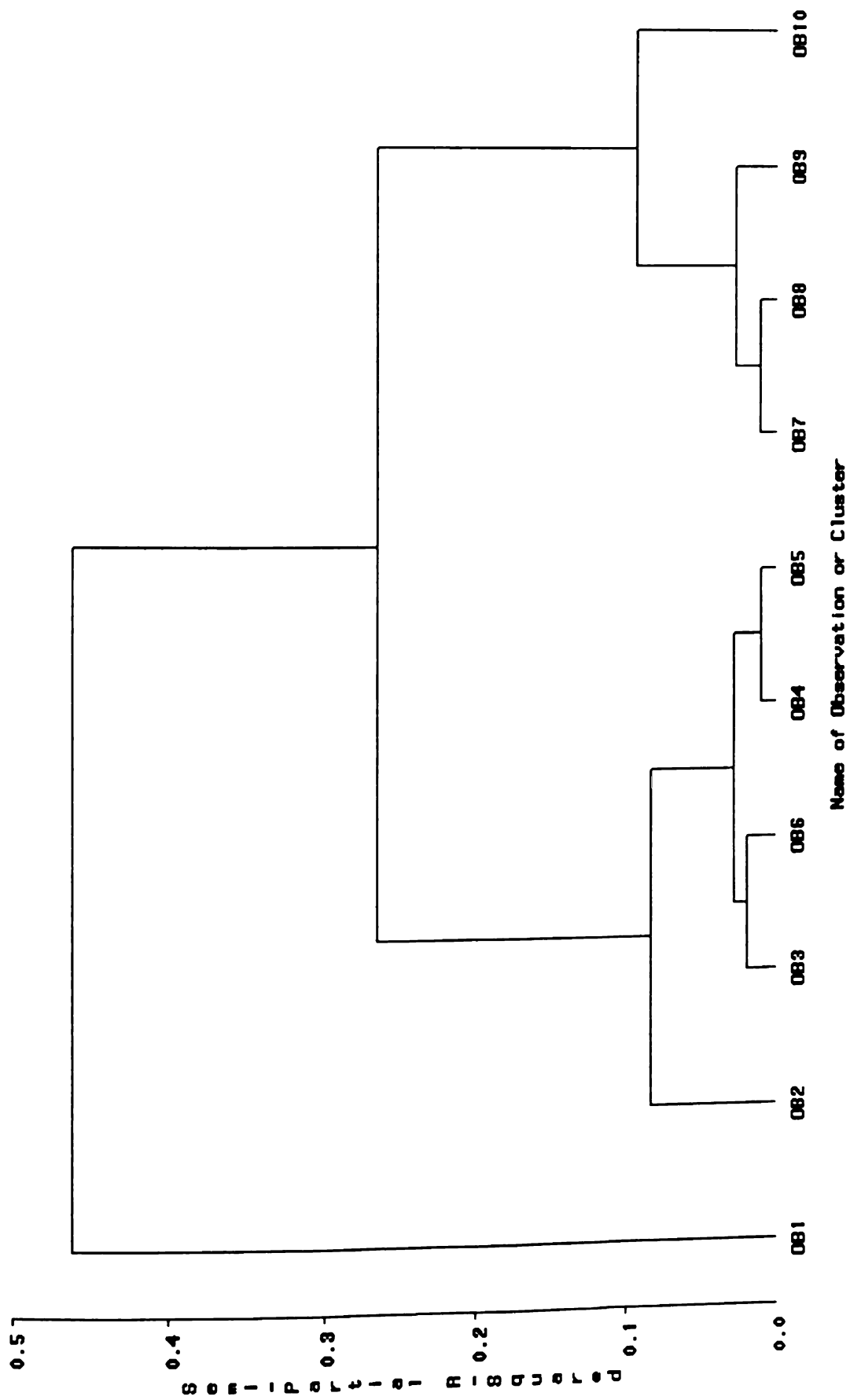
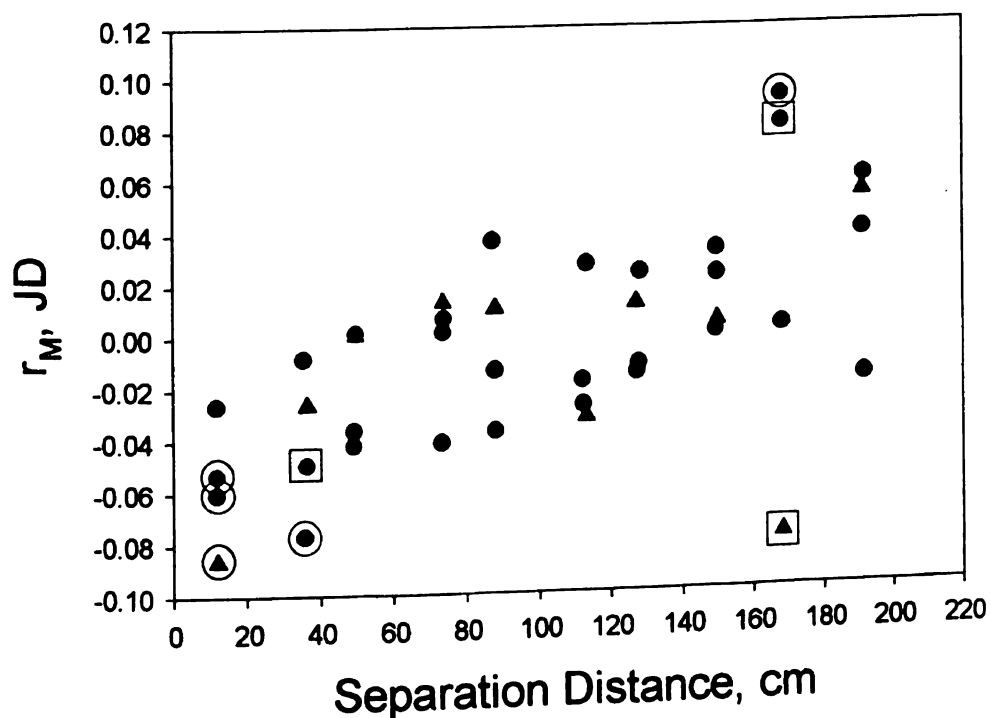
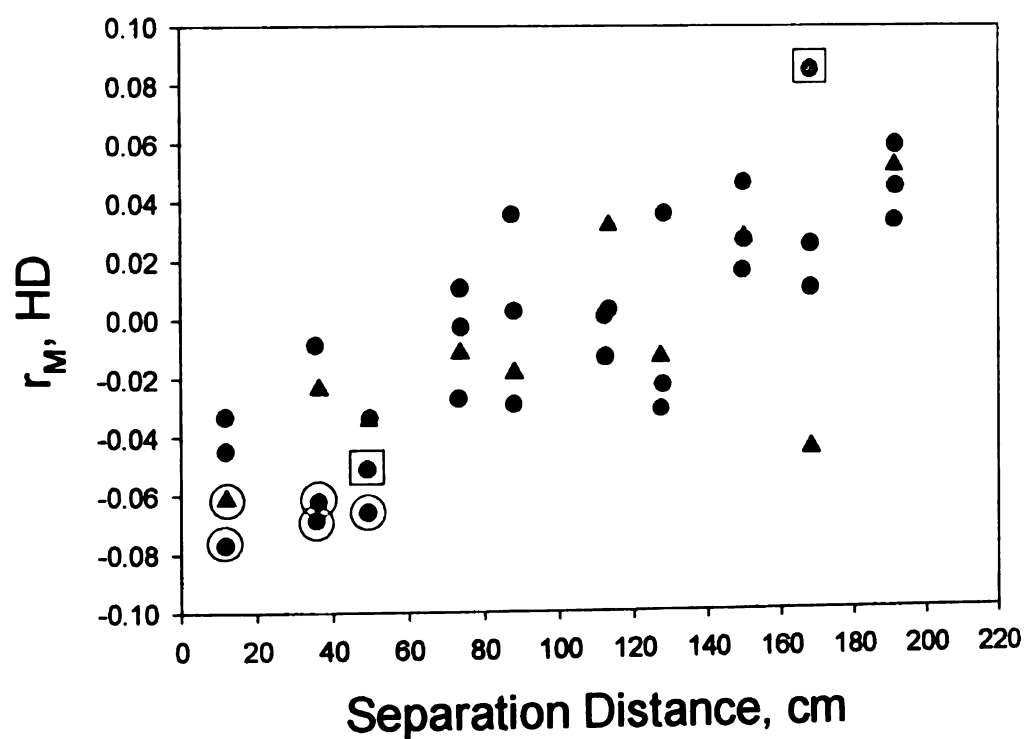


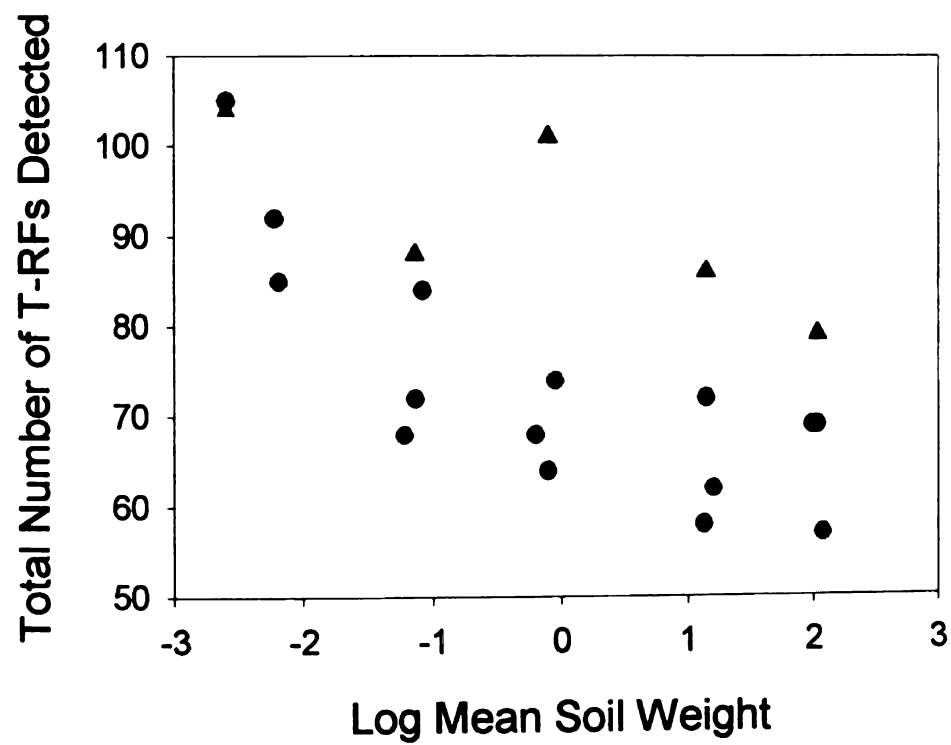


Figure 8: Normalized Mantel correlogram of Hellinger and Jaccard distances for all 10 g samples. Colors indicate the three different grid replicates (red=grid 1, blue=grid 2, green=grid 3). Circles are sets of RsaI digests, triangles are sets of MspI digests. Circled datapoints are significantly different from zero using the progressive Bonferroni correction and boxed datapoints are significant using uncorrected tests ($p < 0.05$). *This figure is in color.*





Appendix A: Total number of T-RFs detected in sets of samples at multiple-grain sampling locations. Note that this is not the average number of T-RFs per sample. Colors indicate the three different grid replicates (red=grid 1, blue=grid 2, green=grid 3). Circles are sets of RsaI digests, triangles are sets of MspI digests. *This figure is in color.*



believed a 391-T to maximum inlet

170
160
150
140
130
120
110
100
90
80
70
60
50
40
30
20
10
0

1

Appendix A: Total number of 391-T
sampling locations. Note that the
Colors indicate the three different
Circles are size of 1/2 in. diameter

Appendix A: Total number of 391-T
sampling locations. Note that the
Colors indicate the three different
Circles are size of 1/2 in. diameter

